Texas Medical Center Library
DigitalCommons@The Texas Medical Center

UT GSBS Dissertations and Theses (Open Access) | Graduate School of Biomedical Sciences

5-2010

VALIDATION OF THE ACTIVATION OF AURORA B KINASE BY CAENORHABDITIS ELEGANS TOUSLED-LIKE KINASE AND THE IDENTIFICATION OF CYCLIN B3 AS A PHOSPHO-SPECIFIC TLK-1 INTERACTOR

Gary Michael Deyter

Follow this and additional works at: http://digitalcommons.library.tmc.edu/utgsbs_dissertations


Part of the Cell Biology Commons, Developmental Biology Commons, and the Molecular Genetics Commons

Recommended Citation
Deyter, Gary Michael, "VALIDATION OF THE ACTIVATION OF AURORA B KINASE BY CAENORHABDITIS ELEGANS TOUSLED-LIKE KINASE AND THE IDENTIFICATION OF CYCLIN B3 AS A PHOSPHO-SPECIFIC TLK-1 INTERACTOR" (2010). *UT GSBS Dissertations and Theses (Open Access)*. Paper 87.

This Dissertation (PhD) is brought to you for free and open access by the Graduate School of Biomedical Sciences at DigitalCommons@The Texas Medical Center. It has been accepted for inclusion in UT GSBS Dissertations and Theses (Open Access) by an authorized administrator of DigitalCommons@The Texas Medical Center. For more information, please contact laurel.sanders@library.tmc.edu.

The TMC LIBRARY Health Sciences Resource Center

VALIDATION OF THE ACTIVATION OF AURORA B KINASE BY *CAENORHABDITIS ELEGANS* TOUSLED-LIKE KINASE AND THE IDENTIFICATION OF CYCLIN B3 AS A PHOSPHO-SPECIFIC TLK-1 INTERACTOR

by

Gary Michael Deyter, B.A.

APPROVED:

_____
Jill Schumacher, Ph.D., Supervisory Professor

_____
Sharon Dent, Ph.D

_____
Gregory May, Ph.D.

_____
Mong-Hong Lee, Ph.D.

_____
Jeffrey Frost, Ph.D.

APPROVED:

_____

George Stancel, Ph.D., Dean, The University of Texas Health Sciences Center at Houston Graduate School of Biomedical Sciences

VALIDATION OF THE ACTIVATION OF AURORA B KINASE BY *CAENORHABDITIS ELEGANS* TOUSLED-LIKE KINASE AND THE IDENTIFICATION OF CYCLIN B3 AS A PHOSPHO-SPECIFIC TLK-1 INTERACTOR

A

DISSERTATION

Presented to the Faculty of
The University of Texas Health Science Center at Houston
and
The University of Texas
M. D. Anderson Cancer Center
Graduate School of Biomedical Sciences
in Partial Fulfillment

of the Requirements

for the Degree of

DOCTOR OF PHILOSOPHY

by
Gary Michael Deyter, B.A.
Houston, TX
May 2010

VALIDATION OF THE ACTIVATION OF AURORA B KINASE BY *CAENORHABDITIS ELEGANS* TOUSLED-LIKE KINASE AND THE IDENTIFICATION OF CYCLIN B3 AS A PHOSPHO-SPECIFIC TLK-1 INTERACTOR

A

DISSERTATION

Presented to the Faculty of
The University of Texas Health Science Center at Houston
and
The University of Texas
M. D. Anderson Cancer Center
Graduate School of Biomedical Sciences
in Partial Fulfillment

of the Requirements

for the Degree of

DOCTOR OF PHILOSOPHY

by
Gary Michael Deyter, B.A.
Houston, TX
May 2010

ACKNOWLEDGEMENTS

There are many people that have contributed to my success in earning a doctoral degree. I am thankful for the presence of my grandmother and grandfather (Frieda Bertha Deyter-Polz and Wilton Edward Peter Polz) in my childhood and for helping my family through difficult financial times. Above everyone else, I am grateful for Christopher Narcisco and the love, support, and guidance he has shown me. We have grown together, and I would not be where I am today without him. I appreciate the time we have spent with his father Dominick Narcisco and step-mom Cissy. Being with them gave me so much happiness and we shared many great experiences. My basset hounds Bailey and Daisy (my girls!) brought me peace and love when science or life did not unfold as I had hoped. I often stared into their eyes and felt that we understood each other at a level deeper than words. How could we have not shared a word between us, yet understand each other so well? I think the answer is something called love.

I am especially indebted to the great women in science that have taught and guided me through my career. All of the work presented in this dissertation would not have been possible without the guidance of Jill Schumacher. So many great ideas and experiments- I have learned so much and I am so thankful. I am grateful for Sharon Dent and all of the support she has given me during my graduate studies. Lastly, I would not have enrolled in graduate school without the guidance I received from Bonnie Firestein. I learned so much from her during the few years I was in her lab and she provided the foundation for my growth as a scientist.

Blanche: “Oh, Rose’s friend is Lebanese.”
Dorothy: “No, Blanche, LESBIAN.”
Blanche: “Lesbian….*lesbian*….LESBIAN???!!!”
~ Conversation between Dorothy Zbornak and Blanche Devereau, The Golden Girls.

“I was just layin' down some rhymes, with the G-folk, you know, kickin' it on the west siy-eede.”
~ Eric Cartman, South Park.

“You mean, she cocooned herself up there? How dreadful!”
“Oh, a hot dog. I haven’t had one of those in years!”
“Oh, Dominick, you’re making eggs on the grill (since there was no electricity due to the power outage)…I’ll have mine over *EASY*.”
~Jillian, Donny & Cissy’s snobby neighbor from South Africa, Hurricane Ike September 2008.

“You know the worst thing anyone has ever said to me – my friend, a transsexual, called ME BUTCH! Can you believe that?”
~Identity withheld ☺!

To all of the characters that have made me laugh…

LOST! ~ Cold Play

Fix you ~ Cold Play

I Didn't Know My Own Strength ~ Whitney Houston

Hero ~ Mariah Carey

To all of the artists that have touched my soul…

VALIDATION OF THE ACTIVATION OF AURORA B KINASE BY *CAENORHABDITIS ELEGANS* TOUSLED-LIKE KINASE AND THE IDENTIFICATION OF CYCLIN B3 AS A PHOSPHO-SPECIFIC TLK-1 INTERACTOR

Publication No._____

Gary M. Deyter, Ph.D.

Supervisory Professor: Jill M. Schumacher, Ph.D.

A hallmark of tumorigenesis and certain birth defect syndromes is the loss of ploidy that can result from incorrect chromosome segregation. Chromosomes that are not partitioned properly during mitosis are often fragmented, changing the genetic makeup of daughter cells. Inheriting extrachromosomal fragments that contain cell survival genes or losing chromosomal loci that encode tumor suppressors can promote tumor development. Thus, it is essential to elucidate molecular mechanisms required for correct chromosome segregation. Chromosomes are connected to mitotic spindle microtubules by way of a proteinacous, chromosome-bound organelle called the kinetochore. Two decades of research have confirmed that the conserved Aurora B/AIR-2 kinase is required for multiple mitotic events including the proper attachment of microtubules to kinetochores, activation of a checkpoint that monitors kinetochore-microtubule attachment, and separation of daughter cells during cytokinesis. Our previous work identified the *C. elegans* Tousled-like kinase (TLK-1) as an interactor and substrate activator of AIR-2. However, the role of TLK-1 kinase activity in TLK-1-promoted AIR-2 activation remained enigmatic. The research presented herein reveals that the Aurora B-activating role of TLK-1 is independent of TLK-1 kinase activity *in vivo* and suggests that this mechanistic function is conserved. Moreover, we

hypothesized that phosphorylation influences TLK-1 protein-protein interactions. Towards this goal, the execution of a tethered-catalysis yeast two-hybrid screen to discover proteins that bind TLK-1 in a phosphorylation-specific manner was performed. This screen identified cyclin B3 (CYB-3) as a phospho-TLK-1 interactor. The mitotic defects caused by the loss of CYB-3 are profound and suggest that CYB-3 has crucial roles in promoting kinetochore activity necessary for a critical point during mitosis: the irreversible metaphase-to-anaphase transition. Altogether, these results suggest that CYB-3 has an important role in kinetochore function and predict that CYB-3 influences TLK-1-mediated AIR-2 activation.

TABLE OF CONTENTS

LIST OF FIGURES

LIST OF TABLES

CHAPTER ONE: AN INTRODUCTION

The Fundamental Mechanism of Chromosome Segregation is Conserved

The ultimate goal of the cell cycle is to stably transmit the genetic material, DNA, which is compacted into chromosomes. Chromosome segregation occurs during mitosis, and dividing somatic cells of all eukaryotes utilize similar mechanisms for a common purpose: to maintain ploidy. In humans, aneuploidy can result in developmental defects such as Down's syndrome; it can also promote tumorigenesis which often leads to death (1, 2). Cancer biologists initially believed that karyotype changes in tumor cells were simply a consequence of failed molecular events that had occurred early during cancer development (e.g.- loss of tumor suppressor genes resulting in inappropriate cell cycle progression and mitotic defects) (3). However, it is now clear that aneuploidy can be a cause rather than a consequence of cancer (2, 3). Thus, **it is crucial to study the function of mitotic proteins to gain better molecular understanding of mechanisms involved in chromosome segregation**.

DNA is packaged into chromatin by being wrapped around structures called nucleosomes that are formed of histone proteins (4). The importance of histone function is highlighted by the observation that histone proteins and post-translational modifications are extremely conserved (4). In all organisms, most regions of chromosomes play passive roles during mitosis and are not directly involved in segregation. Instead, a specific section of the chromosome called the centromere is the "active" site where kinetochore proteins involved in attaching chromosomes to the mitotic spindle assemble (5, 6). Although there are species-specific variations in kinetochore protein composition, the structure and function of kinetochores are conserved. On the other hand, the absolute requirement of centromeres for chromosome segregation is confounded by the absence of conserved DNA sequences that specify centromere location on chromosomes (7). However, the incorporation of CENP-A, a histone H3 variant, exclusively at centromeres in all eukaryotes suggests that centromere identity is maintained epigenetically (7).

Chromosomes are duplicated during S-phase, a stage that precedes mitosis. Therefore, it is imperative that replicated chromosomes (termed sister chromatids) remain paired to one another so that chromosome segregation is equational. Unpaired,

duplicated chromosomes undergo random, uncontrolled segregation and are likely to result in aneuploidy (8). To avoid this, protein complexes involved in DNA replication interact with complexes that function to generate cohesion between sister chromatids (8). Thus, DNA replication, packaging into chromatin, and cohesion are coupled processes that are critical for subsequent chromosome segregation.

Early mitotic chromosomes are extended and relatively unstructured. This lax morphology of chromosomes would result in chromosome entanglement, catenation, and missegregation (9). Therefore, chromosome condensation is an important facilitator of chromosome segregation. Histone-histone as well as DNA-protein interactions condense chromatin into higher ordered structures that are competent for segregation (10). Chromosome condensation also contributes to the proper orientation of kinetochores, proteinacous organelles that interact with chromosomes and spindle microtubules (9).

Cells use microtubules to create connections between chromosomes and distally localized structures called centrosomes. Microtubules are formed of tubulin dimers, and tubulin protein sequences display little divergence between species (11). Chromosome segregation requires microtubules and most spindles are formed by centrosome-nucleated microtubules (11). However, germ cells and other acentriolar cells rely on chromatin-induced nucleation of microtubules to drive chromosome segregation (12). Microtubules are dynamic structures that are subject to many modes of regulation including post-translational modification of tubulin and binding of microtubule-associated proteins (MAPs) that affect microtubule-based processes (11).

Disrupting the structure/function of many of the mitotic features highlighted above can devastate human health. Molecular techniques including comparative genomic hybridization and fluorescence *in situ* hybridization have revealed that cancer cells are highly aneuploid (13). The "aneuploidy theory" of cancer origin was proposed over a century ago by Theodor Boveri, a german cell biologist studying chromosome segregation in round worms (14). Boveri was the first scientist to suggest that genes were located on chromosomes and discovered that centrosomes (which he named) were critical mitotic structures (14). He suggested that gain of growth-promoting genes or loss of growth-inhibitors in cancer cells due to altered chromosome number could contribute to tumorigenesis. Indeed, the chromosome instability that results from errors in

chromosome segregation is now appreciated as a central factor in cancer development (3).

All together, this brief summary highlights key conserved cellular processes involved in chromosome segregation. The next sections will explore the composition and regulation of mitotic structures in greater depth, with a focus on the interplay between proteins that are required for successful chromosome segregation. The focus will be on conserved kinetochore complexes with an emphasis on results generated from studies with *Caenorhabditis elegans*. The finale of the introduction will describe *C. elegans* in detail and will explain the logic behind utilizing this nematode to study mitosis.

Chromosome condensation

Chromosome segregation would not be possible with an extended chromatin structure due to the size restriction of cells and the propensity for DNA catenation and entanglement (15). Molecular mechanisms compact interphase chromatin 10,000- to 20,000-fold to generate mitotic chromosomes that can be segregated appropriately by spindle microtubules (16). Additionally, the double helical structure of DNA intertwines the nitrogen nucleotide bases and increases the likelihood of DNA catenation (17). The close proximity of chromosomes even in the most compacted structure may lead to chromosome entanglement. Thus, mechanisms must exist to ensure that chromosomes remain as individual entities throughout the cell cycle.

Upon entry into mitosis, histone H3 becomes phosphorylated at S10 (P-H3S10) by Aurora B kinase concomitant with chromosome condensation (18). P-H3S10 is not unique to mitosis and also regulates transcription during interphase (18). Although P-H3S10 is used as a marker for cells in mitosis, accumulating evidence suggests that this modification is neither necessary nor sufficient for complete chromosome condensation. Budding yeast H3S10A phospho-mutants do not have reduced viability suggesting that P-H3S10 is not required for condensation in this organism (18). In *C. elegans*, chromosomes are condensed similar to wild-type levels when AIR-2/Aurora B is depleted (19). In contrast, the best example of a functional role for P-H3S10 comes from studies of chromosome condensation in cultured human cells. A phospho/methyl switch has been identified whereby the P-H3S10 modification inhibits methylation at H3K9

(Me-H3K9) (20, 21). HP1 (**h**eterochromatin **p**rotein 1) is a chromo-domain containing protein that binds Me-H3K9 (22). HP1 molecules self-associate and propagate the formation of silent chromatin by recruiting transcriptional inhibitors to DNA (22). P-H3S10 inhibition of Me-H3K9 promotes chromosome condensation by effectively removing HP1 and associated proteins from chromosomes to promote condensation factor binding/function (20, 21). It is interesting to note that *S. cerevisiae* and *C. elegans* centromeres are not flanked by heterochromatin-bound HP1 and therefore may not require the phospho/methyl circuitry.

Conserved protein complexes called condensins are crucial for chromosome condensation (10). Most organisms have two condensin complexes (I and II) that facilitate condensation by trapping DNA supercoils. The condensin complex is a tetramer composed of a heterodimer of SMC2/4 (**s**tructural **m**aintenance of **c**hromosomes) and three non-SMC proteins (CAP-D2, CAP-G, and CAP-H) (10). The SMC subunits dimerize via a C-terminal coiled-coil region to form a V-shaped structure with the N-terminal ATPase domains associating with the non-SMC trimer (23). ATP hydrolysis provides the energy required for the condensin complex to change conformation and entrap DNA (23). Condensin complexes can also oligomerize and thus contribute to higher order chromatin structure via intermolecular protein-protein interactions (24). Interestingly, Cdk1-mediated phosphorylation of condensin activates the supercoiling activity of the vertebrate condensin complex in vitro (25) and Aurora B targets condensin to chromosomes (26, 27). Thus, phosphorylation is a key modification that affects condensin function.

Topoisomerase II (Topo II) is an ATPase that changes the topography of DNA into different isomers (28). Topoisomerases cause transient breaks in the DNA phosphate backbone resulting in the unwinding of DNA strands and untangling of chromosomes (28). Topo II function is required throughout mitosis for proper chromosome structure and segregation. During early chromosome condensation, Topo II activity is essential for chromosome individualization by decatenating intertwined chromosomes (15). Chromosome individualization is important since in its absence chromosome condensation would led to entangled chromosomes that are broken by anaphase segregation (15). Topo II is also involved in sister chromatid resolution, a

process during prophase in which the geometry of sister chromatid kinetochores becomes back-to-back (28). A centromere-specific function for Topo II has been suggested by the enrichment of the enzyme at centromeres as well as kinetochore defects that result from chemical inhibition of Topo II (29). Similar to condensin function, phosphorylation by a variety of kinases including Cdk1, Aurora B, Casein Kinase II, and protein kinase C influence Topo II activity (30, 31).

Although the condensin complex and Topo II are involved in events concomitant with condensation, both proteins are not sufficient for complete chromosome condensation. For instance, the depletion of condensin subunits in many organisms does not cause a complete loss of chromosome condensation (24). In *C. elegans*, the depletion of the SMC-4 or HCP-6 condensin subunits results in severely defective chromosome condensation and the complete absence of distinct linear chromosomes (19). However, chromosomes show some degree of condensation at nuclear envelope breakdown suggesting the presence of condensation pathways independent of condensins (19). Lines of investigation in other organisms also suggest multiple pathways of chromosome condensation independent of condensin and Topo II (32). Although their precise roles in chromosome condensation remain unclear, the functions of the condensin complex and Topo II are required for normal chromosome segregation. Topo II function is absolutely required for normal anaphase chromosome segregation (33). Interestingly, **the primary function of condensins may be to stabilize or shape compacted metaphase chromosomes** (34).

Kinetochore assembly and function

The kinetochore is an organelle composed of protein complexes that mediate interactions between centromeres and spindle microtubules (11). Transmission electron microscopy (EM) has revealed the trilaminar structure of the human kinetochore that is composed of a so-called inner plate (made of proteins involved in centromere binding), outer plate proteins that bind to microtubules, with a space between the plates termed the inner space (35, 36). However, the inner space has not been identified upon treatment of cells with more advanced EM techniques, suggesting that the inner plate may be an artifact of fixation (37).

A fibrous corona extends from the outer plate in the absence of microtubule binding (37). The function of this network is relatively unknown and unstudied. *C. elegans* chromosomes are holocentric and build kinetochores along the entire length of condensed mitotic chromosomes (38). In contrast, most species have monocentric chromosomes that build kinetochores at a specific region on the chromosome called the primary constriction (7). Despite this macroscopic difference, *C. elegans* holocentric chromosomes display a similar trilaminar geometry when analyzed by EM (39), suggesting that *C. elegans* kinetochores are extended versions of conventional kinetochores. It is important to note that electron micrographs reveal the architecture of fixed, static kinetochores, a representation that undermines the dynamic biology of kinetochore structure/function.

Macromolecular complexes can be assembled in a variety of ways. For instance, ribosomes are composed primarily of a dimer of a 60S and a 40S subunit. Other biological processes including transcription rely on the coordinated activities of multiple protein complexes (e.g.- histone modifying enzymes, nucleosome remodelers, basal transcription factors, enhancer-binding entities, etc.). Research aimed at deducing kinetochore protein composition in model organisms including *C. elegans* has revealed that the kinetochore is assembled in a hierarchal manner from distinct complexes (38). The proper function of the kinetochore depends on the interplay between the proteins described below.

Centromeres contain the histone H3 variant CENP-A

Chromosome segregation demands that only one kinetochore assembles on each sister chromatid at a region of the chromosome called the centromere. Dicentric chromosomes that build two microtubule-binding kinetochores are fragmented during anaphase segregation and contribute to chromosomal instability (40). Thus, centromere location on chromosomes must be specified and maintained throughout cell division. In most organisms, centromeric DNA is composed of highly repetitive 171-base pair α-satellite sequences embedded in peri-centromeric heterochromatin (7). No particular DNA sequence elements define the centromere in higher eukaryotes. However, centromeres in *S. cerevisiae* are unique and have a defined 125-bp CEN sequence

containing three conserved elements (CDEI, CDEII, and CDEIII) with no surrounding heterochromatin (41, 42). CDE1 and CDEII DNA interact with a single nucleosome containing the histone H3 variant Cse4/CENP-A (43, 44).

CENP-A/cenH3 is incorporated into nucleosomes specifically at centromeres and is the epigenetic determinant of centromere identity. HCP-3 (**h**olo**c**entric **p**rotein) is the *C. elegans* CENP-A homolog and it is present in nucleosomal arrays throughout the entire length of each chromosome (45). Higher-order chromatin compaction during mitosis tethers these arrays (or HCP-3 patches) together to form chromosome-long centromeres (38). Thus, mitotic chromosomes contain coalesced HCP-3-containing nucleosomes that act as a single element consistent with the repeat subunit model of kinetochore architecture (Figure 1) (46). HCP-3 is required for kinetochore assembly and embryos treated with *hcp-3(RNAi)* can not build kinetochores nor undergo chromosome segregation (47). Lastly, centromeric chromatin is an integral part of the kinetochore and in most organisms CENP-A is at the forefront of kinetochore assembly (7). Many investigators have defined the kinetochore as a chromosomal domain or a DNA-protein complex (48). Therefore, it is a matter of semantics whether the kinetochore is defined with or without a chromatin component. The bottom line is: **no centromere formation = no kinetochore structure or function**.

There are two species-specific molecules that participate in localizing kinetochores to centromeres via binding to specific DNA sequences. Budding yeast CDEIII is recognized by Ndc10, which is part of the CBF3 complex (which also includes Ctf13, Cep3, and Skp1) (49). The CBF3 complex is essential for the localization of all other kinetochore components and *cbf3* mutants do not form functional kinetochore-microtubule attachments *in vivo* (49). Thus, two DNA sequence-dependent pathways contribute to kinetochore assembly in budding yeast: (1) CBF3 is the most upstream kinetochore factor and is required for the centromere localization of Cse4/CENP-A and (2) CENP-A incorporation into the single centromeric nucleosome at CEN DNA (44). In vertebrates, CENP-B localizes to centromeres in a sequence-dependent manner. CENP-B binds to CENP-B boxes that are present at regular intervals in α-satellite DNA (50).

Figure 1. The repeat subunit model of kinetochore assembly

Kinetochore assembly and function during mitosis requires a specialized chromatin structure at centromeres and incorporation of the CenH3 histone variant. CenH3 exists in repetitive nucleosomal patches (green) interspersed by nucleosomes containing canonical H3 (blue) (46). During interphase, CenH3 nucleosomes in monocentric species are limited to a confined chromosomal region while CenH3 patches exist throughout holocentric chromosomes. Mitotic chromosome condensation tethers CenH3 chromatin domains together to form the centromere foundation for kinetochore assembly.

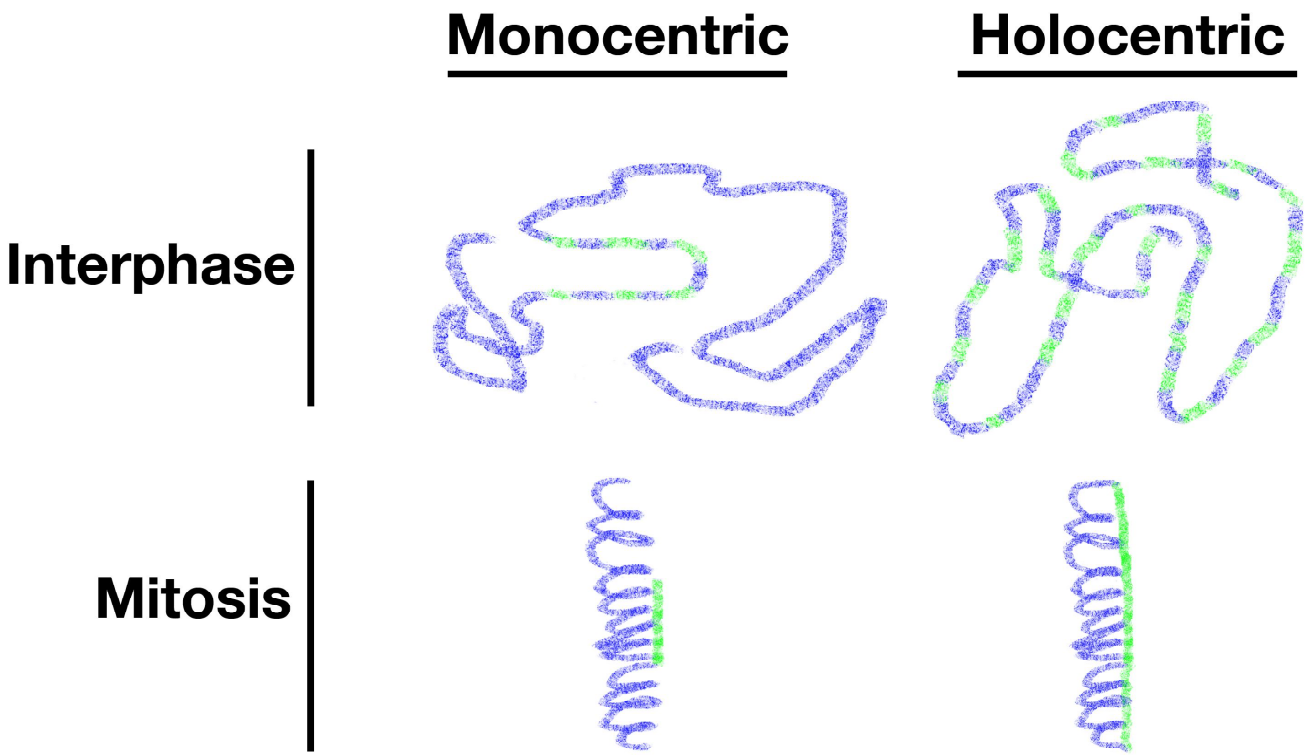
Monocentric
Holocentric
Interphase
Mitosis

Mammalian artificial chromosomes (MAC) have been an important biological context to study centromere formation on chromosomes. MACs do not have centromeric DNA sequences yet they can incorporate cenH3, assemble kinetochores, and are segregated by the mitotic spindle (51). Investigations of MAC segregation in the absence of CENP-B binding revealed that CENP-B and α-satellite DNA is essential for the production of CENP-A chromatin and kinetochore assembly (51). Interestingly, CENP-B that is targeted to non-centromeric chromosomal domains promotes heterochromatin production but not de novo centromere formation (52). This suggests that CENP-B stimulates centromere formation but also prevents the formation of excess centromeres on chromosomes. However, given that CENP-B-null mice do not display kinetochore defects (53), the epigenetic mechanism of CENP-A deposition appears to be most crucial for centromere identity.

Mechanisms to selectively incorporate CENP-A at centromeric nucleosomes are beginning to be identified. The Mis16-Mis18 complex in *S. pombe* was one of the first molecular players involved in CENP-A deposition to be identified (54). Centromeres in *mis16* and *mis18* mutants have increased levels of histone H3 and H4 acetylation (54). With this insight, post-translational modification of core histones likely plays a crucial role in promoting the centromeric chromatin structure required for CENP-A deposition. RbAp46 and RbAp48 are human orthologs of Mis16 and are part of the NuRD histone deacetylase complex (55). The human complex consists of RbAp46/48 associated with a conserved Mis18 complex (55). In *C. elegans*, KNL-2 shares sequence homology with Mis18BP1 and is essential for CENP-A centromere targeting (56). Lastly, budding and fission yeast Scm3 were found to be CenH3 assembly factors (57-59). *Sc*Scm3 binds Ndc10, a critical component of the CBF3 complex that specifies centromere function (58). *Sp*Scm3 co-purifies with cenH3 from yeast cell extract and aides in cenH3 replacement of canonical H3 at centromeres in cooperation with Mis16 and Mis18 (59). HJURP, a protein involved in DNA damage repair, is a human homolog of Scm3 and is also required for efficient CENP-A centromere deposition (60).

Proteins that link centromere-proximal and microtubule-interacting kinetochore complexes

Biochemical purification of CENP-A from human cells has identified a network of proteins that are constitutively present at centromeres even during interphase. These proteins are called CCAN (constitutive centromere-associated network) and include CENP-C and 13 interacting proteins (CENP-H, CENP-I, and CENP-K-U) (61). CENP-A acts upstream of CCAN, and all CCAN members require CENP-A for centromere localization. However, CCAN may reinforce or stabilize CENP-A-containing nucleosomes once they are established (61).

The molecular dissection of the *C. elegans* kinetochore has been aided by biochemical and cytological experiments with *C. elegans* embryos. The screening of monoclonal antibodies isolated from hybridoma cell lines identified anti-sera that co-localized with the bona fide kinetochore protein HCP-3/CENP-A (62). This protein, HCP-1, harbors coiled-coil domains and shares partial sequence homology with human CENP-F. CENP-F is a highly conserved protein that influences multiple cell cycle functions including microtubule dynamics and transcriptional regulation (63). The localization of HCP-1 partially co-localized with HCP-3-containing centromeric chromatin and was the second kinetochore protein identified in *C. elegans* (62). Searches of the *C. elegans* genome with HCP-1 revealed homology with ~50% sequence similarity to HCP-1 that was subsequently named HCP-2 (62). The combined depletion of HCP-1/2 via RNAi resulted in chromosome segregation defects including anaphase bridging. Further studies revealed that HCP-4 (*C. elegans* CENP-C) is required for kinetochore assembly downstream of HCP-3 but upstream of HCP-1 (64, 65). Although human CENP-C is part of CCAN, HCP-4 is not detected on interphase chromosomes (64). This species-specific difference in the temporal localization of CENP-C may correspond to differences in peri-centromeric chromatin structure. Monocentric centromeres are surrounded by constitutive heterochromatin that remains relatively condensed throughout the cell cycle. Holocentric centromeres are not embedded in heterochromatin and may require mitotic chromosome condensation as a prerequisite for HCP-4 kinetochore localization. Regardless, the results of these experiments revealed an important detail

regarding *C. elegans* kinetochores: conservation of an ordered assembly pathway with conserved kinetochore proteins.

RNAi-based genomic approaches have identified essential proteins required for chromosome segregation during *C. elegans* embryogenesis (66). Genomic screens are important since more directed approaches could miss important mitotic players that lack sequence similarity in other organisms. Function-based genomic approaches revealed that loss of KNL-1 results in a "kinetochore-null" phenotype similar to that caused by CENP-A/CENP-C depletion (67). Unlike HCP-3/CENP-A and HCP-4/CENP-C, KNL-1 is not required for the proper structure of centromeric chromatin. Instead, KNL-1 links centromere-proximal kinetochore proteins to outer kinetochore microtubule-binding complexes (67). KNL-1 co-immunoprecipitates with chromatin-proximal HCP-4 in addition to NDC-80 and HIM-10/Nuf2, two subunits of the conserved microtubule-binding Ndc80 complex (67). Moreover, many outer kinetochore proteins including NDC-80 and HIM-10 require KNL-1 for proper targeting (67). Interestingly, budding yeast Spc105 and human AF15q14 share limited homology to KNL-1 and are also required for chromosome segregation (68).

Tandem affinity purification techniques utilizing *C. elegans* embryo extracts have gleaned biochemical insight into KNL-1-interacting proteins (69). Mass spectrometry analysis of KNL-1 immunoprecipitates revealed the presence of several novel proteins including KNL-3, KBP-1 - KBP-5 (**K**NL **B**inding **P**rotein), and MIS-12, a *C. elegans* homolog of the Mis12 family (70). KNL-3 is similar to *Sc*Spc25, a kinetochore protein that interacts with the *Sc*Ndc80 complex. The chromosome segregation defects resulting from *knl-3(RNAi)* phenocopies *ndc-80(RNAi)*, suggesting a conservation of function between these two proteins (70). Importantly, the depletion of MIS-12, KBP-1, or KBP-2 from *C. elegans* embryos results in the delayed recruitment of outer kinetochore proteins and transient instability of kinetochore-microtubule attachments (70). Biochemical work with purified kinetochore complexes revealed two microtubule-binding sites in the *C. elegans* kinetochore, one in the NDC-80 complex and the other in KNL-1 (71). Altogether, this protein network was termed KMN (**K**NL-1, **M**IS-12, and **N**DC-80) (71).

Outer kinetochore proteins interact with microtubules and respond to their presence

The proteins of the kinetochore function as a singular molecular machine whose ultimate goal is to interact with microtubules to achieve bipolar spindle attachment. As discussed above, the Ndc80 and Knl1 complexes form the microtubule-binding interface at kinetochores. However, another class of bifunctional proteins can interact with microtubules independent of the kinetochore and can also bind kinetochore proteins. The Dam1 complex in yeast is a ten subunit microtubule-binding complex at kinetochores (72). The kinetochore localization of Dam1 requires Ndc80 and microtubules, and Dam1 interacts with microtubules *in vitro* (73). Interestingly, ultrastructural investigations of recombinant Dam1 complexes reconstituted *in vitro* revealed that Dam1 complexes can self-associate to form ring-like structures around microtubules (73). The Dam1 complex slides along microtubules and may couple microtubule plus-end depolymerization at anaphase to chromosome movement (74). However, *in vivo*, Dam1 complex-oligomerization occurs between one to four Dam1 complexes, a size that would preclude ring formation around microtubules (75). Although sequence-based searches failed to uncover Dam1 homologs in other organisms, recent evidence suggests that the Ska complex is a higher eukaryotic functional homolog (76). Similar to the Dam1 complex, the Ska1 complex interacts with microtubules, forms homo-oligomers, and couples chromosome movement to microtubule depolymerization (77). Moreover, Ska1 oligomers do not form rings and ring formation is not required for Ska1 complex function (77). Lastly, the Ska1 complex and the KMN network complement each other to generate stable kinetochore-microtubule attachments (76).

Although several microtubule motor proteins localize to kinetochores, two key motors required for multiple kinetochore functions are dynein and CENP-E. Dynein serves many microtubule-related functions including vesicle and organelle transport, centrosome separation and bipolar spindle formation, nuclear envelope breakdown by microtubule puncture, and spindle assembly checkpoint silencing (78). Dynein is a 1.5 Megadalton complex composed of approximately twelve subunits (79). The two dynein heavy chains dimerize and have ATPase activity, which is used for movement along microtubules toward their minus ends at the centrosomes (79). The carboxy-termini of

the heavy chains are responsible for microtubule binding whereas their amino-termini interact with various dynein light and intermediate chains (80). Cargo proteins including vesicles and organelles interact with the light and intermediate chains to facilitate intracellular movement (80). CENP-E is a plus-end directed kinesin that contributes to chromosome congression toward the mitotic spindle equator (81). CENP-E also influences the spindle assembly checkpoint (see below).

In conclusion, the kinetochore is a large multi-protein machine that must be temporally and spatially built and functionally modified to achieve equational chromosome segregation. Kinetochore proteins represent critical understudied candidates for mutation in cancer. In fact, four out of eight genes whose mutation contributes to chromosome instability in colon cancer cells encode kinetochore proteins (48). Moreover, the interdependency of kinetochore protein complexes for one another and the large molecular weight and multiple functions of the vertebrate organelle (detailed below) suggest many levels of regulation that could be lost due to mutation.

The Interplay Between Kinetochores and Microtubules

The spindle cytoskeleton is composed of α,β-tubulin dimers that assemble into microtubules when nucleated from distinct cellular structures (Figure 2) (11). Microtubules are energy-generating macromolecules: β-tubulin is a GTPase that releases the energy stored in GTP during microtubule plus-end growth and energy is also released when tubulin dimers are removed from shrinking microtubule plus-ends (11). A key requirement of kinetochores is that they must be able to couple the dynamic properties of microtubules to directed chromosome movement. After nuclear envelope breakdown, kinetochores make monorientated and lateral attachments to microtubules resulting in chromosome movement to centrosomes. This movement is mainly due to the activity of minus-end-directed cytoplasmic dynein (82). Lateral attachments to microtubules would not produce sufficient force for proper sister chromatid segregation nor permit the generation of tension between sister chromatids that is required for anaphase entry. Thus, mechanisms exist to antagonize dynein function and the poleward movement of chromosomes.

Figure 2. Microtubule nucleation at chromosomes and centrosomes

A) Chromosome-induced microtubule nucleation contributes to mitotic spindle assembly. An activity gradient of RanGTP around mitotic chromosomes produced predominately at kinetochores influences microtubule nucleation, most likely by regulating the function of microtubule-stabilizing proteins. RanGTP activating proteins (RanGAPs) negatively regulate RanGTP kinetochore localization to inhibit chromosome-induced microtubule nucleation. B) Centrosome-induced microtubule nucleation is the major mechanism of mitotic spindle assembly and requires the function of multiple mitotic kinases and microtubule stabilizing/nucleating factors.

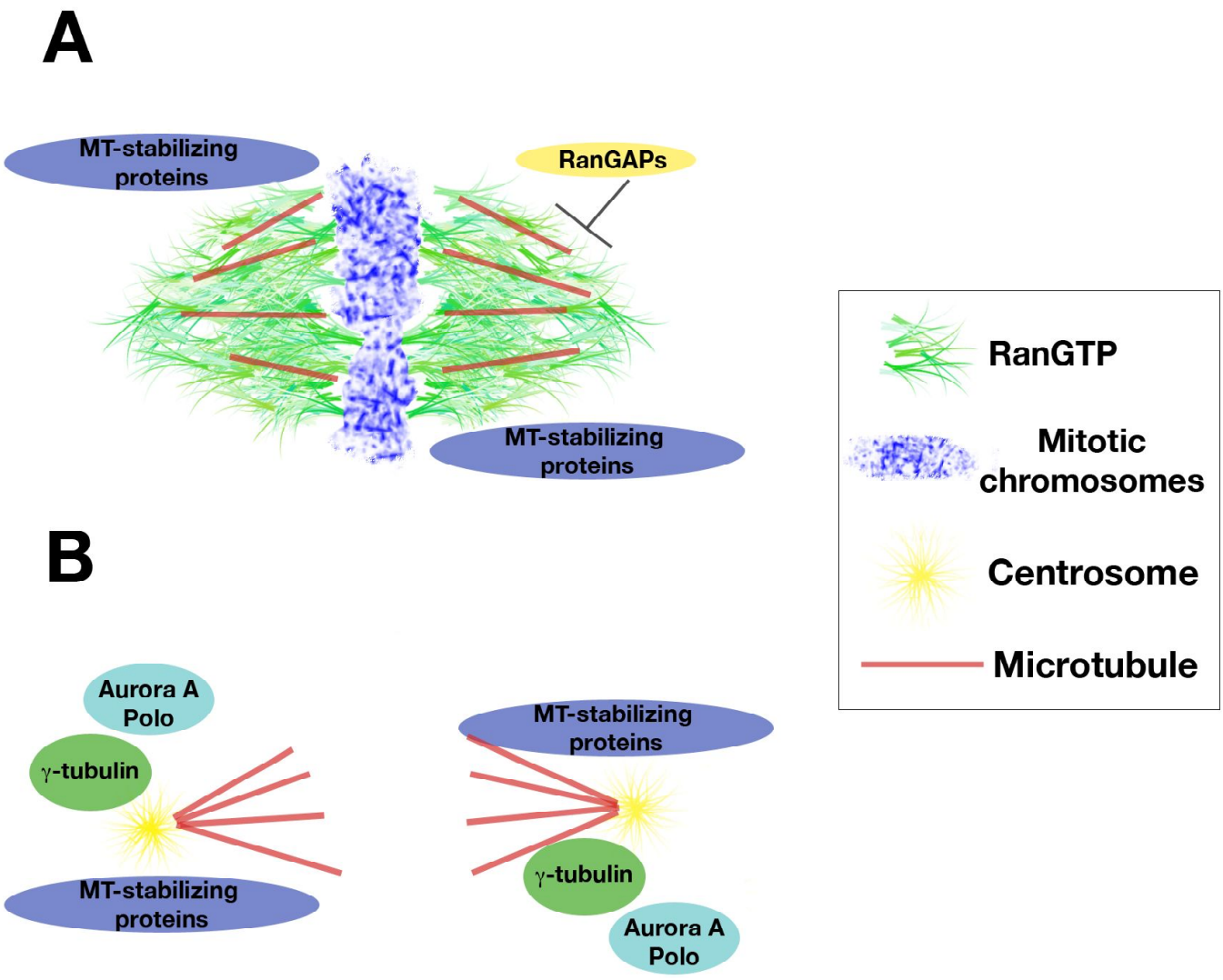
A
MT-stabilizing proteins
RanGAPs
MT-stabilizing proteins
B
Aurora A Polo
γ-tubulin
MT-stabilizing proteins
MT-stabilizing proteins
γ-tubulin
Aurora A Polo
RanGTP
Mitotic chromosomes
Centrosome
Microtubule

Elaborate experiments performed three decades ago revealed that the spindle itself produces a "polar ejection force" that antagonizes the poleward pull on kinetochores by bound microtubules (Figure 3) (83). These experiments were aimed at determining if both sister kinetochores are required for prometaphase chromosome oscillations of a monoriented chromosome. They were testing the accepted notion that microtubule attachment from the opposite spindle pole to the unattached kinetochore of a monoriented sister chromatid pair was required to move the chromosomes to the spindle equator (84). In these assays, laser microsurgery was performed on kinetochores in newt lung cells to ablate one metaphase sister kinetochore while keeping the other microtubule-bound kinetochore intact (83). The irradiated chromosome moved toward the attached spindle pole as expected from laser-induced monorientation. If forces generated by microtubule attachment to the normally non-irradiated kinetochore were needed for subsequent congression to the spindle equator, the experimentally damaged chromosomes should not undergo congression. However, robust chromosome oscillations similar to wild-type prometaphase kinetics were observed, suggesting that spindle poles generate a force that pushes chromosomes away from the pole (83). This "polar ejection force" was also witnessed on chromosome arms that lack kinetochores. This outward force results from astral microtubules acting along the chromosome to eject it from the polar region. Finally, the authors suggest that the ejection force must decrease during anaphase and predict that astral microtubule density changes may accompany anaphase onset (83). Although the complete nature of these forces remain enigmatic, research in many organisms including *C. elegans* has revealed that plus-end microtubule motor protein chromokinesins (*Ce*KLP-19) associates with non-kinetochore chromosomal regions to generate a polar ejection force that is required for accurate chromosome segregation (85, 86). CENP-E, a plus-end directed kinetochore kinesin, also participates in moving chromosomes away from spindle poles to the cell equator (81). Thus, microtubules and microtubule-associated proteins produce forces driving sister chromatids away from spindle poles.

Figure 3. Polar ejection forces influence chromosome congression

The results of laser ablation studies on kinetochore function and chromosome motility revealed that the spindle poles/centrosomes generate a pushing force against chromosome arms (83). Prometaphase/metaphase kinetochores (purple figures) (A, one sister chromatid pair is depicted) were subjected to laser microsurgery to create monooriented chromosomes containing one functional, unperturbed kinetochore. As expected, sister chromatids rapidly moved toward the centrosome of the attached sister kinetochore due to the loss of kinetochore-microtubule attachment (green lines) to the damaged kinetochore (B). If the laser-ablated kinetochore was required for subsequent sister chromatid oscillations on the mitotic spindle (black lines), the chromatids were expected to remain near the centrosomes (Outcome 1; size of arrow indicates magnitude of force toward the centrosome). However, the chromosome oscillations witnessed in these experiments revealed that chromosome arms are subject to kinetochore-independent spindle forces (mainly from astral microtubules) that eject chromosomes from the centrosome (Outcome 2).

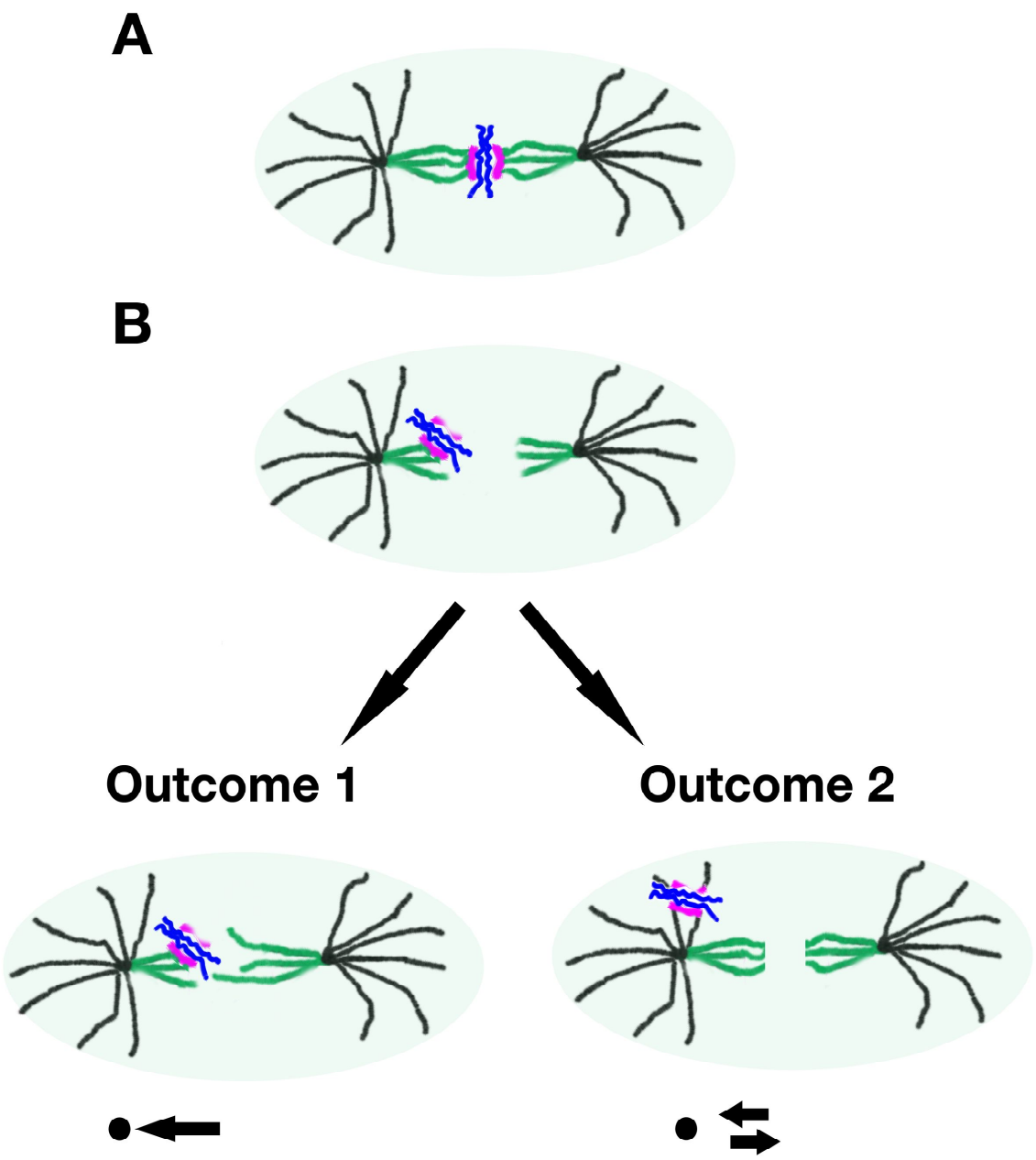
A
B
Outcome 1
Outcome 2

The initial attachment of chromosomes to spindle microtubules is by chance encounters. Microtubules emanating from centrosomes randomly search the cytoplasm and eventually capture a sister chromatid pair via kinetochore interaction (87). This "search and rescue" mode of kinetochore-microtubule attachment is error-prone. The proximity of a sister chromatid pair to one centrosome during early prometaphase increases the likelihood that microtubules emanating from the centrosome will interact with both sister kinetochores instead of only one. The syntelicity that results from this incorrect attachment would be devastating to chromosome stability should it remain uncorrected since segregation would not be equivocal (88). To correct aberrant attachments, the spindle assembly checkpoint (SAC) is at work to lengthen the duration of prometaphase and inhibit anaphase onset to offer time for correction mechanisms and chromosome biorientation (89). Proteins involved in correcting improper kinetochore-microtubule interactions function in parallel with the SAC to produce amphitelic chromosome-spindle attachment (90). Lastly, in a 1997 Science review of how cells obtain the correct number of chromosomes, Dr Nicklas wrote: "When cells divide, the chromosomes must be delivered flawlessly to the daughter cells…chance events are the starting point for chromosome delivery, which makes the process prone to error…tension (between sister chromatids) stabilizes the proper chromosome configuration, controls a cell cycle checkpoint, and changes chromosome chemistry" (87). In my opinion, a more accurate and succinct account of global biochemical in mitotic chromosomes has never been written. The next sections will explore in detail the tension that Dr. Nicklas was referring to and why tension between bioriented sister chromatids is vital for maintaining chromosome stability.

Kinases are Required for the Fidelity of Multiple Mitotic Events

Kinases influence all aspects of cell biology, including the cellular recognition and cellular response to mitogens (mainly tyrosine receptor kinases), transcription of developmental genes (hormone receptor kinases), and entry and progress through the cell cycle (soluble serine/threonine kinases) (91). Kinases and cancer go hand-in-hand, and much research has been devoted toward developing drug inhibitors of the aforementioned classes of kinases for therapeutic benefit (92). Drugs that target mitogen-activated

tyrosine kinases (including those inhibiting Abl and EGF (**e**pidermal **g**rowth **f**actor **r**eceptor)) have proven successful at ameliorating certain cancer types (93). However, it is now appreciated that mitotic kinases can play a direct role in cancer by promoting mitotic entry at inappropriate times and also by influencing chromosome stability. For example, the analysis of gene expression profiles in a variety of tumors suggests that mitotic kinases are at the top of the list of genes that, with altered expression/function, contribute to chromosome instability (94). Drugs targeting mitotic kinases have the potential to inhibit mitotic entry and stop tumor cell division. Also, the inherit genetic instability of cancer cells might worsen and become detrimental to tumor growth upon pharmacological antagonization of kinases involved in promoting chromosome stability (95).

The functions of cyclin-dependent kinases (cdks) are most crucial for cell cycle progression. Cdks are heterodimeric proteins consisting of an enzyme and a regulatory subunit (cyclin) (96). The binding of cyclins to Cdks partially activates Cdk kinase activity, yet full activation requires post-translational modifications at conserved Cdk residues (96). The crystal structure of monomeric Cdk2 was the first to be resolved and revealed that unphosphorylated Cdk2 is inactive due to an incorrectly orientated ATP molecule and a T-loop configuration that occludes substrates from the active site (97). Cyclin A binding to Cdk2 reorientates the ATP for phospho-transfer and moves the T-loop away from the substrate docking site, and an activating phosphorylation stabilizes this conformation (98). Importantly, cyclins are expressed in a temporally controlled manner throughout the cell cycle. Since all Cdks have a similar consensus sequence for phosphorylating target proteins, the different Cdk tertiary structure resulting from cyclin binding is unique for each cyclin and is essential for substrate specificity (99). Although yeast express only one Cdk (cdc28 in *S. cerevisiae* and cdc2 in *S. pombe*), higher eukaryotes have between two and twelve loci encoding Cdks (100) .

Cdk mutations rarely occur in tumor cells. Instead, downregulation of Cdk inhibitors including the INK4 and Cip/Kip families and upregulation of cyclins are frequently detected in most human cancers (100). Interestingly, not all Cdks are involved in cell cycle progression but rather influence diverse processes including transcription via RNA polymerase II phosphorylation (Cdk7 and Cdk8), and are components of the TFIIH

transcription factor complex and Cdk activating kinase complex (Cdk7) (101). Cdk1 is the mitotic kinase that, when bound to either A- or B-type cyclins, promotes centrosome duplication, spindle assembly, chromosome condensation, nuclear envelope breakdown, spindle assembly checkpoint function, and anaphase onset by APC phosphorylation (100). Key substrates of Cdk1 include Histone H1 (102) and HMG to facilitate chromosome condensation, lamin phosphorylation leading to nuclear envelope breakdown (103), and positive-feedback regulation by cdc25 phosphorylation (104).

The Aurora kinases are a family of conserved serine/threonine proteins involved in nearly all aspects of chromosome segregation (105). The founding member of the Aurora kinases was first identified from genetic screens performed with *S. cerevisiae* aimed at identifying gene products required to maintain ploidy (106). This screen identified two alleles of a gene that resulted in chromosome missegregation and increased ploidy at restrictive temperatures (106). This gene was named *ipl1* (**i**ncrease in **pl**oidy) and its product encodes the only Aurora homolog in budding yeast, which is most functionally similar to Aurora B. The vertebrate Aurora family consists of three members: Aurora A, B, and C (105). Aurora A localizes to centrosomes and peri-centrosomal microtubules and is involved in centrosome maturation, separation, and nucleation of microtubules that make up the mitotic spindle (105). Aurora B associates with chromosomes during mitotic stages up to anaphase, at which point it dissociates from chromosomes and relocalizes to the spindle midzone (105). As discussed below, Aurora B has many pivotal functions in mitotic chromosome and microtubule dynamics. Thus, it is not surprising that small molecule inhibitors of Aurora kinases are currently under clinical investigation (107), given the crucial role these kinases play in promoting spindle formation (Aurora A) and the association of microtubules with chromosomes (Aurora B). Interestingly, an Aurora A mutant that is experimentally mislocalized to chromosomes can efficiently substitute for Aurora B (108). This result confirms the importance of targeting Aurora kinases to distinct subcellular destinations for substrate specificity and undermines the difficulty in producing drugs that inhibit a specific Aurora kinase. Lastly, Aurora C is expressed in germ cells and influences meiotic chromosome segregation (109).

Aurora B (and the entire chromosomal passenger complex) initially localizes to chromosomes during prophase and is a mitotic histone H3 (S10) kinase (18). As discussed above, P-H3S10 may not be a critical mitotic post-translation modification. Instead, Aurora B-mediated phosphorylation of the Scc1 subunit of the cohesin complex has a bona fide functional role and contributes to loss of cohesion from chromosomal arms during prophase (88). Cohesin must be removed from chromosomal arms during prophase to facilitate efficient sister chromatid separation at anaphase onset. However, cohesin at the centromere must remain intact and functional until the metaphase-anaphase transition to inhibit precocious sister chromatid segregation. Aurora B-mediated phosphorylation of centromeric cohesin complexes is minimized by Shugoshin-dependent centromere localization of PP1, a phosphatase that antagonizes Aurora B function (110). Aurora B contributes to chromosome condensation by targeting the condensin complex to chromosomes in some but not all organisms (105). As discussed above, the precise role of Aurora B with regard to condensin function remains elusive and condensin subunits have not been shown to be substrates of the kinase (105). Aurora B has many kinetochore functions including spindle attachment and checkpoint signaling. Investigations of Ipl1/Aurora kinase targets in budding yeast have revealed functional phosphorylation of the Dam1 and Ndc80 microtubule-binding complexes. Phosphorylation of Dam1 by Ipl1 results in the dissociation of the microtubule-associated Dam1 complex from kinetochores and thus kinetochore unoccupancy (111). Importantly, Dam1 phospho-mutant yeast phenocopy *ipl1ts* growth defects, suggesting that Dam1 is a critical target of Ipl1 (111). Ndc80 is a conserved Aurora B target that, once phosphorylated, has reduced affinity for microtubules (71). Another Aurora B substrate is MCAK, a microtubule depolymerase at metazoan kinetochores. Phosphorylation of MCAK by Aurora B inhibits its depolymerase activity and therefore stabilizes kinetochore-microtubules (112). Lastly, Aurora B influences the spindle midzone localization and function of MKLP1 (**m**itotic **k**inesin-**l**ike **p**rotein) and MKLP2 during anaphase/telophase to promote microtubule dynamics required for appropriate cytokinetic furrow function and the completion of mitosis (88).

All Aurora B homologs share a common function: to destabilize incorrect kinetochore-microtubule interactions that do not produce tension between sister

chromatids. They perform their various tasks by serving as the enzymatic core of the conserved chromosomal passenger complex (CPC) that consists of INCENP (*Ce*ICP-1), Survivin (*Ce*BIR-1), and Dasra/Borealin (*Ce*CSC-1) (105). ICP-1 influences proper AIR-2 function by mediating the interaction between AIR-2 and the CSC-1/BIR-1 subcomplex (113). In monocentric organisms, each of the CPC subunits is interdependent for complex formation and localization. However, a *C. elegans* ICP-1/BIR-1/CSC-1 subcomplex can form in the absence of AIR-2 (113). Since the chromosome-long kinetochores built on holocentric chromosomes may be more prone to incorrect attachments to the mitotic spindle, these results suggest that additional levels of AIR-2 regulation may exist that involve an ICP-1/BIR-1/CSC-1 complex.

Several lines of evidence suggest species-independent modes of Aurora B regulation. First, Aurora B homologs share striking primary sequence similarity (Figure 6). The kinase domain is at the carboxy-terminus of the protein and shows little sequence divergence. Second, Aurora B activity is crippled by mutations at conserved residues. For example, the *ipl1-1* allele in budding yeast (106) causes a P340L amino acid substitution and results in a temperature-sensitive (ts) phenotype (Figure 6). *air-2(or207ts)* is an AIR-2 allele that results in an identical amino acid change and a similar ts lethality (114). Third, INCENP is a conserved substrate activator of Aurora B. Aurora B phosphorylates conserved C-terminal residues of INCENP, a modification that positively feeds back on Aurora B activity (115).

There are a variety of ways that protein function can be influenced including cycles of phosphorylation and dephosphorylation, subcellular localization, and the binding of regulatory proteins. Aurora B activity is impacted by each of these mechanisms. PP1 (**p**rotein **p**hosphatase 1) has a conserved antagonistic function against Aurora B and dephosphorylates Aurora B and its substrates (116, 117). How can a phosphorylation event on an Aurora B substrate be maintained in a cellular environment where PP1 levels are not limiting? One method to potentiate Aurora B signaling is by enriching the CPC at subcellular locations including chromatin (118). CPC enrichment increases the substrate phosphorylation/dephosphorylation ratio by decreasing substrate accessibility to PP1. In these experiments, anti-INCENP antibodies were used to cluster Aurora B-Incenp molecules together, resulting in autoactivation of Aurora B (118).

These conclusions are consistent with structural studies of Aurora B bound to INCENP that suggested *in trans* phosphorylation of INCENP by Aurora B (i.e.- neighboring Aurora B complexes phosphorylate one another) (119). Therefore, CPC activation is concentration and localization dependent.

Protein interactors that influence Aurora B activity include CPC and non-CPC proteins. As described above, INCENP is a critical Aurora B regulator in the CPC. TD60 (**t**elophase **d**isc-**60**kd) is a non-CPC inner centromere protein required to localize the *Xenopus* CPC to centromeres (120). TD60 cooperates with microtubules to activate Aurora B and stimulate *in trans* CPC phosphorylation and activation (121). Our lab has identified CDC48.3, a AAA-ATPase protein, as a direct interactor and inhibitor of AIR-2 protein levels and kinase activity (122). We also determined that TLK-1 (**T**ousled-**l**ike **k**inase) serves as a substrate activator of AIR-2 to influence chromosome segregation (123, 124).

Tousled kinases target serine/threonine residues in their substrates to influence a variety of cellular processes. The prototype TLK (termed Tousled (TSL)) was first identified in Arabidopsis as a gene product required for proper organ development in flowers (125). Mammalian Tlk1 and Tlk2 were cloned and discovered to be highly active and linked to DNA replication during S-phase (126). hTLK1 and hTLK2 dimerize, autophosphorylate, and are subject to functional regulation by phosphorylation during the cell cycle (126). The identification of the chromatin assembly factor Asf1 as a Tlk1 substrate and interactor suggested a mechanism by which Tlk1 may influence chromatin structure (127, 128). However, the *in vivo* functional consequence of Tlk1-mediated Asf1 phosphorylation remains largely elusive but may regulate the stability of Asf1 (129).

The initial characterization of Tlk1 and Tlk2 revealed that DNA damaging agents and drugs that inhibited replication led to a rapid downregulation of Tlk kinase activity (126). Further investigation of the molecular mechanism of Tlk1 inactivation revealed ATM and Chk1 as critical upstream factors in the process (130). Chk1 phosphorylates and inactivates Tlk1 during the cellular response to DNA damage (131). Although the link between Chk1 and Tlk1 is interesting, these results will remain enigmatic until downstream targets and exact cellular processes influenced by Tlk1 are discovered.

Moreover, the nature of the signal that triggers ATM-dependent downregulation of Tlk1 remains unknown but may involve changes to chromatin structure rather than specific DNA lesions (130, 132). It has also been suggested that "…the cell cycle arrest following the alteration of chromatin structure due to TLK misregulation may occur through the activation of the DNA damage checkpoint pathway." (128). Thus, a correlative relationship exists in higher eukaryotes between TLK and the assembly of chromatin structures that affect cell cycle progression.

C. elegans TLK-1 is required for transcription during embryogenesis although its exact role in transcriptional events is unknown (133). Interestingly, yeast Asf1 participates in histone eviction during transcription of *pho5* and *pho8* genes (134). Thus, it is possible that TLK-1 functions with ASF-1 to remove histones from promoters or other critical chromatin regions to generate a chromatin environment permissive for transcription. Although Tousled kinases are most highly expressed during S-phase, Tousled function is not limited to S-phase events. We have also shown that TLK-1 participates in chromosome segregation by influencing AIR-2 activity (123). AIR-2 phosphorylates TLK-1 at S634 *in vitro* and *in vivo*, a modification that increases TLK-1 kinase activity and positively feeds-back on AIR-2 activity (123). The activation of AIR-2 by TLK-1 does not require TLK-1 kinase activity but does depend on the presence of ICP-1 *in vitro* (123). Also, the chromosome segregation defects in embryos harboring a hypomorphic temperature-sensitive allele of *air-2* at semi-permissive temperatures are enhanced by *tlk-1(RNAi)* (123). These results strongly suggest that TLK-1 is necessary for proper AIR-2 function during mitosis.

Similar to the Aurora kinases, Polo kinases target serine/threonine residues of many proteins to influence virtually all aspects of mitosis. Polo was first identified in *Drosophila* as a gene product required for embryonic and larval viability via regulation of appropriate centrosome number, structure, and function (135). Human Plk1 participates in mitotic entry by phosphorylating and activating Cdc25C, a phosphatase that removes inhibitory phosphorylations on Cdk1 (136). In fact, Cyclin B-Cdk1 phosphorylates Cdc25C and serves to prime Cdc25 for Plk1 interaction (137). This interaction is mediated by conserved Plk1 residues that make up the PBD (**p**olo **b**ox **d**omain), a motif that binds phosphorylated S/T residues. Binding of the PBD to Plk1 substrates results in

a conformational change in Plk1 and increased kinase activity (137). In addition, Plk1 phosphorylates and inactivates Wee1, a kinase that negatively regulates Cdk1 (138). A prerequisite for Plk1-mediated Wee1 inhibition is Cdk1-dependent phosphorylation of Wee1. Plk1 also phosphorylates Cyclin B at centrosomes to contribute to Cdk1 activation and the cellular commitment to mitosis (139).

Plk1 is essential for bipolar spindle assembly in many organisms. Depletion of Plk1 in human cells causes monopolar spindle formation due to centrosome maturation and separation defects (140). Plk1 directly associates with γ-tubulin and may help facilitate its incorporation at centrosomes (141). Chromosome-localized Plk1 cooperates with Aurora B during the phosphorylation- promoted removal of chromosomal arm cohesin during prophase (142). Plk1 participates in the spindle assembly checkpoint by facilitating BubR1 kinase activation by Cdk1 (143). During later mitotic stages, Plk1 promotes APC activation by phosphorylating multiple APC subunits (144). However, Plk1 is not essential for APC function, but may cooperate with Cdk1 to augment APC activity (145). Lastly, Plk1 translocates from chromosomes to the central spindle via recruitment by proteins including Mklp1 and Mklp2 that also serve as Plk1 substrates (146). Plk1 also appears to influence abscission, a very late stage of cytokinesis, through an as yet unclear pathway (145).

Recent evidence suggests that Cdk1 and Plk1 converge on Aurora B signaling. Cdk1 phosphorylates INCENP, a subunit of the CPC, to promote Plk1 binding via its PBD (147). The interaction of Plk1 with INCENP is essential for the relocation of the chromosomal passenger complex from chromosomes to the spindle midzone at the metaphase-anaphase transition (147). Moreover, *Xenopus* Polo kinase phosphorylates and primes substrates for subsequent Aurora B phosphorylation (121). Thus, a kinase cascade is beginning to emerge that involves Plk, Cdk1, and Aurora B signaling that ultimately influences entry into anaphase.

C. elegans homologs of Cdk1, Aurora B, and Plk1 have been cloned and functionally characterized. CDK-1 (also called NCC-1 for **n**ematode **c**ell **c**ycle) has been shown to influence nuclear envelope breakdown during oocyte maturation and is required for mitotic divisions in the germline, embryo, and adult proliferative tissue (148, 149). Wee1 homologs (WEE-1.1, WEE-1.2, and WEE-1.3) negatively regulate CDK-1

function and are required to limit CDK-1-mediated maturation of oocytes to those that are most proximal to the spermathecae (150).

AIR-2 (**A**urora and **I**pl1 **r**elated) is required for proper meiotic and mitotic chromosome segregation (151). AIR-2 phosphorylates the REC-8 subunit of the cohesin complex during meiosis to remove sister chromatid cohesin at anaphase of the second meiotic division (152). *air-2(RNAi)* results in failure of polar body extrusion (remnants of the two meiotic divisions that follow fertilization) (151). The first mitotic division also requires AIR-2 for appropriate anaphase segregation (153). Similar to other organisms, AIR-2 exists and is functionally active in the chromosomal passenger complex (CPC) that includes ICP-1 (INCENP, BIR-2 (Survivin), and CSC-1 (similar to hBorealin) (113). Importantly, loss of AIR-2 has not yet been shown to cause improper kinetochore-microtubule attachments as would be expected from conclusions drawn about Aurora B in other organisms. Unlike the substantiated role that Aurora B plays in SAC signaling (90), AIR-2 is not required for SAC activation in response to monopolar spindles (154), although its role in bipolar SAC activity has not been researched. Thus, although AIR-2 displays much functional homology with Aurora B**,** the requirement of AIR-2 for certain Aurora B-influenced mitotic events remains inconclusive. Lastly, AIR-2 contributes to cytokinesis by influencing the spindle midzone localization of ZEN-4 kinesin (also known as MKLP1) (114). AIR-2 binds ZEN-4 in vitro, suggesting that AIR-2 recruits ZEN-4 to the central spindle to influence microtubule bundling at that location (114). AIR-2 is not required for cleavage furrow invagination but rather for the continued maintenance or function of proteins involved in actomyosin ring contraction (114).

PLK-1 is required for oocyte nuclear envelope breakdown prior to fertilization and polar body extrusion (149). *plk-1(RNAi)* does not result in centrosome maturation defects or monopolar spindle formation, suggesting that PLK-1 does not contribute to these events in the early embryo. Instead, *plk-1(RNAi)* results in chromosome missegregation with no evidence of anaphase figures (149). Moreover, cytokinesis furrow invagination begins but is not completed in embryos depleted of PLK-1, indicating a conserved function for Polo kinases during the final stages of cytokinesis.

The Spindle Assembly Checkpoint

Kinetochores are neither static nor passive microtubule-binding structures. Instead, kinetochores actively monitor the attachment state of microtubules to kinetochores. After nuclear envelope breakdown during prometaphase, microtubules emanating from centrosomes execute a search-and-capture activity as they randomly probe the cytoplasm for a kinetochore connection (89). Kinetochores initially bind microtubules laterally resulting in the translocation of the entire chromosome to the spindle pole/centrosome (monopolar attachment) (89). This movement results from the activity of kinetochore-bound dynein, a minus-end directed microtubule motor protein (82). Microtubules are polar structures with stable minus ends (congregated at centrosomes) and dynamically growing and shrinking plus ends that are localized distal to centrosomes (i.e.-kinetochores). Thus, dynein contributes to the centrosome localization of chromosomes during prometaphase (82). Although the search-and-capture model is attractive, a novel mechanism of kinetochore-microtubule attachment has been identified. This model suggests that chromosomes themselves nucleate microtubules (likely catalyzed by chromosome-localized Ran GTPase) that interact with centrosome-generated microtubules to facilitate kinetochore-spindle association (155, 156).

After the initial monopolar attachment of one sister kinetochore of a sister chromatid pair, various types of microtubule attachment can occur to the unoccupied kinetochore during prometaphase chromosome congression (Figure 4). Sister kinetochores that have not established attachments with microtubules or have incorrectly established attachments produce a "wait-anaphase" signal (157). Types of inappropriate attachments include syntelic (both sister kinetochores bind microtubules from the same pole), merotelic (one sister kinetochore interacts with microtubules emanating from both poles), and monotelic (same as monopolar) (158). Moreover, the close proximity of sister kinetochores to centrosomes during early prometaphase increases the likelihood of merotelic attachments. Thus, a mitotic checkpoint called the spindle assembly checkpoint (SAC; also known as spindle checkpoint) surveys kinetochore-spindle attachments and inhibits anaphase until all metaphase chromosomes have bipolar, amphitelic (both sister kinetochores interact with microtubules arising from the appropriate pole) character (158).

Figure 4. Kinetochore-microtubule attachments and the spindle assembly checkpoint

A variety of wrong kinetochore-microtubule (K-Mt) attachments exist during chromosome congression (Prometaphase) that activate the spindle assembly checkpoint (SAC). Monotelic: Spindle microtubule attachment (green lines) to one sister kinetochore (purple ovals) and microtubule unoccupancy at the paired kinetochore. Syntelic: Both sister kinetochores interact with microtubules emanating from the same spindle pole. Merotelic: Microtubules originating from both poles interact with the same sister kinetochore. Red arrows indicate the incorrect K-Mt interactions. Monotelic and syntelic attachments are recognized (by relatively enigmatic mechanisms), leading to SAC activation and attempts at reorientation. However, merotelic attachments generate enough tension between sister chromatids to silence the SAC. Chromosome biorientation at the metaphase plate and amphitelic K-Mt attachment generate spindle tension, SAC silencing, and anaphase onset.

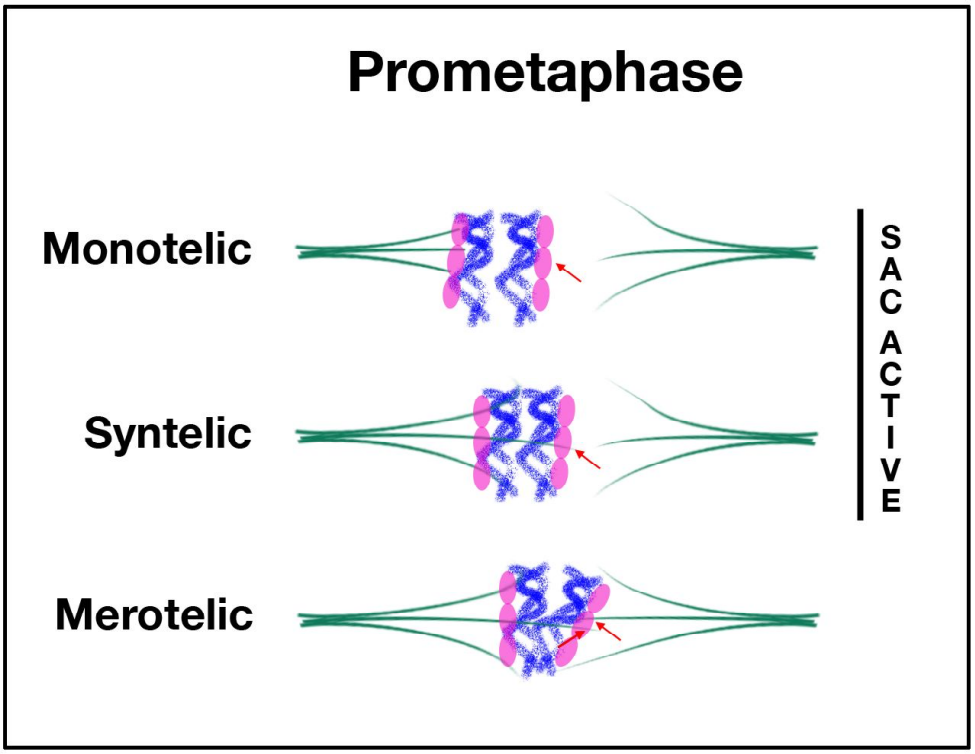
Prometaphase
Monotelic
Syntelic
Merotelic
SAC ACTIVE

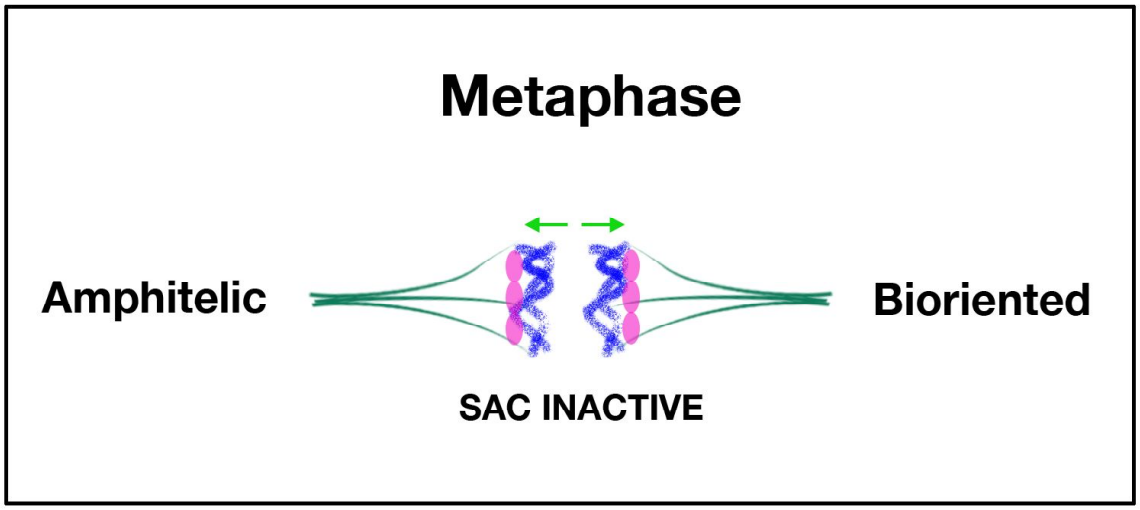
Metaphase
Amphitelic
Bioriented
SAC INACTIVE

Key proteins involved in SAC signaling have been identified. Several SAC proteins were identified from genetic screens performed in budding yeast selecting for mutants that could not inhibit mitotic progression in the presence of spindle poisons (159). These screens identified Mad1, Mad2, and Mad3 (**m**itotic **a**rrest **d**eficient) as well as Bub1 and Bub3 (**b**udding **u**ninhibited by **b**enzimidazoles). SAC proteins are highly conserved, and research utilizing model organisms including *Xenopus* egg extracts and cultured human cells has revealed the molecular details of SAC activity. Mad2 can exist in two structurally distinct conformations (open (O) vs. closed (C)) (89). C-Mad2 is a more potent inhibitor of Cdc20, an activator of the APC (**A**naphase **P**romoting **C**omplex, an E3 ubiquitin ligase that targets key proteins for proteolysis), than is O-Mad2 (89). Thus, the ratio of C-Mad2/O-Mad2 is important and suggests the need to propagate the production of C-Mad2 when the SAC is engaged. A "template model" has been proposed whereby a complex of Mad1 and C-Mad2 at the kinetochore recruits O-Mad2 from the cytosol via Mad2 dimerization to generate more C-Mad2 (160). C-Mad2 is removed from kinetochores when bound to Cdc20, effectively disrupting APC activation (161). Also, the released C-Mad2/Cdc20 complex likely catalyzes the conversion of cytosolic O-Mad2 to C-Mad2, amplifying the originally weak, kinetochore-produced signal (162).

Although kinetochores produce a "wait anaphase" signal, evidence suggests that additional kinetochore-independent signals can be generated and propagated. Biochemical purifications from HeLa cells isolated a mammalian cytosolic MCC (**m**itotic **c**heckpoint **c**omplex) that contains BubR1, Bub3, Cdc20, and Mad2 (163). The MCC is a much better *in vitro* inhibitor of the APC than is recombinant C-Mad2. Moreover, the MCC is present during interphase when mature, fully assembled kinetochores do not exist (163). Thus, kinetochore-generated SAC signaling is thought to cooperate and potentiate the ability of the MCC to inhibit the APC, perhaps by modifying the APC at kinetochores (89). The MCC is conserved and exists in eukaryotes from yeast to human (164). In *C. elegans*, biochemical attempts to identify cytosolic MCC from embryo extract have not been attempted. However, a functional SAC exists during *C. elegans* embryogenesis and is activated when kinetochore-microtubule attachments are perturbed (154, 165). Recent analysis of the *C. elegans* SAC has identified bipartite characteristics,

with a largely cytosolic BUB-3/MDF-3 (Mad3, also known as SAN-1) component and kinetochore-based MDF-1 (Mad1)/MDF-2 (Mad2) signaling (154). Kinetochore complexes including KNL-1, NDC-80, and Rod/Zwilch/Zw10, as well as BUB-1 influence the generation of the kinetochore-based signal (154). SPDL-1, a *C. elegans* Spindly homolog, interacts with and targets MDF-1 to kinetochores (166). Interestingly, Spindly also associates with dynein at kinetochores to promote SAC silencing (167), suggesting that Spindly and dynein might compete for Mad1 binding during SAC activation and inactivation, respectively.

SAC activation is coordinated with the status of kinetochore-microtubule attachments largely by way of kinase signaling. The conserved Aurora B kinase (AIR-2 in *C. elegans*) somehow recognizes non-amphitelic attachments and destabilizes them so that bipolarity can be reattempted (168, 169). In budding yeast, Ipl1/Aurora kinase creates unattached kinetochores that activate the SAC (168). However, metazoan Aurora B appears to have separable functions in SAC activation and destabilizing wrong kinetochore-microtubule attachments (90). Intriguing evidence suggests that a subcomplex of Sli15 (*Ce*INCENP) and Bir1 (*Ce*Survivin) interacts with centromeres and microtubules to activate Ipl1 when microtubules are not under tension (170), indicating that the CPC may directly monitor spindle tension. Therefore, it is important to note that although Aurora B is part of a major tension-sensing mechanism, it itself is unlikely to be part of the mechanosensing machinery. Instead, proteins that associate with Aurora B may relay the state of sister kinetochore tension to Aurora B to activate (no tension) or inhibit (full tension) its kinase activity.

Although Ipl1 is indirectly involved in SAC activation (by creating unattached kinetochores), Aurora B activity in higher eukaryotes, however, is required to localize the SAC proteins Bub1 and Mad2 to kinetochores (171). Also, human Aurora B inhibits the association of dynein with the ZW10 and Rod subunits of the RZZ kinetochore complex at tensionless kinetochores, blocking dynein-dependent SAC silencing (see below and (172)). Thus, Aurora B may couple the status of sister chromatid tension to SAC activation. Curiously, *C. elegans* AIR-2/Aurora B is not necessary for SAC activity during embryogenesis, since *air-2(RNAi)* does not inhibit SAC signaling that is induced by monopolar spindles (154). However, profound anaphase chromosome bridging occurs

in AIR-2-defective embryos, likely caused by incorrect kinetochore-microtubule attachments (153). Besides Aurora B, Polo kinase (Plk1) also has a conserved role in regulating kinetochore-microtubule attachments in part by phosphorylating BubR1, a kinase involved in SAC signaling that also influences kinetochore-microtubule stability (173).

That proteins involved in SAC activation would participate in establishing stable attachments (to ultimately inactivate the SAC) might seem paradoxical, yet other SAC proteins including Bub1 and Bub3 also contribute to bipolar attachments (174, 175). Similarly, kinetochore proteins that bind microtubules also influence the SAC. For instance, the KMN network that forms the key microtubule-binding interface at kinetochores regulates SAC activity. Human blinkin (a *C. elegans* KNL-1 homolog found in the metazoan KMN complex) directs Bub1 and BubR1 to kinetochores for SAC activation (176). The KMN component Mis12 is required for checkpoint signaling and recruits the RZZ complex to kinetochores to facilitate Mad1 and Mad2 signaling (177). Additionally, the Ndc80 complex is also required for SAC activation. Yeast mutants of the Ndc80 complex cannot activate the SAC yet global kinetochore structure and assembly remains intact (178). Since the SAC requires intact outer-kinetochore structural proteins, the absence of the SAC in Ndc80 mutants is consistent with the notion that kinetochore-microtubule interactions directly affect the checkpoint.

Although mechanisms that maintain SAC activity are known, less is understood at the molecular level about SAC inactivation. Yet, Bub1 and BubR1 are kinases that are mutated in several colorectal, lung, and breast malignancies and their inactivation also contributes to premature chromatid separation syndrome (179, 180). **It is therefore imperative to elucidate molecular mechanisms that contribute to SAC silencing, since upregulation of these pathways could contribute to premature SAC inactivation, chromosome instability, and cancer.** Cdc20 is an important APC activator and must be removed from the inhibitory binding of C-Mad2. One method of Cdc20 regulation involves interaction of p31comet with C-Mad2 to release Cdc20 and promote APC activation (181). p31comet interacts with residues in Mad2 responsible for homodimerization, effectively inhibiting the production of C-Mad2 from O-Mad2 (181). Another SAC silencing mechanism involves microtubule binding to kinetochore-

localized CENP-E resulting in the inhibition of BubR1 SAC signaling (182).

An additional level of SAC silencing at kinetochores involves dynein-dependent removal of SAC proteins from kinetochores. SAC proteins including Mad1 are cargo for the light chains of the dynein complex (183, 184). Dynein attenuates the SAC by binding to SAC proteins at kinetochores and moving along kinetochore-microtubules to centrosomes (82). Proteins including the RZZ complex and Spindly target dynein to kinetochores to deactivate the SAC (185). Finally, the outer kinetochore proteins Ska3 in human cells contributes to SAC silencing. Ska3 is a recently identified protein that is part of the microtubule-binding Ska1 complex (77). Ska3 shRNA in HeLa cells results in improper prometaphase chromosome congression and a block at metaphase (186). This block requires SAC proteins and therefore results from continued SAC activity. Importantly, kinetochore-microtubule attachments are robust in Ska3-depleted cells (76). These data led to a model suggesting that Ska3 "reads" the tension-specific status of multiple microtubule attachments at each kinetochore. Even in the presence of bipolar attachment of chromosomes to the mitotic spindle, the absence of Ska3 results in the inability of kinetochores to recognize that proper attachments have been achieved, resulting in prolonged SAC activity (76).

Recent evidence suggests that Aurora B-mediated signaling must also be silenced so that kinetochore-microtubule attachments are stabilized. For instance, the kinetochore structure achieved when sister chromatids are properly bioriented at the metaphase plate influences Aurora B substrate availability (187). In this model, tension between sister chromatids physically sequesters kinetochore targets from Aurora B. Moreover, this model suggests that decreasing Aurora B activity is unnecessary for SAC inactivation (187). However, there are outstanding questions about the "metaphase kinetochore structure" model including: 1) Why would Aurora B not be able to interact with kinetochore proteins even at tensed kinetochores? What would physically block Aurora B from diffusing within the inner centromeric space to interact with kinetochores under tension? 2) What magnitude of incorrect kinetochore-microtubule attachments would generate a kinetochore structure permitting Aurora B phosphorylation of kinetochore proteins? Would this amount be physiologically relevant in relation to the number of microtubules that interact with kinetochores? Lastly, the PP1 phosphatase contributes to

SAC inactivation by counteracting Aurora B substrate phosphorylation (188, 189). These observations suggest that active mechanisms to silence Aurora B-dependent SAC activation are at play, with kinetochore structure playing a more passive role.

Studying Mitosis Utilizing *Caenorhabditis elegans* as a Model Organism

All organisms require stable chromosome segregation for proper embryonic development and a disease-free adulthood. Accurate division of single-cell organisms like *S. cerevisiae* is important for population growth and survival. In *C. elegans,* mitotic chromosome segregation is important for pre-meiotic germ cell proliferation, embryonic development, and post-embryonic somatic divisions of adult tissues including intestine, ventral cord, and germline (190). Although nematodes do not develop cancer, loss of chromosome segregation fidelity can lead to embryonic lethality or defects in the development of adult tissue (190). Also, *C. elegans* is suitable for forward and reverse genetic analyses and is also a proven biochemical system for defining protein complexes (69, 191).

C. elegans is a terrific model organism to study meiotic and mitotic processes. The hermaphrodite gonad is a U-shaped symmetrical structure with the proximal gonad close to the spermathecea and the distal gonad near the apical surface of the animal (192). The distal tip of the gonad contains primordial cells that function as a stem cell-like population for the generation of oocytes (192). Cells in the distal tip divide mitotically and transition into oogenesis spatially, with progressive meiotic prophases occurring in the proximal gonad. Diakinetic oocytes near the spermathecea contain 6 bivalents that each contain two paired homologous chromosomes (192). MSP (**m**ajor **s**perm **p**rotein) promotes oocyte maturation, consisting of morphological changes in oocyte shape, oocyte cell growth, nuclear envelope breakdown, and activation of kinases including MPK-1 (ERK), CDK-1, and AIR-2 (193). Fertilization occurs when oocytes traverse the spermathecea, sperm entry defines the embryo posterior and stimulates exit from meiotic prophase and the two meiotic divisions of the maternal pronucleus at the anterior cell cortex (190). Two polar bodies are extruded, resulting in a haploid complement of chromosomes that, paired with the paternal chromosomes, produces a

Figure 5. The first mitotic division in the *C. elegans* embryo

After fertilization and meiotic chromosome segregation (not shown), the maternal (M) and paternal (P) pronuclei replicate their DNA and pronuclear migration ensues. The maternal pronucleus migrates toward the paternal pronucleus at the posterior cortex (arrows indicate the migration distance of each pronucleus away from the respective cortex). Centrosomes (purple circles) separate on the paternal pronuclear membrane and begin to build the mitotic spindle (purple circles and lines). After pronuclear meeting (PNM), the nucleus/spindle apparatus rotates to align with the A-P axis and is asymmetrically localized to the posterior of the embryo. Nuclear envelope breakdown defines the start of prometaphase and chromosomes congress by kinetochore attachment to spindle microtubules. Chromosomes align at the metaphase plate concomitant with amphitelic K-Mt attachment and the generation of tension between sister chromatids (green arrows). Sister chromatids separate at anaphase, chromosomes decondense during telophase, and cytokinesis completes the first mitotic division.

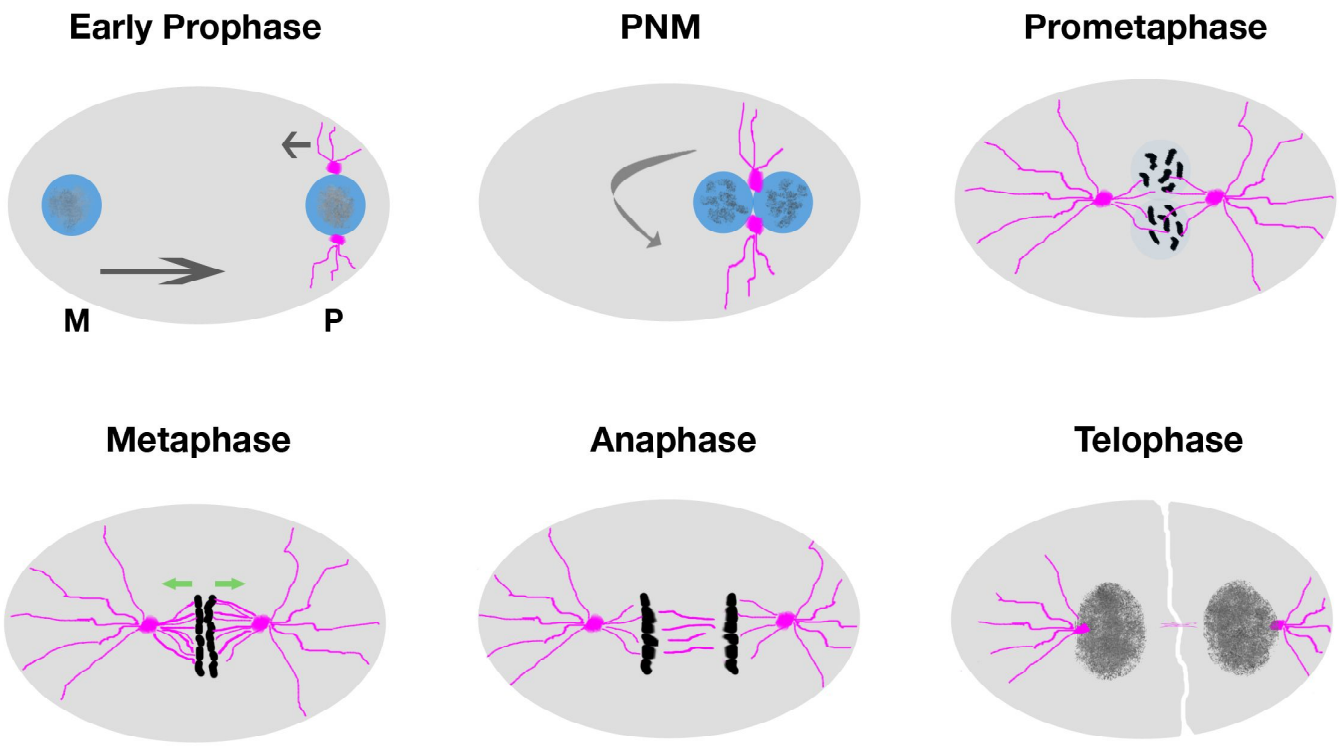
Early Prophase
PNM
Prometaphase
M
P
Metaphase
Anaphase
Telophase

diploid embryo with six pairs of chromosomes (190). The sperm-derived centrosome and the condensed paternal pronucleus remain at the posterior end of the embryo as the maternal pronuclear divisions occur. Subsequently, the paternal chromatin decondenses, centrosomes and chromosomes duplicate, and pronuclear meeting occurs near the posterior embryo cortex (190).

Pronuclear meeting marks the onset of prophase of the first mitotic division (Figure 5). The spindle-nucleus apparatus rotates 90° to align with the A-P axis of the embryo. During this period or shortly thereafter, the nuclear envelope disassembles and prometaphase chromosome congression ensues. Chromosomes align at the spindle equator during metaphase, but the spindle equator is not equivalent to the embryo equator. That is, the mitotic spindle is localized asymmetrically toward the posterior of the embryo to give rise to daughter cells that differ in size (194). Anaphase chromosome segregation and cytokinesis complete the first mitotic division.

Various methods exist to introduce dsRNA into *C. elegans* larvae for RNAi-mediated depletion of germline and embryonic proteins (190). These include soaking worms in dsRNA solution, ingestion of *E. coli* with plasmid-based expression of dsRNA, and microinjection of dsRNA directly into the larval gonad. Protein levels after RNAi-targeting are reduced 90-95% compared to wild-type (190). Therefore, meiotic divisions and the first embryonic mitosis can be studied after selective deprivation of a protein of interest.

As mentioned previously, mechanisms underlying chromosome segregation are largely conserved. Moreover, the *C. elegans* genome encodes homologs of mitotic proteins that function in similar ways regardless of species (e.g. Aurora B, Cdk1, Ndc80, Knl1) (190). *C. elegans* offers a unique opportunity for studying kinetochore biology since its chromosomes are holocentric and build kinetochores that represent elongated conventional kinetochores (38). The increased size of *C. elegans* kinetochores facilitates phenotypic analyses of centromere/kinetochore architectural changes during sister chromatid resolution and kinetochore-microtubule attachment. Another factor that aids in studies of kinetochore geometry is the rigidity and rod-like structure of *C. elegans* mitotic chromosomes (38). Chromosome rigidity reduces the uncertainty that changes in

kinetochore architecture are due to chromosome stretching/bending rather than altered kinetochore function.

The *C. elegans* researcher has a molecular toolkit from which to choose the appropriate experimental procedure to answer a biological question. Transgenic animals expressing proteins tagged with short epitopes (e.g.- HA, myc, etc) can be generated to perform *in vivo* localization and immunoprecipitation assays with highly specific commercially available antibodies. Since not all attempts at generating antibodies are successful, epitope tags can be crucial for determining protein interactions and subcellular localization. Also, the expression of fluorophore-conjugated (e.g.- GFP, mCherry) proteins permits live-cell imaging of embryos under diverse experimental conditions (195). Data gleaned from live imaging does not suffer from fixation artifacts and reveal a clearer picture of alterations in the temporality and spatiality of mitotic processes in mutant or RNAi-treated animals. The generation of stable transgene expression in the germline and early embryos, however, has been difficult. Although transgenes can be injected into young adults and exist in oocytes as extrachromosomal arrays, germline silencing of the arrays mediated by HMG and Polycomb group proteins is common (196). A newer technique called bombardment uses high velocity to deliver DNA-coated beads into animals (197). This technique is advantageous because the transgene is often integrated into the genome at a single locus and mimics the expression level of the native protein. However, it can be extremely difficult to generate transgenic animals due to the low frequency of successful transgene delivery, large number of animals from which to screen for positive transformants, and low expression of the transgenic protein (196). Recently, a Mos transposon technique has been developed for targeted integration of transgenes in *C. elegans* (198). Although this procedure has been suggested to be highly efficient and noncomplex, results from our lab and others suggest that the method is riddled with difficulties.

The results described in this dissertation were obtained by research performed with two model organisms: *Saccharomyces cerevisiae* and *Caenorhabditis elegans*. The data explained in the next chapter focuses on the heterologous expression of TLK-1, a *C. elegans* AIR-2/Aurora B activator, in yeast to gain insight into the mechanism of TLK-1-induced Aurora B activation. Chapter Three discusses a tethered catalysis yeast two-

hybrid screen that was performed to identify proteins that interact with TLK-1 in a phosphorylation-specific manner. Chapter Four reveals pivotal mitotic roles for CYB-3, one protein identified from the two-hybrid screen, during *C. elegans* embryogenesis. Lastly, Chapter Five reiterates several key conclusions drawn from my experimental results. In addition, Chapter Five presents interesting hypotheses and experiments that expand on the data presented within these pages. Altogether, **my data indicate that TLK-1 contributes to chromosome segregation at least in part by functioning as a platform for mitotic kinase signaling.**

CHAPTER TWO: DETERMINING IF TLK-1 KINASE ACTIVITY IS REQUIRED FOR TLK-1-MEDIATED AURORA B ACTIVATION

Introduction

Our previous results revealed a critical role for TLK-1-mediated AIR-2 activation during *C. elegans* embryogenesis (123). However, several open questions remained. For one, is TLK-1 kinase activity required for its activation of AIR-2 *in vivo*? It is important to ascertain if TLK-1 kinase activity is required to potentiate AIR-2 function since many kinase cascades rely on activating phosphorylations. As an example, the DNA-damage response requires activating phosphorylations of Chk1 and Chk2 kinases by ATM and ATR kinases (199). Although we found no evidence that AIR-2 is a substrate of TLK-1 *in vitro* (123), it is possible that TLK-1 phosphorylates AIR-2 or another member of the CPC *in vivo* to increase AIR-2 activity. We also desired to determine if TLK-1 expression and S634 phosphorylation were sufficient for AIR-2 activation *in vivo*.

Advantages of utilizing *Saccharomyces cerevisiae* for analyzing the *in vivo* sufficiency of TLK-1-promoted AIR-2 activation

Establishing *C. elegans* transgenic lines can be difficult due to transgene silencing, lethality resulting from ectopic expression of essential genes with non-inducible promoters, and low probability of chromosome integration causing variable expression (197). Our previous results suggested that AIR-2-mediated phosphorylation of TLK-1 at S634 was both necessary and sufficient for *in vitro* AIR-2 activation by kinase-inactive TLK-1 (123). However, it remained unclear if S634 modification or TLK-1 kinase activity was sufficient to activate AIR-2 *in vivo*. In order to answer these questions, multiple transgenic animals would have had to been generated (e.g.- animals expressing S634A phospho-mutant and S634E/D phospho-mimetic TLK-1 with or without kinase domain mutations). What is more, overexpression of *Drosophila* TLK results in embryonic lethality indicating that the level of TLK must be strictly regulated (128). Also, endogenously produced wild-type TLK-1 would have confounded the conclusions drawn from the TLK-1-mutant phenotypes since TLK-1 molecules likely dimerize (126, 200). This issue could have been circumvented by performing selective RNAi degradation of the wild-type transcript and sparing of the transgenic product by codon substitution (i.e.- replacing nucleotides of the transgene with nucleotides that

would generate identical amino acids) (201). However, several models suggest that RNAi can progressively recognize sequences outside of the targeted region so there is no guarantee that codon substitution would have completely shielded the transgene from degradation (202).

Budding yeast offer several advantages for the molecular dissection of TLK-1-induced AIR-2 activation. Firstly, Aurora B, AIR-2, and Ipl1 are highly conserved in sequence and function (Figure 6). Secondly, genomic sequence searches have failed to identify Tousled homologs in *S. cerevisiae*. Therefore, TLK-1 mutant-induced changes in budding yeast viability could be reasonably attributed to the TLK-1 mutations and would not have to rely on a dominant-negative function of the mutant protein. Thirdly, the level of wild-type and mutant TLK-1 expression is expected to be nearly equal since each protein is transcribed by the same Gal4 promoter and the cultures are induced at similar time points during culture growth. Fourthly, biochemical purification from yeast extract can be efficiently performed and a variety of epitope-tagged Ipl1/Aurora strains are available. The ability to synchronize yeast at a particular cell cycle stage, which is not possible in *C. elegans*, would also clarify temporal interactions between TLK-1 and Ipl1.

Results

TLK-1 mutants that mimic AIR-2-directed S634 phosphorylation suppress *Ipl1* mutants independent of TLK-1 kinase activity

Previous results suggested that heterologous expression of hTlk1 suppresses the growth defect of yeast harboring a ts *ipl1* allele (203). The conclusions drawn in this manuscript suggested that hTLK1 substituted for Ipl1 in histone H3S10 phosphorylation (203). Our previous work suggested that TLK-1 does not phosphorylate H3 at S10 *in vitro* or *in vivo* (133). Although we cannot exclude the possibility that TLK-1 acts in a redundant fashion towards H3S10 phosphorylation, it is fully feasible that hTlk1 suppressed the *ipl1ts* phenotype by acting as a substrate-activator of Ipl1. Moreover, H3S10 phosphorylation is not required for chromosome segregation in budding yeast, so

Figure 6. Comparison of Ipl1, AIR-2, and Aurora B primary protein structure and hypomorphic alleles relevant to the present study

Amino acid sequence alignment of the Aurora B homologs from *S. cerevisiae* (ScIpl1), *C. elegans* (CeAIR-2), and *H. sapiens* (HsAurora) displays the positions of identical amino acids (black), amino acids with similar biochemical properties (grey), and dissimilar residues (white). The kinase domain (highlighted with a grey bar) encompasses a significant portion of the protein. Both an asterisk and an arrow denote the IPL1 alleles utilized in this study. Of note, one of the *IPL1* alleles, *ipl1-1*, shares the exact same point mutation as a hypomorphic allele of AIR-2, *air-2(or207ts),* previously shown to impair AIR-2 function at restrictive temperatures (114). The other allele of *IPL1*, *ipl1-2*, also changes a conserved amino acid within the kinase domain (116).

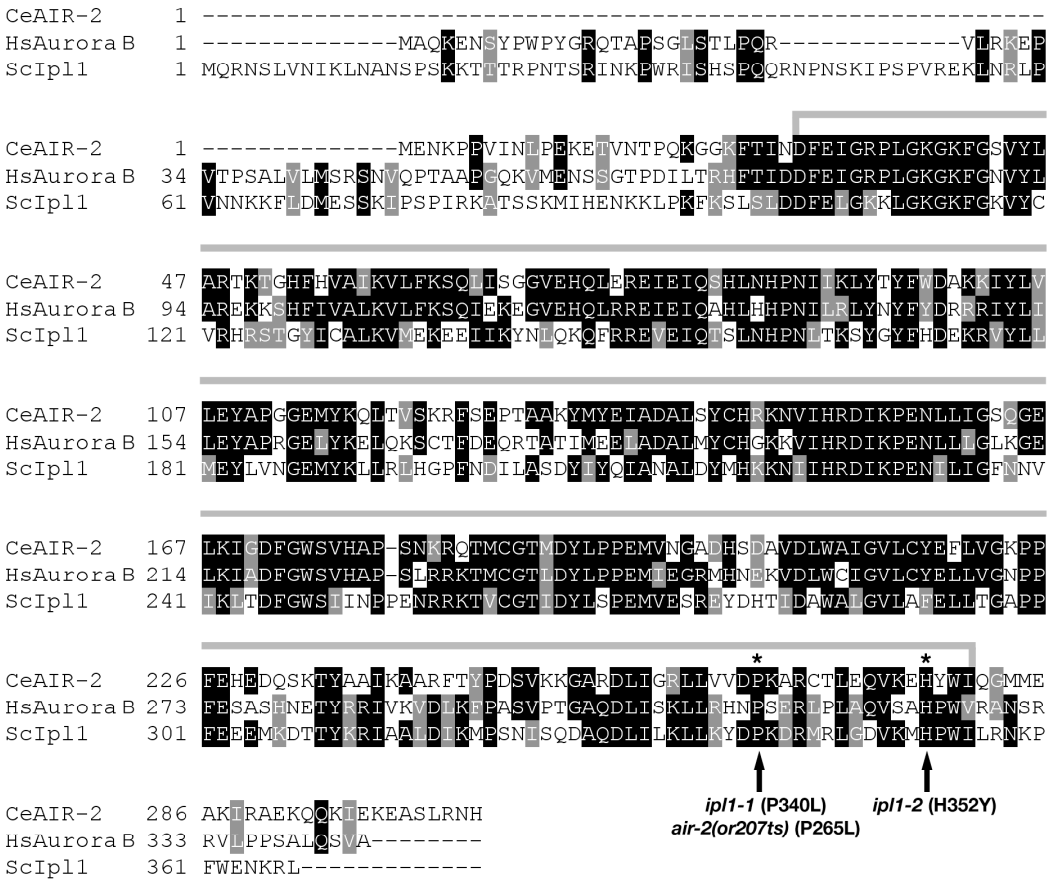
CeAIR-2
HsAurora B
ScIpl1
ipl1-1 (P340L)
air-2(or207ts) (P265L)
ipl1-2 (H352Y)

it is unlikely that increased P-H3S10 levels contributed to *ipl1ts* suppression by hTlk1 (18).

To determine if TLK-1 can suppress *ipl1ts* growth defects, wild type and *ipl1-1* mutant yeast were transformed with either an empty vector control or wild type TLK-1. The vector contains a galactose-inducible promoter and expresses V5-tagged TLK-1 when galactose is used as a carbon source. Equal concentrations of wild type and *ipl1-1* cells were serially diluted and plated on either glucose or galactose medium with incubation at 30°C (permissive) or 35°C (semi-permissive) (Figure 7). *Ipl1-1* cells containing an empty expression vector grew similar to wild type cells at 30°C (Figure 7A), consistent with previous data on the range of temperatures that make cell proliferation sensitive to *ipl1-1*-related defects. The growth of *ipl1-1* cells at 30°C on galactose medium was slightly defective, suggesting that Ipl1 is a positive regulator of galactose catabolism or, more likely, that galactose stresses the cell division process. *Ipl1-1* cells exhibited a growth defect on glucose or galactose-containing medium at 35°C that was strongly suppressed by wild type TLK-1 (Figure 7B). There are a few explanations for the suppression of *ipl1-1* defects on medium that should not drive TLK-1 expression (glucose). The suppression of *ipl1-1* defects by TLK-1 on glucose medium suggests incomplete *GAL1* promoter repression in the presence of glucose. Also, cell growth is more efficient when glucose is used as a carbon source compared to galactose because the latter sugar stresses yeast metabolism.

A previous study suggested that Tlk1 alleviates *ipl1ts* lethality through a TLK-1 kinase activity-dependent bypass suppression mechanism (203). However, our data suggest that TLK-1 kinase activity is dispensable for AIR-2 activation *in vitro* (123). To ascertain if TLK-1 must be catalytically active to suppress *ipl1ts* growth defects, a TLK-1 mutant harboring a missense mutation in the kinase domain that cripples TLK-1 activation was expressed in *ipl1-1* and an isogenic wild type strain. Kinase-inactive TLK-1 suppressed the *ipl1-1* growth defect nearly as well as wild-type TLK-1 (Figure 7B). In addition, the kinase-independent suppression of crippled Ipl1 function by TLK-1 was not specific for the *ipl1-1* allele. Kinase-dead TLK-1 also suppressed the cell lethality of an *IPL1* strain harboring a stronger allele, *ipl1-2*, in a ts fashion (Figure 8, A and B) (106). These results suggest that the functional contribution of TLK-1 with

Figure 7. Kinase-independent suppression of *ipl1-1* cells by TLK-1

ipl1-1 cells and an isogenic wild type strain were transformed with the indicated galactose-driven plasmids, serially diluted five-fold on glucose or galactose medium, and incubated at 30°C or 35°C for five days. Cells containing an empty vector served as controls.

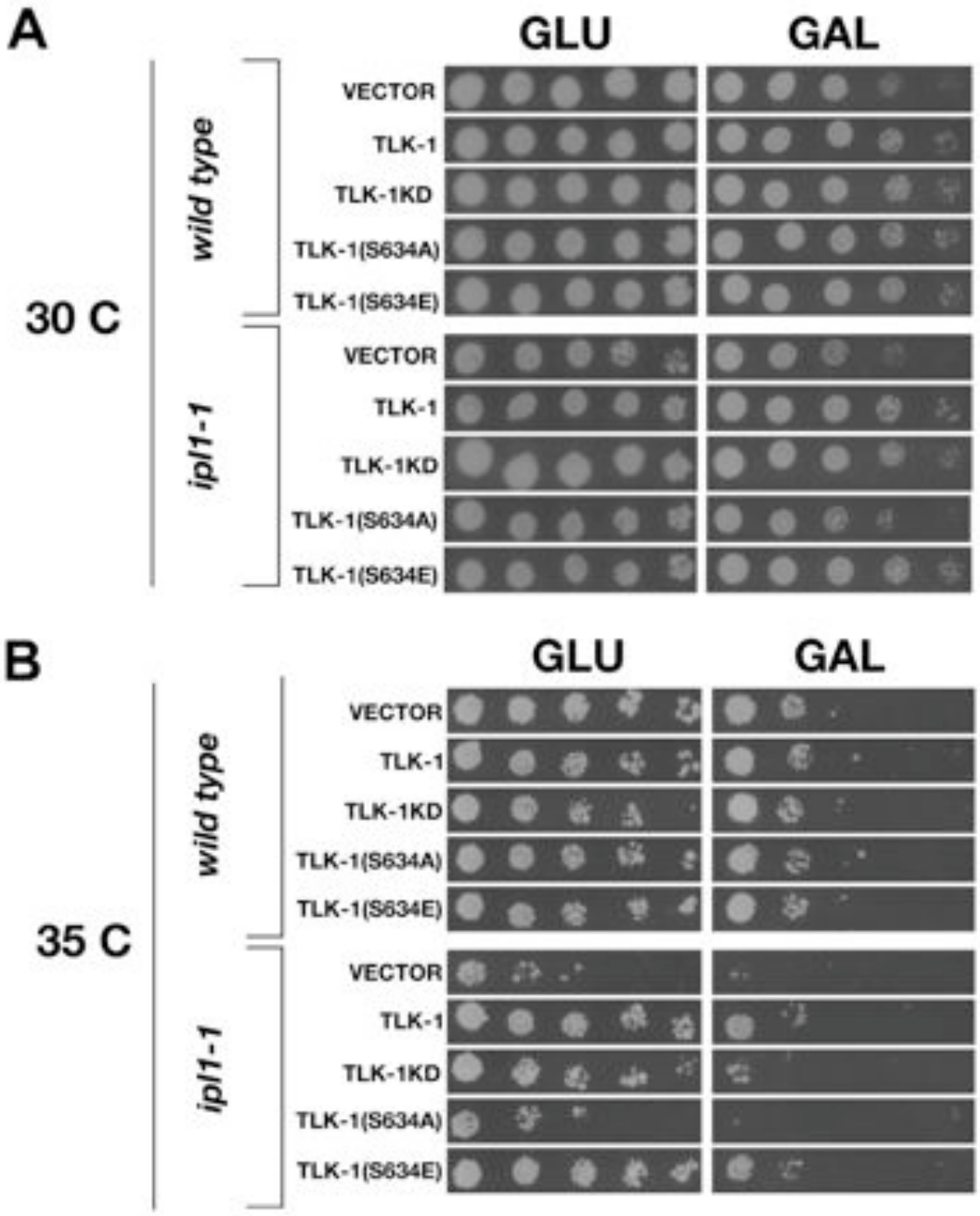
A
GLU
GAL
30 C
wild type
VECTOR
TLK-1
TLK-1KD
TLK-1(S634A)
TLK-1(S634E)
ipl1-1
VECTOR
TLK-1
TLK-1KD
TLK-1(S634A)
TLK-1(S634E)
B
GLU
GAL
35 C
wild type
VECTOR
TLK-1
TLK-1KD
TLK-1(S634A)
TLK-1(S634E)
ipl1-1
VECTOR
TLK-1
TLK-1KD
TLK-1(S634A)
TLK-1(S634E)

regard to *ipl1ts* suppression is unlikely to be due to a parallel pathway stimulated by TLK-1 that increases the fidelity of chromosome segregation. Instead, these results provide compelling evidence that kinase-dead TLK-1 is sufficient to activate Aurora B *in vivo*.

Our previous results suggested that TLK-1 S634 is a critical residue that, once phosphorylated by AIR-2, increases AIR-2 activity (123). We hypothesized that TLK-1-mediated *ipl1ts* suppression might also be dependent on S634 phosphorylation. To test the contribution of TLK-1 S634 to Ipl1 kinase activity *in vivo*, the growth of wild type and *ipl1-1* yeast cells expressing full-length TLK-1 harboring the phospho-mutant S634A or the phospho-mimetic S634E were compared (Figure 7, A and B). The growth of *ipl1-1* cells was suppressed by TLK-1(S634E) at each condition (30°C or 35°C, glucose or galactose) similar to the suppression of *ipl1-1* by wild type TLK-1 (Figure 7, A and B). In contrast, TLK-1(S634A) was unable to suppress *ipl1-1* growth defects. These data indicate that phosphorylation of TLK-1 at S634 enhances Ipl1 function and promotes colony growth. Since *ipl1-1* and *ipl1-2* defects are attributed to chromosome missegregation (106), these results imply that TLK-1 attenuates *ipl1ts* lethality by enhancing the fidelity of chromosome segregation.

Ipl1 co-purifies with TLK-1 isolated from yeast extract

Our model suggests that TLK-1 interacts with Ipl1 to potentiate Ipl1 kinase activity. Although kinase-substrate interactions are often transient, we sought to determine if TLK-1 interacts with Ipl1 *in vivo*. A strain expressing myc-tagged Ipl1 under its native promoter was transformed with an empty vector control or V5-tagged WT TLK-1, TLK-1KD, TLK-1(S634A), and TLK-1(S634E) (Figure 9A). Protein extracts were made from these myc-Ipl1/V5-TLK-1 strains after growth in galactose to induce TLK-1 expression. V5-TLK-1 was immunopurified with the V5 antibody and the presence of myc-Ipl1 was assessed by western blot analysis (Figure 9A). Myc-Ipl1 co-purified with TLK-1 regardless of the mutational status of TLK-1. V5 immunoprecipitations from empty vector-containing cells did not display myc-Ipl1 confirming the specificity of the TLK-1/Ipl1 interaction. These results suggest that

Figure 8. Kinase-inactive TLK-1 suppresses *ipl1-2* lethality

ipl1-2 cells and a wild type isogenic strain were transformed with the empty vector (control) or a galactose-inducible plasmid expressing catalytically inactive TLK-1, serially diluted five-fold, plated and grown on galactose or glucose medium at (A) 25°C or B) 30°C for five days.

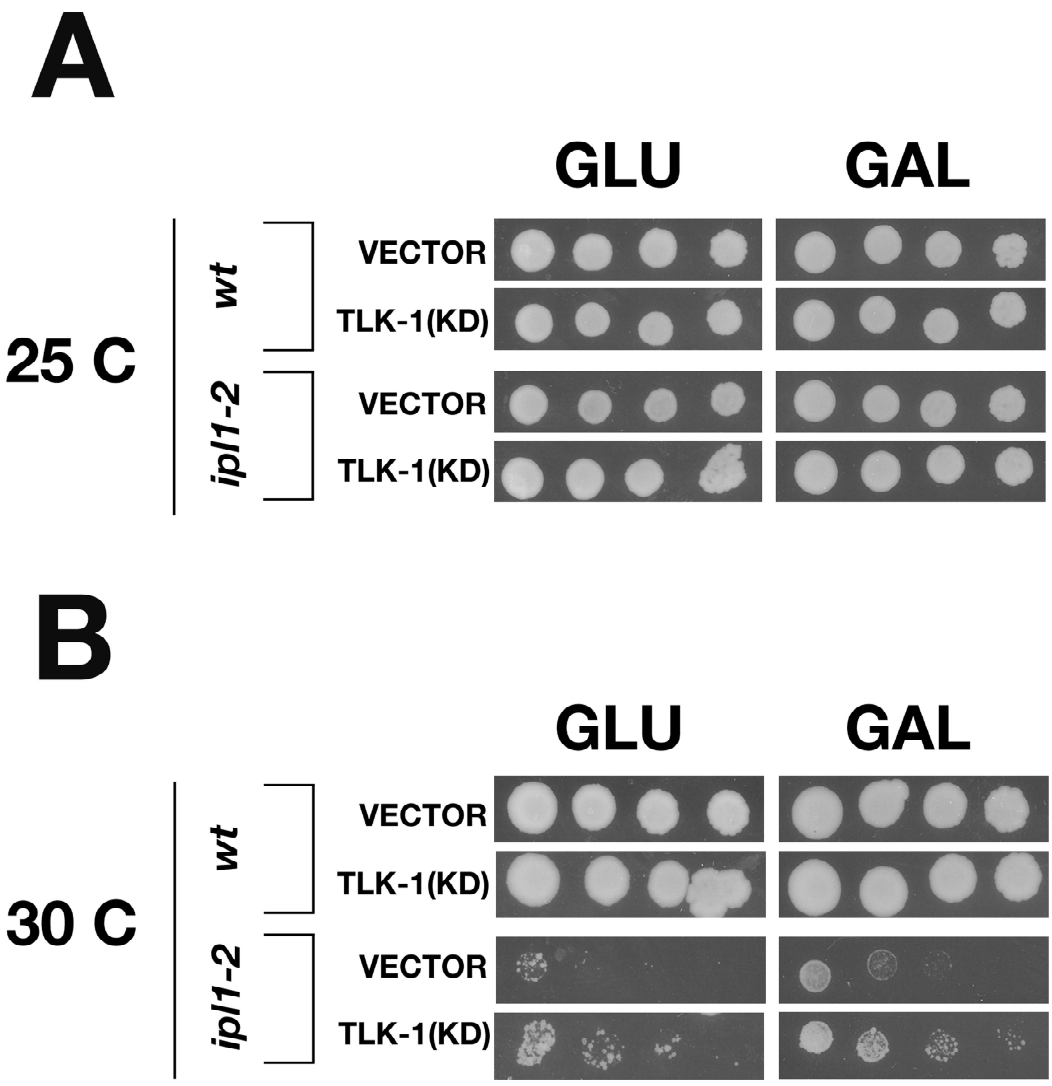
A
GLU
GAL
25 C
wt
ipl1-2
VECTOR
TLK-1(KD)
VECTOR
TLK-1(KD)
B
GLU
GAL
30 C
wt
ipl1-2
VECTOR
TLK-1(KD)
VECTOR
TLK-1(KD)

Figure 9. TLK-1 immunopurifications contain Ipl1

A) The indicated V5-tagged TLK-1 proteins were isolated from a myc-Ipl1 expressing strain using an anti-V5 antibody, separated on SDS-PAGE, and subject to Western analysis. The blots were probed with an anti-myc antibody to visualize the co-precipitation of myc-Ipl1 and then stripped and reprobed with an anti-V5 antibody to detect TLK-1. An anti-V5 IP from myc-Ipl1 cells transformed with an empty vector served as a negative control. Lanes are as follows: LD: load; S: supernatant after pelleting V5 Protein G beads; P: washed V5 Protein G bead pellet. B,C) The myc-Ipl1 strain transformed with wt V5-TLK-1 was arrested in G1 with alpha-factor, followed by wash-out and resuspension into fresh medium without the drug. The mitotic index was assessed by visual examination of bud size (large indicates mitosis) from aliquots taken 0, 1, 2, and 3 hours post-release, and cells were subjected to lysis followed by B) Western analysis of whole cell extract with V5 and myc antibodies, and C) Immunoprecipitation with V5 antibodies followed by western analysis with the indicated antibodies. Extracts from each time point had similar amounts of protein as visualized by Ponceau S staining (Load).

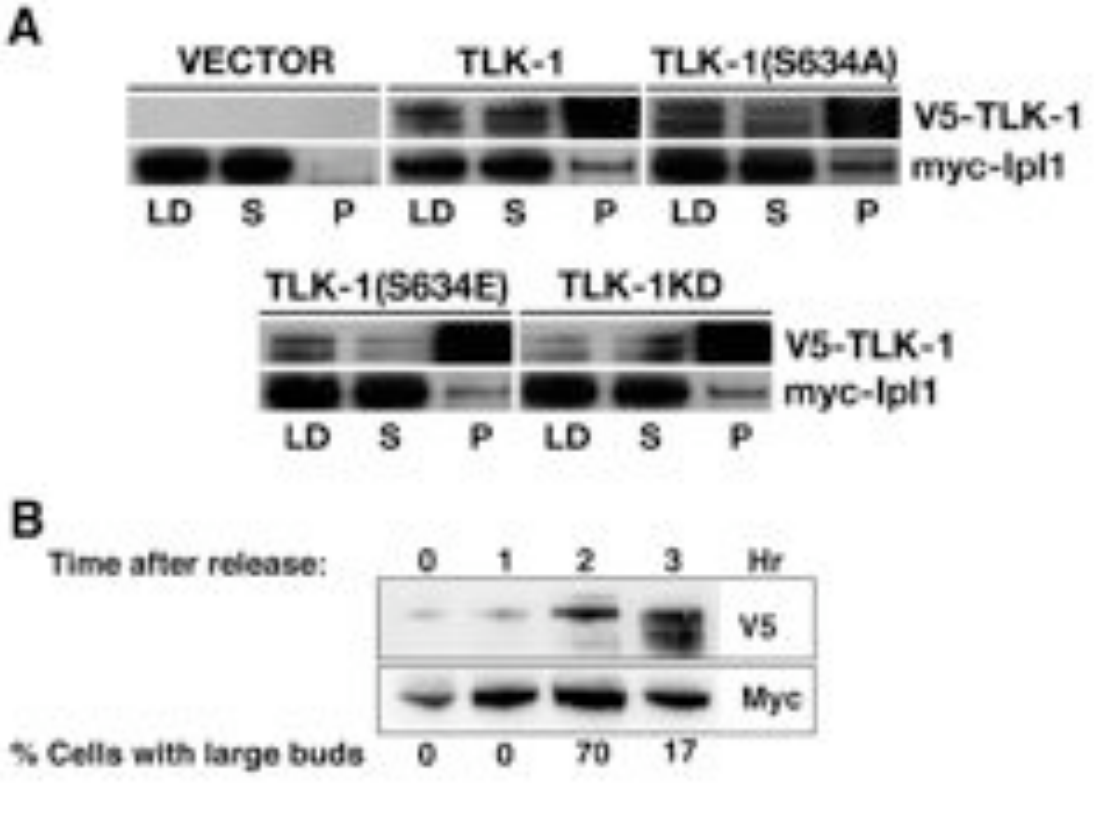
A
VECTOR
TLK-1
TLK-1(S634A)
V5-TLK-1
myc-Ipl1
LD S P LD S P LD S P
TLK-1(S634E)
TLK-1KD
V5-TLK-1
myc-Ipl1
LD S P LD S P
B
Time after release:
0 1 2 3 Hr
V5
Myc
% Cells with large buds
0 0 70 17
C
IP:V5
Time after release:
0 1 2 3 Hr
V5-TLK-1
myc-Ipl1
Load
% Cells with large buds
0 0 70 17

TLK-1 incorporates into an Ipl1-containing complex *in vivo* and that the TLK-1 mutants are not grossly defective in protein folding or stability.

Ipl1 is highly active during mitosis but is also expressed in S-phase, albeit at reduced levels (204). Because Tousled kinases function predominantly during S-phase, we wanted to determine if TLK-1 co-purifies with Ipl1 during mitosis. Moreover, yeast kinetochores bind microtubules throughout the cell cycle suggesting that TLK-1 may be enhancing potential S-phase Ipl1 functions related to the kinetochore (205). To determine the temporal association of Ipl1 and TLK-1, the myc-Ipl1 strain was grown in galactose to promote wild type V5-TLK-1 expression followed by an alpha-factor G1 arrest. Aliquots taken at 0,1, 2, and 3 h after release into fresh medium were visually inspected for the presence of large buds (indicative of mitosis) and subjected to immunoprecipitation with the anti-V5-TLK-1 antibody. Although the galactose concentration remained constant throughout the experiment, V5-TLK-1 protein levels were highest during mitosis (Figure 9B) and V5 immunoprecipitates contained myc-Ipl1 (Figure 9C). Therefore, we conclude that TLK-1 robustly associates with Ipl1 during mitosis. Furthermore, TLK-1 appears to become stabilized specifically during mitosis, perhaps via Ipl1 binding or phosphorylation.

Although V5-TLK-1 immunopurifications contained Ipl1, high concentrations of TLK-1 had to be isolated to detect the interaction (Figure 9A). We were comforted by the fact that *S. cerevisiae* kinetochore proteins are expressed at very low levels, making their identification by immunoprecipitation technically difficult by requiring large volumes of yeast extract (205). However, we reasoned that confirming the TLK-1/Ipl1 interaction via an independent and more stringent method would support our conclusion that TLK-1 associates with Ipl1.

The TAP-tag method is a tandem-affinity purification procedure consisting of two rounds of protein purifications (206). The TAP tag consists of a TEV protease cleavage site floxed by protein A and calmodulin-binding peptide domains. TAP-tagged proteins and their interactors are precipitated by IgG::Agarose, re-solubilized by TEV cleavage of crude complexes, and re-purified with a calmodulin-immobilized resin (206). This two-step procedure has been utilized to elucidate the molecular composition of many protein complexes in a variety of organisms. To determine if TLK-1 associates with highly

purified Ipl1 complexes, a strain expressing TAP-Ipl1 from the *IPL1* endogenous locus was transformed with the wild type TLK-1 plasmid. Cells were incubated in galactose-containing medium to induce TLK-1 expression and protein extracts were generated for immunoprecipitation. Western analysis of the eluates after the two-step purification revealed the presence of V5-TLK-1 in samples enriched for TAP-Ipl1 (Figure 10). Moreover, V5-TLK-1 protein levels were proportional to the amount of TAP-Ipl1 suggesting a likely 1:1 or 1:2 (due to TLK-1 dimerization) stochiometric relationship (Figure 10). These results provide strong evidence that TLK-1 incorporates into Ipl1 complexes *in vivo*.

Ipl1 isolated in the presence of TLK-1 exhibits increased kinase activity

We speculated that TLK-1-induced suppression of *ipl1ts* lethality correlated with increased Ipl1 kinase activity that was dependent on TLK-1 S634 phosphorylation (123). To decipher if V5-TLK-1 augments myc-Ipl1 activity *in vivo*, we transformed kinase-dead (KD) TLK-1 constructs into the myc-Ipl1 strain. The myc-Ipl1 strains were grown in galactose to induce TLK-1KD, TLK-1KD(S634A), and TLK-1KD(S634E) expression followed by protein purification and immunoprecipitation with the V5 antibody. In parallel cultures, myc-Ipl1 complexes were isolated from the myc-Ipl1 strain transformed with the empty V5 vector by α-myc immunoprecipitation. We compared the level of myc-Ipl1 kinase activity in the presence or absence of the TLK-1 mutants by performing kinase assays with the precipitated proteins and endogenously added MYBP as substrate (Figure 11, A and B). Protein levels of V5-TLK-1 and myc-Ipl1 were assessed by western analysis with the appropriate antibodies. TLK-1KD immunoprecipitations showed a significant increase (~6-8-fold) in MYBP phosphorylation compared with myc-Ipl1 immunoprecipitations (Figure 11, A and B). However, the phosphorylation status of TLK-1 at S634 did not influence Ipl1 activity in this assay since TLK-1KD increased Ipl1 activity to similar levels irrespective of the S634A or S634E mutations. Altogether, we conclude that TLK-1 interacts with Ipl1 and, by a function independent of TLK-1 kinase activity, increases Ipl1 function to suppress *ipl1ts* defects.

Figure 10. TLK-1 co-precipitates with TAP-Ipl1 from yeast extract after a stringent two-step purification

Western analysis of the eluates obtained after the two-step purification for detection of V5-TLK-1 and TAP-Ipl1.

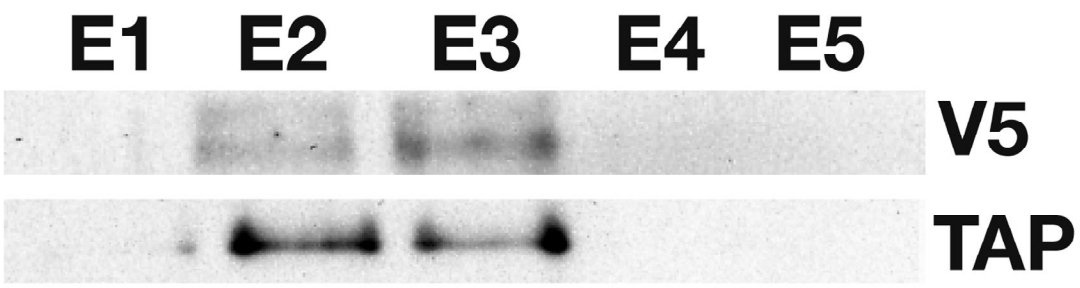
E1
E2
E3
E4
E5
V5
TAP

Figure 11. Kinase-dead TLK-1 increases the kinase activity of Ipl1 immunoprecipitates

(A) The indicated V5-TLK-1 proteins were isolated from myc-Ipl1 yeast extract via V5 immunoprecipitation (IP:V5) and incubated with myelin basic protein (MYBP) to assess the kinase activity of myc-Ipl1 within TLK-1 immunoprecipitates. Myc-Ipl1 was isolated from vector-transformed cells to determine the activity of Ipl1 against MYBP in the absence of kinase-dead TLK-1 (IP::MYC). Lanes labeled 1-4 indicate increasing amounts of myc precipitates to ensure that increased P-MYBP correlates with greater concentrations of Ipl1. (B) Quantitation of MYBP phosphorylation in the indicated TLK-1(KD)-containing Ipl1 immunoprecipitates compared to Ipl1 isolated without TLK-1 (labeled Ipl1). Error bars indicate standard deviations from the means of three independent experiments.

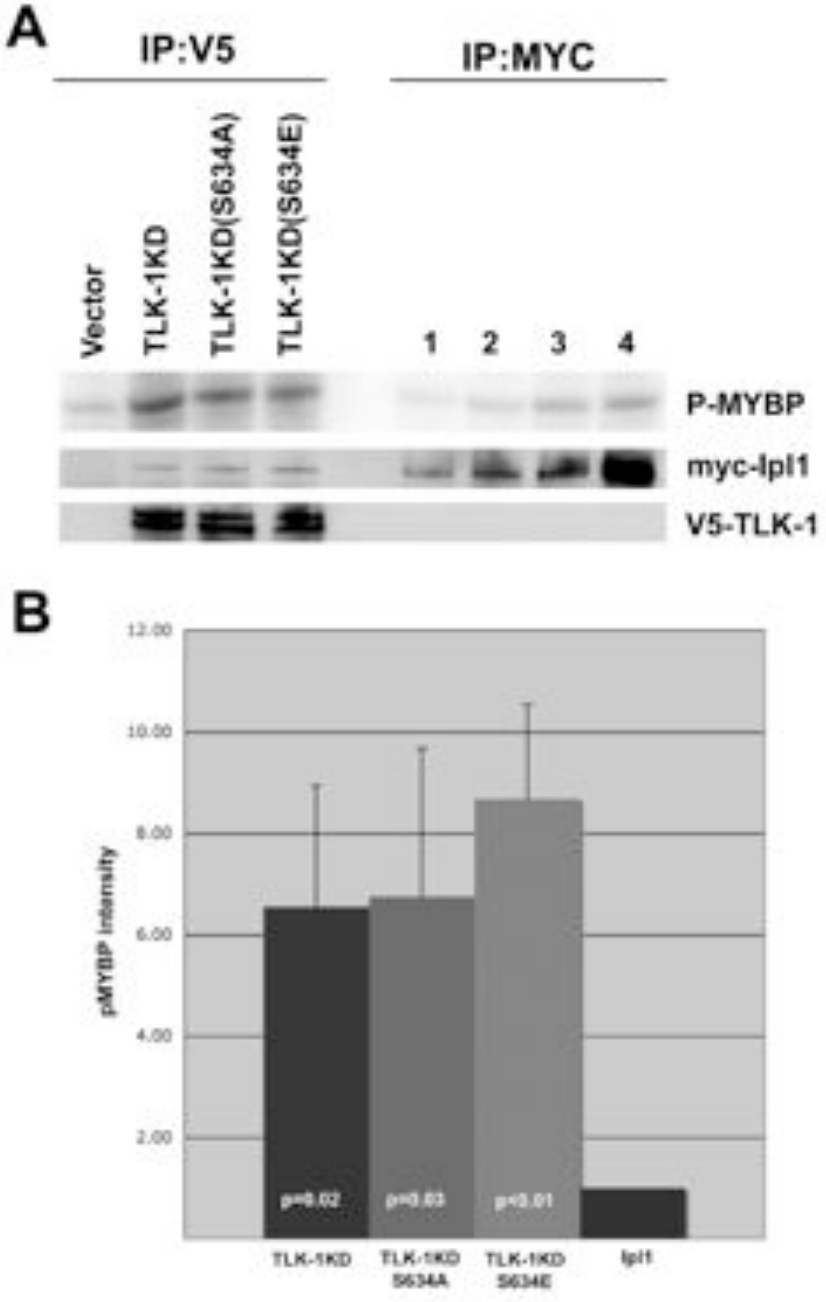
A
IP:V5
IP:MYC
Vector
TLK-1KD
TLK-1KD(S634A)
TLK-1KD(S634E)
1
2
3
4
P-MYBP
myc-Ipl1
V5-TLK-1
B
pMYBP intensity
12.00
10.00
8.00
6.00
4.00
2.00
p=0.02
p=0.03
p=0.01
TLK-1KD
TLK-1KD S634A
TLK-1KD S634E
Ipl1

ZM447439, an Aurora B inhibitor, inhibits AIR-2 but not Ipl1 *in vitro*

We have shown that TLK-1 binds and activates AIR-2 and also associates with and activates Ipl1 (124). These results suggest a conserved mechanism of TLK-1-mediated Aurora B activation independent of TLK-1 kinase activity. However, the functional consequence of Aurora B-mediated TLK-1 S634 phosphorylation remains somewhat unclear. Although TLK-1(S634A) did not suppress *ipl1ts* growth defects (Figure 7, A and B), Ipl1 isolated via TLK-1(S634A) immunoprecipitation displayed kinase activity similar to Ipl1 in wild-type TLK-1 purifications (Figure 11, A and B). Also, *in vitro* assays revealed that TLK-1(S634E) did not significantly increase the kinase activity of Ipl1, yet TLK-1(S634E) suppressed *ipll1ts* lethality (Figure 11 and Figure 7, respectively). If phosphorylation of TLK-1 by AIR-2 confers a subtle structural change to the kinase domain of AIR-2 (similar to the slight conformational change of just a few residues within the Aurora B kinase domain by phospho-INCENP (pg. 44)), the inability of the *in vitro* kinase assays to reveal a TLK-1(S634E)-dependent increase in Ipl1 activity could be due to evolutionary differences in kinase domain residues or tertiary structures of Aurora B homologs.

Drug inhibition can provide evidence of structural changes in homologous proteins. For instance, structure-based approaches utilizing three-dimensional structural models of Aurora kinase domains have been instrumental in designing small molecule inhibitors selective for Aurora A or Aurora B (207). Thus, an drug inhibitor of higher eukaryotic Aurora B may not efficiently inhibit Aurora B homologs in lower eukaryotes due to subtle changes in the kinase domain. ZM447439 is a selective small molecule inhibitor of human Aurora B and is twenty-times more potent against Aurora B than Aurora A (107). To determine if ZM447439 inhibits lower eukaryotic Aurora B homologs at similar concentrations, bacterially-expressed recombinant AIR-2 and Ipl1 were purified and used for *in vitro* kinase assays with MYBP serving as a substrate. The reactions were separated by SDS-PAGE, transferred to a nitrocellulose membrane, Ponceau S stained to determine the amount of MYBP, and probed with the GST antibody to detect AIR-2 and Ipl1 (Figure 12, A and B). Autoradiography revealed a pronounced decrease in AIR-2 phosphorylation of MYBP in the presence of 500nM ZM447439 (Figure 12A). In stark contrast, MYBP phosphorylation by Ipl1 was not

Figure 12. ZM447439, an Aurora B inhibitor, does not inhibit Ipl1 catalytic activity
A) Bacterially expressed GST::AIR-2 was incubated with MYBP as substrate and either DMSO vehicle control (0) or increasing concentrations of ZM447439. AIR-2 activity was determined by MYBP phosphorylation (P-MYBP). The amount of AIR-2 was determined by western analysis with GST antibody while Ponceau S staining revealed MYBP levels. B) Parallel reactions were performed as in (A) with *E. coli* expressed GST::Ipl1 substituting for AIR-2.

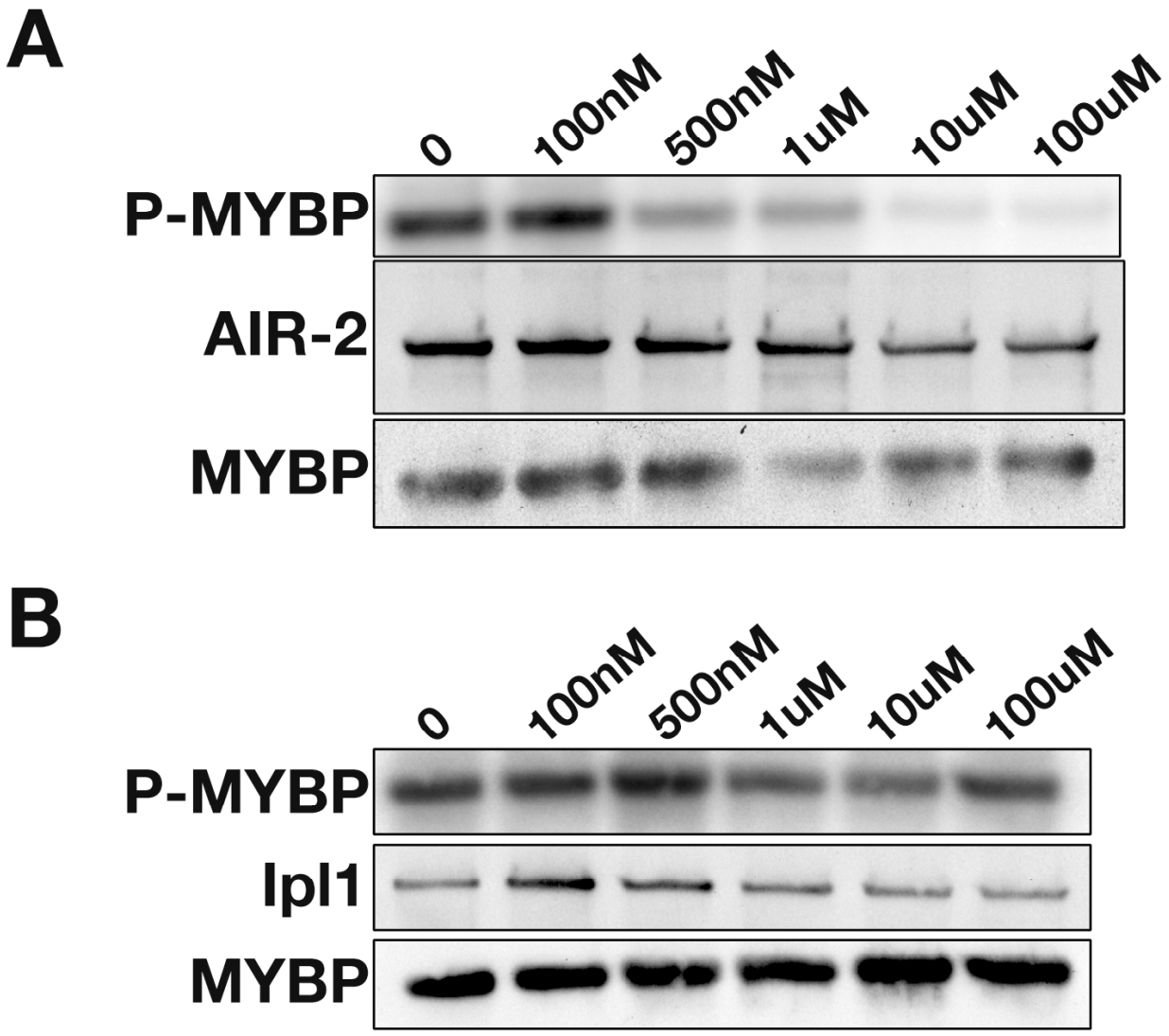
A
0
100nM
500nM
1uM
10uM
100uM
P-MYBP
AIR-2
MYBP
B
0
100nM
500nM
1uM
10uM
100uM
P-MYBP
Ipl1
MYBP

greatly affected by ZM447439 (Figure 12B). These data imply that Aurora B kinase domains have diverged during evolution to be differentially susceptible to Aurora B-specific drugs that inhibit kinase domain function. However, Aurora B homology among species is most conserved in kinase domain residues (Figure 6). These points suggest that the tertiary structure of the Ipl1 kinase domain has subtle differences compared to its higher eukaryotic counterparts.

The expression of ICP-1 also suppresses *Ipl1* mutants

Genetic screens performed with *S. cerevisiae* have identified conserved proteins that function in critical cellular pathways including the SAC (89). In principle, a genetic screen for suppression of *ipl1ts* growth defects by the heterologous expression of higher eukaryotic Aurora B activators may identify novel Aurora B agonists. To determine if another bona fide Aurora B activator suppresses *ipl1ts* growth defects, ICP-1-mediated suppression of the *ipl1-2* phenotype was an analyzed. Indeed, ICP-1 expressed from a high-expression vector rescued *ipl1-2* growth defects at the restrictive temperature (Figure 13). Surprising, AIR-2 expression from the same plasmid could not efficiently substitute for Ipl1 function (Figure 13). This result implies that Aurora B activators but not Aurora B itself can be substituted across species to functional complement Ipl1 function. In light of the drug inhibition studies, the inability of AIR-2 to substitute for Ipl1 corroborates the idea that Aurora B kinase domains have diverged through evolution. Altogether, these data provide proof-of-principle that *ipl1ts* suppression by higher eukaryotic Aurora B activators will help identify additional regulators of Aurora B.

Discussion

C. elegans TLK-1 suppresses the lethality of multiple *Ipl1ts* mutants

The data presented here provide clear evidence that TLK-1 kinase activity is not a functional requirement for Aurora B activation. TLK-1 suppressed the growth defects of two *ipl1ts* alleles (124). Two different biochemical approaches confirmed the TLK-1/Ipl1 interaction and cell synchronization studies determined that the interaction is

Figure 13. AIR-2 and ICP-1 suppress the growth defect of an *ipl1* mutant

Wild type and ipl1-2 yeast transformed with either an empty vector, or galactose-inducible plasmids expressing *Ce*ICP-1 and *Ce*AIR-2 were plated on galactose medium and incubated at the restrictive temperature (30°C) for five days.

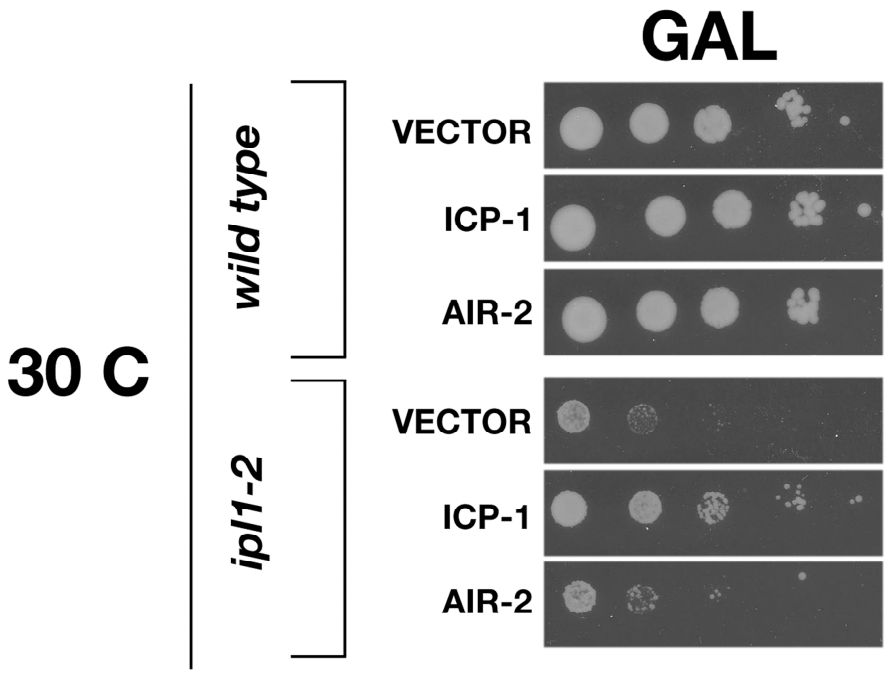
GAL
30 C
wild type
ipl1-2
VECTOR
ICP-1
AIR-2
VECTOR
ICP-1
AIR-2

prevalent during mitosis. Also, TLK-1 activates the kinase activity of Ipl1 complexes purified from yeast extract. Altogether, these data complement our previous studies highlighting a crucial role for TLK-1 in Aurora B activation (123).

Ipl1-1 and *ipl1-2* cells have defective chromosome segregation at non-permissive temperatures (106). Ipl1 function is critical for bipolar spindle attachment of kinetochores to microtubules (204). Therefore, TLK-1-promoted *ipl1ts* suppression likely corresponds to activation of Ipl1-dependent correction mechanisms at kinetochores. However, *ipl1-315* cells that carry a temperature-sensitive allele of *IPL1* are defective in spindle assembly and not kinetochore correction mechanisms (208). Since Ipl1 participates in spindle assembly independent of its role at kinetochores, an alternative conclusion is that TLK-1 increases this function of Ipl1 to promote *ipl1ts* cell growth. To void this argument, chromosome-sectoring assays in TLK-1-expressing *ipl1ts* cells would confirm increased rates of equivocal chromosome segregation. Another method to study chromosome movement *in vivo* is to express fluorophore-conjugated Lac repressor protein in *ipl1ts* strains harboring chromosomal Lac operator arrays. Lastly, determining the localization of V5-TLK-1 in *ipl1ts* cells by immunofluorescence would provide evidence of either a kinetochore or spindle pole-based function of TLK-1.

The discrepancy between the genetic versus biochemical evidence that TLK-1 S634 phosphorylation plays on TLK-1-mediated Ipl1 suppression

Our genetic analyses revealed that TLK-1 S634 phosphorylation likely plays a critical role in Ipl1 activation since TLK-1 S634A could not suppress *ipl1ts* growth defects. However, Ipl1 isolated in the presence of TLK-1 S634A displayed higher kinase activity compared to Ipl1 without TLK-1 *in vitro*. Although the latter results seem to contradict the activating function of TLK-1 S634 phosphorylation to Ipl1, several explanations for this discrepancy are possible. Firstly, the genetic suppression assays may be more sensitive to Ipl1 function than the kinase assays. Secondly, myelin basic protein is a ubiquitously-used substrate for kinase assays and may not be a perfect indicator of Ipl1 activity. Ipl1 has many substrates *in vivo*, and TLK-1 may be activating Ipl1 function toward a subset of these proteins. Thirdly, TLK-1 S634 phosphorylation

may promote *in vivo* substrate/Ipl1 interactions and this function of TLK-1 would not be revealed by *in vitro* kinase assays. Fourthly, TLK-1 phosphorylation may influence Ipl1 subcellular localization in addition to Ipl1 kinase activity, with both contributing to *ipl1ts* suppression. Regardless of the exact mechanism, the data presented here show that TLK-1 S634 phosphorylation but not kinase activity is critical for Ipl1 activity *in vivo*.

Elucidating mechanisms of Aurora activation will greatly inform the design of therapeutic interventions to reduce Aurora activity in cancer cells. The analysis of gene expression profiles in a variety of human tumors suggests an expression signature linked to chromosomal instability. Interestingly, this expression profile revealed increased levels of Aurora family members (94). Since TLK-1 kinase activity is dispensable for Aurora B activation, pharmacological intervention of S634 phosphorylation but not TLK-1 kinase activity may be a targeted approach for decreasing Aurora B activity in tumors. The biostructural mechanism of Aurora activation by protein interactors is beginning to be unveiled. TPX2-mediated Aurora A activation is elicited by a dramatic conformational change of the Aurora A kinase domain by TPX2 binding (209, 210). Aurora A auto-phosphorylation of critical kinase domain residues exposed by the TPX2 interaction greatly facilitates Aurora A activation (211). In addition, TPX2 prolongs Aurora A activity by shielding the auto-phosphorylated residues from PP1-dependent dephosphorylation (212). Structural studies have revealed that the binding of INCENP to Aurora B causes a subtle alteration and partial activation of the kinase domain of Aurora B (119). Aurora B-mediated phosphorylation of INCENP changes intramolecular amino acid interaction in Aurora B to achieve full kinase activation (115, 213). Future studies will determine the exact structural mechanism of TLK-1-mediated AIR-2 activation. Recently it was reported that Aurora B in trypanosomes interacts with and becomes activated by a Tousled homolog in that organism (214). These data indicate that Aurora B activation by Tousled kinases is a conserved functional interaction. Future research will discover if this particular function of Tousled kinases is conserved in mammals.

CHAPTER THREE: A TETHERED-CATALYSIS YEAST TWO-HYBRID SCREEN IDENTIFIES CANDIDATE PHOSPHO-TLK-1 INTERACTORS

Introduction

The TLK-1 domain surrounding S634 may be functionally influenced by additional phosphorylations

The data presented in Chapter Two revealed that TLK-1 phosphorylation at S634 (P-S634) was critical to activate *ipl1ts* function. Interestingly, the TLK-1 domain in which S634 lies is structurally related to a region of PKA (**p**rotein **k**inase **A)** that is highly post-translationally modified (Maria Schumacher, personal communication) (215). We therefore hypothesized that phosphorylation of TLK-1 at S634 and nearby residues may influence protein interactions with TLK-1.

Post-translational modifications impact a myriad of protein functions including protein-protein interactions. For example, the polo box domain of Plk1 binds target proteins after they are "primed" by Cdk1 or Plk1 phosphorylation (216). 14-3-3 σ proteins are another class of molecules that interact specifically with phosphorylated proteins (217). The phosphorylated residues of 14-3-3 σ and Plk1 interactors directly mediate the interaction. However, not every protein that interacts with a phosphorylated target does so by binding directly to phospho-residues. For example, cyclin B1 interacts with separase downstream of a Cdk1-primed phosphorylation site (218). This interaction is dependent on the phosphorylation, but does not bind directly at the phospho-site. Each of the phosphorylation-promoted interactions described above influence critical cell cycle events confirming that phosphorylation is a key regulator of functional protein-protein interactions.

A tethered-catalysis yeast two-hybrid screen to identify phospho-specific binding partners

The yeast two-hybrid (Y-2-H) screen has been instrumental in the identification of novel protein-protein interactions that influence particular biological processes (219). In a conventional Y-2-H screen, the "bait" is a protein of interest fused to the Gal4 DNA binding domain (DBD). "Prey" constructs consist of proteins fused to the Gal4 transactivation domain (ACT). Protein interaction between the bait and prey brings the

two essential Gal4 modules together to facilitate Gal4-dependent transcription of reporter genes (219).

Y-2-H screening for phosphorylation-specific interactions presents an obstacle since phosphorylation events are notoriously labile (116). One method to obtain phosphorylated bait is to co-express a kinase *in trans* from a separate vector. Although this method is feasible, phosphorylation of the bait would be dependent on several factors: 1) Since the Gal4 DBD contains a nuclear localization sequence, the phosphorylation event must occur or persist in the nucleus; 2) The kinase vector would require an additional auxotrophic selection marker, stressing the cells; 3) potential cell lethality caused by kinase overexpression.

Recently, a tethered-catalysis Y-2-H screen was devised to allow for constitutive *in cis* bait phosphorylation (220). The bait protein in a tethered-catalysis screen is a chimera of an enzyme tethered to its substrate. The strength of this method for identifying phospho-specific interactions is that substrate phosphorylation is constitutive. The developers of this modified screen successfully identified proteins that interact with acetylated residues of histone H3 in a Gcn5::H3 peptide chimera (220). Also, a separate screen identified proteins that bind phosphorylated residues within the CTD of RNA polymerase II (RNA pol II) (220).

The master bait: A chimera of AIR-2 and a TLK-1 peptide

We hypothesized that AIR-2 phosphorylation of TLK-1 at S634 promoted TLK-1 interactions. Since the majority of AIR-2 residues (82.6%) constitute the functional kinase domain (Figure 6), full-length AIR-2 was used as the enzymatic core of the bait chimera. The ideal length of the TLK-1 peptide used in the chimera was difficult to determine since the function of residues neighboring S634 were unknown. Considering that phospho-TLK-1 interactors may bind upstream or downstream of P-S634, a sixty-one amino acid TLK-1 peptide surrounding S634 was used as the substrate. Thus, the bait protein was full-length AIR-2 tethered to a sixty-one amino acid sequence of TLK-1 surrounding S634 (notated **Wt-S**) (Figure 14A). The chimera also contained a Gal4

Figure 14. Outline of the tethered-catalysis yeast two-hybrid (Y-2-H) screen

A) Diagram of the bait chimeras used in the initial screening of a *C. elegans* cDNA prey library. B) Outline of the screening procedure (see Materials and Methods for a more detailed description).

A

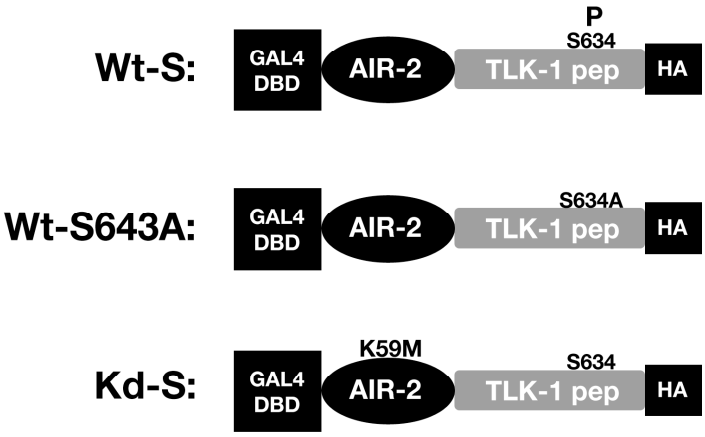

B

Transform PJ694a strain with Wt-S

↓ trp selection

Transform with *C. elegans* cDNA pACTII prey library

FIRST ROUND ↓ trp & leu selection; *GAL1-HIS3* reporter

Isolate pACTII plasmid from yeast that grow in the absence of histidine

↓ leu selection

Re-transform PJ694a with empty bait vector control or Wt-S

SECOND ROUND ↓ trp & leu selection; *GAL1-HIS3* reporter

Isolate pACTII plasmid from yeast that grow with Wt-S expressed but not vector control

↓ leu selection

Sequence pACTII plasmid to determine the identity of the interactors

↓

Determine if the interactions require TLK-1 S634 or AIR-2 kinase activity within the bait chimera

DBD and an HA-tag for biochemical identification (Figure 14A).

The screening procedure

The Wt-S chimera was used to screen a *C. elegans* cDNA prey library for potential phospho-TLK-1 interactors. "Hits" were then rescreened with empty bait vector to rule out non-specific interactions. The yeast strain used for the screening had a GAL1 promoter upstream of a *HIS3* gene so that growth on medium lacking histidine was used as a sensitive reporter. Additional screening consisted of isolating the prey plasmid and retransforming Wt-S-expressing yeast to confirm the potential phospho-TLK-1/prey interaction. A final round of screening utilized chimeras that would distinguish whether the identified interactions require AIR-2 kinase activity and TLK-1 P-S634. These constructs included kinase-dead AIR-2 tethered to a wild-type TLK-1 peptide (Kd-S) and full-length AIR-2 fused to a TLK-1 peptide harboring the S634A mutation (Wt-S634A) (Figure 14A). Prey plasmids were isolated by auxotrophic selection and sequenced to determine the identity of the candidate phospho-TLK-1 binding proteins. A brief outline of the screening procedure is given in Figure 14B.

Results

The AIR-2::TLK-1 chimera is phosphorylated at S634 in yeast

We posited that TLK-1 S634 phosphorylation would be enriched by tethering AIR-2 to TLK-1. To determine if S634 is phosphorylated in the bait chimera in yeast, protein extracts were obtained from yeast expressing an empty vector control or the Wt-S, Wt-A, and Kd-S chimeras in the presence of phosphatase inhibitors. A TLK-1 P-S634 antibody (described in detail below and (123)) was used to immunoprecipitate chimeric proteins from equal concentrations of protein extract. The immunopurifications were assessed by western analysis with an HA antibody to confirm the presence of the chimeras (Figure 15). As expected, the P-S634 antibody immunoprecipitated the Wt-S chimera suggesting that S634 is phosphorylated *in vivo* (Figure 15). The Wt-A chimera was not recognized by the P-S634 antibody confirming

Figure 15. The AIR-2::TLK-1 chimera is phosphorylated at TLK-1 S634

Yeast expressing the indicated chimeras were grown to log phase, and an antibody that recognizes TLK-1 phosphorylated at S634 (P-S634) was used to immunoprecipitate the chimeras from whole cell extracts (WCE). An immunoblot was probed with an HA antibody to detect the presence of the chimeras in the P-S634 immunoprecipitates (top panel) or WCE (bottom panel). Lane (-): empty vector control.

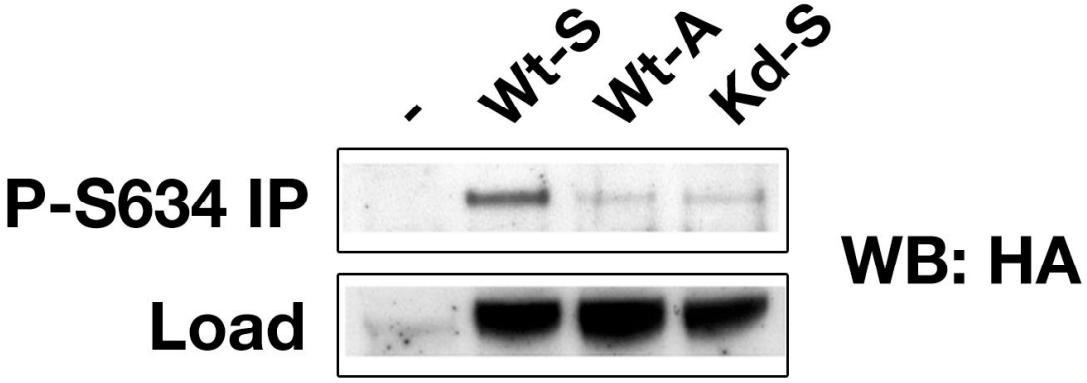
-
Wt-S
Wt-A
Kd-S
P-S634 IP
Load
WB: HA

the specificity of the antibody for the P-S634 epitope. Lastly, the P-S634 antibody did not show immunoreactivity toward Kd-S indicating that AIR-2 kinase activity is required for TLK-1 S634 phosphorylation (Figure 15).

Candidate phospho-TLK-1 interactions require active AIR-2, but not S634

Amazingly, of the thirty-four candidate phospho-TLK-1 interactors identified from this screen (Table 1), each required AIR-2 kinase activity but not P-S634 to interact with the bait (for an example see Figure 16A; the TLK-1/CYB-3 binding results are described in this chapter). These unexpected results did not support the hypothesis that AIR-2-mediated TLK-1 phosphorylation at S634 promotes TLK-1 interactions. However, the requirement of AIR-2 activity in the bait chimera suggested that phosphorylation of other TLK-1 residues promoted the bait-prey interactions. Also, none of the candidate TLK-1 binding proteins interacted with untethered AIR-2 or TLK-1 peptide indicating that the tethering of AIR-2 to TLK-1 is required for the prey interactions (Figure 16A). Intriguingly, the molecular identity of several of these binding proteins indicated that the screen may have uncovered TLK-1 interactors that are related to chromatin biology and mitotic processes.

The candidate TLK-1 interactors can be classified into different groups based on function (Table 1). F54D5.5, NTL-2, and Y18D10A.1 appear to influence chromatin-related processes (WormBase web site, http://www.wormbase.org, release WS204, date 29 Jul 2009). F54D5.5 encodes a protein with ~32% homology with the yeast set2 methyltransferase that influences transcription but does not have a SET domain. Set2 methylates Lys36 of histone H3 and co-purifies with RNA pol II phosphorylated at serine 2 within the CTD repeats (221). Interestingly, *tlk-1(RNAi)* results in decreased RNA pol II P-S2 and transcription defects in embryos (133). Thus, the protein product of the F54D5.5 gene may facilitate TLK-1 function with respect to transcription. NTL-2 (**NO**T-**l**ike) shares homology with the yeast CCR4/NOT complex, which is a basal transcription factor (222). The CCR4/NOT complex is a global regulator of RNA pol II transcription and associates with the chromatin assembly factor CAF1 (222). Since Tousled influences transcription and chromatin assembly, NTL-2 may bridge these TLK-1 functions. The protein encoded by Y18D10A.1 is predicted to contain a region

GENE NAME	SEQUENCE NAME	DESCRIPTION
-	F54D5.5	Homology with *Sc*Set2
-	Y37H2A.1	TatD-related DNase
NTL-2	B0286.4	NOT-like (ScCCR4/NOT complex)
-	Y18D10A.1	Contains HMG domain
CYB-3	T06E6.2	B3-type cyclin involved in sister chromatid separation
TAC-1	Y54E2A.3	Functions with ZYG-9 to promote spindle assembly
-	T09B9.4	Homology with human CCDC6
-	F52H3.2	Meiotic chromosome segregation
TAG-304	F53E2.1	Contains LisH motif involved in MT and dynein binding
CGH-1	C07H6.5	Conserved germline helicase
HEL-1	C26D10.2	Homology to *Hs*UAP56 helicase and splicing factor
FOG-1	Y54E10A.4	cytoplasmic polyadenylation element binding protein
EST-1	Y54F10AL.2	Homology with Ever-short telomere mRNA survelliance
-	Y47G6A.25	Unknown function
LEC-1	W09H1.6	Galectin that forms part of cuticle
UNC-87	F08B6.4	Structure of myofilaments in body wall muscle cells
-	F35H12.1	Unknown function

GENE NAME	SEQUENCE NAME	DESCRIPTION
-	H02I12.1	Unknown function
-	C14A4.11	Putative apoptosis-related protein similar to *Hs*PDCD10
-	Y47G6A.4	Unknown function
-	C15C6.2	Unknown function
SYD-1	F35D2.5	synapse defective PDZ domain protein
-	F36G3.1	Unknown function
EGL-45	C27D11.1	Egg laying defective; homolog of euk translation factor 3
-	C29F9.4	Unknown function
BRA-2	F23H11.1	BMP Receptor Associated Family TGF-beta signaling
SNA-2	T13F2.7	snRNP-binding protein
IFB-2	F10C1.7	Intermediate filament B
RPL-22	C27A2.2	Large ribosomal subunit L22 protein
CCO-1		Cytochrome C Oxidase
TAG-309		Endosome protein sorting
-	C04C3.3	Pyruvate dehydrogenase
ACDH-1		Acyl CoA dehydrogenase
-	F22B3.4	Glucosamine-fructose-6-phosphate aminotransferase

with homology to HMG-1 and HMG-Y (**h**igh **m**obility **g**roup) proteins that regulate transcription and chromosome organization (WormBase web site, http://www.wormbase.org, release WS204, date 29 Jul 2009).

A second group of TLK-1 interactors uncovered in our screen (CYB-3, TAC-1, TAG-304, F52H3.4, and T09B9.4) likely participate in chromosome segregation, particularly by regulating microtubule-related processes. CYB-3 encodes a B3-type cyclin that is required for proper chromosome segregation and SAC silencing (see Chapter 4). TAC-1 (**t**ransforming **a**cid **c**oiled coil (TACC) protein family) activity is essential for microtubule processes including pronuclear migration and mitotic spindle elongation (223). TAC-1 is a crucial centrosomal component that functions with ZYG-9 during spindle assembly to stabilize astral microtubules (224). TAG-304 contains a LisH motif implicated in microtubule dynamics and dynein regulation (225). *tag-304(RNAi)* results in defective adult locomotion and TAG-304 is expressed predominantly during larval and adults stages of development (WormBase web site, http://www.wormbase.org, release WS204, date 29 Jul 2009). Thus, TAG-304 is unlikely to influence TLK-1 functions during embryogenesis. The F52H3.4 gene encodes an uncharacterized protein that may play a role in meiotic chromosome segregation as suggested from genome-wide RNAi screens (66). T09B9.4 is orthologous to human CCDC6 (also known as H4), a putative cytoskeletal protein which when mutated leads to disease (226, 227). The other candidates function in RNA metabolism, energy biosynthetic pathways, and other miscellaneous pathways (Table 1). I chose to pursue the characterization of the interaction between TLK-1 and CYB-3 because the functions of B-type cyclins during *C. elegans* embryogenesis remain largely unexplored. Moreover, results from genome-wide RNAi screens suggested that CYB-3 is involved in sister chromatid separation (66).

Key TLK-1 residues mediate the interaction of TLK-1 with CYB-3

The tethered-catalysis Y-2-H screen was designed to identify phospho-specific interactions (220). However, several caveats are at play when using chimeric proteins. First, a chimera is essentially an "unnatural" protein (protein Z) that is formed from two genuine proteins (protein X and protein Y). Thus, any protein identified in the screen may be interacting nonspecifically with multiple protein Z residues that normally do not

exist in the same molecule. Also, the interactions may occur at the synthetic junction between protein X and protein Y. To gain better insight on the requirement of chimera regions for CYB-3 binding, yeast co-expressing CYB-3 and an empty vector control, Wt-S, Wt-S634A, or Kd-S were serially diluted on non-selection and (-) his-selection plates (Figure 16A). Yeast cell growth was equivalent on non-selection medium regardless of bait construct expression. However, growth on –his medium did not occur in cells expressing vector control or Kd-S, indicating that the kinase activity of AIR-2 is required for CYB-3 binding (Figure 16A). Cells expressing Wt-S and Wt-S634A grew on –his plates, suggesting that the interaction of CYB-3 with these chimeras activated HIS reporter expression (Figure 16A). These data suggest that AIR-2 kinase activity but not TLK-1 S634 phosphorylation contributes to the CYB-3 interaction.

Our previous studies revealed that S634 is a major TLK-1 residue targeted by AIR-2 phosphorylation (123). The requirement for AIR-2 kinase activity within the chimera for interaction with CYB-3 suggested that AIR-2 may phosphorylate additional sites within the TLK-1 peptide. To discern if any of the six S/T residues in the TLK-1 peptide participate in CYB-3 binding, chimeras containing singular alanine substitutions were expressed with CYB-3 and assessed for growth on –his medium (Figure 16B). Interestingly, five of the six TLK-1 residues were dispensable for CYB-3 binding. However, yeast cell growth on selective medium was deficient in cells co-expressing the T610A chimera and CYB-3 (Figure 16B). However, cell growth on non-selective medium was identical for all bait plasmids (Figure 16B). These data implicate T610 as a critical TLK-1 residue that participates in CYB-3 binding.

The failure of CYB-3 to bind the T610A mutant chimera suggested that T610 phosphorylation contributes to this interaction. To determine if the negative charge created by phosphorylation at T610 is critical for the CYB-3 interaction, a T610E chimera was generated. Indeed, the Wt-T610E chimera interacted with CYB-3 similar to Wt-S indicating that a negative charge at T610 is important for the chimera/CYB-3 association (Figure 16C). These data suggest that TLK-1 phosphorylation at T610 is important for CYB-3 binding.

Figure 16. Y-2-H-mediated identification of key TLK-1 residues that are required for the TLK-1/CYB-3 interaction

A) Yeast co-transformed with the indicated bait plasmids and CYB-3 were serially diluted 5-fold and spotted onto non-selective (left panel) and selective (right panel) medium. Wt AIR-2: untethered wild-type AIR-2; Kd AIR-2: untethered AIR-2(K59M); TLK-1(S634): untethered wild-type TLK-1 peptide; TLK-1(S634A): untethered TLK-1(S634A) peptide. B-D) Yeast transformed with plasmids expressing the indicated phospho-mutant and phospho-mimetic chimeras and CYB-3 were serially diluted 5-fold and spotted onto nonselective (left panel) and selective (right panel) medium. E) Yeast treated as in A-D were transformed with the denoted RXL mutant TLK-1 chimeras and CYB-3. R628L; L630R: chimera with TLK-1 R628L and L630R mutations; R645L; L647R: chimera with TLK-1 R645L and L647R mutations; R650L; L652R: chimera with TLK-1 R650L and L652R mutations. F) Amino acid sequence of the TLK-1 peptide highlighting the positions of S/T residues and the RXL motifs.

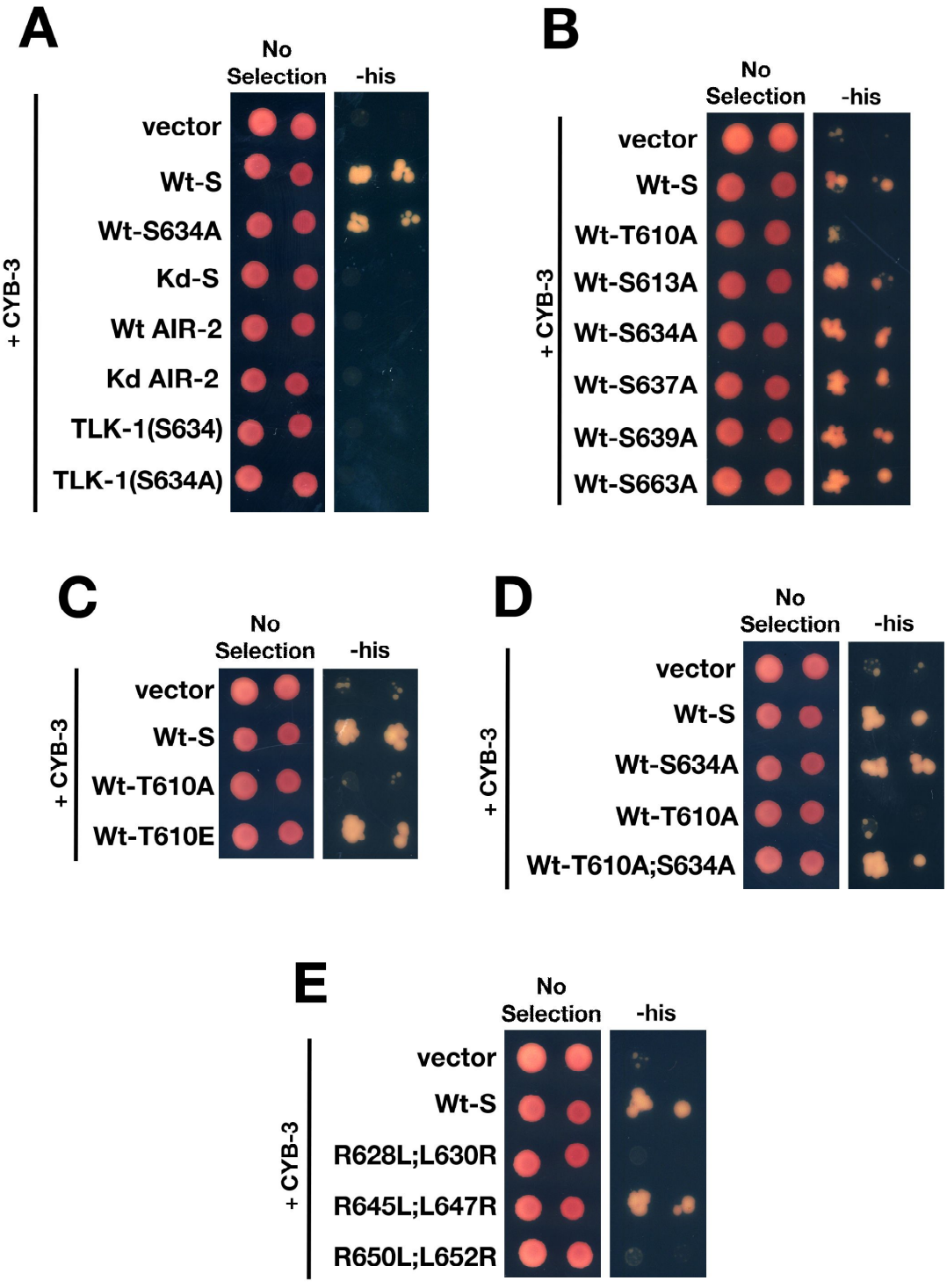

F

TLK-1

AIR-2::HLRKEE**T**DL**S**MEKERLEKEKQHHV**REL**KRA**S**NE**S**A**S**QFNDH**RLL**HK**RYL**MLNLLGKGGF**S**E

610 613 634 637 639 663

We hypothesized that T610 phosphorylation may change the structure of TLK-1 to facilitate CYB-3 binding to residues elsewhere within the TLK-1 peptide. Excitingly, visual inspection of the TLK-1 peptide revealed three RXL motifs within the 60 amino acid sequence. RXL domains mediate interactions with cyclin box folds of cyclin proteins (228). For example, Rb (retinoblastoma protein) harbors RXL motifs that interact with cyclins A and E (229). To ascertain if the TLK-1 RXL motifs influence CYB-3 binding, RXL residues within the chimera were mutated to LXR and their binding to CYB-3 was assessed as above. Indeed, mutation of the first and third RXL motifs of TLK-1 completely abolished CYB-3 binding (Figure 16E). The second RXL sequence was dispensable for the TLK-1/CYB-3 interaction (Figure 16E). Interestingly, the first and third RXL motifs are completely conserved in tousled orthologs (Figure 17) indicating that tousled/cyclin interactions occur outside of nematodes.

Curiously, the first RXL motif in TLK-1 neighbors S634 (Figure 16F). Our biochemical experiments revealed that TLK-1 S634 within the chimera is robustly phosphorylated by AIR-2 in yeast (Figure 15). We hypothesized that phosphorylation at T610 limits P-S634 to facilitate CYB-3 binding to the neighboring RXL motif since post-translational modification (PTM) cross-talk can alter protein function (e.g. the histone "code") (230). Thus, the inability of the T610A chimera to bind CYB-3 may result from the loss of the PTM cross-talk and unrestricted S634 phosphorylation masking the first RXL domain of TLK-1. To determine if limiting P-S634 in the T610A chimera would affect CYB-3 binding, growth on –his medium of yeast co-expressing CYB-3 and a T610A;S634A double mutant chimera was assessed (Figure 16D). Indeed, CYB-3 interacted with the Wt-T610A;S634A chimera similar to Wt-S (Figure 16D) indicating that P-T610 antagonizes P-S634 to promote CYB-3 binding in this system.

TLK-1 P-T610 interacts with CYB-3 *in vitro*

The tethered-catalysis Y-2-H data indicated that phosphorylation at T610 (P-T610) plays a pivotal role in CYB-3 binding. To confirm the necessity of P-T610 for CYB-3 binding, *in vitro* phospho-peptide binding assays were performed with recombinant CYB-3 expressed and purified from bacteria. Due to financial

Figure 17. An alignment of the TLK-1 region used in the chimera with the positions of *C. elegans* T610 and RXL motifs denoted

Clustal W alignment of Tousled homologs with T610 (asterisk) and three RXL motifs (bars) highlighted.


HsTlk2
HsTlk1
DmTlk
CeTLK-1
AtTousled

considerations, the minimal TLK-1 peptide required to interact with CYB-3 was determined by the Y-2-H method (data not shown). These assays suggested that the forty N-terminal residues (harboring only one RXL motif) of the sixty amino acid TLK-1 peptide were sufficient for the CYB-3 interaction. Biotinylated TLK-1 peptides containing no phosphate groups (NON-P), phosphorylated T610 (P-T610), phosphorylated S634 (P-S634), and the dual modification (P-T610;P-S634) were synthesized. These peptides were immobilized on a streptavidin-coated resin and used for pull-down assays with CYB-3. Indeed, CYB-3 interacted with the P-T610 peptide better than the non-phosphorylated or P-S634 peptides confirming the critical nature of P-T610 (Figure 18). CYB-3 did not bind the P-T610;P-S634 peptide suggesting that phosphorylation of S634 inhibits the CYB-3 interaction regardless of the phosphorylation status of T610 (Figure 18). This result confirms the Y-2-H data that suggested that one main function of P-T610 is to inhibit P-S634 since S634 in the P-T610;P-S634 peptide is obligedly phosphorylated, preventing CYB-3 binding. In contrast, if P-T610 is required only to inhibit P-634 to promote the CYB-3 interaction, the non-phospho TLK-1 peptide should have interacted with CYB-3 (Figure 18). Since it did not, these data suggest that P-T610 also appears to promote the CYB-3 interaction independent of P-S634.

TLK-1 phospho-isoforms localize to kinetochores

Our previous immunolocalization studies with a full-length TLK-1 antibody revealed nuclear TLK-1 expression during S-phase and early mitosis (prophase) in *C. elegans* embryos (133). In contrast, the TLK-1 P-S634 antibody displays a peri-chromosomal immunoreactivity during prophase, prometaphase, and metaphase (123). The TLK-1 P-S634 phospho-epitope was severely reduced in *air-2(RNAi)* embryos confirming that TLK-1 S634 is an *in vivo* AIR-2 phosphorylation event (123). To determine if TLK-1 T610 is phosphorylated *in vivo*, a phospho-specific T610 polyclonal antibody was produced and utilized for immunocytochemistry. Interestingly, the P-T610 antibody stained the nuclei of prophase embryos but was enriched near chromosomes (Figure 19A). At prometaphase, P-T610 staining revealed two parallel lines on each sister chromatid pair, a localization consistent with kinetochore proteins (Figure 19A).

Figure 18. Phosphorylation of TLK-1 at T610 enhances CYB-3 binding *in vitro*
Biotinylated TLK-1 peptides were immobilized on streptavidin-coated beads, incubated with recombinant CYB-3 protein, and bound material was run on SDS-PAGE followed by western analysis. The presence of CYB-3 in the load (LD) and TLK-1 peptide bead pellets (BEADS: streptavidin-coated beads with no conjugated TLK-1 peptide; NON-P: an unphosphorylated TLK-1 peptide; P-T610: TLK-1 with phosphorylated T610; P-S634: TLK-1 with phosphorylated S634; P-T610;P-S634: TLK-1 containing both P-T610 and P-S634) was assayed by immunoblotting with the CYB-3 antibody.

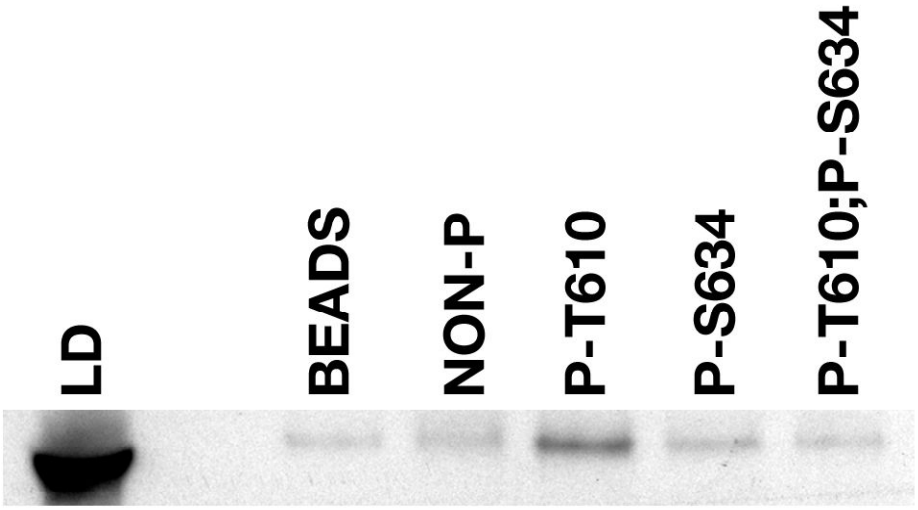

WB: CYB-3

Clear kinetochore and kinetochore-microtubule staining of P-T610 was evident at metaphase, followed by the loss of immunoreactivity during anaphase and telophase (Figure19A). The depletion of TLK-1 by RNAi or genetic deletion consistently reduced P-T610 staining confirming antibody specificity (data not shown). These data provide critical support for mitotic TLK-1 T610 phosphorylation and suggest that P-T610 may influence kinetochore function.

Protein-protein interactions can influence subcellular localization and biological properties. To determine if CYB-3 mediates proper P-T610 localization, embryos were depleted of CYB-3 via RNAi and fixed for immunostaining. The prophase and prometaphase staining of P-T610 in CYB-3-depleted embryos was similar to control (Figure 19A). Interestingly, metaphase P-T610 staining in embryos treated with *cyb-3(RNAi)* did not reveal clear parallel lines flanking sister chromatid pairs and kinetochore-microtubule staining was absent. Robust depletion of CYB-3 results in molecular changes that inhibit entry into anaphase (see Chapter 4). However, P-T610 was not detected during a defective anaphase/telophase in embryos with partial CYB-3 depletion (Figure 19A). These results suggest that CYB-3 may influence the kinetochore localization of P-T610 specifically at metaphase but is not required for P-T610 degradation/dephosphorylation. Additional staining and functional assays have generated support for the alternative explanation that CYB-3 promotes the appropriate architecture of the entire metaphase kinetochore (see Chapter 4).

The localization of TLK-1 P-S634 was initially characterized using limited microscopic resolution without the benefit of deconvolution (123). In these experiments, P-S634 localization was descriptively termed a “halo” around the metaphase chromosomes (123). TLK-1 phosphorylated at S634 activates AIR-2 *in vivo* (123, 124) so it is critical to determine the spatial distribution of P-S634. In light of P-T610 kinetochore staining, P-S634 localized to tensionless/non-amphitelic kinetochores may function to activate AIR-2, severing incorrect attachments to promote biorientation. On the other hand, P-S634 localized as a “halo” around kinetochores would be less likely to interact with AIR-2 at the inner centromere and may not activate AIR-2. To determine the localization of P-S634 with high resolution and deconvolution, embryos treated with control and *cyb-3(RNAi)* were fixed and stained with the P-S634 antibody fractions

Figure 19. TLK-1 phospho-isoforms localize to kinetochores and kinetochore-microtubules

A) Embryos excised from control and *cyb-3(RNAi)*-treated embryos were fixed and stained with DAPI to visualize DNA, an α-tubulin antibody for mitotic spindle detection, and an antibody raised against a TLK-1 P-T610 peptide. B) Embryos treated as in (A) were subject to immunofluorescence with a TLK-1 P-S634 antibody. Scale bar = 10 μm.

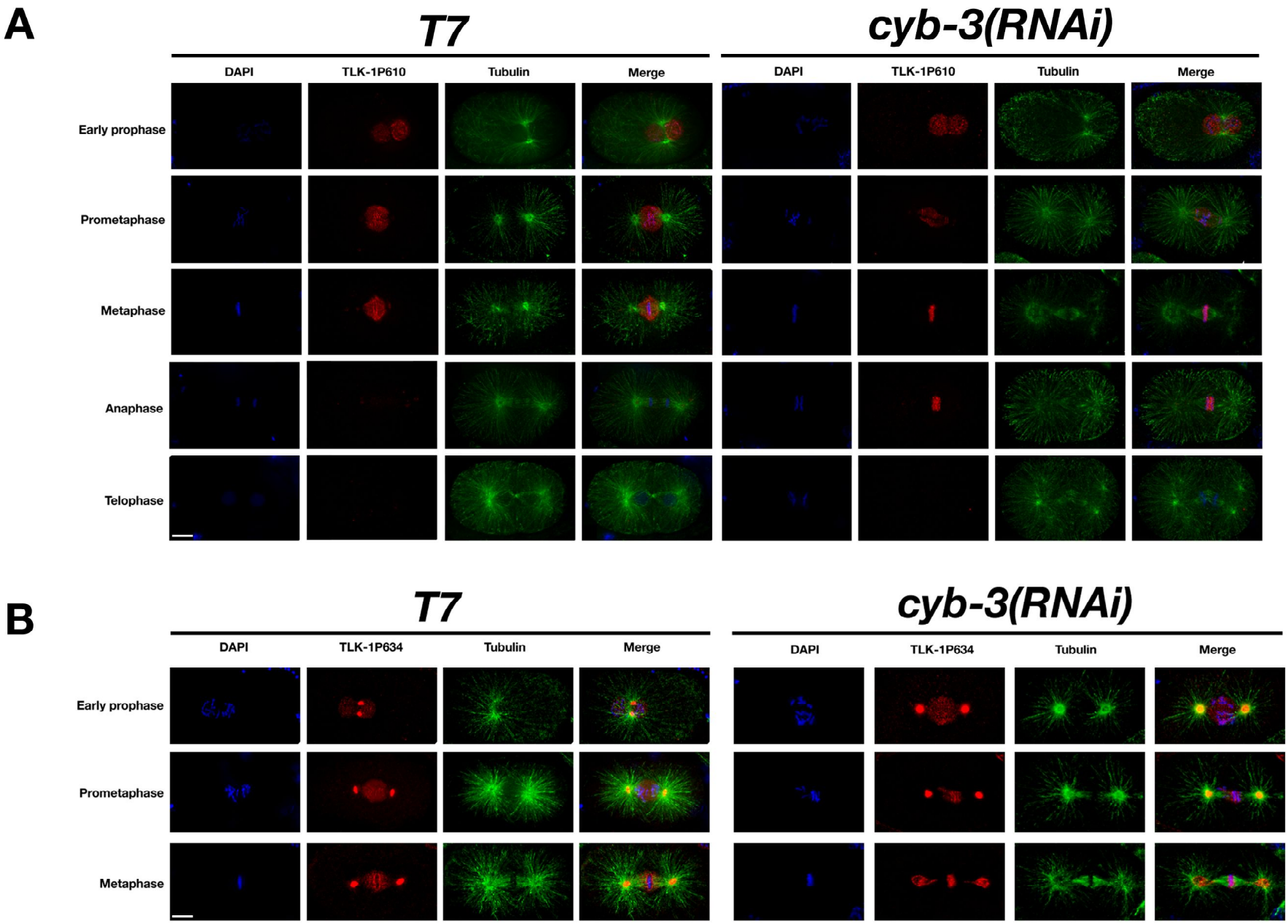
A
T7
cyb-3(RNAi)
DAPI
TLK-1P610
Tubulin
Merge
Early prophase
Prometaphase
Metaphase
Anaphase
Telophase
B
T7
cyb-3(RNAi)
DAPI
TLK-1P634
Tubulin
Merge
Early prophase
Prometaphase
Metaphase

previously utilized for immunostaining (123). Indeed, P-S634 presented parallel stripes of kinetochore staining from prophase to metaphase, and metaphase kinetochore-microtubule staining was obvious (Figure 19B). The localization of P-S634 mimicked that of P-T610 in embryos depleted of CYB-3 with a profound alteration of staining specifically at metaphase (Figure 19B). Lastly, immunostaining with P-T610 and P-S634 revealed centrosome staining (Figure 19, A and B). Our previous data showed that *air-2(RNAi)* decreased peri-chromosomal P-S634 staining but centrosome staining persisted (123). This suggests that P-S634 centrosomal localization is largely artifactual (Figure 19B). The centrosomal staining of P-T610 is much less pronounced than P-S634 and becomes largely depleted in *cyb-3(RNAi)* embryos suggesting that CYB-3 may have play a role in P-T610 localization to centrosomes (Figure 19A). Altogether, these results suggest that phosho-TLK-1 isoforms are produced during mitosis and localize to kinetochores, kinetochore-microtubules, and possibly centrosomes.

AIR-2 does not phosphorylate TLK-1 at T610 in vitro

To begin to characterize the biochemical nature of T610 phosphorylation, we initially focused on AIR-2. AIR-2 kinase activity in the Y-2-H chimera was required for the CYB-3 interaction as was P-T610 (Figure 16A), suggesting that AIR-2 may be the T610 kinase. However, the TLK-1 [K-E-E-T_{610}] amino acid sequence does not match the Aurora B/Ipl1 [K/R-X-S/T_{P}-I/L/V] phosphorylation consensus (111). Also, previous mutagenesis studies did not reveal T610 as an AIR-2 phosphorylation site (123). To determine if AIR-2 phosphorylates TLK-1 at T610, *in vitro* kinase assays were performed with recombinant AIR-2 and full-length TLK-1 kinase-dead (KD) proteins. Corroborating our previous results, TLK-1 (KD) was robustly phosphorylated by AIR-2 but was not phosphorylated when S634 was mutated to alanine (Figure 20, A and B). In contrast, the T610A mutation did not affect AIR-2-mediated TLK-1 phosphorylation (Figure 20, A and B). These data suggest that AIR-2 does not phosphorylate TLK-1 at T610.

Figure 20. AIR-2 does not phosphorylate TLK-1 at T610 *in vitro*

A) Bacterially-expressed recombinant AIR-2 was incubated with the indicated recombinant kinase-dead TLK-1 proteins in kinase reaction buffer. The level of phosphorylated TLK-1 (P-TLK-1) was assessed by autoradiography. The amount of MBP::TLK-1 and GST::AIR-2 was assessed by Ponceau S staining. B) Quantitation of AIR-2-dependent phosphorylation levels of the indicated TLK-1 substrates. Error bars indicate standard deviations from the means of three independent experiments.

A

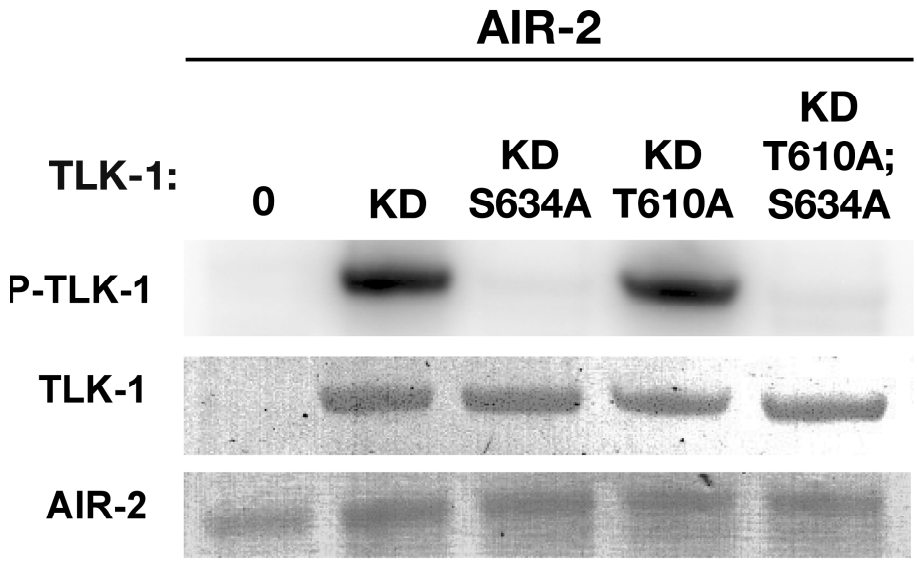
AIR-2
TLK-1:
0
KD
KD S634A
KD T610A
KD T610A; S634A
P-TLK-1
TLK-1
AIR-2

B

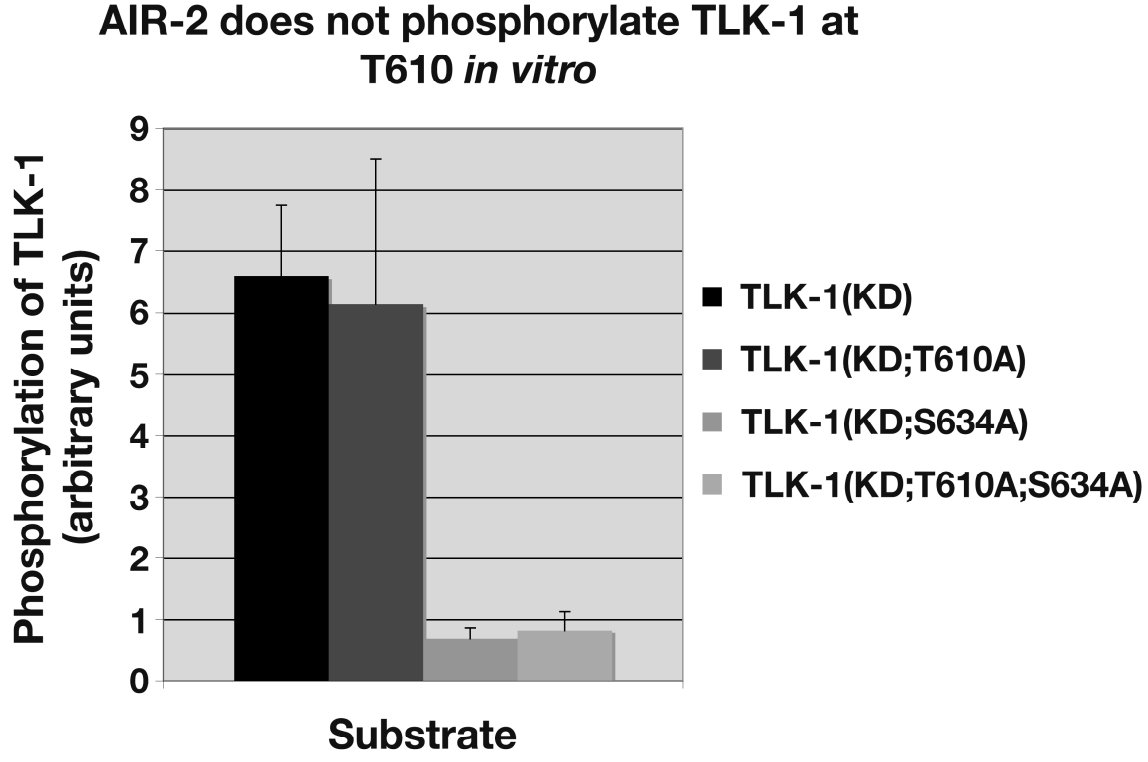
AIR-2 does not phosphorylate TLK-1 at T610 *in vitro*
Phosphorylation of TLK-1 (arbitrary units)
0
1
2
3
4
5
6
7
8
9
Substrate
TLK-1(KD)
TLK-1(KD;T610A)
TLK-1(KD;S634A)
TLK-1(KD;T610A;S634A)

Chk1 phosphorylates TLK-1 at T610

The identification of the kinase that phosphorylates TLK-1 at T610 is a necessary next step to decipher the function of the TLK-1/CYB-3 interaction. However, the identity of kinases that produce particular phospho-epitopes often remains unknown for decades (e.g. the 3F3/2 epitope) (231). *In vitro* kinase assays revealed that P-T610 is not a TLK-1 autophosphorylation event (data not shown). Intriguingly, the TLK-1 [K-E-E-T_{610}] sequence matches the Chk1 phosphorylation sequence (199). Chk1 is a conserved kinase that mediates DNA damage checkpoint signaling during S-phase (199). Interestingly, critical mitotic functions for Chk1 were recently unveiled. Chk1 phosphorylates Aurora B, potentiating Aurora B activity to maintain SAC activation under conditions of altered microtubule dynamics (232). Another Chk1 function is to phosphorylate and inhibit Plk1 activity at metaphase in order to promote the metaphase-anaphase transition (233). These results suggest that Chk1 plays critical roles during mitosis by phosphorylating mitotic kinases. This discovery, combined with the published phosphorylation of human Tousled by Chk1 during the S-phase DNA damage response (131), promoted the exploration of Chk1 as the T610 kinase.

To determine if Chk1 phosphorylates TLK-1, a TLK-1 peptide that contained T610 was tagged with MBP (**m**altose **b**inding **p**rotein), expressed in *E. coli*, and used for *in vitro* kinase assays with human Chk1 (purchased from Active Motive, Carlsbad CA). Unfortunately, several attempts to isolate active bacterially-expressed *C. elegans* CHK-1 failed so the highly homologous hChk1 was substituted. The TLK-1 peptide was strongly phosphorylated by hChk1 and the robustness of this phosphorylation depended on T610 (Figure 21). However, when full-length kinase-dead TLK-1 was used as a substrate for these assays, the T610A mutation had no discernible affect on hChk1-mediated TLK-1 phosphorylation (data not shown). These results suggest additional residues in full-length TLK-1 are targeted by Chk1 phosphorylation and are consistent with previous data showing that human Tlk1 S695 is a major Chk1 phosphorylation site (131). Lastly, qualitative data from immunostaining experiments revealed that P-T610 levels are decreased in embryos derived from a *chk-1* deletion mutant (Figure 22). When taken together, the evidence presented here combined with the newly appreciated

Figure 21. Active human Chk1 phosphorylates TLK-1 at T610 *in vitro*

Human Chk1 was incubated with the indicated *E. coli*-produced recombinant MBP-tagged TLK-1 peptides in kinase reaction buffer. Autoradiography revealed the auto-phosphorylation of Chk1 (to estimate the amount of Chk1 in the reactions) and phosphorylation of TLK-1 (P-TLK-1). An anti-MBP antibody was used to detect the amount of MBP in all reactions including control (MBP). Two reactions containing TLK-1(T610A) purified from two independent *E. coli* cultures are shown.

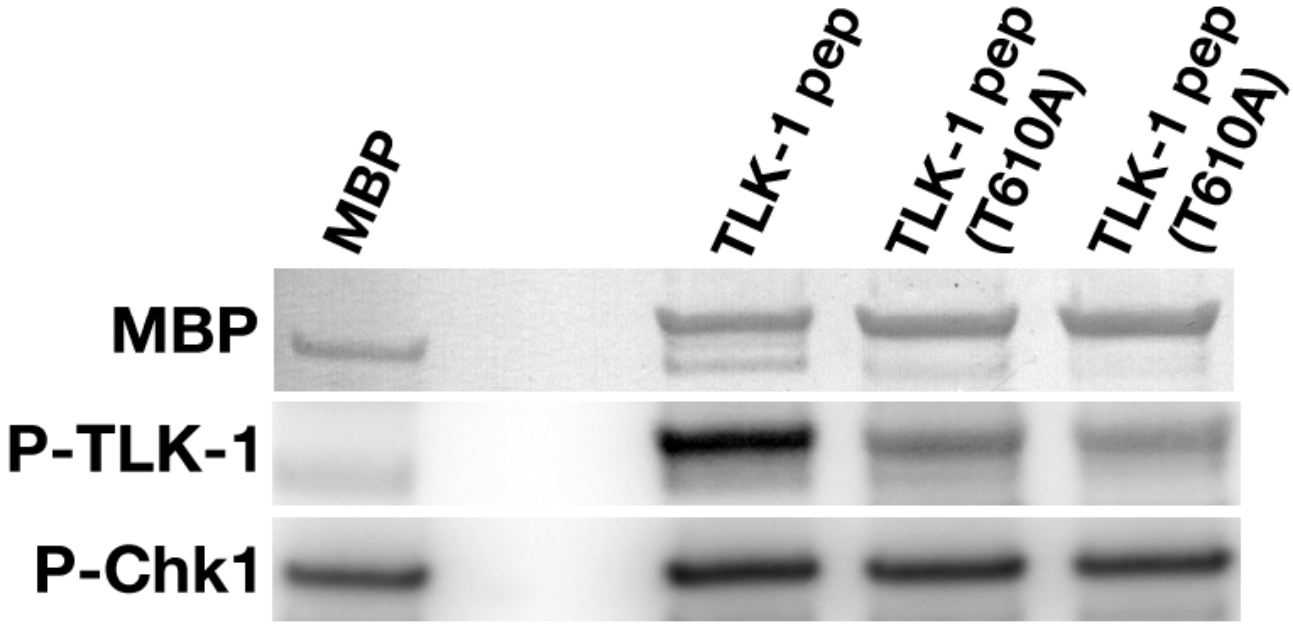
MBP
TLK-1 pep
TLK-1 pep (T610A)
TLK-1 pep (T610A)
MBP
P-TLK-1
P-Chk1

Figure 22. Phosphorylation of TLK-1 at T610 is reduced in *chk-1* embryos

N2 and *chk-1* mutant hermaphrodites were fixed and stained with DAPI (DNA), α-tubulin, and the TLK-1 P-T610 antibody. Shown are representative images of the indicated embryonic stages. Scale bar = 10 μm.

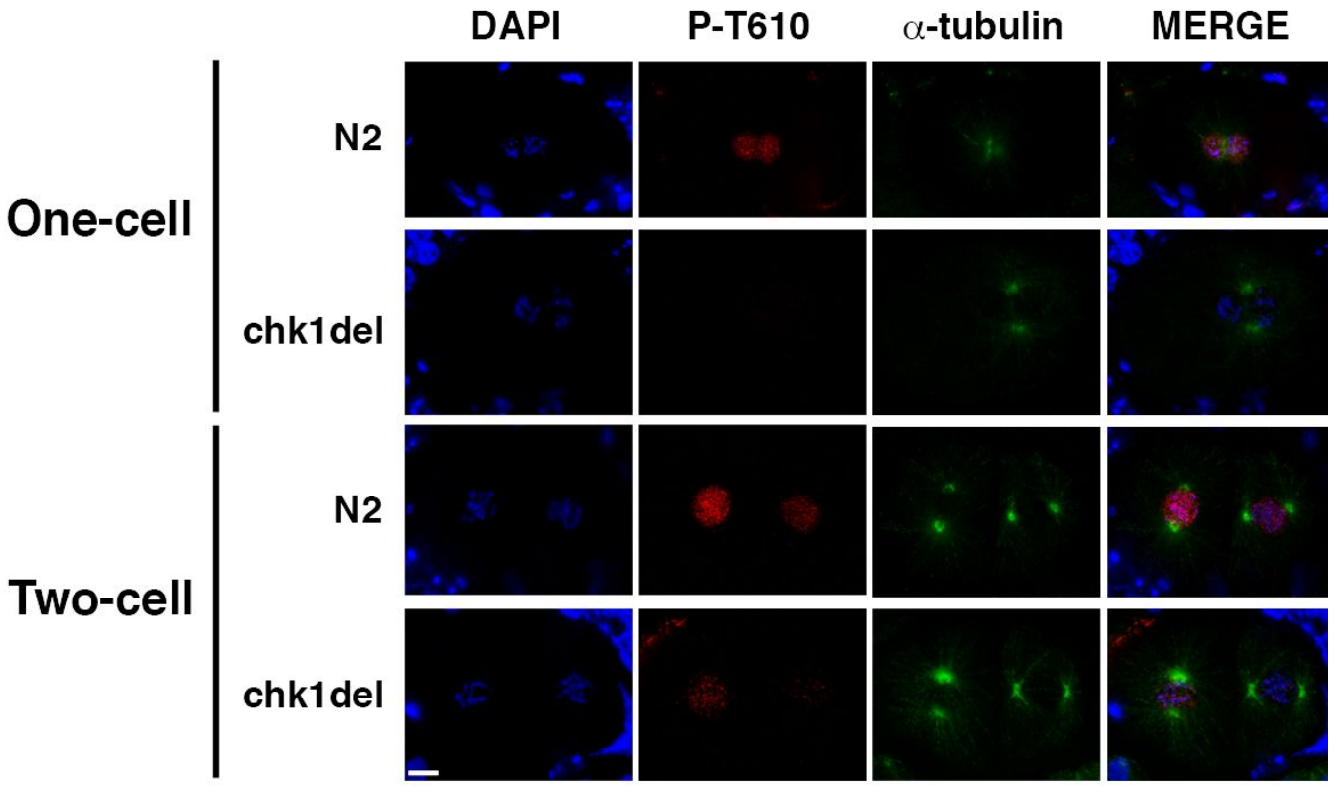
DAPI
P-T610
α-tubulin
MERGE
One-cell
N2
chk1del
Two-cell
N2
chk1del

mitotic functions for hChk1 indicate that CHK-1-mediated TLK-1 phosphorylation promotes CYB-3 binding during mitosis.

Active CHK-1 localizes to the mitotic spindle

C. elegans DNA damage checkpoint proteins influence meiotic and mitotic processes. In the germline, checkpoint proteins are required for a UV-induced DNA damage checkpoint (234, 235). However, this checkpoint is silenced in embryos and CHK-1 contributes to the asynchrony of the second cell division by delaying mitotic entry in the P1 blastomere (236) (234). These functions of CHK-1 are consistent with the dual role this effector kinase plays during the cellular response to DNA damage and cell cycle progression in the absence of DNA lesions in higher eukaryotes. Atm1 is a conserved upstream kinase that phosphorylates Chk1 at S345 to activate Chk1 kinase activity (131). S345 is conserved in *C. elegans* CHK-1 (S344) indicating that an antibody recognizing P-S345 Chk1 would be a good indicator of active CHK-1 localization *in vivo*.

To determine the localization of P-CHK-1 in *C. elegans* embryos, control and *cyb-3(RNAi)*-treated embryos were fixed and prepared for immunofluorescence with P-CHK-1 and α-tubulin antibodies (Figure 23, A and B). Rewardingly, P-CHK-1 localized to centrosomes and spindle microtubules throughout mitosis. Punctate nuclear P-CHK-1 staining was also apparent during telophase and interphase (Figure 23A and data not shown). Depletion of CYB-3 had no affect on P-CHK-1 localization (Figure 23B). These results indicate that active CHK-1 localizes to the mitotic spindle and may couple spindle microtubule dynamics to TLK-1 T610 phosphorylation and CYB-3 association.

Discussion

Unexpected *trans*-acting protein requirements for bait-prey interactions in the tethered-catalysis yeast two-hybrid system

Modification of the traditional Y-2-H screen with tethered-catalysis bait proteins was designed to identify proteins requiring *in cis* PTM of the bait (220). Therefore, we

Figure 23. Active CHK-1 localizes to the mitotic spindle

A) Control and (B) *cyb-3(RNAi)*-treated N2 hermaphrodites were fixed and stained with the indicated antibodies. P-CHK-1 is an antibody that recognizes conserved phosphorylated residues of active human Chk1 (Bartek 2003). Scale bars = 10 μm.

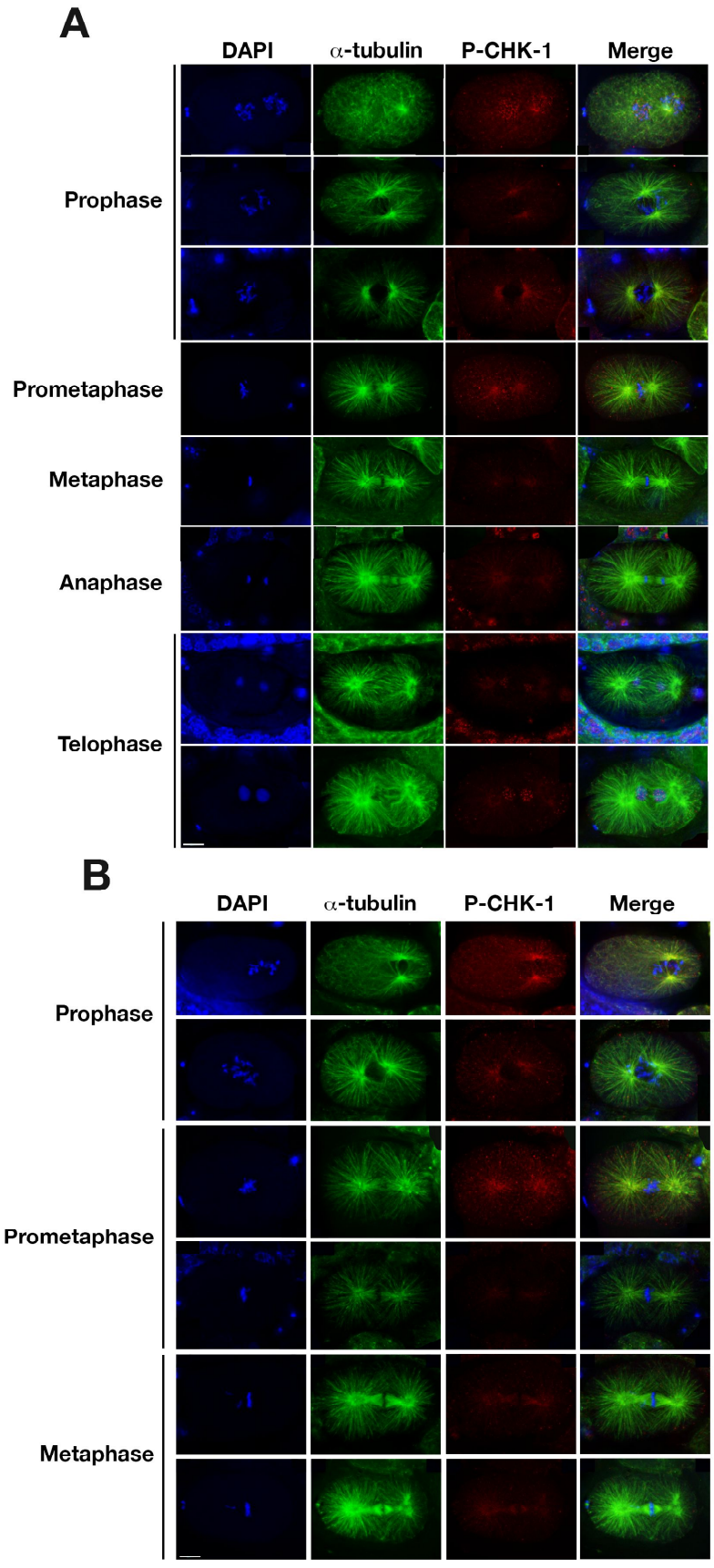
A
DAPI
α-tubulin
P-CHK-1
Merge
Prophase
Prometaphase
Metaphase
Anaphase
Telophase
B
DAPI
α-tubulin
P-CHK-1
Merge
Prophase
Prometaphase
Metaphase

hypothesized that performing a Y-2-H screen with an AIR-2::TLK-1 peptide bait would uncover TLK-1 interacting proteins dependent on S634 phosphorylation. Importantly, our previous data indicated that P-S634 would be the only AIR-2-dependent phosphorylation of the TLK-1 peptide (123). Therefore, we were surprised to discover that none of the thirty-four potential phospho-TLK-1 interactors required P-S634. Interestingly, eight of these prey proteins (including CYB-3) required P-T610 for binding and others required phosphorylation of additional TLK-1 peptide S/T residues (data not shown). Although the screen was not saturated, the lack of P-S634 interactors suggests that the main function of P-S634 may be to positively reinforce AIR-2 activity. It is possible that proteins interacting with P-S634 or nearby residues may sterically hinder AIR-2 activation by P-S634. Thus, a second function of P-S634 may be to inhibit instead of promote protein interactions with TLK-1. Hence, the screen can be modified to identify proteins that bind to the S634A (or AIR-2KD) mutant chimera but not the wild-type construct.

Each phospho-TLK-1 interactor identified from the screen required AIR-2 kinase activity within the chimera but not S634. If other TLK-1 peptide residues are unlikely to be targeted by AIR-2 phosphorylation, why is AIR-2 activity required for the interactions? One possibility is that AIR-2 kinase activity may be required to "present" the TLK-1 peptide for phosphorylation by an endogenous yeast kinase (Figure 24A). The TLK-1 peptide within the AIR-2 K59M kinase-dead chimera may lie internal within the tertiary structure of the chimera and be shielded from phosphorylation. This model is similar to the regulation of Plk1 structure by auto-phosphorylation. C-terminal residues of Plk1 that form the polo-box domain fold back on the kinase domain to inhibit Plk1 activation (216). Plk1 autophosphorylation results in a conformational change to its C-terminus to promote polo-box-mediated protein-protein interactions. Hence, AIR-2 autophosphorylation may cause a conformational change in the C-terminus of the chimera to promote phospho-TLK-1 interactions.

Another potential influence AIR-2 activity may play on phospho-TLK-1 interactions is to activate yeast kinases that phosphorylate the TLK-1 peptide (Figure 24B). In addition, AIR-2 may stably bind to a yeast kinase to potentiate TLK-1

Figure 24. Models for the dependency of AIR kinase activity for bait-prey Y-2-H interactions

A) AIR-2 kinase activity is required to "present" the TLK-1 peptide for the phospho-transfer reaction. (a) AIR-2-dependent phosphorylation of itself or TLK-1 residues other than T610 or S634 promote the TLK-1 architecture required for kinase X to phosphorylate T610. (b) The K59M AIR-2-kinase dead mutant chimera causes a conformational change to the TLK-1 peptide, masking T610 and inhibiting phosphorylation at that residue. B) The kinase activity of AIR-2 is more directly required for T610 phosphorylation by an endogenous yeast kinase. (a) AIR-2-mediated phosphorylation of kinase X activates its catalytic activity or the binding affinity of kinase X to the chimera. (b) Protein Y serves as a third-party participant in T610 phosphorylation by activating yeast kinase X activity or the binding affinity of kinase X to the chimera in an AIR-2-dependent manner.

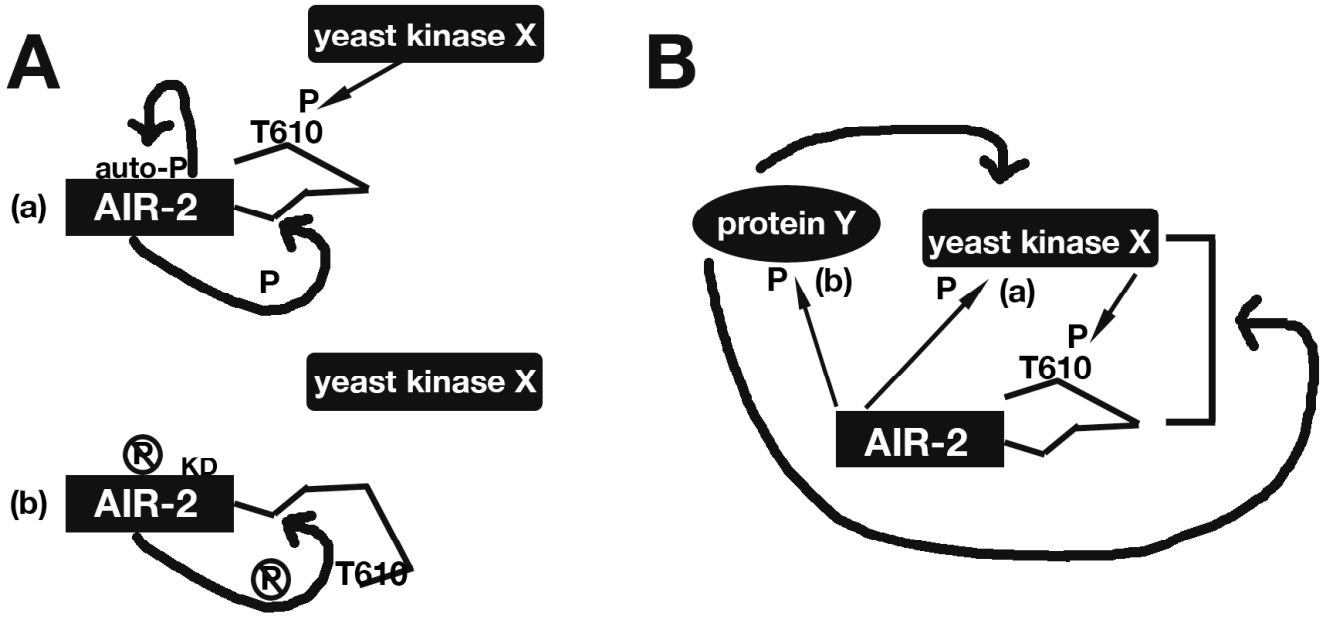
A
yeast kinase X
P
T610
auto-P
(a)
AIR-2
P
yeast kinase X
KD
(b)
AIR-2
T610
B
protein Y
P (b)
yeast kinase X
P (a)
P
T610
AIR-2

phosphorylation. The data presented here suggest that CHK-1 is a T610 kinase that promotes CYB-3 binding to TLK-1. Interestingly, human Chk1 binds, phosphorylates, and activates Aurora B (232). Thus, AIR-2 within the chimera may facilitate T610 phosphorylation by promoting complex formation with yeast Chk1. Alternatively, AIR-2 may also augment Chk1 kinase activity.

Phosphorylation as a key regulator of TLK-1-protein interactions

Our Y-2-H discovery of potential phospho-TLK-1 interactors suggests that multiple residues of TLK-1 are phosphorylated to mediate protein-protein interactions. Eight of the thirty-four proteins identified from the screen failed to interact with the T610A chimera (data not shown). Other phospho-TLK-1 interactors failed to bind chimeras that had different singular serine-to-alanine mutations. Interestingly, the region of TLK-1 containing T610 and S634 is structurally similar to a flexible region of PKA that is subject to phosphorylation (Maria Schumacher, personal communication). This region of PKA is also modified by myristolation and deamidation (215), suggesting that TLK-1 function may similarly be modified by a variety of PTMs. Moreover, cross-talk between PTMs in flexible domains such as the N-termini of histones is an emerging paradigm of protein regulation (230). The potential cross-talk between P-T610 and P-S634 is exciting and suggests that CHK-1 may downregulate AIR-2 by two methods: (1) promoting the CYB-3-dependent kinetochore architecture that decreases the probability of TLK-1-dependent AIR-2 activation; (2) inhibiting phosphorylation at S634 via negative cross-talk by P-T610.

The founding member of the Tousled family was identified in *Arabidopsis* seventeen years ago (125). The only bona fide substrate of Tousled kinases is the chromatin assembly factor Asf1, and Asf1-phosphorylation by Tousled is conserved (127, 128, 237). However, phosphorylation of Asf1 by Tlk1 does not affect histone binding or deposition onto a chromatin template *in vitro* (128). It is intriguing to speculate that the majority of Tousled-influenced processes during mitosis are independent of Tousled kinase activity. From this perspective, a main function of Tousled may be to serve as a platform for kinase signaling integration. The results presented here suggest that TLK-1 serves as a nexus for AIR-2, CHK-1, and CYB-

3/CDK-1 signaling. Additionally, several observations indicate that TLK-1 kinase activity may play a minimal role in the regulation of these kinases. TLK-1 kinase activity is not required to activate AIR-2 (Chapter 2) and is likely dispensable for CHK-1-promoted CYB-3 binding since a small fragment of TLK-1 was sufficient to bind CYB-3. Presumably, the phospho-TLK-1/CYB-3 interaction also includes CDK-1 *in vivo*, since B-type cyclins specifically and functionally interact with CDK-1. Lastly, CHK-1-mediated phosphorylation of TLK-1 at T610 is likely concomitant with phosphorylation at additional residues that may regulate Tousled kinase activity as in higher eukaryotes.

Tousled and cyclin protein function likely overlap throughout the cell cycle

Tousled kinases appear to impact chromatin biology during two vital S-phase processes: chromatin assembly and transcriptional activation (127, 133). The evidence of a mitotic interaction between TLK-1 and CYB-3 suggests that Tousled may also influence chromatin-related cyclin/cdk S-phase functions. Although the majority of cyclin/cdk complexes influence cell cycle division, cyclinH/cdk7 also participates in transcriptional activation as part of the TFIIH basal transcription factor complex (238). We have shown that conserved TLK-1 RXL motifs mediated its interaction with CYB-3 most likely by binding cyclin-box fold domains in CYB-3. Therefore, Tousled may globally affect transcription by influencing cyclin H/cdk7 function within the basal transcriptional complex. Our previous results uncovered a role for TLK-1 in transcription during *C. elegans* embryogenesis (133). *Ce*CDK-7 phosphorylates serine 2 and serine 5 of RNA pol II CTD, and late-stage *tlk-1(RNAi)* embryos showed significantly reduced P-S2 RNA pol II staining (133). It will be interesting to determine if TLK-1 modifies CDK-7 activity vis-à-vis cyclin H binding.

Potential mitotic roles for CHK-1

Recently, the embryonic localization of active *C. elegans* CHK-1 was assessed by immunostaining with the human P-S345 Chk1 antibody and was found to localize to P-granules (234). P-granules are germline-specific RNPs that function in relatively unknown ways to influence RNA metabolism to promote the maintenance of the

germline (239). The localization of active P-CHK-1 to P-granules does not correspond well with known Chk1 functions. P-granules are RNA-containing structures, the function of a DNA damage checkpoint kinase at this organelle seems implausible especially when no CHK-1 substrate has been identified at P-granules. Since P-granules are highly antigenic and react to multiple rabbit preimmune and immune sera, we suspect that this P-granule staining may be an artifact.

The newly discovered roles for Chk1 during mitosis suggest that DNA damage checkpoint proteins influence the metaphase-anaphase transition. Why would enzymes that become activated by DNA lesions function during mitosis? A pivotal paper published in Nature in 2003 revealed that the rapidity of the cellular response to DNA damage does not present enough time for DNA damage proteins to interact directly with DNA lesions (132). Instead, their results indicate that DNA damage changes the configuration of chromatin leading to ATM kinase activation and checkpoint signaling (132). Thus, it is feasible that chromatin configuration is monitored by a DNA damage-like checkpoint during mitosis. The chromatin configuration (especially at the centromere) or microtubule architecture that results from incorrect kinetochore-microtubule attachments may activate ATM to elicit a kinase cascade that includes Chk1 (Figure 25, Prometaphase). As in response to DNA damage, these structural changes may lead to TLK-1 phosphorylation by CHK-1 to inhibit TLK-1 kinase activity. Since the kinase activity of TLK-1 is not required for TLK-1-mediated AIR-2 activation, AIR-2 activation by TLK-1 would remain. In addition, CHK-1 may activate AIR-2 as it does in higher eukaryotes. These two converging modes of AIR-2 activation may serve to weaken improper kinetochore-microtubule attachments and increase SAC activity to allow time for sister chromatid biorientation.

Once all chromosomes biorientate on the metaphase spindle, CHK-1 activity may be directed predominantly at TLK-1 P-T610 phosphorylation (Chapter 25, Metaphase). Since biorientation results in dramatic conformational stretching of sister centromeres (240), ATM-dependent signaling may be modified to allow CHK-1 activity toward T610 of TLK-1. P-T610 stimulates the TLK-1/CYB-3 interaction that may influence dynein activity (see Chapter 4). Dynein-dependent removal of P-T610/CYB-3 from kinetochores could participate in stabilizing bipolar kinetochore-microtubule

Figure 25. Speculative model of the influence CHK-1 has on mitotic TLK-1 functions

The model presented here speculates that CHK-1 (and likely other S-phase DNA-damage checkpoint kinases) plays a fundamental mechanosensory role at the microtubule-kinetochore interface. Similar to the activation of checkpoint kinases by DNA damage-induced changes in chromatin configuration (see text), the model speculates that the microtubule and/or kinetochore architecture that results from non-amphitelic attachment activates CHK-1. Given that human Chk1 phosphorylates and activates Aurora B when the SAC is active, I speculate that CHK-1 positively regulates AIR-2 function to destabilize incorrect K-Mt attachments. Phosphorylation of TLK-1 by CHK-1 may inhibit TLK-1 activity (similar to hChk1 inhibiting Tlk1 during S-phase) against mitotic substrates, the identities of which remain unknown. However, TLK-1-mediated AIR-2 activation may purdure since TLK-1 kinase activity is NOT necessary to activate AIR-2 (see Chapter 2). At metaphase, the TLK-1 P-T610 modification promotes the TLK-1/CYB-3 interaction. CYB-3 appears to be a positive regulator of dynein activity (see Chapter 4), a critical SAC silencer. TLK-1-mediated AIR-2 activation may be inhibited by the translocation of TLK-1/CYB-3 from kinetochores to centrosomes by dynein transport. As a result, bipolar K-Mt attachments would be stabilized and the SAC silenced by dynein-dependent mechanisms.

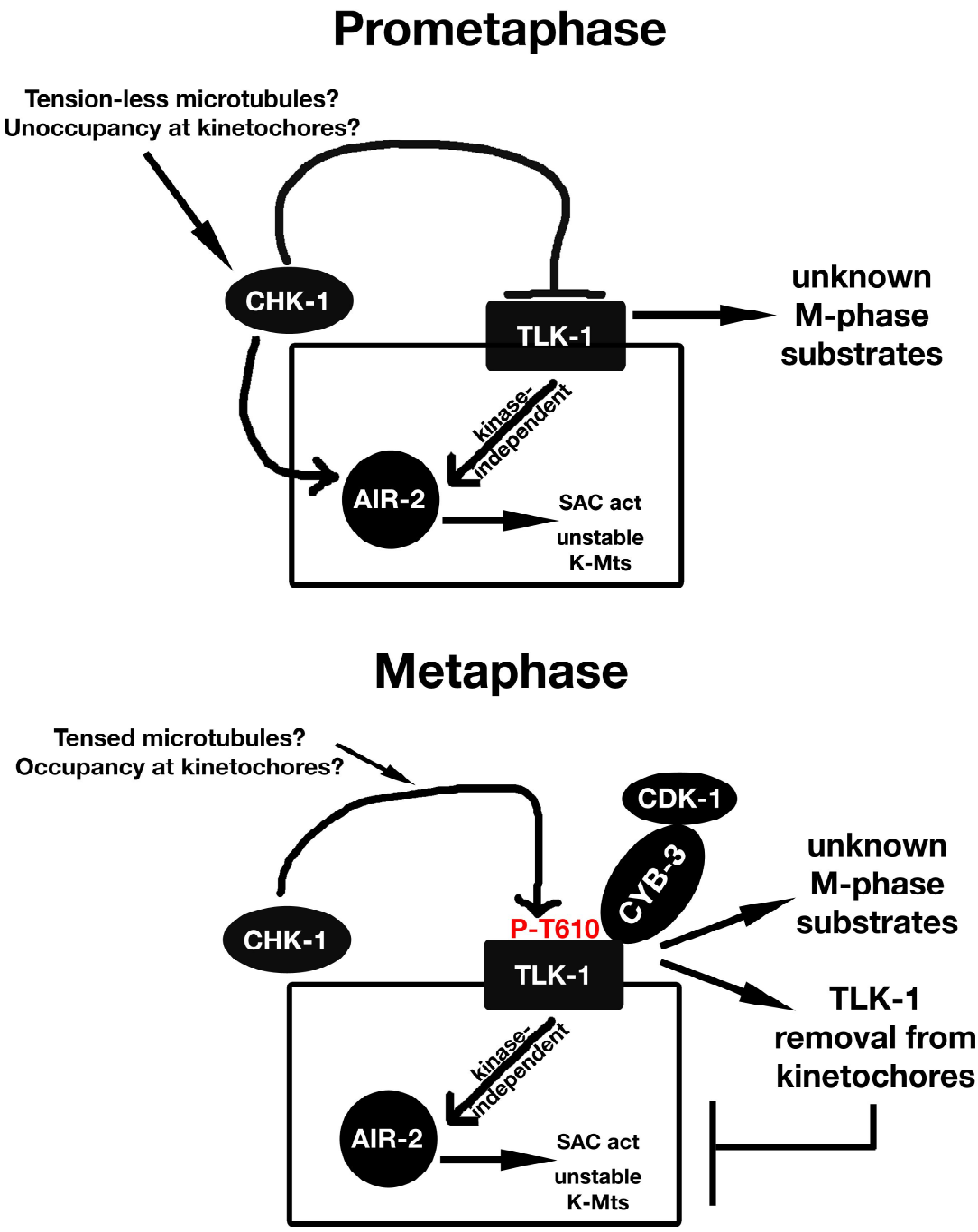
Prometaphase
Tension-less microtubules?
Unoccupancy at kinetochores?
CHK-1
TLK-1
unknown
M-phase
substrates
kinase-
independent
AIR-2
SAC act
unstable
K-Mts
Metaphase
Tensed microtubules?
Occupancy at kinetochores?
CDK-1
CYB-3
unknown
M-phase
substrates
CHK-1
P-T610
TLK-1
TLK-1
removal from
kinetochores
kinase-
independent
AIR-2
SAC act
unstable
K-Mts

attachments by physically sequestering TLK-1-mediated AIR-2 activation (Figure 25, Metaphase). These molecular mechanisms may be difficult to decipher, but experimental designs aimed at supporting these hypotheses are explored in Chapter 5.

CHAPTER FOUR: CYB-3 INFLUENCES THE GENERATION OF STABLE KINETOCHORE-MICROTUBULE ATTACHMENT AND EXTINGUISHES THE SPINDLE ASSEMBLY CHECKPOINT IN *C. ELEGANS*

Introduction

The function and localization of cdk1/cyclin B complexes

Cdk1 is a crucial enzyme required for entry into mitosis (241). Multiple mechanisms regulate Cdk1 function to guarantee that mitotic entry does not occur prematurely. Inhibitory phosphorylations, binding of negative regulators, and restriction of cyclin protein levels contribute to the temporality of Cdk1 activation (241). A- and B-type cyclins bind mitotic Cdk1 leading to partial Cdk1 activation and also provide substrate specificity to Cdk/cyclin complexes (242).

The subcellular localization of Cdk1/cyclin complexes is an important mechanism regulating Cdk1 function since most proteins contain the short Cdk1 phosphorylation consensus sequence [(S/T)/P]. Immunofluorescence performed with antibodies recognizing autophosphorylated active cyclin B1/Cdk1 complexes revealed that Cdk1 first appears on centrosomes during prophase (139). Centrosome-enrichment of Cdk1 complexes contributes to the commitment of cells to mitosis and spindle assembly (139), while phosphorylation of the cytoplasmic retention sequence in cyclin B1 stimulates prophase nuclear enrichment of Cdk1 and nuclear envelope breakdown (243). Immunostaining of *S. pombe*, *Drosophila* embryos, and human cells revealed that cyclin B1 localizes throughout the cytoplasm but is enriched at centrosomes and spindle astral microtubules (244-246). In contrast, cyclin A is predominately associated with chromosomes during S-phase and mitosis (244).

Molecular details of the mitotic mechanisms directly influenced by Cdk1 are being revealed and suggest that Cdk1 function is required throughout mitosis. Microtubule associated proteins (MAPs) are an important class of proteins targeted by Cdk1. *Xenopus* Cdk1 phosphorylates the BimC kinesin Eg5 (kinesin-5 in vertebrates) and enhances its affinity for microtubules (247). Eg5 influences spindle assembly by crosslinking and sliding microtubules thereby driving microtubule flux (248). Thus, positive regulation of Eg5 by Cdk1 contributes to spindle formation. Budding yeast Cdk1/cdc28 participates in centrosome separation by stabilizing MAPs that are required for microtubule bundling (249). Cdk1 protects the Cin8, Kip1, and Ase1 MAPs that are essential for centrosome separation from degradation by phosphorylating and inactivating Cdh1, an activator of the APC E3 ligase (249). After spindle assembly, a

range of mechanisms contribute to nuclear envelope breakdown including dynein-dependent fenestration of the nuclear envelope lamina by microtubules (250, 251), Cdk1/cyclin B1 phosphorylation of the nucleoporin gp210 to facilitate nuclear pore complex disassembly (252), and lamina phosphorylation by Cdk1 (253).

Recent evidence has revealed that Cdk1 has pivotal roles at kinetochores. The kinetochore localization of Cdk1/cyclin B1 had remained elusive due to difficulties in antibody recognition after cell fixation. However, live-cell imaging of GFP-tagged cyclin B1 has confirmed kinetochore localization of Cdk1/cyclin B1 in human cells (254). Mammalian cyclin b1 influences the production of proper kinetochore-microtubule attachments and is subject to dynein-dependent removal from kinetochores (255). Cdk1 function also regulates SAC activity. Mammalian Cdk1 phosphorylates and inhibits separase via direct phosphorylation of separase (256). Phosphorylation of separase by Cdk1 also promotes cyclin B1 binding to inhibit separase activity (218, 257). Therefore, Cdk1/cyclin B complexes appear to influence the metaphase-anaphase transition through a variety of ways.

Diversity of mitotic cyclins

Cyclins display species-specific functional redundancy. *S. cerevisiae* has six B-type cyclins (Clb1-6), with Clb1-4 involved in mitosis (258). Mutational analysis has revealed that each cyclin gene is individually dispensable. However, various combinations such as the s*clb1 clb2*, the *clb1 clb2 clb3*, and the *clb1 clb2 clb3 clb4* mutants are inviable (259, 260). *Drosophila* has three mitotic cyclins, CycA, B, and B3, which are sequentially degraded as mitosis progresses (261). Recent RNAi experiments revealed that CycB is required for the syncytial mitotic divisions of the early embryo but is dispensable zygotically, while co-depletion of CycA and CycB3 resulted in delayed but ultimately successful nuclear divisions (262). Mammals have three B-type cyclins, B1, B2, and B3, which appear to have both overlapping and specific functions. While cyclin B1-null mice die early in development (< day 10 of embryogenesis), cyclin B2-deficient mice grow to be healthy and fertile adults (263). Mammalian cyclin B3 is highly expressed in male and female meiotic germ cells, suggesting a specific role in meiotic progression (264).

Cdk1-related processes that are influenced by B3-type cyclins remain elusive. The evolutionary conservation of cyclin B3 is unique since interspecies B3-type cyclin homology is greater than the similarity of B3 to cyclin B proteins within the same species (265). Although cyclin B3 is highly expressed in testis, it is expressed in a variety of human tissues at very low levels (266). Importantly, no mitotic event directly influenced by cyclin B3 has been identified. Therefore, molecular mechanisms that are influenced by cyclin B3/Cdk1 remain enigmatic.

The mitotic cell cycle machinery in *C. elegans*

The *C. elegans* Cdk1 homolog (CDK-1 or NCC-1) is required for oocyte maturation and entry into embryonic and larval mitoses (148). CDK-7 positively regulates CDK-1 and is a crucial and conserved CAK (**c**dk1-**a**ctivating **k**inase) . Combined inactivation of *cdk-7* through a temperature-sensitive mutation and RNAi resulted in a *cdk-1(RNAi)*-like one-cell embryonic arrest (267). *C. elegans* harbors four partially redundant cyclin B family members called CYB-1, CYB-2.1, CYB-2.2, and CYB-3 (Figure 26A)(66). CYB-1/CDK-1 participates in nuclear envelope breakdown by phosphorylating the nuceloporin gp210 (252). Maturation and ovulation of *C. elegans* oocytes is dependent on the presence of sperm, and the meiotic divisions of the oocyte nucleus take place immediately after fertilization. Previous studies revealed a role for CYB-3 in the duration of the second meiotic division (MII) (268, 269) and the timely destruction of maternal gene products as embryos transition from meiosis to mitosis (270). Embryos depleted of all four cyclin B proteins arrest at the one-cell stage and phenocopy *cdk-1(RNAi)* (271). Thus *C. elegans* B-type cyclins appear to have distinct yet partly overlapping functions. Here, we focus on CYB-3 functions during mitosis and reveal surprising requirements for this B-type cyclin during chromosome congression and spindle checkpoint regulation.

Results

CYB-3 is required for proper mitotic progression

To determine the consequence of CYB-3 depletion during *C. elegans* embryogenesis, L4 larval stage hermaphrodites were fed bacteria expressing *cyb-3*

Figure 26: A protein alignment of *C. elegans* B-type cyclins

A) Clustal-W alignment of approximately 1000 nucleotides the N-terminal protein coding regions of CYB-1, CYB-2.1, CYB-2.2, and CYB-3 cDNAs. The percent homology among the four *C. elegans* B-type cyclins is listed in the table below. B) Protein extracts from control and *cyb-3(RNAi)* embryos were immunoprecipitated with a CYB-3 antibody and subjected to western analysis with the same antibody. α-tubulin was used as a loading control. Asterisk: non-specific protein band.

A

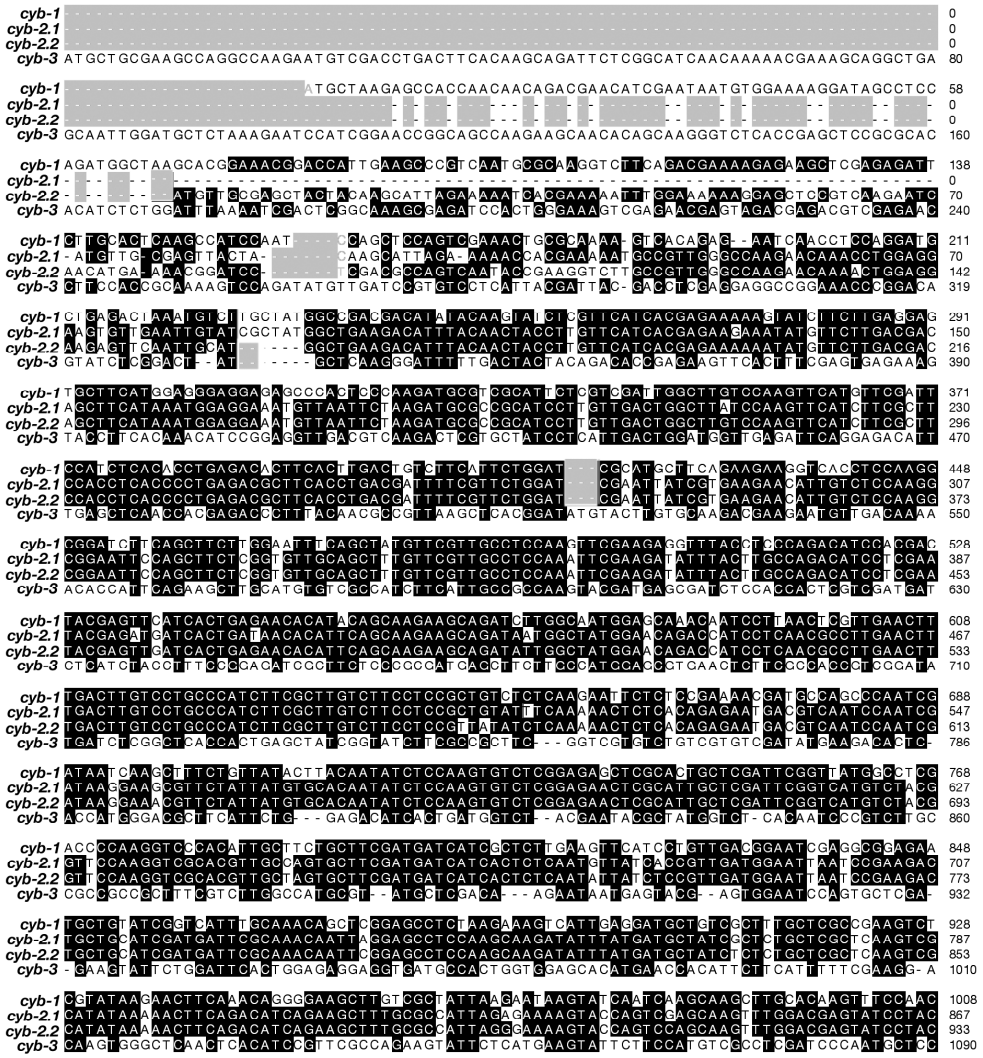

Cyclin cDNAs compared	% homology
cyb-1 and *cyb-2.1*	71.1
cyb-1 and *cyb-2.2*	68.9
cyb-1 and *cyb-3*	41.8
cyb-2.1 and *cyb-2.2*	95.3
cyb-2.1 and *cyb-3*	43.5
cyb-2.2 and *cyb-3*	43.0

B

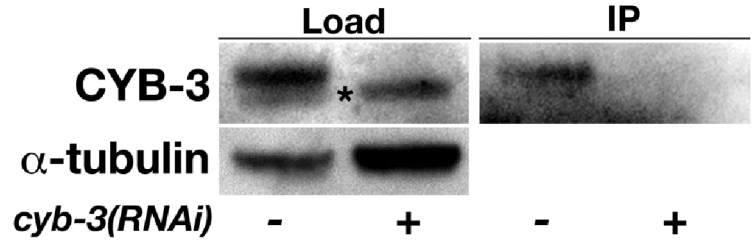

dsRNA, leading to the efficient depletion of CYB-3 (Figure 26B). The first mitotic division of *C. elegans* embryogenesis occurs after the fertilization-induced completion of the meiotic divisions of the oocyte nucleus. Subsequently, the anterior-localized maternal pronucleus then migrates towards the paternal pronucleus at the posterior end of the embryo. The two pronuclei then traverse to the center of the embryo as the growing mitotic spindle undergoes a rotation to align with the long axis of the embryo. Nuclear envelope breakdown and prometaphase chromosome congression culminate in complete metaphase alignment. Anaphase sister chromatid segregation immediately ensues and mitotic exit occurs.

We quantified the duration of the first mitotic division in embryos treated with control or *cyb-3(RNAi)* using specific cellular events as landmarks. We defined pronuclei meeting (PNM) as the initial joining of the maternal and paternal pronuclei, and nuclear envelope breakdown (NEB) as the absence of a clear nucleoplasm and nuclear envelope. Moreover, mitotic exit was defined as the time interval between the start of chromosome decondensation and the beginning of centrosome breakdown. Mitotic progression was monitored by spinning disk confocal microscopy of one-cell embryos expressing mCherry::Histone H2B and GFP::α-Tubulin to visualize the chromosomes and mitotic spindle, respectively. In both control and *cyb-3(RNAi)* treated embryos, the maternal pronucleus migrated towards the posterior region of the embryo prior to PNM with subsequent movement and rotation of the mitotic apparatus to generate a centrally localized equatorial bipolar spindle (Figure 27A). However, the duration between PNM and NEB was delayed approximately 2.5-fold in *cyb-3(RNAi)* embryos compared to control (Figure 27, A and B). After NEB, control-treated embryos showed robust congression of prometaphase chromosomes to the metaphase plate within ~1.5 minutes. However, the period of time required for chromosome congression in CYB-3-depleted embryos was 3-fold longer, and was often incomplete (Figure 27, A and B). 4 out of 10 embryos displayed chromosomes that initially aligned to the metaphase plate but subsequently underwent movement towards the centrosome, followed by re-alignment.

Most striking, however, was the metaphase arrest induced by *cyb-3(RNAi)*. Metaphase was the shortest mitotic stage in control-treated embryos, lasting an average

Figure 27. CYB-3 depletion increases the duration of early mitotic stages and inhibits anaphase chromosome segregation

A) Embryos from OD57 L4 hermaphrodites fed control and *cyb-3(RNAi)* were subjected to live imaging. Time 0:00 corresponds to metaphase chromosome alignment. Frames to the right of 0:00 depict mitotic progression 1, 3, and 6 minutes after metaphase. PNM: Pronuclear meeting; NEB: nuclear envelope breakdown; META: metaphase. Scale bar = 10 μm. B) Mitotic progression in control and *cyb-3(RNAi)* treated OD57 embryos undergoing the first mitotic division. Error bars: mean +/- s.e.m, n = 4 embryos for each condition.

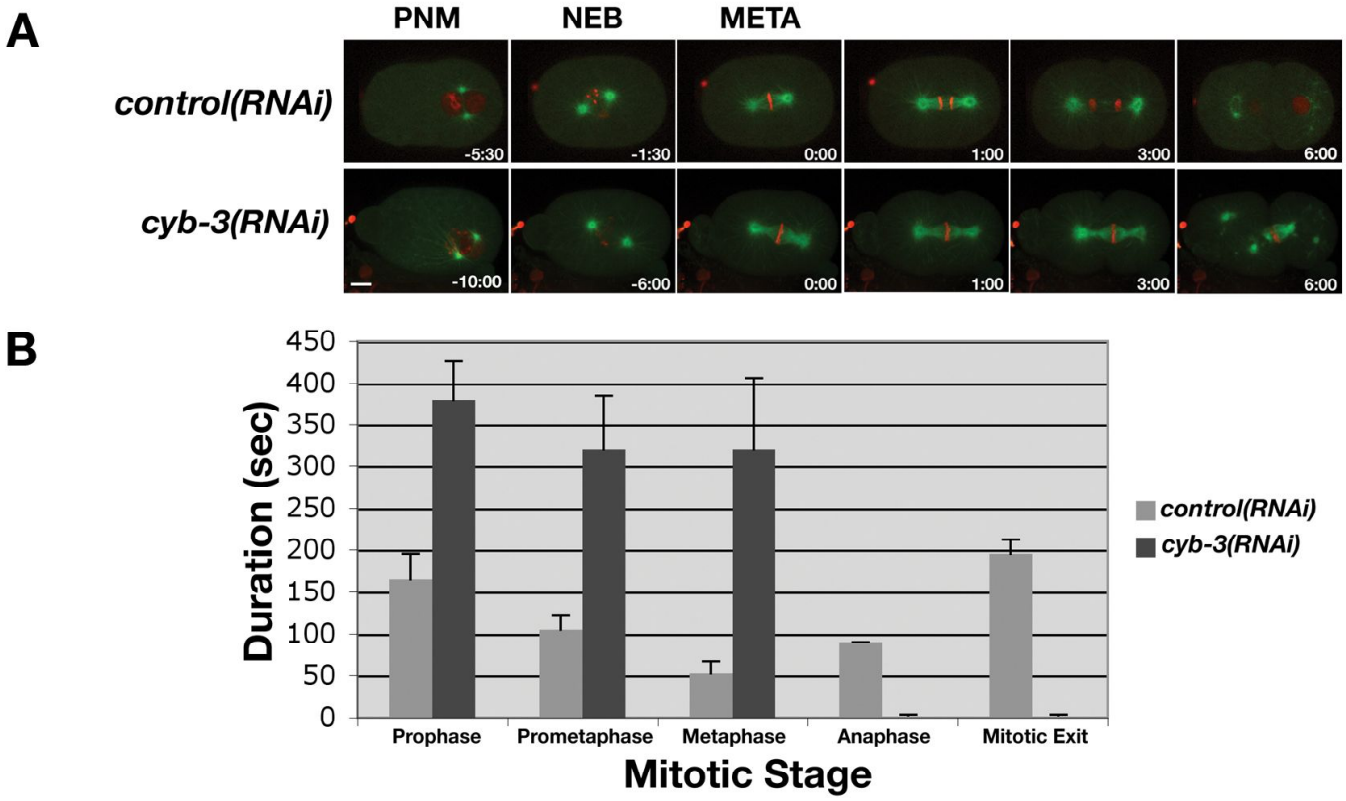
A
PNM
NEB
META
control(RNAi)
cyb-3(RNAi)
-5:30
-1:30
0:00
1:00
3:00
6:00
-10:00
-6:00
0:00
1:00
3:00
6:00
B
Duration (sec)
450
400
350
300
250
200
150
100
50
0
Prophase
Prometaphase
Metaphase
Anaphase
Mitotic Exit
Mitotic Stage
control(RNAi)
cyb-3(RNAi)

of 52 seconds. The loss of CYB-3 resulted in a striking 6-fold increase in the duration of metaphase (287 seconds) (Figure 27, A and B). Anaphase chromosome segregation and telophase chromosome decondensation did not occur in the absence of CYB-3. Therefore, the duration of metaphase in *cyb-3(RNAi)* embryos was defined as the continued alignment of chromosomes at a metaphase-like plate until centrosome breakdown. In these embryos, cleavage furrow ingression occurred while chromosomes remained condensed and aligned at the metaphase plate. Indeed, the cleavage furrow often "cut" the metaphase chromosomes depending on the position of the chromosomes relative to the furrow (data not shown). Entry into the next cell cycle in both daughter cells (as evidenced by centrosome duplication and separation) was also apparent, but occurred in the presence of aligned chromosomes from the first mitotic division (Figure 27A). Lastly, a meiotic role for CYB-3 was also corroborated, and embryos treated with *cyb-3(RNAi)* only extruded the first polar body and were unable to segregate sister chromatids during anaphase II (data not shown). Importantly, meiotic segregation defects do not result in mitotic metaphase delays in *C. elegans* embryos (9, 151). Therefore, the metaphase delay in *cyb-3(RNAi)*-treated embryos is not a secondary consequence of the meiotic defects. These data suggest that CYB-3 is required for the timely execution of mitosis and is essential for the metaphase-to-anaphase transition during mitosis and meiosis.

The phenotype observed upon loss of CYB-3 is distinct from that caused by the depletion of other B-type cyclins

CYB-3 is one of four B-type cyclins in *C. elegans*. The remaining three cyclin B proteins include CYB-1, the closest homolog to mammalian Cyclin B1, and two B2-like proteins. CYB-1, CYB-2.1, and CYB-2.2 are highly homologous to one another and can be targeted for elimination using a single dsRNA (Figure 26A). Embryos were co-depleted of CYB-1, CYB-2.1, and CYB-2.2 (*cyb-1&2(RNAi)*) and mitotic progression assessed via live cell imaging. Interestingly, chromosomes from one-cell embryos treated with *cyb-1&2(RNAi)* did not align to a metaphase plate but still underwent anaphase chromosome and spindle movements (Figure 28). The duration from NEB to the onset of anaphase spindle movements in CYB-1&2 depleted embryos was similar to

Figure 28. The phenotype resulting from the concomitant loss of CYB-1, CYB-2.1, and CYB-2.2 is distinct from *cyb-3(RNAi)* defects

Live imaging of embryos from OD57 hermaphrodites subjected to mock, *cyb-3*, or *cyb-1&2* dsRNA microinjection. Time 0:00 = NEB. Frames to the right of 0:00 correspond to 1, 2, 4, 6, and 8 mins after NEB. Scale bar = 10 μm.

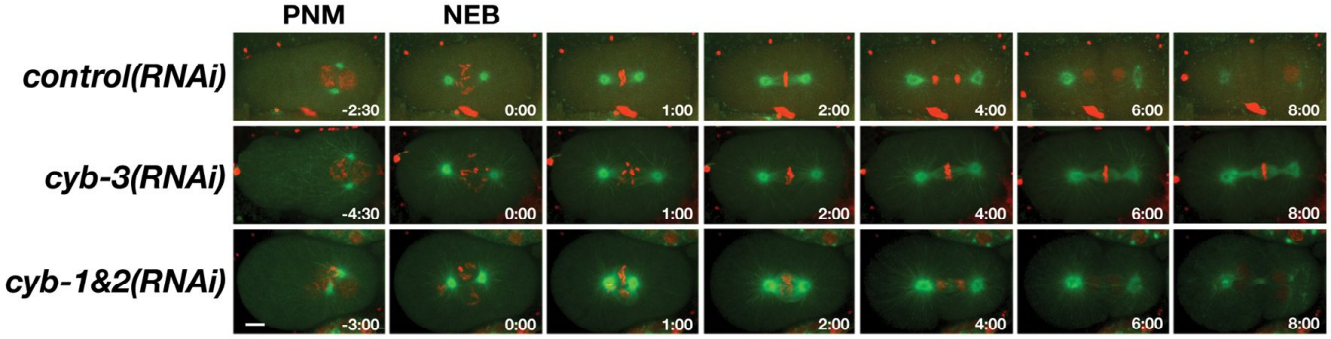
PNM
NEB
control(RNAi)
cyb-3(RNAi)
cyb-1&2(RNAi)
-2:30
0:00
1:00
2:00
4:00
6:00
8:00
-4:30
0:00
1:00
2:00
4:00
6:00
8:00
-3:00
0:00
1:00
2:00
4:00
6:00
8:00

control embryos (average of 150 secs for control (n=2; SD=0) and 124 secs for *cyb-1&2(RNAi)* (n=7; SD=20), suggesting that the SAC is not activated in *cyb-1&2(RNAi)* embryos. Thus, embryos depleted of CYB-3 exhibit a phenotype distinct from that caused by co-depletion of CYB-1 and CYB-2.

CYB-3 depletion activates the spindle assembly checkpoint

Amphitelic metaphase chromosome alignment results in the generation of tension between sister kinetochores (interkinetochore) as well as within each sister kinetochore (intrakinetochore), two prerequisites for anaphase chromosome segregation (272, 273). Kinetochores as well as centromeric chromatin undergo stretching at metaphase due to tension that results from bipolar K-Mt attachment (240). Sister centromere and kinetochore stretching produces spindle tension that is a requirement for anaphase onset. Therefore, we hypothesized that the robust metaphase delay in *cyb-3(RNAi)* embryos was caused by SAC activation. The 3F3/2 antibody has been used to study sister chromatid tension and SAC activation in many experimental systems (274). Recently, the 3F3/2 epitope was identified as Plk1-dependent phosphorylation of the SAC component BubR1 (274). The 3F3/2 epitope is generated when no or reduced tension is present between sister chromatids and is a marker of SAC activity (231). Thus, the 3F3/2 antibody stains tension-less kinetochores during prometaphase, as well as metaphase sister chromatids that are unable to generate tension. To determine if *cyb-3(RNAi)* causes a loss of metaphase tension, control and *cyb-3(RNAi)* embryos were fixed and co-stained with 3F3/2 and BUB-1 antibodies. As expected, the 3F3/2 antibody faintly stained prometaphase chromosomes in control and *cyb-3(RNAi)* embryos, corresponding to a lack of tension prior to bipolar K-Mt attachment and metaphase chromosome alignment (Figure 29). Although control embryos did not show 3F3/2 metaphase chromosome staining, the 3F3/2 antibody strongly recognized *cyb-3(RNAi)* metaphase chromosomes (Figure 29). On a final note, embryos were treated with the microtubule-stabilizer Taxol that inhibits the generation of sister chromatid tension leading to 3F3/2 production. Indeed, the 3F3/2 antibody recognized nuclei from Taxol-treated but not vehicle-control multi-cellular embryos (Figure 44B). This result reveals that the absence of sister chromatid tension leads to 3F3/2 epitope production in *C.*

Figure 29. The 3F3/2 antibody stains *cyb-3(RNAi)* metaphase kinetochores

Control and *cyb-3(RNAi)* embryos were fixed and stained with DAPI (blue) and 3F3/2 (green) and BUB-1 (red) specific antibodies. Scale bar = 10 μm.

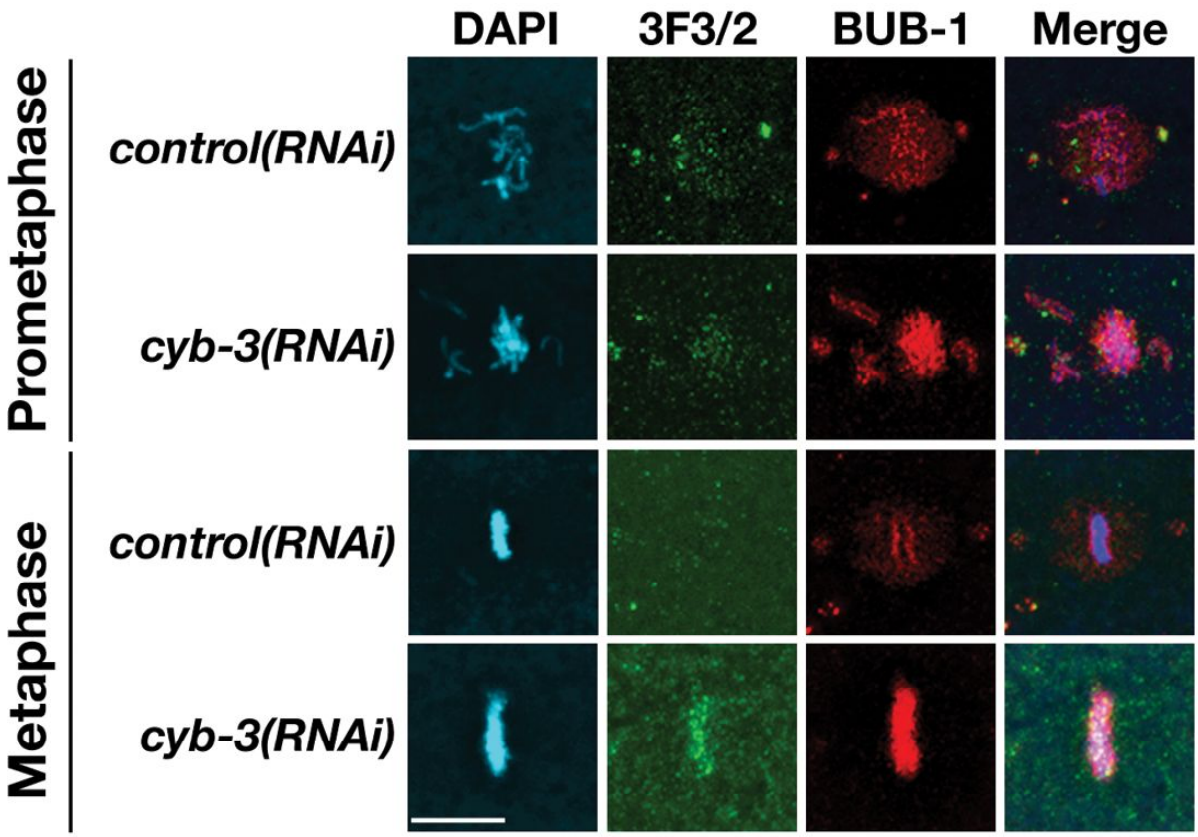
DAPI
3F3/2
BUB-1
Merge
Prometaphase
control(RNAi)
cyb-3(RNAi)
Metaphase
control(RNAi)
cyb-3(RNAi)

elegans similar to other organisms. Taken together, these data suggest that the altered geometry of metaphase kinetochores and centromeres upon CYB-3 depletion is the result of decreased metaphase chromosome tension.

The Spindle Assembly Checkpoint (SAC) monitors chromosome alignment to the metaphase plate and allows for the timely onset of anaphase (89). *C. elegans* embryos have a functional, conserved SAC that responds to perturbations in mitotic spindle dynamics elicited by chemical or genetic manipulation (154, 165). Recent work revealed that the *C. elegans* SAC is bipartite, consisting of a largely cytosolic CeMad3/CeBub3 network, as well as kinetochore-based CeMad1/CeMad2 signaling (154). GFP::MDF-2 (CeMad2) is a nuclear protein that does not show clear kinetochore localization in wild type embryos (154). However, GFP::MDF-2 is targeted to the kinetochore in embryos where the SAC is activated (i.e. by the presence of monopolar spindles) (154, 275). Since the kinetochore localization of MDF-2 is a read-out of SAC activity (154, 275), we determined the localization of GFP::MDF-2 upon loss of CYB-3. Live imaging of embryos expressing GFP::MDF-2 and mCherry::Histone H2B confirmed that MDF-2 is nuclear and is not apparent on kinetochores in control-treated embryos (Figure 30). Conversely, GFP::MDF-2 localized to sister chromatid kinetochores during both prometaphase and metaphase in *cyb-3(RNAi)* embryos (Figure 30). These data suggest that *cyb-3(RNAi)* activates the SAC resulting in the recruitment of MDF-2 to defective kinetochores.

The Spindle Assembly Checkpoint is required for the metaphase block in CYB-3 depleted embryos

Since CYB-3 depletion results in SAC activation and a metaphase block, we determined whether the SAC was required for inhibition of anaphase chromosome segregation in *cyb-3(RNAi)* cells. To this end, GFP::α-Tubulin; mCherry::Histone H2B embryos co-depleted of MDF-1 (CeMad1) (276) and CYB-3 were subjected to live imaging. To control for the effect of co-depletion, *cyb-3* dsRNA and *mdf-1* dsRNA-expressing bacteria were diluted with control bacteria (hereafter noted T7, see Methods and Materials). *mdf-1+T7(RNAi)* did not result in any apparent defects in the timing or execution of mitosis as compared to *T7(RNAi)* treated embryos (Figure 31, A and B).

Figure 30. The conserved spindle assembly checkpoint protein MDF-2 localizes to kinetochores in CYB-3-depleted cells

Selected live images of control and *cyb-3(RNAi)* embryos co-expressing GFP::MDF-2 and mCherry::Histone H2B are shown. Time 0:00 = 30 seconds prior to complete NEB. Scale bar = 10 μm.

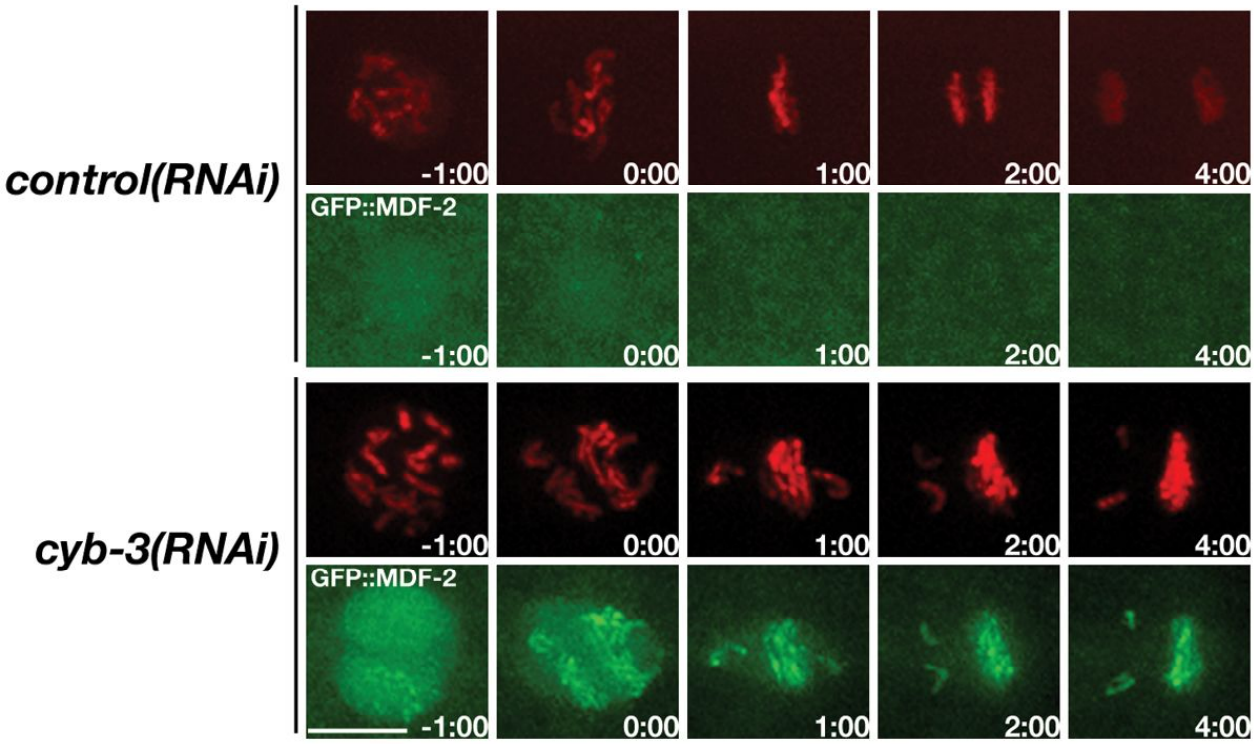
control(RNAi)
-1:00
0:00
1:00
2:00
4:00
GFP::MDF-2
-1:00
0:00
1:00
2:00
4:00
cyb-3(RNAi)
-1:00
0:00
1:00
2:00
4:00
GFP::MDF-2
-1:00
0:00
1:00
2:00
4:00

The mitotic defects of *cyb-3+T7(RNAi)* embryos were indistinguishable from undiluted *cyb-3(RNAi)*, and the one-cell embryos arrested at metaphase. MDF-1 contributed to the prometaphase delay in *cyb-3(RNAi)* embryos, since the duration of prometaphase in *cyb-3+mdf-1(RNAi)* embryos was shortened compared to *cyb-3+T7(RNAi)*, however this interval remained lengthened compared to *T7(RNAi)* (Figure 31, A and B). Strikingly, *cyb-3+mdf-1(RNAi)* embryos entered anaphase after a brief metaphase delay, suggesting that MDF-1 function is required for the metaphase delay in *cyb-3+T7(RNAi)* embryos (Figure 31, A and B). Importantly, GFP::MDF-2 was not recruited to *cyb-3+mdf-1(RNAi)* kinetochores confirming SAC inactivation in these embryos (data not shown). The suppression of the *cyb-3(RNAi)*-induced metaphase block was not specific to MDF-1 depletion, since co-depletion of CYB-3 and either CeMad3 or CeBub1 also resulted in anaphase onset (data not shown). Finally, embryonic lethality remained completely penetrate in embryos co-depleted of CYB-3 and various SAC proteins, suggesting incorrect anaphase segregation of sister chromatids and/or additional cell-cycle defects. Altogether, these results confirm that the metaphase delay elicited by *cyb-3(RNAi)* requires the SAC.

CYB-3 is required for the geometry of metaphase kinetochores

The *C. elegans* embryo has proven to be a powerful platform to study kinetochore function. *C. elegans* chromosomes are holocentric, and the large centromeric chromatin domain provides an advantage for studying changes in kinetochore structure and centromere resolution (45). We reasoned that the chromosome congression defects and SAC activation in *cyb-3(RNAi)* embryos may correlate with defective kinetochore architecture and inappropriate K-Mt attachments. Hence, control and *cyb-3(RNAi)* embryos were fixed and co-stained with antibodies recognizing two kinetochore proteins, HCP-1/CeCENP-F and BUB-1/CeBub1. During prophase in wild-type cells, sister centromeres are resolved from one another, resulting in the orientation of sister kinetochores towards opposite spindle poles (64). This geometry of late prophase sister chromatid centromeres/kinetochores lessens the probability of kinetochores interacting with microtubules emanating from the wrong spindle pole. Prophase sister chromatid resolution occurred in both control and CYB-3-depleted

Figure 31. The metaphase block in *cyb-3(RNAi)* embryos is dependent on the SAC
A**)** Selected live images of OD57 embryos treated with the indicated RNAi combinations. 0:00 = metaphase. Images immediately to the left of 0:00 correspond to NEB. The left most images represent PNM. B) Duration of mitotic stages after treatment with various RNAi combinations. *: $p<0.05$ compared to T7 control. Error bars: mean +/-s.e.m; control, n = 7; *cyb-3+T7(RNAi),* n = 8; *mdf-1+T7(RNAi),* n = 10; *cyb-3+mdf-1(RNAi),* n = 17. Scale bar = 10 μm.

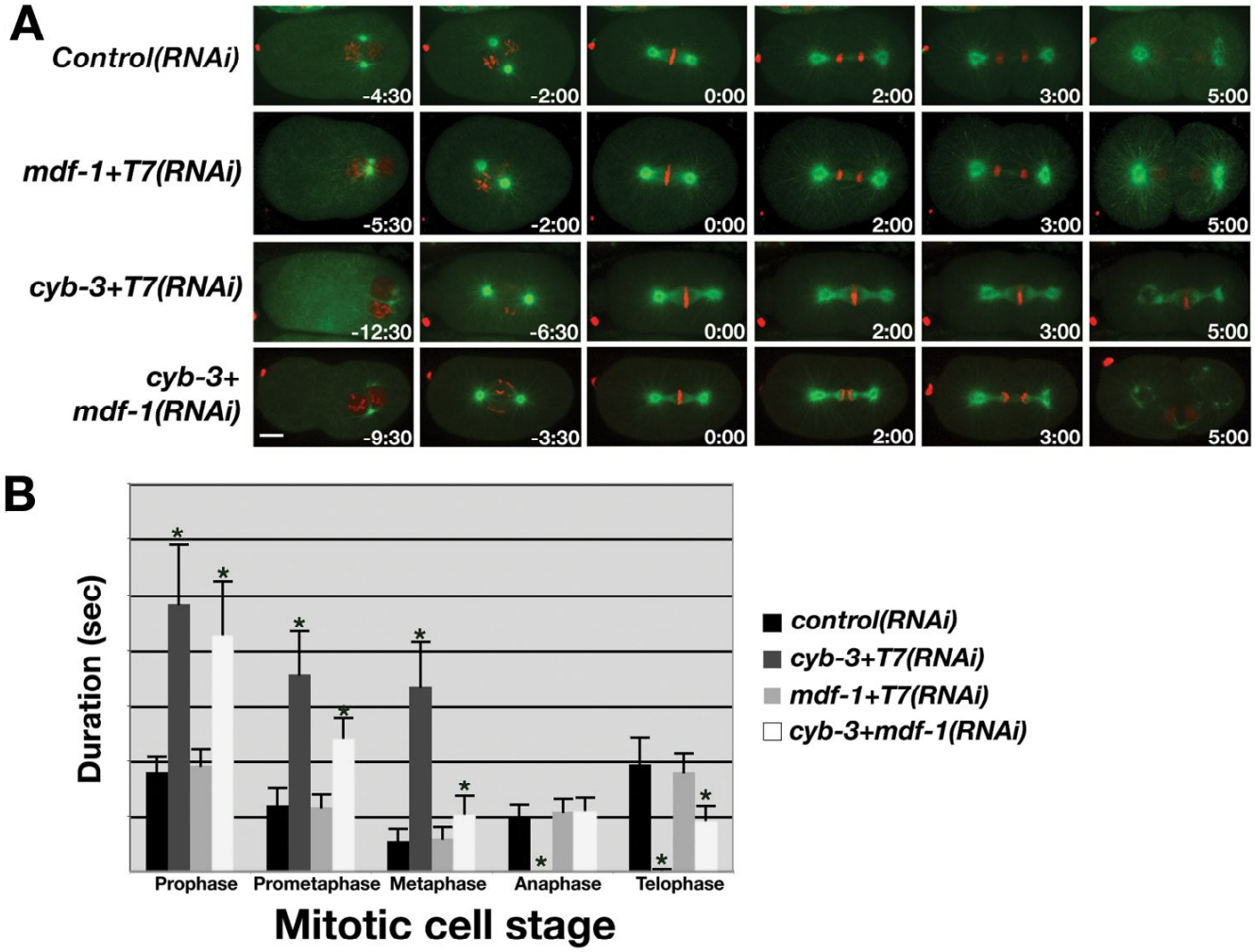
A
Control(RNAi)
mdf-1+T7(RNAi)
cyb-3+T7(RNAi)
cyb-3+
mdf-1(RNAi)
-4:30
-2:00
0:00
2:00
3:00
5:00
-5:30
-2:00
0:00
2:00
3:00
5:00
-12:30
-6:30
0:00
2:00
3:00
5:00
-9:30
-3:30
0:00
2:00
3:00
5:00
B
Duration (sec)
Prophase
Prometaphase
Metaphase
Anaphase
Telophase
Mitotic cell stage
control(RNAi)
cyb-3+T7(RNAi)
mdf-1+T7(RNAi)
cyb-3+mdf-1(RNAi)

embryos, as evidenced by parallel stripes of BUB-1 and HCP-1 staining on prophase chromosomes (Figure 32A). This kinetochore geometry was maintained under both conditions through prometaphase. At metaphase, 100% of control-treated embryos had two clearly defined stripes of BUB-1 and HCP-1 staining, as well as punctate staining of K-Mts (Figure 32A). Loss of CYB-3 resulted in two morphologically distinct classes of metaphase kinetochores, both significantly different from control. The majority of *cyb-3(RNAi)* embryos (81.8%) had no evidence of parallel BUB-1 or HCP-1 metaphase kinetochore staining, as well as the complete absence of BUB-1 or HCP-1 localization to metaphase K-Mts (Figure 32A). Rather, BUB-1 and HCP-1 staining was coincident with the body of the metaphase chromosomes. A small percentage of embryos (18.2%) showed patches of BUB-1 and HCP-1 parallel stripes but no retention of BUB-1 or HCP-1 K-Mt localization (Figure 32A). Immunolocalization performed with antibodies recognizing five additional kinetochore proteins (SEP-1, KLP-7, KNL-2, and two phospho-TLK-1 antibodies) confirmed the alteration of *cyb-3(RNAi)* metaphase kinetochores (data not shown) suggesting that the architecture of the entire metaphase kinetochore was specifically and significantly altered. Finally, live cell imaging revealed that the kinetochore protein GFP::NDC-80 also co-localized with the bulk of metaphase chromosomes in *cyb-3(RNAi)* embryos (data not shown).

As in other organisms, the *C. elegans* kinetochore is built on centromeric chromatin which contains the histone variant CENP-A (HCP-3 in *C. elegans*) (47). In fact, centromeric chromatin is the upstream-most crucial kinetochore component (65). HCP-3 depletion leads to a kinetochore-null phenotype and chromosome segregation defects (65). Thus, the altered metaphase kinetochore architecture that occurred in the absence of CYB-3 could coincide with changes in centromere geometry. To determine the state of sister chromatid centromeres, fixed embryos were co-stained with antibodies recognizing BUB-1 and HCP-3 to simultaneously visualize the outer kinetochore and centromere. Parallel stripes of BUB-1 and HCP-3 were evident on control and *cyb-3(RNAi)* prophase and prometaphase chromosomes, consistent with sister chromatid centromere resolution occurring under both conditions (Figure 32B). At metaphase, 100% of control embryos showed clear stripes of HCP-3 and BUB-1 staining, whereas most embryos depleted of CYB-3 had no clearly resolved HCP-3 and BUB-1 stripes

Figure 32. CYB-3 influences the geometry of metaphase kinetochores

A) Control and *cyb-3(RNAi)* embryos were fixed and stained with DAPI and antibodies recognizing the kinetochore proteins HCP-1 (green) and BUB-1 (red). Arrowheads: resolved sister chromatids. Arrows: K-Mt immunostaining. B) Embryos treated as in (A) were stained with DAPI and antibodies recognizing HCP-3 (green) and BUB-1 (red). Arrowheads: resolved sister chromatids. C) Selected live images of control and *cyb-3(RNAi)* embryos expressing GFP::HCP-3 and mCherry::H2B are shown. Time 0:00: first evidence of nearly complete metaphase chromosome alignment. The first panels in each row correspond to NEB. For each RNAi condition, the top panel is GFP::HCP-3 and mCherry::H2B while the bottom panel is GFP::HCP-3 alone. Scale bars = 10 μm.

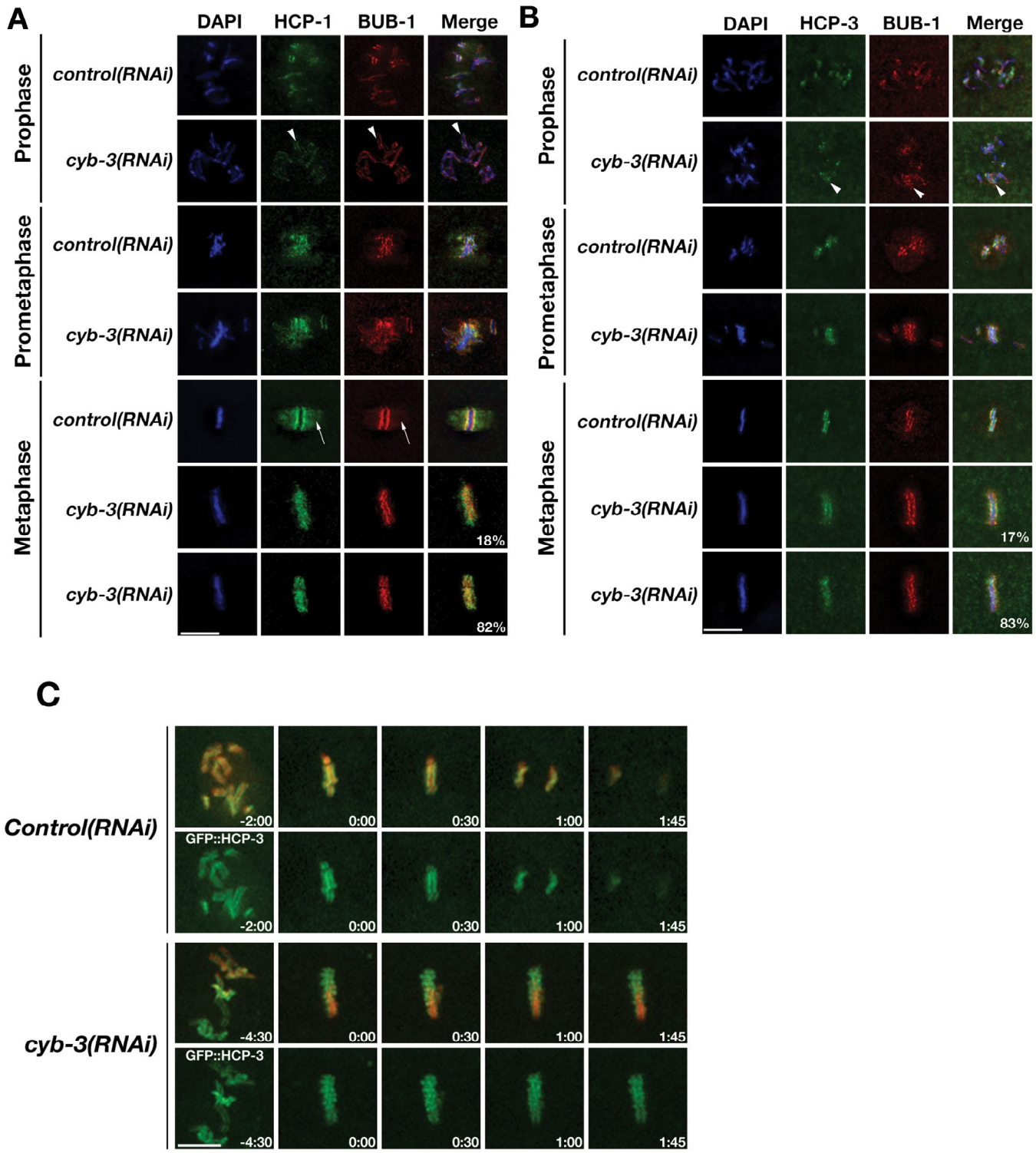
A
DAPI
HCP-1
BUB-1
Merge
Prophase
control(RNAi)
cyb-3(RNAi)
Prometaphase
control(RNAi)
cyb-3(RNAi)
Metaphase
control(RNAi)
cyb-3(RNAi)
18%
cyb-3(RNAi)
82%
B
DAPI
HCP-3
BUB-1
Merge
Prophase
control(RNAi)
cyb-3(RNAi)
Prometaphase
control(RNAi)
cyb-3(RNAi)
Metaphase
control(RNAi)
cyb-3(RNAi)
17%
cyb-3(RNAi)
83%
C
Control(RNAi)
GFP::HCP-3
-2:00
0:00
0:30
1:00
1:45
cyb-3(RNAi)
GFP::HCP-3
-4:30
0:00
0:30
1:00
1:45

(83%) (Figure 32B). Importantly, the loss of metaphase BUB-1 stripes was always coincident with unresolved, "twisted" HCP-3 stripes, suggesting a correlation between kinetochore and centromere morphological changes.

Next, we generated time-lapse movies of embryos expressing GFP::HCP-3 and mCherry::H2B to visualize centromeric chromatin and entire chromosomes in live cells. In control and *cyb-3(RNAi)* embryos, sister chromatid resolution occurred prior to NEB with GFP::HCP-3 lines orientated on the poleward face of mCherry::H2B-labeled chromatin (Figure 32C). This geometry was maintained throughout prometaphase under both conditions. In control embryos, parallel lines of GFP::HCP-3 were not apparent during initial metaphase chromosome alignment but became visible just prior to anaphase chromosome segregation in the majority of embryos (9/12) (Figure 32C). Parallel GFP::HCP-3 lines were never apparent during metaphase in *cyb-3(RNAi)* cells (n=9) (Figure 32C). Altogether, these results suggest that the geometry of metaphase centromeric chromatin is altered in *cyb-3(RNAi)* embryos.

CYB-3 influences kinetochore-microtubule dynamics

Chromosome congression requires kinetochore attachment to the mitotic spindle and is supervised by a surveillance mechanism that corrects improper, non-amphitelic attachment of kinetochores to microtubules (89). The lengthened interval of prometaphase and metaphase in CYB-3-depleted embryos suggested that kinetochore microtubule interactions may be defective. Interestingly, staining with an α-tubulin specific antibody revealed that the density of metaphase kinetochore-microtubules (K-Mts) was increased, and the metaphase spindle appeared "pinched" at the centrosomes in *cyb-3(RNAi)* treated embryos compared to control (Figure 33A). Similar abnormalities were apparent in live *cyb-3(RNAi)* embryos, suggesting that fixation is not the cause of the altered K-Mts (Figure 33B). A qualitative increase or decrease in astral microtubule density was not apparent in fixed or live embryos.

In control-treated embryos, chromosome alignment occurred with precision and 100% of fixed metaphase one-cell embryos had all twelve pairs of sister chromatids aligned at the metaphase plate (Figure 33C). Upon CYB-3 depletion, only 71% of one-cell embryos had complete metaphase chromosome alignment, whereas 29% had at least

Figure 33. *cyb-3(RNAi)* embryos exhibit metaphase chromosome malorientation and altered spindle morphology

A) Control and *cyb-3(RNAi)* embryos were fixed and stained with DAPI (blue) and an α-tubulin (green) antibody. One-cell embryos at metaphase are shown. Arrow: unaligned chromosome. B) Selected live images of control or *cyb-3(RNAi)* OD57 embryos at metaphase are shown. Arrows: unaligned chromosomes. Panel labels are the same as in (A). Scale bars = 10μm. C) Percentage of fixed control and *cyb-3(RNAi)* one-cell embryos with complete metaphase chromosome alignment (control, n = 25; *cyb-3(RNAi),* n = 42; Error bars: mean +/- s.e.m; p = 0.001).

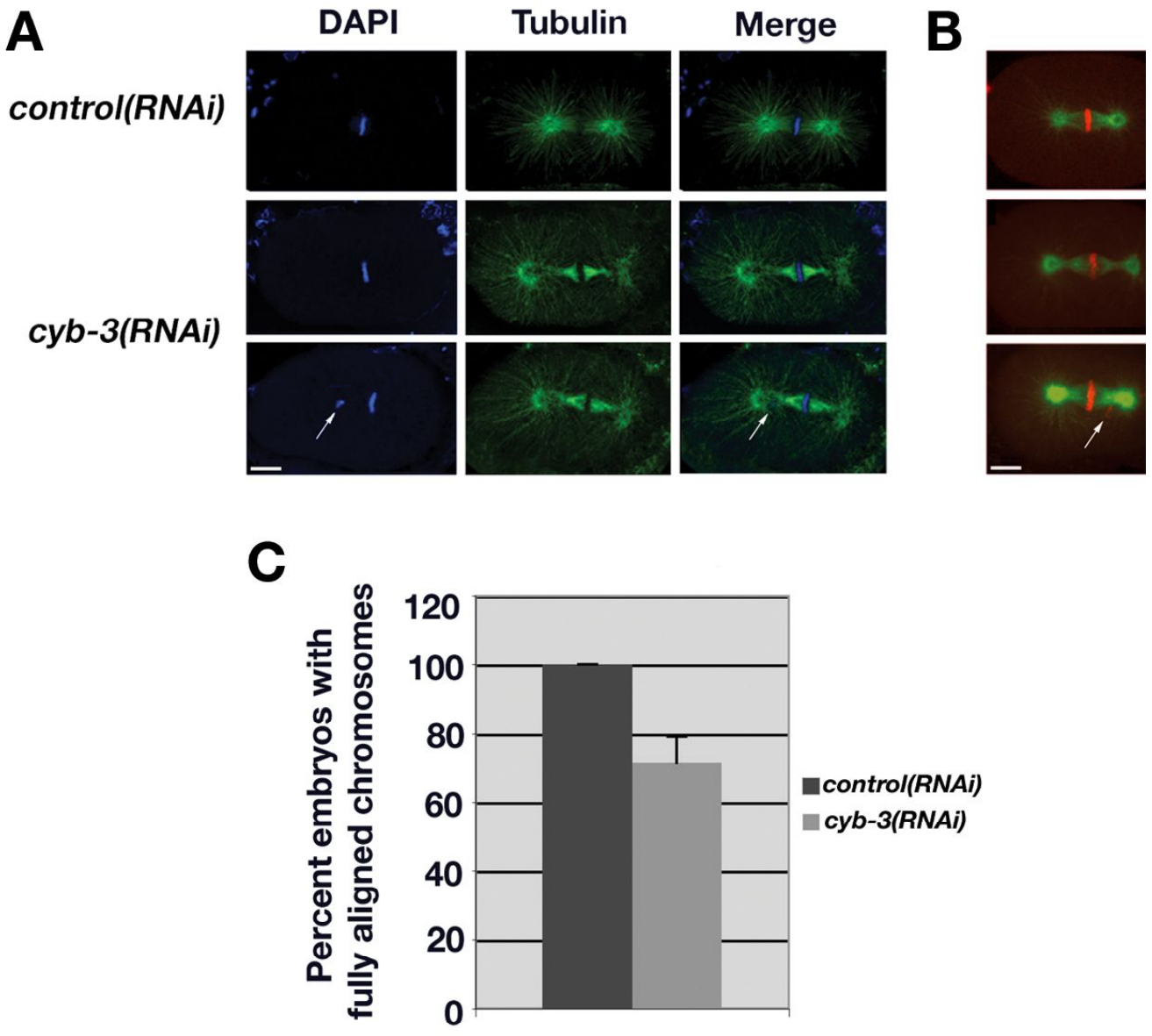
A
DAPI
Tubulin
Merge
control(RNAi)
cyb-3(RNAi)
B
C
Percent embryos with fully aligned chromosomes
120
100
80
60
40
20
0
control(RNAi)
cyb-3(RNAi)

one pair of sister chromatids that was not at the metaphase plate (Figure 33C). Real-time analysis of CYB-3 depleted embryos expressing GFP::α-Tubulin and mCherry::Histone H2B also revealed metaphase chromosome malorientation (3/10 *cyb-3(RNAi)* embryos), an event not witnessed in control embryos (n = 18) (p = 0.01) (Figure 33B). Thus, CYB-3 depletion leads to an alteration in K-Mt organization as well as metaphase chromosome alignment defects.

The increased duration of prometaphase, chromosome congression defects, and continued SAC activation in *cyb-3(RNAi)* embryos suggested that CYB-3 is required for the appropriate attachment of kinetochores to microtubules. Most organisms undergo two stages of anaphase chromosome movements termed anaphase A and B. Anaphase A occurs in early anaphase, when depolymerization of kinetochore-proximal microtubules results in chromosome movement to centrosomes. Anaphase B segregation occurs when spindle poles are pulled towards the cell cortex by cortical microtubules. *C. elegans* embryos only undergo anaphase B segregation, so the pole-pole distance is a measure of the strength of cortical pulling forces (67). Cortical pulling forces are antagonized by stable K-Mt interactions, so the pole-pole distance is an indirect measure of the strength of K-Mt attachments (67). To determine if CYB-3 influences the generation of stable K-Mt attachments, embryos were co-depleted of CYB-3 and known microtubule-binding kinetochore proteins. Two Mt binding entities exist within the *C. elegans* kinetochore: one in the NDC-80 complex and another in the KNL-1 complex (71). Indeed, live cell imaging performed with embryos expressing GFP::α-tubulin and mCherry::H2b revealed that the pole-pole distance of embryos co-depleted of CYB-3 and either NDC-80 or KNL-1 was greater than singular depletions (Figure 34, A and B). These results suggest that loss of CYB-3 weakens K-Mt interactions, resulting in increased cortical pulling forces on centrosomes and increased pole-pole separation. On a final note, spindle length measurements assessed in embryos co-depleted of MDF-1 and CYB-3 revealed robust anaphase pole-pole separation that was delayed compared to control (Figure 34B). Additionally, experiments described below reveal that CYB-3 depletion delays chromosome condensation. However, spindle pole separation in embryos depleted of SMC-4, a critical condensin subunit, was similar to control suggesting that defective chromosome condensation does not significantly alter K-Mt stability.

Figure 34. Kinetochore-microtubule attachments are weakened in the absence of CYB-3

A) Embryos isolated from OD57 hermaphrodites treated with the indicated RNAi combinations were mounted and subject to live imaging. Still images derived from the movies are shown, with NEB = 0:00. Note the increased pole-pole distance in embryos treated with *cyb-3(RNAi)* and RNAi directed against bona fide kinetochore microtubule binding complexes (bottom two rows) compared to single-depletion conditions. Scale bar = 10 μm. B) The pole-pole distance was measured as a function of time relative to NEB from movies generated with OD57 embryos treated with the indicated RNAi conditions.

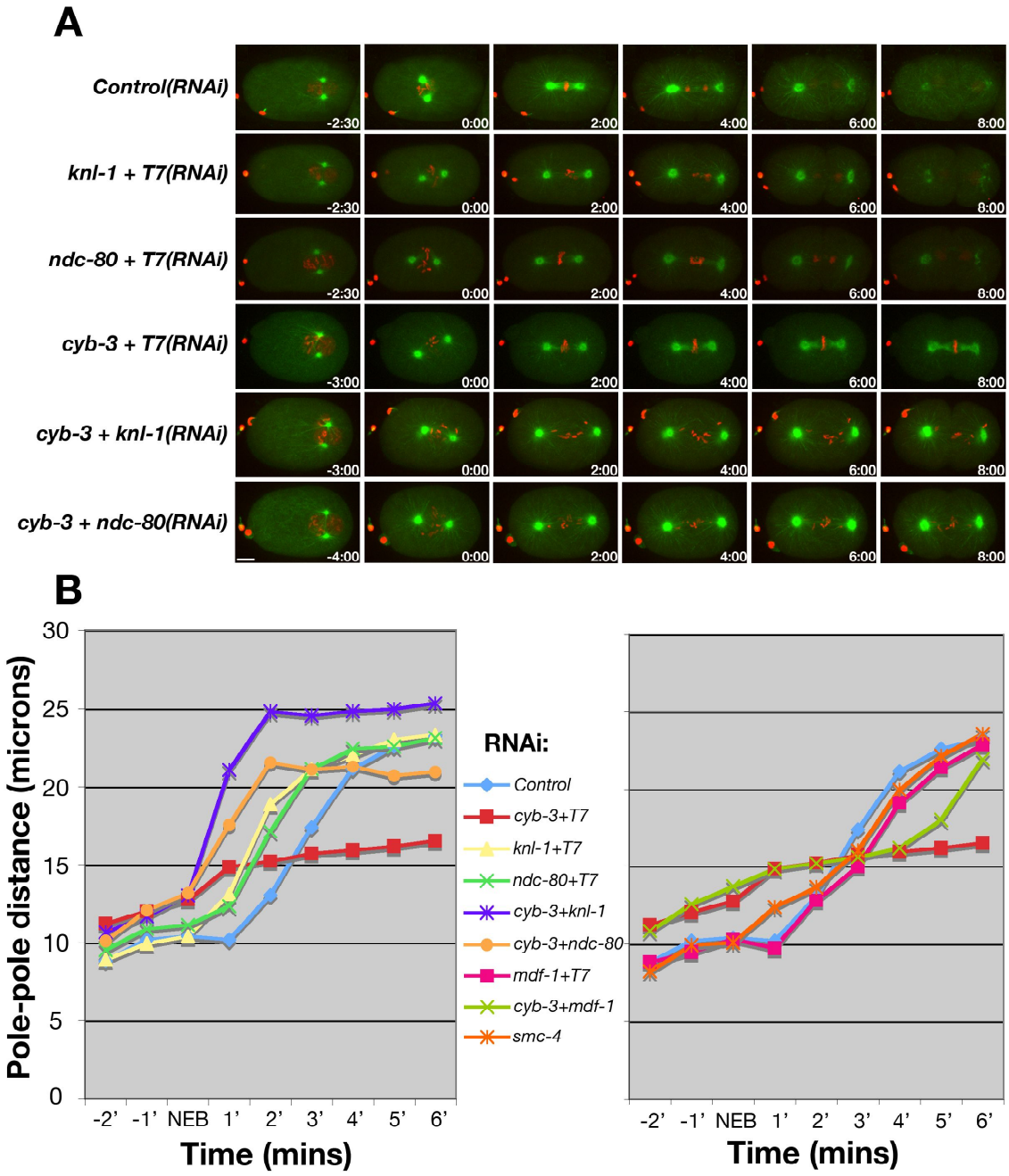
A
Control(RNAi)
knl-1 + T7(RNAi)
ndc-80 + T7(RNAi)
cyb-3 + T7(RNAi)
cyb-3 + knl-1(RNAi)
cyb-3 + ndc-80(RNAi)
-2:30
-3:00
-4:00
0:00
2:00
4:00
6:00
8:00
B
Pole-pole distance (microns)
0
5
10
15
20
25
30
-2' -1' NEB 1' 2' 3' 4' 5' 6'
Time (mins)
RNAi:
Control
cyb-3+T7
knl-1+T7
ndc-80+T7
cyb-3+knl-1
cyb-3+ndc-80
mdf-1+T7
cyb-3+mdf-1
smc-4
-2' -1' NEB 1' 2' 3' 4' 5' 6'
Time (mins)

Kinetochore and kinetochore-microtubule localization of CYB-3 at metaphase

The data presented above suggest that CYB-3 influences K-Mt binding and loss of CYB-3 leads to a deregulation of this particular kinetochore function. Therefore, CYB-3 likely has a regulatory rather than a structural role at kinetochores. To determine the subcellular localization of CYB-3, embryos expressing GFP::CYB-3 were fixed and stained with the GFP antibody and α-tubulin as a fixation control (Figure 35). CYB-3 displayed nuclear localization during prophase and concentrated to the vicinity of prometaphase chromosomes. At metaphase, CYB-3 was enriched on both sides of the metaphase plate indicative of kinetochore and K-Mt localization (Figure 35). As expected, CYB-3 levels were greatly reduced at anaphase consistent with the anaphase-promoting machinery targeting B-type cyclins for proteolysis (Figure 35). These data indicate that CYB-3 has the appropriate localization to regulate kinetochore function during prometaphase and metaphase.

Dynein is retained at kinetochores in the absence of CYB-3

Although much is known about SAC activation, the mechanism by which the SAC becomes silenced remains largely elusive. Dynein, a microtubule motor protein, actively removes SAC proteins from properly attached kinetochores, trafficking along K-Mts to shuttle SAC proteins from kinetochores to centrosomes (82, 184). Since the SAC could not be satiated in embryos depleted of CYB-3, we analyzed whether DHC-1 (CeDynein heavy chain) was properly localized by examining embryos expressing GFP::DHC-1 and mCherry::Histone H2B. Under control conditions, GFP::DHC-1 localized to the nuclear periphery at prophase and was faintly associated with chromosomes upon nuclear envelope breakdown (Figure 36). At metaphase, kinetochore and K-Mt localization was evident. The relocation of DHC-1 from kinetochores to centrosomes occurred during anaphase and was most obvious by mid-anaphase (Figure 36). In embryos depleted of CYB-3, GFP::DHC-1 localized to the nuclear periphery during prophase as in control. Strikingly, DHC-1 was strongly detected at *cyb-3(RNAi)* kinetochores during prometaphase and metaphase, while the K-Mt signal at metaphase was greatly reduced (Figure 36). The dynactin complex is a conserved positive regulator of dynein function (185). The failure of minus-end directed

Figure 35. GFP-conjugated CYB-3 localizes to the vicinity of kinetochores

Embryos expressing GFP::CYB-3 were fixed and stained with DAPI, and antibodies that recognize α-tubulin and GFP. The inset is a blow-up of the chromatin region of an embryo at metaphase. Scale bar = 10 μm.

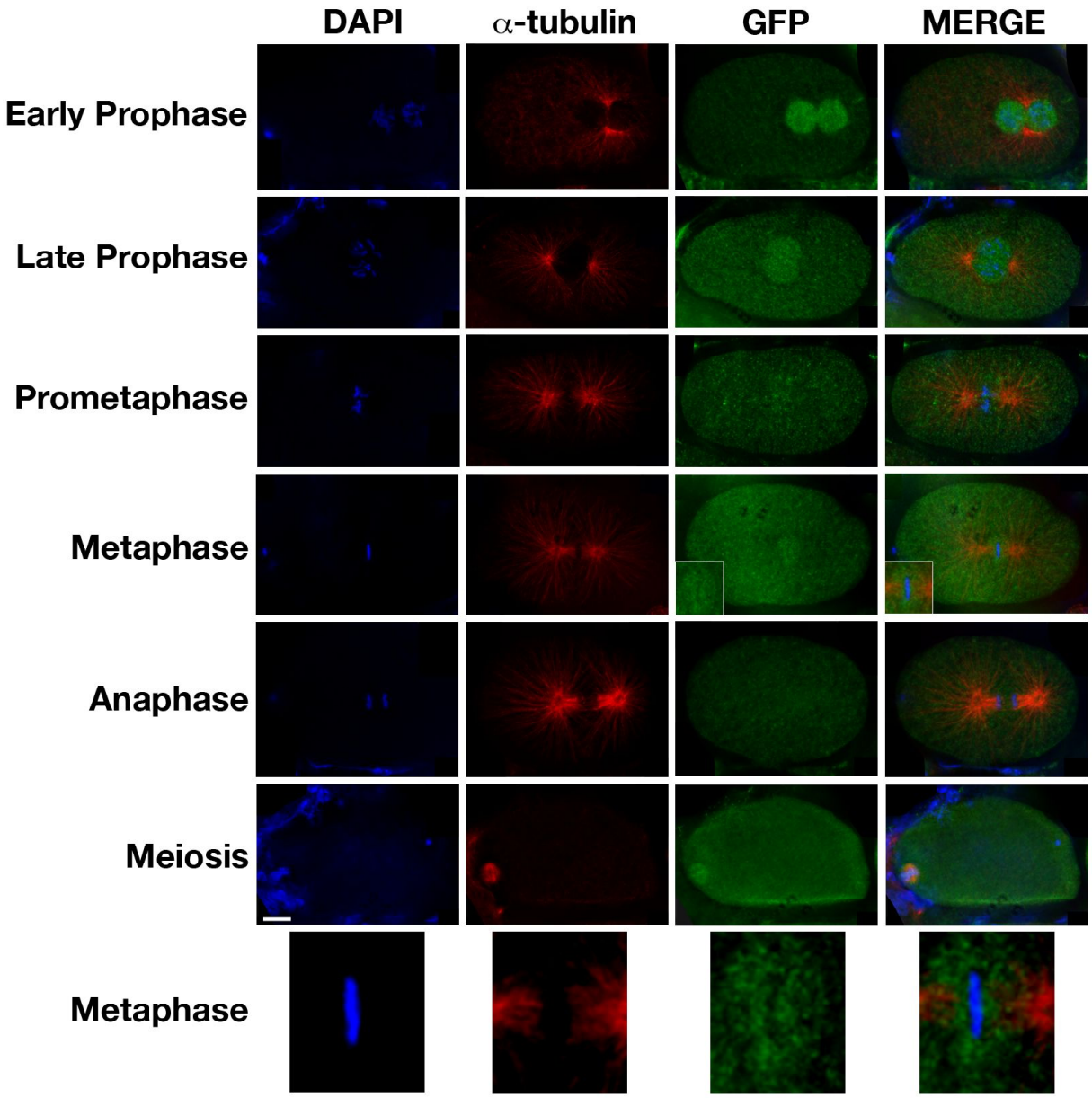
DAPI
α-tubulin
GFP
MERGE
Early Prophase
Late Prophase
Prometaphase
Metaphase
Anaphase
Meiosis
Metaphase

Figure 36. Dynein fails to translocate away from *cyb-3(RNAi)* kinetochores

Selected live images from control and *cyb-3(RNAi)* embryos expressing GFP::DHC-1 and mCherry::Histone H2B are shown. Time 0:00 = PNM. Arrows: spindle and centrosome localization of GFP::DHC-1. Time 0:00 = PNM. Scale bar = 10 μm.

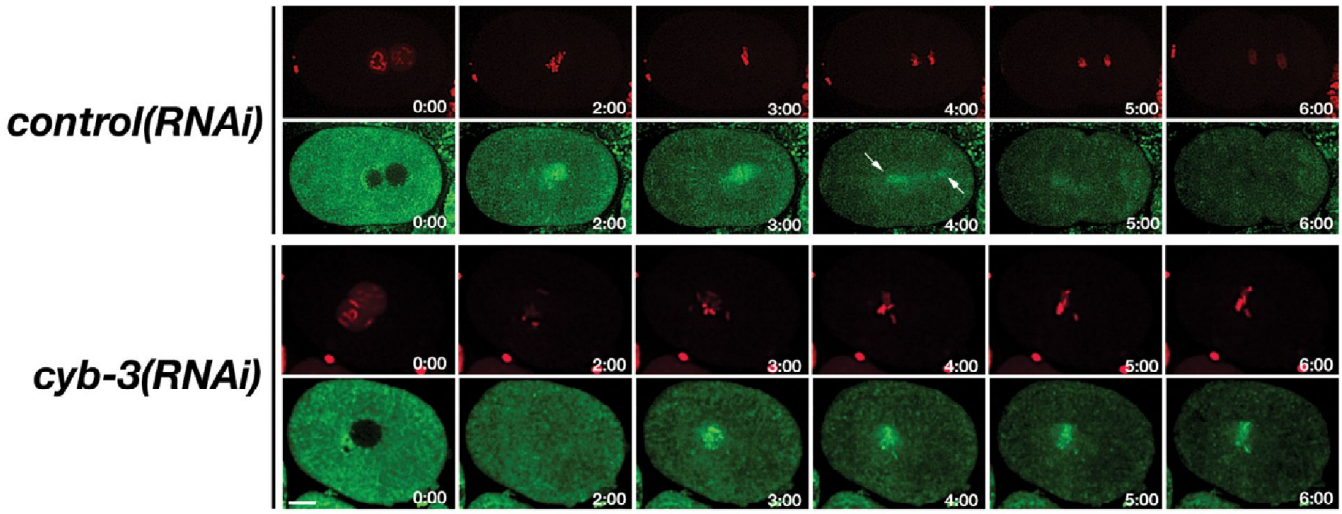
control(RNAi)
cyb-3(RNAi)
0:00
2:00
3:00
4:00
5:00
6:00

dynein to translocate from kinetochores to centrosomes (from microtubule plus- to minus-ends, respectively) suggested that CYB-3 is required for some aspect of dynein activation and/or microtubule binding. The localization of dynactin was assessed to determine if the absence of dynactin contributes to the retention of dynein at *cyb-3(RNAi)* kinetochores (277). Surprisingly, live cell analysis of GFP::DNC-2 (p50/dynamitin) revealed robust kinetochore localization of DNC-2 to prometaphase and metaphase chromosomes upon *cyb-3(RNAi)* treatment but little K-Mt recruitment (data not shown). Immunostaining performed with an antibody recognizing the dynactin subunit DNC-1 (p150(glued)) also revealed the localization of DNC-1 to *cyb-3(RNAi)* prometaphase and metaphase kinetochores with a concomitant decrease in K-Mt and centrosome association (Figure 37). These results indicate that CYB-3 positively regulates dynein and/or dynein-accessory protein function.

The inability of dynein and dynein-related proteins to associate with the mitotic spindle in *cyb-3(RNAi)* embryos could reflect a global defect in microtubule-associated protein (MAP) binding to K-Mts due to altered microtubule morphology. However, the MAP BMK-1(CeBimC kinesin) (278), a substrate of AIR-2 that depends on AIR-2 to target to microtubules, localizes to K-Mts in control and *cyb-3(RNAi)* embryos (Figure 38). Thus, a plus-end directed kinesin but not minus-end dynein show appropriate microtubule localization in embryos depleted of CYB-3. Altogether, these data indicate that K-Mts are not totally inconducive to MAP binding and suggest that CYB-3 is required for the movement of dynein from kinetochores as sister chromatids congress to, align with, and segregate from the metaphase plate.

Depleting a negative dynein regulator suppresses the metaphase delay associated with partial CYB-3 depletion

Conserved positive regulators of dynein include the dynactin complex and Lis1, and proper dynein function requires homologous proteins in *C. elegans* (277, 279). Mechanisms that negatively regulate dynein activity remain largely unknown. However, an RNAi-based screen in *C. elegans* revealed that DYLT-1 and DYRB-1, two dynein light chains, negatively regulate dynein function but are otherwise dispensable for viability (280). We predicted that dynein-related defects associated with strong CYB-3

Figure 37. Dynein-accessory proteins are retained at *cyb-3(RNAi)* metaphase kinetochores

Control and *cyb-3(RNAi)* embryos were fixed and stained with DAPI (blue) and antibodies recognizing α-tubulin (green) and DNC-1/p150(glued) (red). Arrows: DNC-1 centrosome staining in control embryos that is clearly decreased upon CYB-3 depletion. Arrowhead: centrosome breakdown. Scale bar = 10 μm.

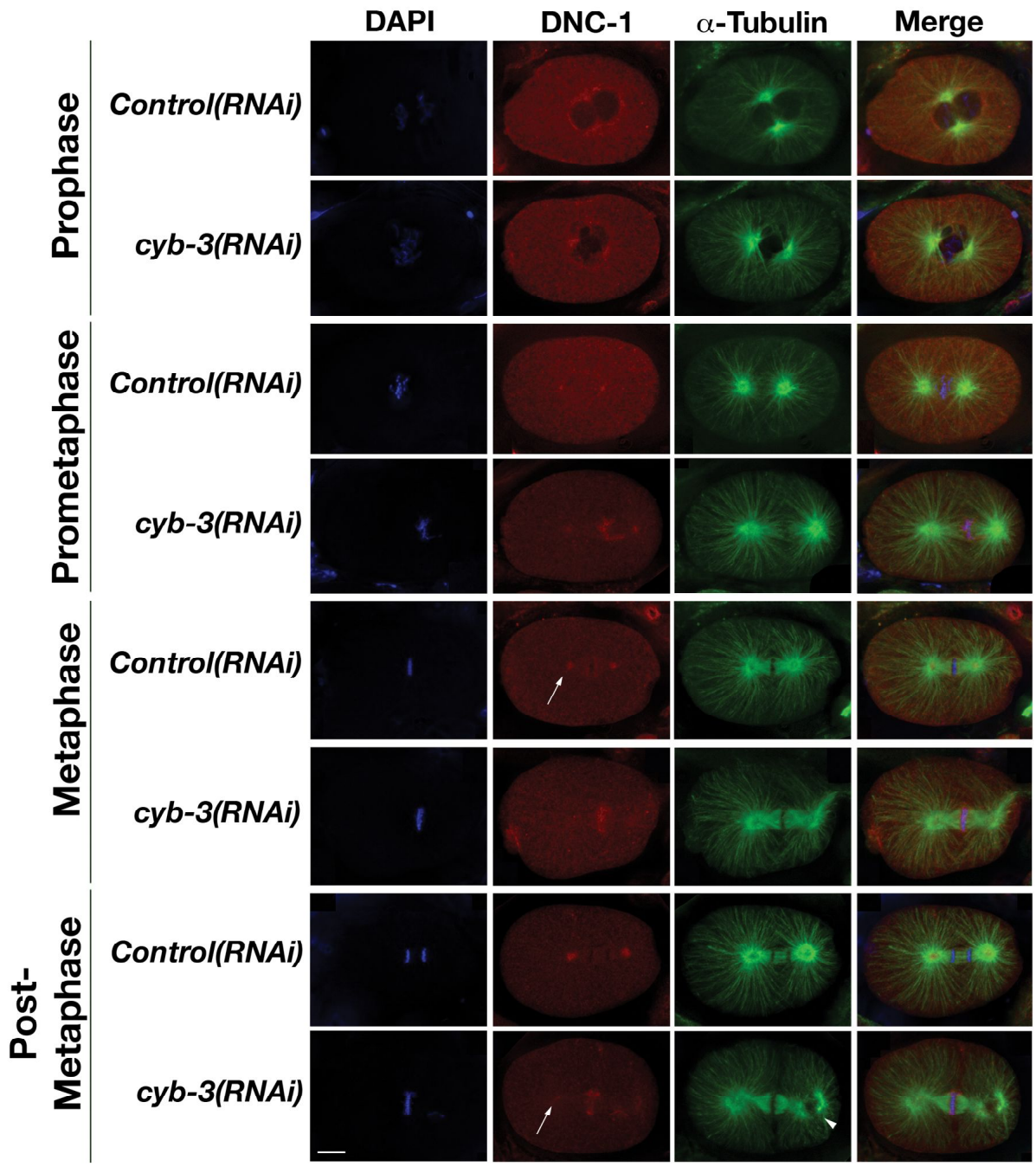
DAPI
DNC-1
α-Tubulin
Merge
Prophase
Control(RNAi)
cyb-3(RNAi)
Prometaphase
Control(RNAi)
cyb-3(RNAi)
Metaphase
Control(RNAi)
cyb-3(RNAi)
Post-Metaphase
Control(RNAi)
cyb-3(RNAi)

Figure 38. *cyb-3(RNAi)* K-Mts are accessible to microtubule-associated proteins
Control and *cyb-3(RNAi)* embryos were fixed and stained with DAPI (blue) and antibodies recognizing α-tubulin (green) and BMK-1 (red). Scale bar = 10 μm.

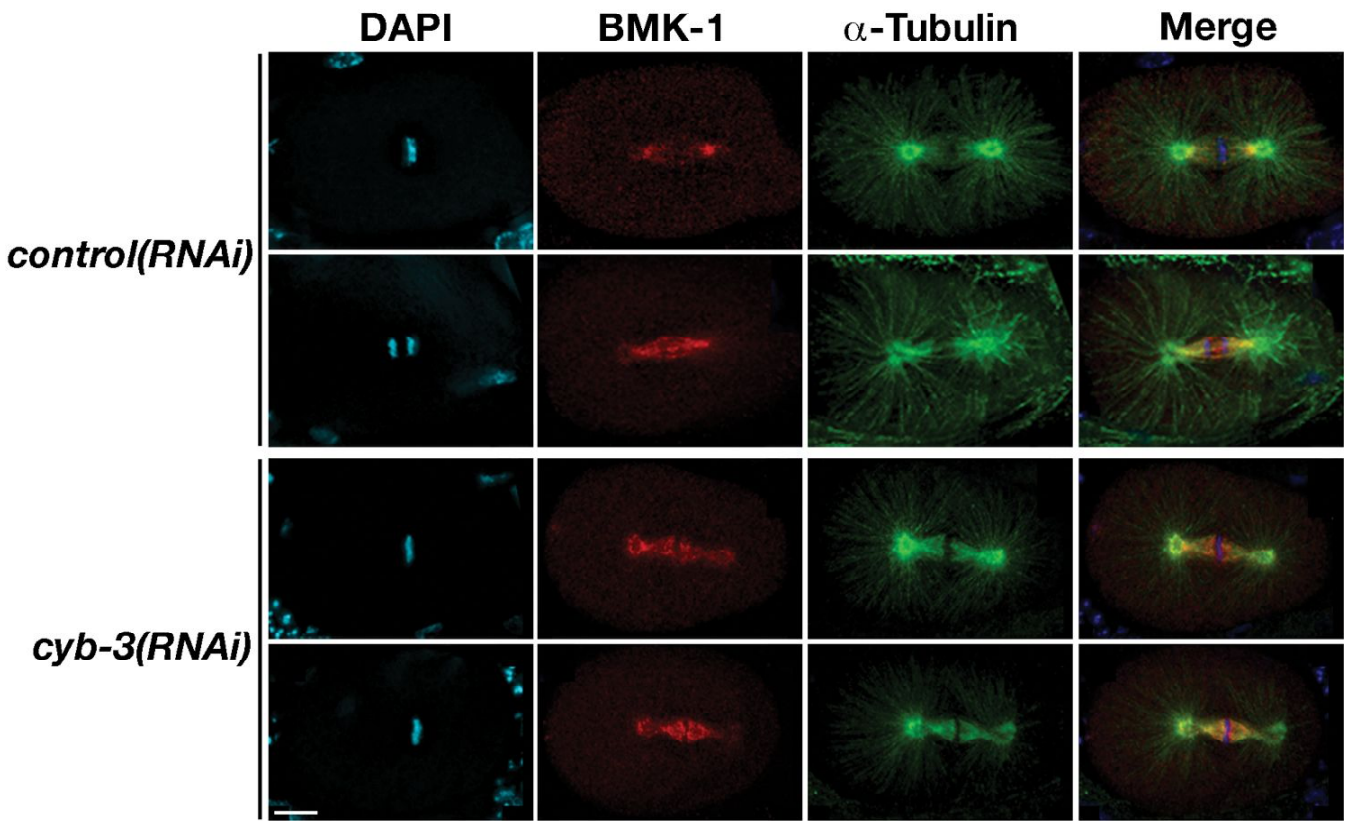
DAPI
BMK-1
α-Tubulin
Merge
control(RNAi)
cyb-3(RNAi)

depletion would not be feasibly suppressed by the loss of a dynein inhibitor. Therefore, we hypothesized that removing an inhibitor of dynein in embryos partially depleted of CYB-3 would facilitate dynein activity and suppress the metaphase delay. Live-cell imaging was performed with GFP::α-tubulin and mCherry::histone H2B-expressing embryos cut from hermaphrodites treated with *cyb-3(RNAi)* diluted with control or *dylt-1(RNAi)*. Under these conditions, CYB-3 depletion results in a significant metaphase delay (approximately two-fold) compared to control-treated embryos yet anaphase segregation eventually occurs (Figure 39A). Interestingly, the duration from nuclear envelope breakdown to anaphase in *dylt-1(RNAi)*-treated embryos is significantly shorter than control indicating that upregulated dynein activity may facilitate chromosome congression and/or SAC silencing (Figure 39B). Consistent with our predication, the co-depletion of DYLT-1 and CYB-3 suppressed the *cyb-3(RNAi)* metaphase delay and the duration from nuclear envelope breakdown to anaphase was similar to control (Figure 39, A and B). When taken together, these results provide strong evidence of decreased dynein function in embryos depleted of CYB-3.

Genetically reducing dynein function in *cyb-3(RNAi)* embryos enhances prometaphase defects

The data presented above suggest that CYB-3 positively regulates dynein function to silence the SAC. However, DYLT-1 may have dynein-independent mitotic functions and we therefore sought to determine if dynein activity is directly altered in *cyb-3(RNAi)* embryos. *dhc-1(or195ts)* mutants (hereafter referred to as *dhc-1ts*) harbor a hypomorphic temperature-sensitive allele of the dynein heavy chain (78). *dhc-1ts* embryos at restrictive temperatures display mitotic delays (including a delay at metaphase) but progress through the early embryonic divisions albeit with chromosome missegregation and penetrant lethality (78). With the prediction that genetically dampening dynein function would enhance *cyb-3(RNAi)*-related defects, *dhc-1ts* hermaphrodites or a wild-type strain were treated with control or dilute *cyb-3(RNAi)* and incubated at semi-permissive temperatures (22°C and 24°C) for 24 hours. Embryos were fixed and stained with an α-tubulin antibody and DAPI and the percentage of one-cell embryos at prometaphase, metaphase, and anaphase was scored for each condition.

Figure 39. Loss of a negative dynein regulator suppresses the metaphase latency in embryos partially depleted of CYB-3

A) Still images obtained from movies of OD57 embryos treated with *control (RNAi*), dilute *dylt-1(RNAi)*, dilute *cyb-3(RNAi)*, and dilute *cyb-3(RNAi)* and *dylt-1(RNAi)*. NEB = nuclear envelope breakdown. Scale bar = 10 μm. B) The time interval between NEB and the beginning of anaphase chromosome movements was quantified for the indicated RNAi movies. Asterisk = significantly different from control; control, n = 11; *dylt-1;control(RNAi)*, n = 2; dilute *cyb-3(RNAi)*, n = 6; dilute *cyb-3;dylt-1(RNAi)*, n = 7.

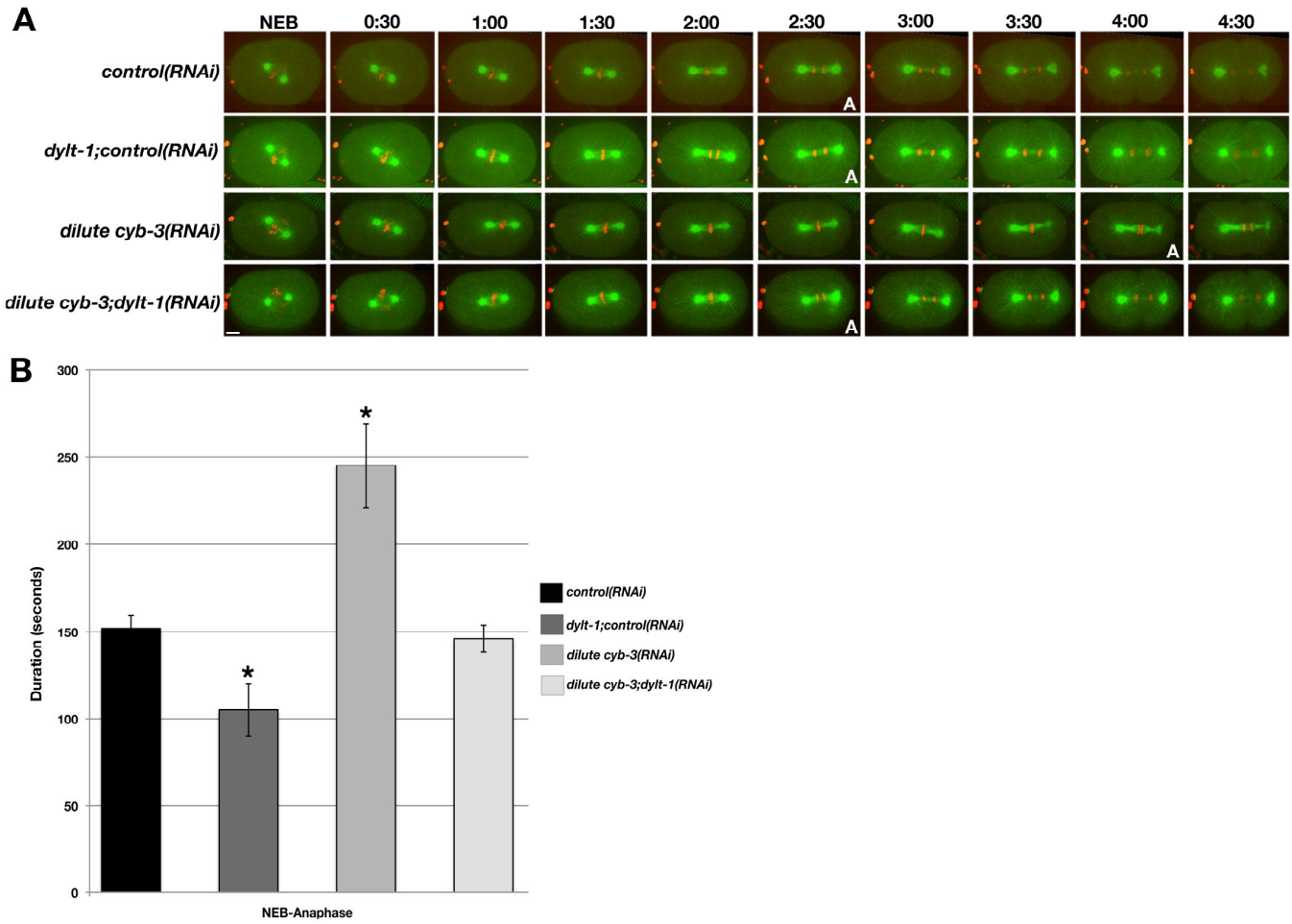
A
NEB
0:30
1:00
1:30
2:00
2:30
3:00
3:30
4:00
4:30
control(RNAi)
dylt-1;control(RNAi)
dilute cyb-3(RNAi)
dilute cyb-3;dylt-1(RNAi)
A
B
300
250
200
150
100
50
0
Duration (seconds)
NEB-Anaphase
*
*
control(RNAi)
dylt-1;control(RNAi)
dilute cyb-3(RNAi)
dilute cyb-3;dylt-1(RNAi)

The percentage of *dhc-1ts* control-treated embryos at prometaphase was significantly greater than wild-type at 24°C but not 22°C, confirming the temperature-sensitive nature of the *dhc-1ts* allele (Figure 40). These results are in line with the initial characterization of *dhc-1(or195ts)* that revealed an increase in the duration of prometaphase due to crippled dynein function (78). Interestingly, the percentage of anaphase control-treated *dhc-1ts* embryos at 24°C was significantly less than wild-type (Figure 40). The increased and decreased percentage of *dhc-1ts* embryos at prometaphase and anaphase, respectively, are completely consistent with dynein function influencing chromosome congression and/or SAC silencing.

Partial CYB-3 depletion did not increase the percentage of one-cell prometaphase, metaphase, or anaphase wild-type embryos compared to control-treated embryos at either temperature (Figure 40). However, multi-cellular embryos depleted of CYB-3 displayed chromosome missegregation and ploidy changes confirming the partial absence of CYB-3 (data not shown). As expected if CYB-3 positively regulates dynein function, CYB-3 depletion increased the percentage of prometaphase *dhc-1ts* embryos and decreased the number of embryos at anaphase at 22°C compared to wild-type embryos (Figure 40). Decreasing CYB-3 function in *dhc-1(ts)* embryos at 24°C showed a similar pattern (Figure 40). These data are consistent with our model that CYB-3 positively regulates dynein function.

CYB-3 and DHC-1 co-immunoprecipitate from embryo extract

Our model predicts that improper dynein function in CYB-3-depleted embryos is due to missing phospho-regulation of dynein subunits mediated by CYB-3/CDK-1 (Figure 47). Since cyclins direct Cdks to distinct substrates, CYB-3 may provide substrate specificity to the CYB-3/CDK-1 complex and tethers CDK-1 to its substrates. We hypothesized that CYB-3 interacts with dynein to facilitate phosphorylation by CDK-1. The *C. elegans* dynein complex is composed of thirteen subunits that interact with heavy chain (DHC-1) dimers that form the complex's motor core (WormBase web site, http://www.wormbase.org, release WS204, date 29 Jul 2009). Since it is not obvious which dynein subunit(s) CYB-3 binds, we speculated that DHC-1 would be a good candidate for CYB-3 association since phosphorylation of the dynein motor may

Figure 40. Reduction of dynein function enhances the prometaphase defects in CYB-3-depleted embryos

Wild-type (the two leftmost columns of each temperature set) and *dhc-1(ts)* embryos treated with control or dilute *cyb-3(RNAi)* were fixed and visually inspected for one-cell embryos of the indicated mitotic stages. Error bars: mean + S.E.M.; Asterisks: significantly different from control; Wild-type embryos (22°C: *control*, n = 74; *cyb-3 dilute;control*, n = 70), (24°C: *control*, n = 69; *cyb-3 dilute;control*, n = 95); *dhc-1(ts)* embryos (22°C: *control*, n = 73; *cyb-3 dilute;control*, n = 69), (24°C: *control*, n = 64; *cyb-3 dilute;control*, n = 96).

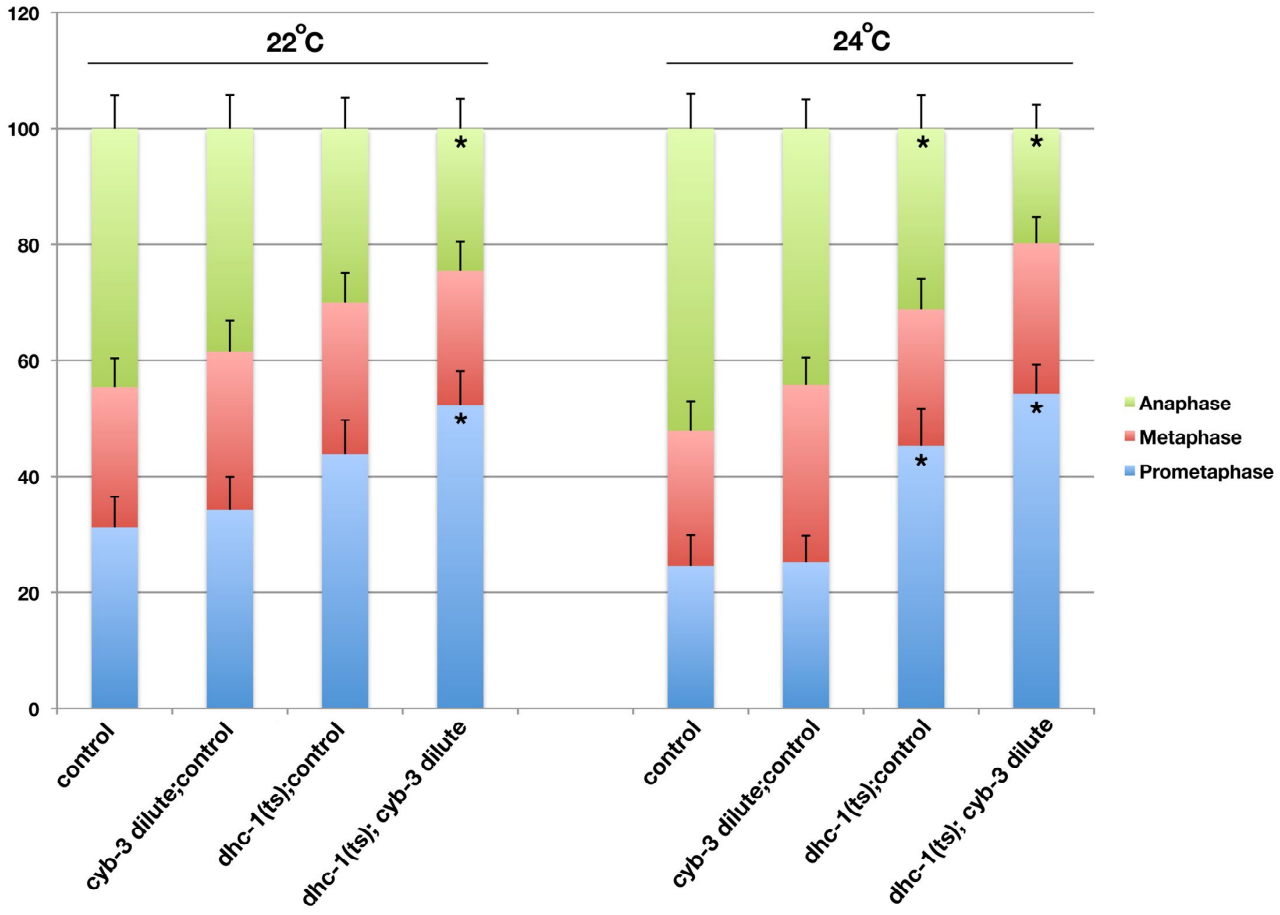
120
100
80
60
40
20
0
22°C
24°C
*
control
cyb-3 dilute;control
dhc-1(ts);control
dhc-1(ts); cyb-3 dilute
Anaphase
Metaphase
Prometaphase

be critical for dynein activation or movement. Moreover, CYB-3 co-immunoprecipitation with DHC-1 would imply that CYB-3 associates with dynein subunit(s), whether they are the light or heavy chains. Embryos expressing GFP::DHC-1 were isolated from control and *cyb-3(RNAi)*-treated hermaphrodites, sonicated, and protein extract was incubated with a polyclonal CYB-3 antibody. The protein G-isolated immunopurifications were washed, and the presence of CYB-3 and GFP::DHC-1 was assessed by western blotting (Figure 41). Interestingly, GFP::DHC-1 levels in *cyb-3(RNAi)* embryos was increased compared to control suggesting that dynein is stabilized at the kinetochore (Figure 41, LOAD). GFP::DHC-1 co-immunoprecipitated with CYB-3 in control but much less so in *cyb-3(RNAi)* immunoprecipitations (Figure 41). Although preliminary, these results indicate that CYB-3 likely interacts with dynein *in vivo*.

MDF-1^{mad1} is aberrantly associated with centrosomes in *dhc-1ts* embryos

Dynein function is required for a wide range of processes during *C. elegans* mitosis including proper centrosome separation, asymmetric spindle positioning, and chromosome congression (78). Embryos harboring a temperature-sensitive allele of *dhc-1* are delayed during prometaphase and metaphase at restrictive temperatures, a result that was interpreted to reflect crippled SAC silencing when dynein function is perturbed (78). However, it is currently unknown if SAC proteins in *C. elegans* serve as dynein cargo. Corroborating a biochemical association of SAC proteins with dynein is likely to be difficult since it is unclear which dynein subunits participate in this interaction.

The subcellular co-localization of proteins hints at their potential interactions. We hypothesized that kinetochore-localized dynein interacts with SAC proteins to coordinate SAC inactivation. Interestingly, the kinetochore localization of dynein in *dhc-1(or195)* embryos fails, and dynein is found predominately at centrosomes (78, 280). If dynein interacts with SAC proteins, we hypothesized that MDF-1^{Mad1} in *dhc-1(or195)* mutants would inappropriately co-localize with dynein at centrosomes. Indeed, immunostaining of wild-type and *dhc-1(or195)* embryos at restrictive temperatures with the MDF-1 antibody revealed robust MDF-1 centrosome staining in *dhc-1(or195)* embryos at prophase, prometaphase, and metaphase (Figure 42B). In stark contrast,

Figure 41. CYB-3 and DHC-1 co-immunoprecipitate from embryo extract

Embryos from GFP::DHC-1 hermaphrodites treated with control and *cyb-3(RNAi)* were isolated, subjected to sonication, and the pre-cleared soluble lysate was used for immunoprecipitation with an anti-CYB-3 antibody. Immobilized Protein G was used to isolate CYB-3-containing immunocomplexes, washed, and boiled in loading buffer. Western analysis was first performed with an anti-GFP antibody to determine the presence of DHC-1. Membranes were stripped and probed with CYB-3-specific antibodies. T7 = control; LOAD = 1/10 of starting material and CYB-3 IP = washed CYB-3 immunoprecipitates.

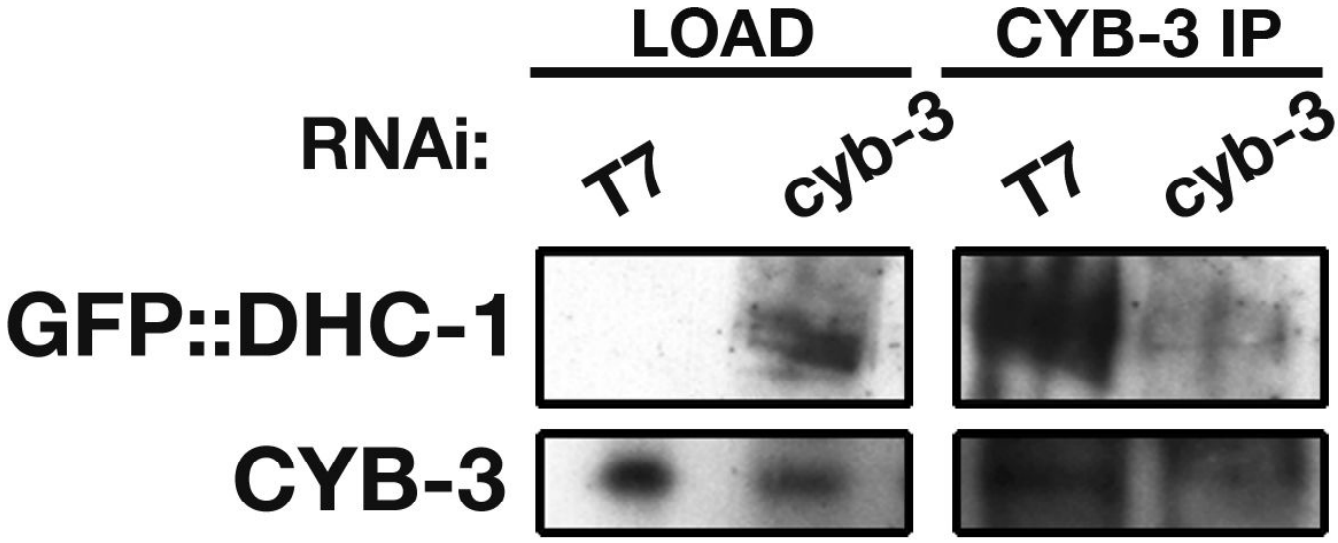
LOAD
CYB-3 IP
RNAi:
T7
cyb-3
T7
cyb-3
GFP::DHC-1
CYB-3

Figure 42. MDF-1^{mad1} is enriched at centrosomes in *dhc-1ts* embryos throughout mitosis

A) Wild-type and B) *dhc-1ts* hermaphrodites were incubated at 22°C and their embryos were fixed and stained with DAPI, α-tubulin, and an antibody recognizing MDF-1. Pro = prophase; Pro-meta = prometaphase; Meta = metaphase; Ana = Anaphase; Arrows = centrosome staining. Scale bar = 10 μm.

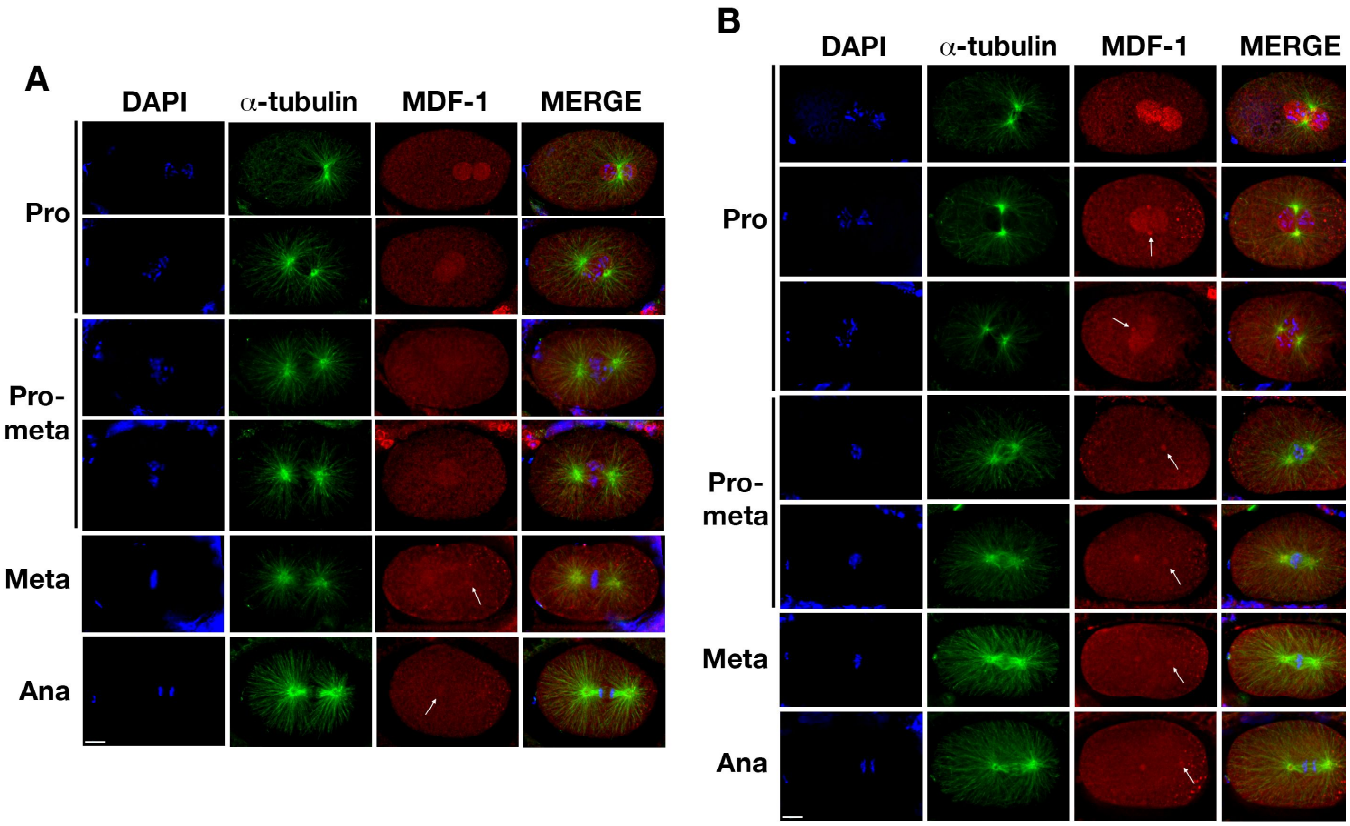
A
DAPI
α-tubulin
MDF-1
MERGE
Pro
Pro-
meta
Meta
Ana
B
DAPI
α-tubulin
MDF-1
MERGE
Pro
Pro-
meta
Meta
Ana

MDF-1 was only apparent with metaphase and anaphase centrosomes in control-treated embryos (Figure 42A). These results are consistent with SAC proteins serving as dynein cargo and indicate that the proper localization of SAC proteins during mitosis requires functional dynein complexes.

K-Mt defects do not contribute to dynein kinetochore retention

It has been proposed that the movement of dynein from kinetochores may be facilitated by proper K-Mt attachments (281). In this model, dynein is retained at kinetochores due to increased microtubule turnover in the presence of incorrect K-Mt interactions. If this model is correct, the inability of dynein to shuttle off of kinetochores may be due to unstable K-Mt attachments in embryos depleted of CYB-3. However, embryos depleted of key microtubule binding complexes at the kinetochore (e.g. NDC-80 and KNL-1) still undergo anaphase spindle movements and thus are unlikely to have SAC silencing defects (67). To determine if dynein is retained at kinetochores in embryos treated with *ndc-80(RNAi)* or *knl-1(RNAi)*, live-cell imaging of embryos expressing GFP::DHC-1 and mCherry::histone H2B was performed. As expected, the inability to generate stable K-Mt interactions did not perturb the dynamic localization of dynein and faint kinetochore localization was only visible at metaphase (data not shown). These results indicate that CYB-3 may have separable roles in the generation of stable K-Mt attachments and dynein-dependent SAC silencing. However, it is likely that decreased dynein function contributes to the malfunction of both processes.

The temporality of chromosome condensation is altered in *cyb-3(RNAi)* embryos

Cdk1 function is required for chromosome condensation in part by phosphorylating condensin subunits that are essential for establishing higher-order chromatin structures (92). We noticed that mitotic chromosomes in CYB-3-depleted embryos were not as condensed as control-treated embryos. Moreover, *C. elegans* embryos depleted of condensin subunits show defects in chromosome condensation and altered architecture of prometaphase and metaphase kinetochores (9, 26). To rule out chromosome condensation defects as the cause of the molecular alterations in embryos depleted of CYB-3, many of the experiments described above were performed with

embryos depleted of essential condensin subunits (e.g. SMC-4 and HCP-6). To quantitatively determine condensation defects in *cyb-3(RNAi)* embryos, live-cell imaging was performed with embryos expressing GFP::γ-tubulin (an independent marker to define the mitotic stage) and GFP::histone H2B. Chromosome condensation in the paternal pronucleus was monitored with an algorithm previously designed for such a purpose (19). This program detects the percentage of pixels that have intensities falling below a defined threshold of the maximum (19). For example, the percentage of pixels falling below 20% of the maximum pixel intensity threshold occurs late during condensation since GFP::histone H2B molecules must be in close proximity to satisfy this value. Embryos treated with *control(RNAi)*, *cyb-3(RNAi)*, and *smc-4(RNAi)* were subject to live-cell imaging and chromosome condensation was analyzed in the paternal pronucleus. In control embryos, chromosome condensation initiated approximately 4.5 mins before nuclear envelope breakdown (Figure 43A, time point -270) and linear chromosomes were apparent 1.5 minutes prior to nuclear envelope breakdown (time point -90). Depletion of SMC-4 greatly perturbed chromosome condensation and compact linear chromosomes were not observed at any mitotic stage (Figure 43A). In contrast, the depletion of CYB-3 did not drastically affect chromosome condensation and chromosome morphology was similar to control at nuclear envelope breakdown (Figure 43A). Quantitation of GFP::histone H2B intensity revealed that CYB-3-depletion slows but does not greatly affect chromosome condensation (Figure 43B; compare the 20% and 35% line traces). However, *smc-4(RNAi)* perturbs chromosome condensation measured at each threshold (Figure 43B). These data indicate that CYB-3 regulates the temporality of condensation but is not required for it per se.

RNAi-mediated silencing of chromosome condensation factors does not phenocopy *cyb-3(RNAi)* defects

Embryos depleted of CYB-3 displayed increases in the duration of prophase and prometaphase, with the complete absence of anaphase sister chromatid separation (Figure 27). To determine if defective chromosome condensation similarly alters cell cycle progression, OD57 embryos expressing GFP::α-tubulin and mCherry:histone H2B were treated with *smc-4(RNAi)* and the first mitotic division viewed with live-cell

Figure 43. CYB-3 influences the timing of chromosome condensation yet loss of condensation does not alter cell cycle progression

A) Hermaphrodites expressing GFP::gamma-tubulin and GFP::Histone H2B were treated with control, *cyb-3*, and *smc-4(RNAi)*. Embryos were isolated and mounted for spinning-disc confocal microscopy. Enlarged images of chromosomes are shown for comparison with time points (in seconds) relative to nuclear envelope breakdown (NEB). B) Quantitation of the percentage of GFP::histone H2B pixels that have intensities below the indicated thresholds. The control plots are superimposed on the *cyb-3(RNAi)* and *smc-4(RNAi)* graphs for comparison. C) Still images from movies generated with OD57 embryos depleted of the indicated proteins via RNAi. Scale bar = 10 μm. The movies were analyzed to obtain time intervals for the mitotic stages indicated in (D).

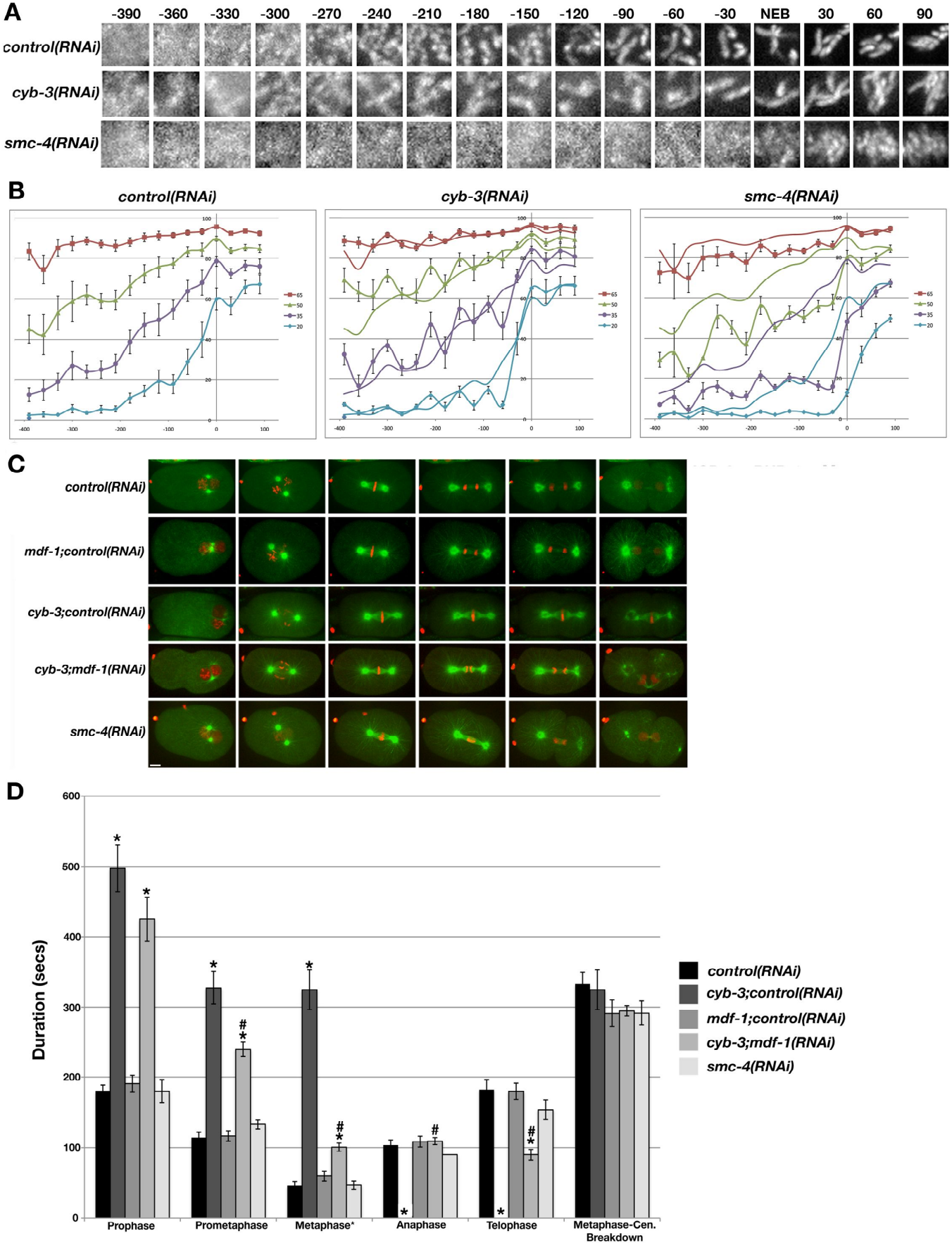
A
-390
-360
-330
-300
-270
-240
-210
-180
-150
-120
-90
-60
-30
NEB
30
60
90
control(RNAi)
cyb-3(RNAi)
smc-4(RNAi)
B
control(RNAi)
cyb-3(RNAi)
smc-4(RNAi)
65
50
35
20
C
control(RNAi)
mdf-1;control(RNAi)
cyb-3;control(RNAi)
cyb-3;mdf-1(RNAi)
smc-4(RNAi)
D
Duration (secs)
600
500
400
300
200
100
0
Prophase
Prometaphase
Metaphase*
Anaphase
Telophase
Metaphase-Cen. Breakdown
control(RNAi)
cyb-3;control(RNAi)
mdf-1;control(RNAi)
cyb-3;mdf-1(RNAi)
smc-4(RNAi)

imaging. Depletion of SMC-4 abruptly compromised chromosome condensation but did not significantly alter cell cycle progression (Figure 43, C and D). The most severe defects occurred during anaphase when uncondensed chromosomes were stretched along the A-P axis of the mitotic spindle with no clear chromosome segregation (Figure 43C) (26). In these experiments, anaphase onset was therefore defined as the beginning of centrosome separation and not by the timing of sister chromatid disjunction. Quantitation of mitotic stage timing revealed that *smc-4(RNAi)* and *control(RNAi)*-treated embryos were nearly identical at each stage of mitosis (Figure 43D). Therefore, the mitotic progression defects resulting from loss of CYB-3 are not due to underlying chromosome condensation defects. These data support the conclusion that deregulated kinetochore function is a central factor that affects cell cycle progression in *cyb-3(RNAi)* embryos.

The normal mitotic progression in *smc-4(RNAi)* embryos suggested that chromosome condensation defects do not activate the SAC. To validate this hypothesis, embryos treated with control, *cyb-3(RNAi)*, *smc-4(RNAi)*, and *hcp-6(RNAi)* were fixed and stained with the 3F3/2 antibody and BUB-1 as a kinetochore marker. In control embryos, BUB-1 localized to parallel kinetochore stripes and K-Mts (Figure 44). 3F3/2 immunoreactivity was highly cytosolic but was not enriched on metaphase chromosomes (Figure 44). In stark contrast, *cyb-3(RNAi)* displayed relatively unstructured BUB-1 stripes, absent K-Mt staining, and robust recognition of metaphase chromosomes by the 3F3/2 antibody (Figure 44). In embryos depleted of SMC-4 and HCP-6, BUB-1 staining was altered compared to control and parallel kinetochore stripes were not obvious. However, decreased chromosome condensation in these embryos did not produce the 3F3/2 epitope (Figure 44). These data reveal an important observation: chromosome condensation defects leading to altered kinetochore architecture do not lead to passive production of the 3F3/2 epitope. Instead, these results confirm that loss of CYB-3 leads to kinetochore dysfunction and active production of the SAC-dependent 3F3/2 phospho-epitope.

CYB-3 depletion leads to SAC activation and recruitment of the SAC protein MDF-2 to kinetochores (Figures 29, 30, and 31). Although metaphase chromosomes in

Figure 44. Depletion of chromosome condensation factors does not result in the recruitment of the 3F3/2 epitope to chromosomes

A) Wild-type hermaphrodites were subjected to the indicated RNAi conditions, and their embryos were fixed and stained with DAPI and antibodies that recognize 3F3/2 and the kinetochore protein BUB-1. B) Embryos were treated with either vehicle (DMSO) or Taxol prior to fixation and staining with DAPI and the 3F3/2 antibody. Shown is 3F3/2 staining of single nuclei obtained from stage matched multi-cellular embryos. Scale bars = 10 μm.

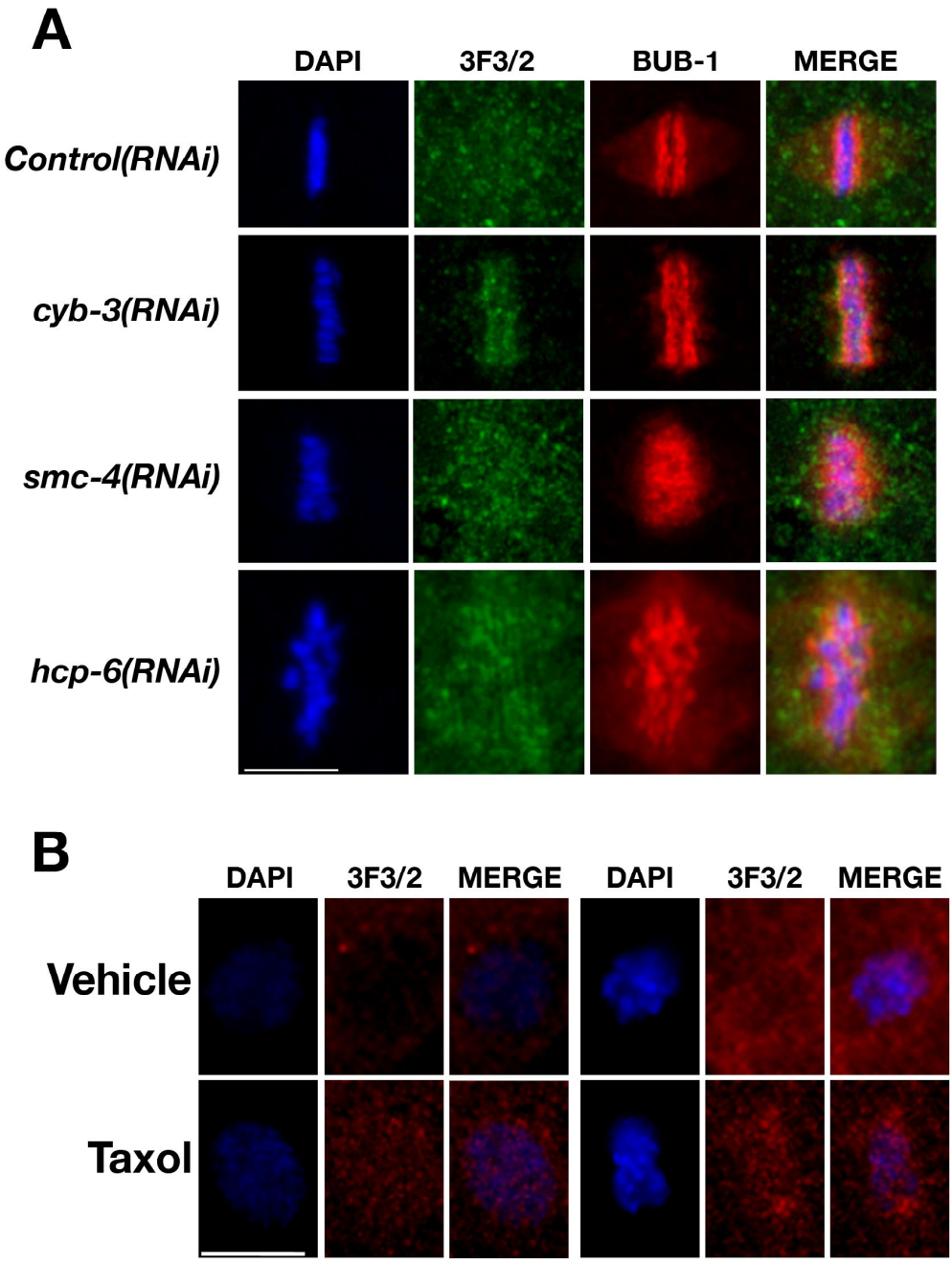
A
DAPI
3F3/2
BUB-1
MERGE
Control(RNAi)
cyb-3(RNAi)
smc-4(RNAi)
hcp-6(RNAi)
B
DAPI
3F3/2
MERGE
DAPI
3F3/2
MERGE
Vehicle
Taxol

embryos depleted of SMC-4 and HCP-6 did not display the 3F3/2 tension-specific epitope, the possibility remained that a MDF-2-dependent SAC pathway was active due to potential K-Mt defects caused by the loss of chromosome condensation. Live-cell analysis of embryos expressing GFP::MDF-2 and mCherry::histone H2B revealed that profound kinetochore recruitment of MDF-2 was exclusive to embryos depleted of CYB-3 (Figure 45). These data reveal that chromosome condensation defects do not appear to activate either branch of the SAC.

In a final line of investigation, dynein localization was analyzed by performing live-cell imaging of embryos expressing GFP::DHC-1 and mCherry::histone H2B. CYB-3 depletion results in dynein kinetochore retention (Figure 46). On the other hand, condensin-subunit depletions did not affect dynein localization and the kinetochore localization of dynein was only visible at metaphase similar to control-treated embryos (Figure 46). Altogether, these data confirm that the subtle condensation defects resulting from depletion of CYB-3 are unrelated to kinetochore dysfunction, SAC activation, or the failure of dynein to translocate from kinetochores.

AIR-2 has increased activity in embryos depleted of CYB-3

The Aurora B kinase corrects K-Mt attachments that do not generate tension, phosphorylating key kinetochore proteins ultimately leading to the dissociation of microtubules from the kinetochore (71, 111, 118). *C. elegans* Aurora B/AIR-2 is required for proper chromosome alignment and segregation during meiosis and mitosis (151, 153). The decreased fidelity of prometaphase chromosome congression and the inability to generate tension between sister chromatids at metaphase alignment suggested improper K-Mt dynamics potentially related to altered AIR-2 function. To test for changes in AIR-2 activity, control and *cyb-3(RNAi)* embryos were fixed and stained with an antibody recognizing ICP-1/CeINCENP phosphorylated at S598 and S599 (pICP-1) (Figure 48A) (122). AIR-2/Aurora B phosphorylation of ICP-1 at S598/S599 elicits a positive feedback increasing AIR-2 kinase activity (115). Immunoquantitation of the level of pICP-1 associated with chromosomes corresponding to chromosomal passenger localization revealed that pICP-1 levels were 1.5-fold higher in *cyb-3(RNAi)* one-cell embryos compared to control (Figure 48B).

Figure 45. Chromosome condensation defects do not promote robust MDF-2 kinetochore recruitment

Selected live images of control, *cyb-3(RNAi), smc-4(RNAi), and hcp-6(RNAi)* embryos co-expressing GFP::MDF-2 and mCherry::Histone H2B are shown. Time 0:00 = NEB. Scale bar = 10 μm.

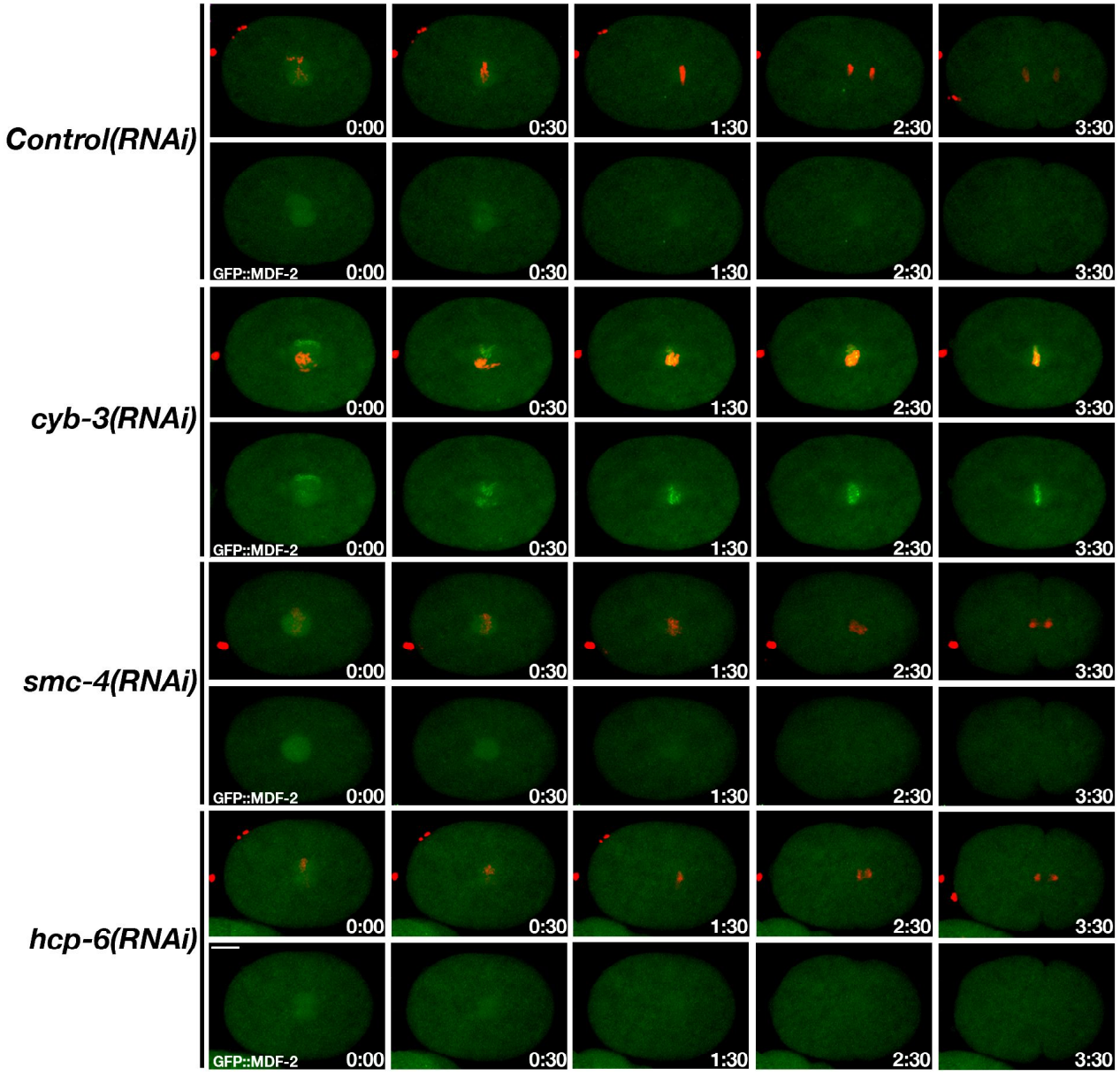
Control(RNAi)
cyb-3(RNAi)
smc-4(RNAi)
hcp-6(RNAi)
GFP::MDF-2
0:00
0:30
1:30
2:30
3:30

Figure 46. Dynein is not retained at kinetochores of under-condensed chromosomes
Selected live images of control, *cyb-3(RNAi), smc-4(RNAi), and hcp-6(RNAi)* embryos co-expressing GFP::DHC-1 and mCherry::Histone H2B are shown. Time 0:00 = NEB. Scale bar = 10 μm. The localization of DHC-1 at the anterior (left) bulge in *cyb-3(RNAi)* embryos corresponds to the polar body.

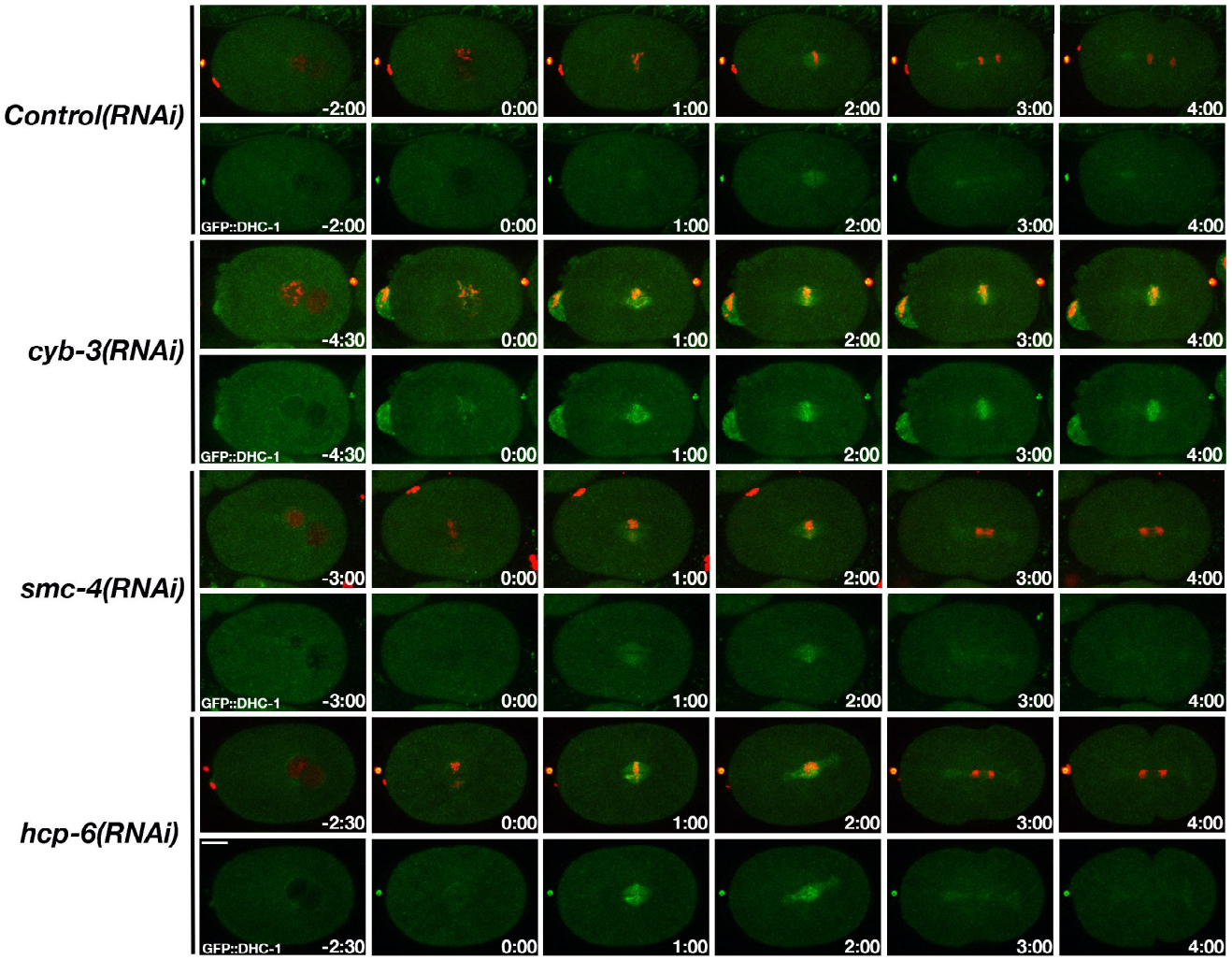
Control(RNAi)
-2:00
0:00
1:00
2:00
3:00
4:00
GFP::DHC-1
cyb-3(RNAi)
-4:30
smc-4(RNAi)
-3:00
hcp-6(RNAi)
-2:30

Figure 47. A model for the influence CYB-3 has on dynein function

During prometaphase, CYB-3 influences the removal of dynein from kinetochores, perhaps by direct phosphorylation of dynein by CDK-1/CYB-3 complexes. Work in other model organisms has revealed that a key role of Cdk1 phosphorylation of dynein light chains is to facilitate cargo binding to dynein. Thus, CYB-3 may also influence cargo binding to dynein (red circles) to coordinate SAC protein removal from kinetochores. In the absence of CYB-3 (bottom left diagram), improper regulation of dynein at kinetochores leads to a propensity for chromosomes to move toward the minus-end of microtubules by dynein motor complexes and chromosome malorientation. At the metaphase-anaphase transition, CYB-3/CDK-1 function is required to silence the spindle assembly checkpoint through dynein mobilization, microtubule binding, and/or interaction with SAC proteins. The metaphase kinetochore architectural change that manifests in the absence of CYB-3 likely reflects a tug-of-war between plus-end-embedded, load bearing kinetochore-microtubule attachments and dynein-mediated pulling of chromosomes away from the metaphase plate. Increased AIR-2 activity in *cyb-3(RNAi)* embryos may also contribute to chromosome congression defects by increasing K-Mt turnover.

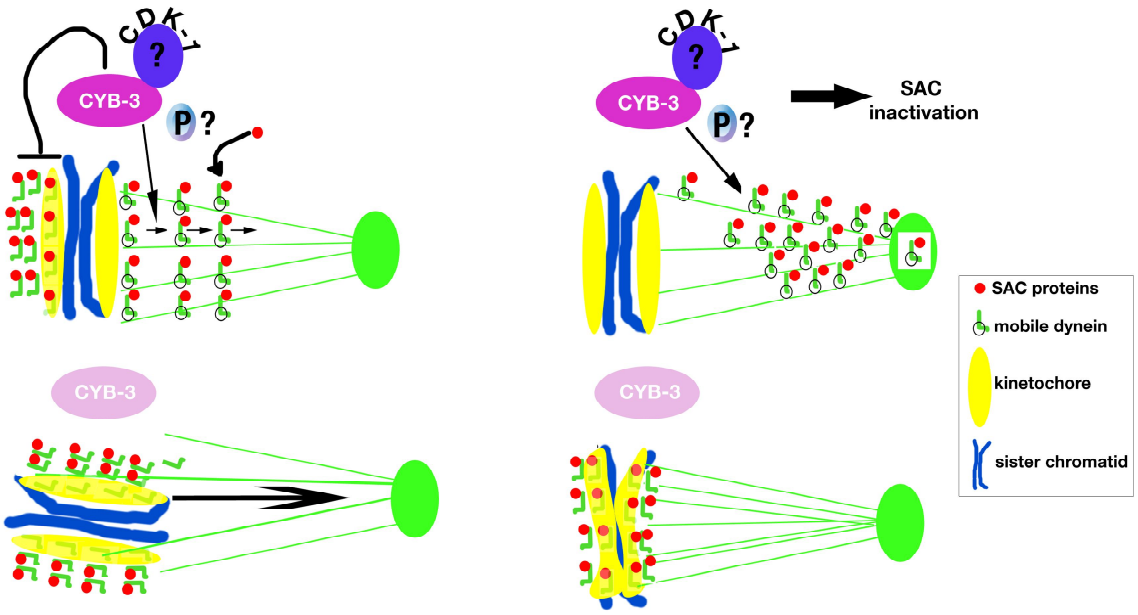
Prometaphase
Metaphase/Anaphase
CDK-1
?
CYB-3
P ?
SAC
inactivation
SAC proteins
mobile dynein
kinetochore
sister chromatid

Since the loss of CYB-3 resulted in increased AIR-2 activity, we postulated that overexpression of AIR-2 would enhance the defects caused by a weak or partial depletion of CYB-3. Previous work revealed that expression of a functional GFP::AIR-2 transgene in *C. elegans* enhanced the meiotic defects caused by the loss of an AIR-2 inhibitor (LAB-1) but did not alter wild-type meiotic progression (282). Hence, embryos co-expressing GFP::AIR-2 and mCherry::Histone H2B were treated with either control (*T7*) or *cyb3-(RNAi)* highly diluted with *T7* (1:30, see Materials and Methods). Parallel experiments were performed with embryos expressing GFP::α-Tubulin and mCherry::Histone H2B. Under these conditions, 88% of *cyb-3(RNAi)* embryos entered anaphase (n=8) whereas only 30.8% of *cyb-3(RNAi)*;GFP::AIR-2-expressing embryos underwent anaphase chromosome segregation (n=13, p=0.005) (Figure 48C). Moreover, AIR-2 levels on prophase, prometaphase, and metaphase chromosomes were decreased in *cyb-3(RNAi)* embryos compared to control, indicating a role for CYB-3 in the expression or stability of AIR-2, or the targeting of AIR-2 to chromosomes (Figure 48C). These results suggest that increased AIR-2 activity contributes to the metaphase arrest in the absence of CYB-3.

Phospho-CDK-1 isoforms localize to distinct subcellular regions

Cdk1 activity is influenced by *in trans* activating and inactivating phosphorylations. Cdk1 phosphorylated at T161 within the activation loop increase whereas N-terminal phosphorylations decrease Cdk1 kinase activity (241). T161 is targeted by Cdk-activating kinase (CAK) while Wee1-related kinases mediate the N-terminal inhibitory phosphorylations (241). The phenotype of *cdk-7(RNAi)* suggests that *Ce*CDK-7 is a CAK that activates CDK-1 during meiosis and mitosis (267). The *C. elegans* genome encodes three WEE-1 isoforms, and WEE-1.3 is required to prevent premature oocyte maturation by inhibiting CDK-1 (150). The Cdk1 residues that are targeted by Wee1 and CAK are conserved in *Ce*CDK-1, indicating that phospho-regulation of cyclin dependent kinases is a conserved mechanism.

To determine the subcellular localization of specific phospho-CDK-1 isoforms, embryos were fixed and stained with antibodies specific for each post-translational modification. Active CDK-1 (P-T161) localized to centrosomes and the mitotic spindle

Figure 48. The activity of AIR-2/CeAurora B is increased in CYB-3 depleted embryos

(**A**) Control and *cyb-3(RNAi)* embryos were fixed and stained with DAPI (blue) and antibodies specific for α-tubulin (green) and pICP-1 (red). Prometaphase and metaphase one-cell embryos are shown. (**B**) pICP-1 prometaphase and metaphase chromosome staining intensity in control and *cyb-3(RNAi)* one-cell embryos. Asterisks: $p < 0.001$. Prometaphase: control, n = 27; *cyb-3(RNAi)*, n = 51; Metaphase: control, n = 34; *cyb-3(RNAi)*, n = 97. Error bars: mean +/- s.e.m. (**C**) Selected live images of OD57 (first and third rows) and GFP::AIR-2 and mCherry::Histone H2B expressing embryos (second and fourth rows) treated with control or diluted *cyb-3(RNAi)*. Time 0:00 = metaphase. Images just left of 0:00 correspond to NEB, and the left most images PNM. Scale bars = 10 μm.

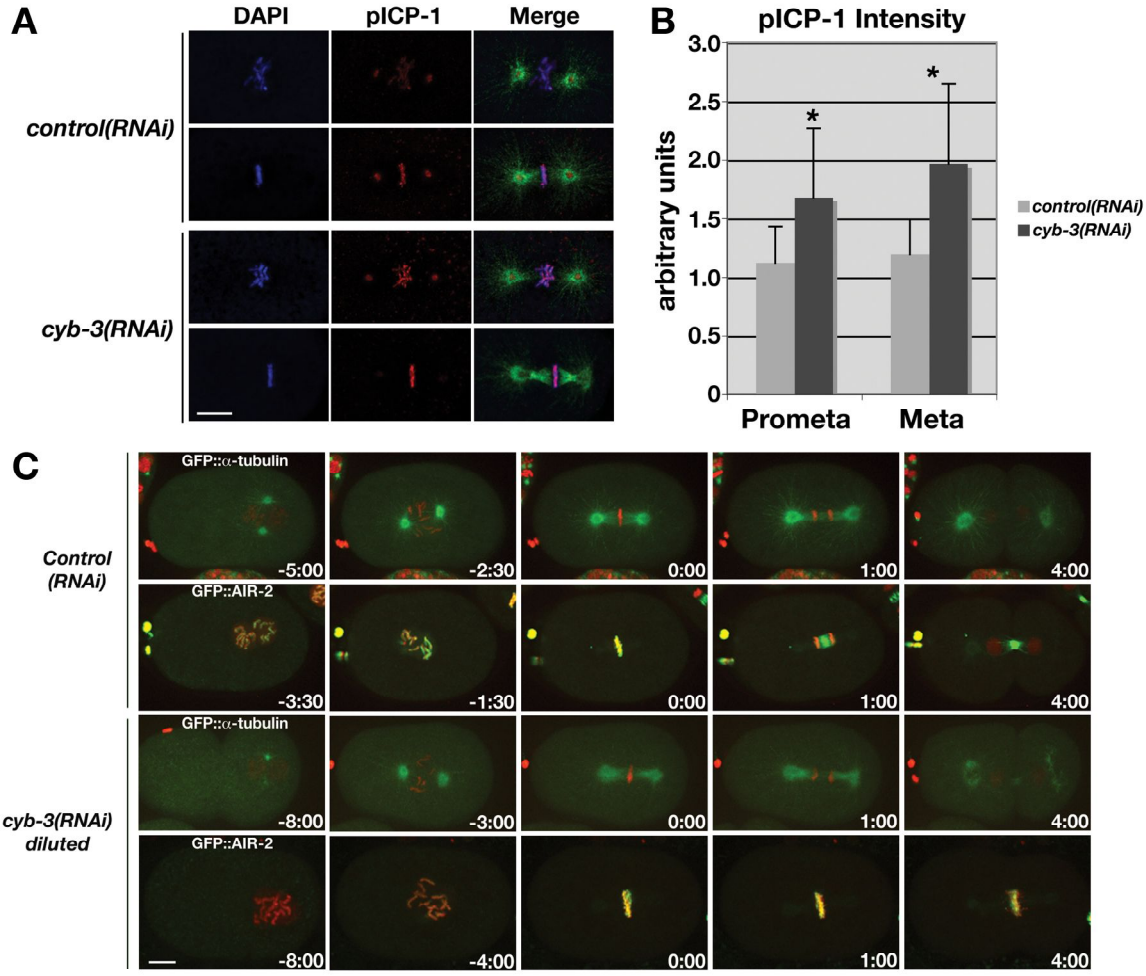
A
DAPI
pICP-1
Merge
control(RNAi)
cyb-3(RNAi)
B
pICP-1 Intensity
arbitrary units
3.0
2.5
2.0
1.5
1.0
0.5
0
Prometa
Meta
control(RNAi)
cyb-3(RNAi)
C
Control (RNAi)
cyb-3(RNAi) diluted
GFP::α-tubulin
GFP::AIR-2
-5:00
-2:30
0:00
1:00
4:00
-3:30
-1:30
-8:00
-3:00
-4:00

throughout mitosis and was nuclear during prophase and late telophase/G1 (Figure 49). Interestingly, kinetochore localization of active CDK-1 (P-T161) was not observed (Figure 49). This localization of T161-phosphorylated CDK-1 is consistent with the spatial regulation of Cdk1 activation in higher eukaryotes in which active Cdk1 first appears at centrosomes and nuclei (139). Inactive CDK-1 (P-T14, Y15) is similarly enriched at nuclei during prophase and late telophase/G1 (Figure 50). This phospho-CDK-1 isoform also localizes to centrosomes throughout mitosis but appears more focused at the centrosome center compared to active CDK-1 (P-T161) (Figure 50). Strikingly, inactive CDK-1 (P-T14, Y15) localizes to kinetochores at prometaphase and metaphase (Figure 50). Interestingly, CDK-1 (P-T14, Y15) does not appear to localize to K-Mts (Figure 50). Although further research is required to determine which kinetochore layer (i.e. inner or outer) the inactive phospho-CDK-1 isoform localizes to, the only kinetochore protein that does not display K-Mt immunostaining is HCP-3, the CENP-A histone H3 variant at centromeres. Hence, the most logical explanation of CDK-1 (P-T14, Y15) localization is that the kinetochore pool of CDK-1 is largely inactive and must be targeted to microtubules for CDK-1 activation. Therefore, CYB-3/CDK-1 complexes at the kinetochore-microtubule interface may require proper microtubule dynamics at kinetochores to promote CDK-1 activation and phosphorylation of critical CDK-1 substrates. This hypothesis is in complete agreement with results gleaned from studies of *S. pombe* that indicate that T14,Y15 dephosphorylation and Cdk1 activation is dependent on proper mitotic microtubule function (245).

Discussion

B-type cyclins in *C. elegans* have largely non-redundant function

Research in many organisms has suggested functional redundancy amongst B-type cyclins. However, cyclins target Cdks to specific substrates so it is probable that key Cdk1 phosphorylations will be lost upon the depletion of individual cyclins. Here, we report that CYB-3 depletion results in profound mitotic defects indicative of a critical kinetochore function for CYB-3 complexes. The altered morphology of kinetochores and K-Mts at metaphase, hyperactivation of AIR-2/Aurora B, and decreased function and failure of dynein and dynein-accessory proteins to move from the kinetochore to the

Figure 49. CDK-1 that is phosphorylated at T161 (active) localizes to the mitotic spindle

Wild-type embryos were fixed and stained with DAPI and antibodies that recognize α-Tubulin and human Cdk1 phosphorylated at T161. P-T161 is a marker of active Cdk1 in humans and is conserved in *C. elegans* CDK-1, although this modification has not been empirically shown to participate in CDK-1 activation in nematodes. Scale bar = 10 μm.

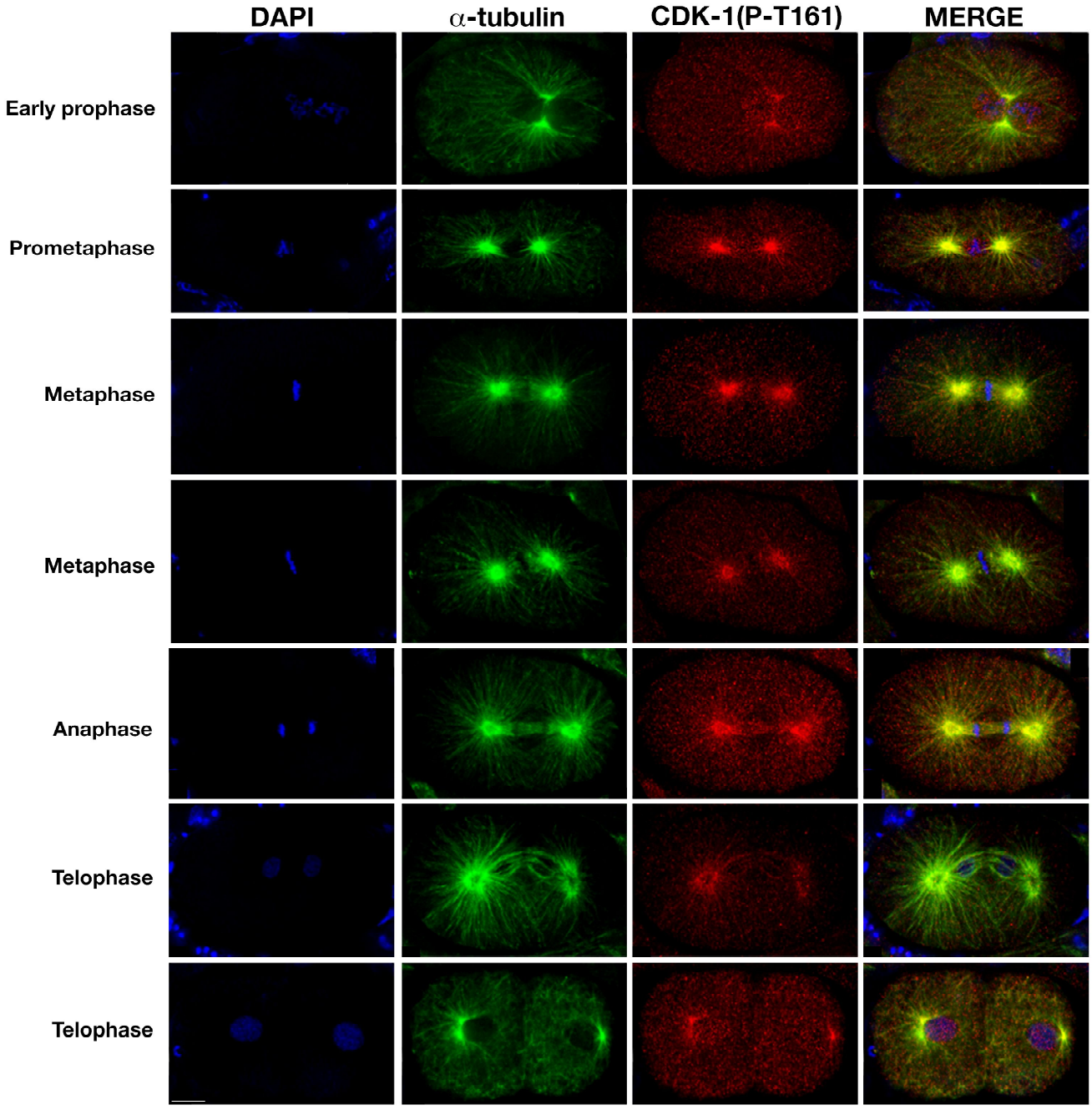
DAPI
α-tubulin
CDK-1(P-T161)
MERGE
Early prophase
Prometaphase
Metaphase
Metaphase
Anaphase
Telophase
Telophase

Figure 50. P-Y14,15-CDK-1 (inactive) localizes to kinetochores and centrosomes
Wild-type embryos were fixed and stained with DAPI and antibodies that recognize α-tubulin and human Cdk1 phosphorylated at T14 and Y15. T14 and Y15 are conserved in *C. elegans* CDK-1, although this modification has not been empirically shown to participate in CDK-1 inactivation in nematodes. Scale bar = 10 μm.

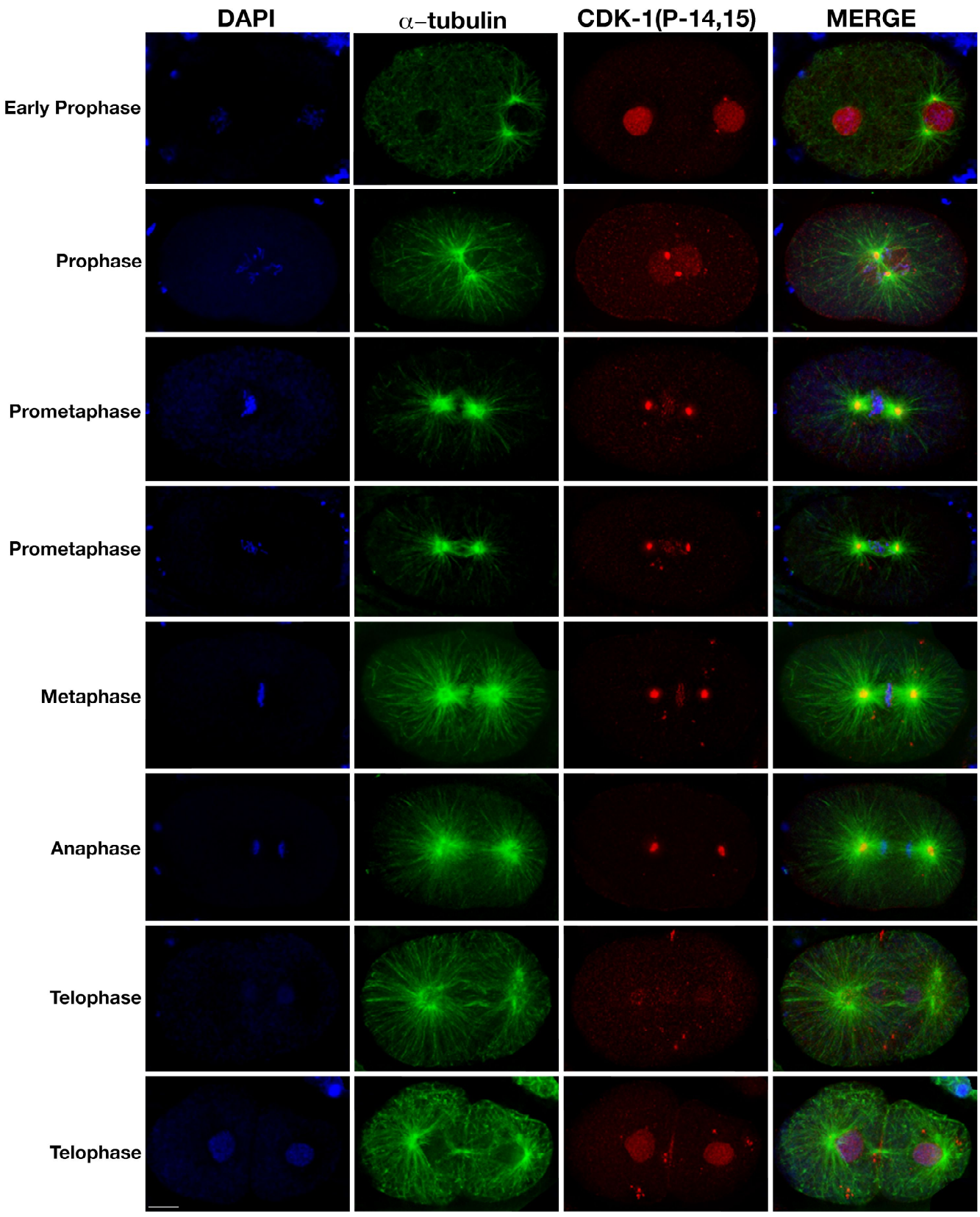
DAPI
α–tubulin
CDK-1(P-14,15)
MERGE
Early Prophase
Prophase
Prometaphase
Prometaphase
Metaphase
Anaphase
Telophase
Telophase

mitotic spindle suggest that CYB-3 couples the fidelity of K-Mt interactions with dynein-dependent SAC inactivation.

Immunostaining of cultured human and chicken cells with cyclin B3 antibodies has suggested that cyclin B3 localizes to the nucleus in interphase and is more nuclear-enriched compared to cyclin B1 (283, 284). Staining of *C. elegans* embryos with a CYB-3 antibody (270) revealed clear nuclear localization during interphase and mitosis prior to NEB, and enrichment around metaphase chromosomes reflecting kinetochore and K-Mt localization (similar to the GFP::CYB-3 staining presented above). Inactive CDK-1 (P-T14,Y15) showed similar nuclear enrichment during interphase and prophase but was exclusive to the metaphase kinetochore and was not detected on K-Mts. In contrast, active CDK-1 (P-T161) localizes to K-Mts and the entire mitotic spindle. Thus, CYB-3 co-localizes with inactive kinetochore-bound CDK-1 and active CDK-1 associated with microtubules. These data indicate that CYB-3 may associate with inactive and active CDK-1 but awaits biochemical confirmation.

Altogether, our data demonstrate that CYB-3 plays a non-redundant role in mitosis by influencing K-Mt dynamics. The next step in further clarifying the molecular mechanism by which CYB-3 influences K-Mt dynamics, AIR-2 activity, and dynein functions will be the identification of CYB-3 partners at the kinetochore. Notably, cyclin B1 harboring a point mutation inhibiting its association with Cdk1 still localizes to kinetochores, suggesting that cyclin B1 may have Cdk1-independent functions (254). Therefore, although cyclins are well-known cofactors of cyclin-dependent kinases, the possibility that cyclins functionally interact with other mitotic partners is an intriguing question for the future.

CYB-3 influences multiple aspects of the spindle assembly checkpoint

The accuracy of kinetochore interactions with spindle microtubules must be relayed to the SAC so that anaphase onset does not occur in the presence of incorrect K-Mt attachments, as these can cause chromosome fragmentation and genome instability (158, 285). The results presented here reveal that CYB-3 function is required to maintain ploidy via two mechanisms: generating stable K-Mt attachments and inactivating the SAC. Both mechanisms may be linked if dynein function is required for

end-on attachments in additional to its established role in silencing the SAC. K-Mt plus-ends that are embedded perpendicular to the kinetochore surface (end-on) display less dynamic instability caused by relatively unknown molecular mechanisms (11). Interestingly, *C. elegans* dynein influences the generation of end-on K-Mt attachments by inhibiting the RZZ kinetochore complex, which antagonizes the switch from lateral to end-on attachments (286). Hence, decreased dynein function in CYB-3-depleted embryos may directly interfere with the production of end-on K-Mt attachments that are a requirement for anaphase.

Human Cdk1 influences SAC inactivation through dynein phosphorylation. Cdk1-mediated phosphorylation of the dynein light intermediate chain stimulates the binding of SAC proteins to dynein and their movement away from kinetochores (184). Cdk1 also influences the kinetochore localization of dynein through intermediate chain phosphorylation-dependent binding of dynein to the zw10 subunit of the RZZ complex (287). However, the identity of the cyclin subunit of the Cdk1 complex that mediates dynein phosphorylation was not verified but was assumed to be cyclin B1. The data presented here suggest that B3-type cyclins may be dispensable for the kinetochore localization of dynein, but may have a critical and direct role mediating Cdk1 phosphorylation of dynein subunits to promote SAC inactivation.

The SAC in the *C. elegans* embryo is not as robust as that in human cells and only provides a transient checkpoint that is eventually overridden or adapted to. Embryos treated with the microtubule-destabilizing drug nocodazole or depleted of K-Mt binding entities at kinetochores only display a transient delay from nuclear envelope breakdown to anaphase onset (~ 250–300s) (165). In embryos depleted of CYB-3, this interval is increased to ~ 600s and anaphase segregation does not occur. Besides CYB-3 depletion, the only other condition that leads to a prominent block at metaphase in *C. elegans* embryos is suspended animation (288). Suspended animation is a phenomenon where unfavorable environmental conditions retard the development of an organism for long durations of time. For example, embryos subjected to an anoxic environment display a SAC dependent block at metaphase (288). This developmental program is reversible as shifting embryos to normal oxygen levels reinstates the cell cycle and anaphase onset (288). Since CYB-3 is required to inactivate the SAC, progression out of

suspended animation may very well depend on CYB-3 as well. Future investigation of CYB-3 function related to suspended animation may lead to a better understanding of exit from this conserved developmental process.

Upregulated AIR-2 activity in the absence of CYB-3

cyb-3(RNAi)-mediated chromosome congression defects and alterations in the structure of metaphase chromosomes suggest that CYB-3 influences the production of tension-generating K-Mt interactions, as does the AIR-2/Aurora B kinase. Although CYB-3-depleted embryos display a modest increase in AIR-2 activity, slight perturbations in Aurora B pathways can have a dramatic impact on mitosis. For instance, mutation of a single residue of the *S. cerevisiae* Ipl1/Aurora substrate Dam1 to a non-phosphorylatable residue severely compromises chromosome segregation and cell viability (111). Similarly, mutation of an Aurora B site in the MCAK kinesin results in severe chromosome segregation defects (112). Thus, the loss of a sole Aurora B phosphorylation in a single substrate can lead to gross mitotic abnormalities.

Since Aurora B phosphorylation leads to the disassociation of K-Mt attachments, its activity must be down-regulated at or isolated from tension-producing interactions. Elegant experiments have recently shown that tension between sister chromatids results in the spatial sequestration of kinetochore substrates from Aurora B at the inner centromere (289). These results suggest that Aurora B kinase activity may not be subject to active down-regulation. Since *cyb-3(RNAi)* results in "twisted" metaphase kinetochores, AIR-2/Aurora B targets may traverse the inner centromere and be prone to phosphorylation. Thus, two events relevant to AIR-2 regulation may occur in *cyb-3(RNAi)* embryos: (i) a subtle increase in AIR-2 kinase activity, and (ii) an alteration in metaphase kinetochore architecture leading to increased phosphorylation of AIR-2 kinetochore targets. Whether these two molecular changes are linked is an important, outstanding question.

We posit that the morphological changes in *cyb-3(RNAi)* metaphase kinetochores are the result of aberrant K-Mts interactions and increased microtubule turnover due to AIR-2 hyperactivation. K-fibers were resistant to cold treatment in control and *cyb-3(RNAi)* embryos, suggesting that kinetochores are attached to K-Mts under both

conditions (data not shown). K-Mt attachment is also supported by anaphase chromosome segregation when the SAC is compromised. Therefore, the absence of kinetochore tension in CYB-3 depleted embryos may reflect either inappropriate K-Mt attachments or an inability to maintain tension-producing K-Mt interactions. An alternative explanation for the altered architecture of metaphase kinetochores is the inability of kinetochore proteins to translocate to K-Mts, leading to their accumulation at kinetochores. The Ndc80 complex is one of several complexes responsible for the K-Mt attachment (71), and is regulated by Aurora B phosphorylation (111, 290). Thus, if Ndc80 components were unable to localize to K-Mts in CYB-3 depleted cells, the sustained proximity of this complex with AIR-2 may lead to increased phosphorylation and high rates of microtubule turnover.

CYB-3 potentially regulates dynein function throughout mitosis

The *cyb-3(RNAi)* phenotype is strikingly similar to that of *Drosophila* S2 cells treated with *spindly(RNAi)* (167). Like *cyb-3(RNAi)*, Spindly-depleted cells undergo a SAC-dependent metaphase arrest characterized by bundled spindles that are pinched at the centrosomes. These cells also fail to silence the spindle checkpoint. However, unlike CYB-3, Spindly is required for the kinetochore localization of dynein (167). *C. elegans* Spindly (SPDL-1) is also required for dynein localization to the kinetochore but is necessary for SAC signaling, acting as a kinetochore-targeting protein for MDF-1/Mad1 and MDF-2/Mad2 (166, 286). Human Spindly is also required for dynein kinetochore recruitment but is not required for SAC activation or the removal of Mad2 from aligned chromosomes (291). Interestingly, inhibition of dynein activity prevented Mad2 removal and SAC silencing in hsSpindly-depleted cells, suggesting that kinetochore recruitment is not necessary for dynein-dependent quenching of the SAC (291). Our results show that dynein, dynein-regulatory proteins, and SAC components all accumulate on *cyb-3(RNAi)* metaphase kinetochores but do not appear to transfer to K-Mts or to centrosomes. Therefore, unlike Spindly, CYB-3 is not required for kinetochore targeting, but rather may be affecting the minus-end directed motor activity of dynein or its association with microtubules.

The research presented here has focused on prometaphase and metaphase abnormalities in the near absence of CYB-3 and suggest that altered dynein function may be a key contributing factor. However, subtle defects in two prophase events occur in embryos depleted of CYB-3. Firstly, the paternal pronucleus of wild-type embryos moves anteriorally away from the posterior cortex during pronuclear migration (PNM). Dynein-mediated pulling forces at the cell cortex mediate this movement (78). In *cyb-3(RNAi)* embryos, the paternal pronucleus does not migrate away from the posterior cortex. Therefore, PNM in CYB-3-depleted embryos occurs at the posterior cortex and not ~ 15 microns from the cortex. Secondly, dynein is a conserved regulator of centrosome separation and influences *C. elegans* spindle rotation during prophase (78). In *C. elegans,* loss of dynein function perturbs centrosome separation and the association of centrosomes with the maternal pronucleus (78). In *cyb-3(RNAi)* embryos, centrosome movement on the maternal pronucleus and spindle rotation are abnormal (data not shown). However, the spindle apparatus in *cyb-3(RNAi)* embryos eventually aligns with the A-P axis and is asymmetrically localized to the embryo posterior as in wild-type. In conclusion, CYB-3 appears to influence dynein-dependent processes at all stages of mitosis, most strikingly SAC silencing.

CHAPTER FIVE: PERSPECTIVES AND SIGNIFICANCE

Summary

The proper development of organisms and the maintenance of cellular ploidy in adult somatic cells both require proper chromosome segregation. Chromosome segregation demands a variety of chromosome-based processes including condensation, kinetochore attachment to spindle microtubules, and a checkpoint that monitors the attachment state of kinetochores to the spindle. These studies utilized two model organisms to glean better insight into TLK-1 function during mitosis. First, TLK-1-mediated AIR-2 activation was proven to be independent of TLK-1 kinase activity. Subsequently, a tethered-catalysis yeast two-hybrid screen was conducted with a bait chimera harboring a fragment of TLK-1 containing a critical residue that is phosphorylated by AIR-2. The results of this screen uncovered a wide range of potential TLK-1 interactors including proteins involved in transcription and mitosis. Further investigation revealed that CYB-3 interacts with TLK-1 phosphorylated at T610 and binds conserved RXL motifs of TLK-1. The conservation of the cyclin-box fold-binding RXL motifs indicate that Tousled homologs may also interact with cyclins to influence Cdk activity during the cell cycle.

The data presented in the previous chapter reveal that CYB-3 is required for the fidelity of chromosome congression and silencing the SAC. This work revealed that dynein activity is decreased in embryos depleted of CYB-3 suggesting that the regulation of dynein by cyclin/Cdk1 is a conserved mechanism. In light of the interaction between CYB-3 and TLK-1 identified in Chapter 3, increased AIR-2 activity in CYB-3-depleted embryos may reflect the inability to remove TLK-1 from kinetochores via dynein transport. TLK-1 at the kinetochore may positively regulate AIR-2 activity to degenerate K-Mt attachments resulting in persistent SAC activation. Taken together, these results indicate that CYB-3 function is crucial to maintain chromosomal stability by influencing the generation of proper K-Mt attachments that guarantee chromosomes remain intact during anaphase segregation.

Hypotheses to be tested in the future

Given the broad scope of these projects, the work presented here offer support for several conclusions regarding TLK-1 and CYB-3 function during *C. elegans* embryogenesis. However, just as many questions have surfaced as conclusions have been drawn. This section highlights several questions evoked from my experimental conclusions. The questions are posed as testable hypothesis and strategies are offered in an attempt to guide future investigations.

Does TLK-1 influence transcription by binding and influencing cyclin H/Cdk7 complexes?

Tousled kinase is unique in that it is highly expressed and active during S-phase but also has important mitotic functions that are likely independent of its own activity. The discovery that TLK-1 interacts with CYB-3 opens up the possibility that hTlk1 interacts with cyclins during S-phase when tlk1 expression and kinase activity is maximal. Binding and functional assays should be pursued to determine if TLK-1 kinase activity influences CYH-1/CDK-7-mediated phosphorylation and activation of RNA pol II. Since hTlk1 binds and phosphorylates the chromatin assembly factor Asf1 (127), it will be interesting to determine if nucleosome eviction by ASF-1 is influenced by TLK-1 to mediate efficient RNA pol II transcription. Lastly, CYH-1/CDK-7 may be an S-phase TLK-1-activating kinase similar to the activation of TLK-1 kinase activity by AIR-2 *in vitro* (123). It should be determined whether TLK-1 is directly phosphorylated by CDK-7 and if TLK-1 kinase activity toward ASF-1 is increased. Since the *in vitro* functionality of Asf1 phosphorylation by human Tlk1 remains enigmatic, identifying Tlk1 sites phosphorylated by Cdk7 may offer mechanistic insight into Asf1 regulation by Tlk1.

The screen described in Chapter 3 and our previous work (133) revealed several potential links between TLK-1 and the transcriptional machinery involving RNA pol II. Since cyclin H/Cdk7 is a transcriptional activator (292) and TLK-1 has cyclin binding motifs, TLK-1 may influence transcriptional events through binding cyclin H to influence Cdk7 activity. Our previous results suggested that RNA pol II CTD

phosphorylation, a read-out of its transcription activity, is decreased in *tlk-1(RNAi)* embryos. However, a direct molecular link between TLK-1 and RNA pol II was not studied. Therefore, the loss of RNA pol II activity in *tlk-1(RNAi)* embryos may reflect decreased cyclin H (CYH-1)/Cdk7 (CDK-7) activity. To test this, the phenotypes that result from singular or combined *tlk-1(RNAi); cyh-1(RNAi)* depletions will reveal if TLK-1 functions in the same or a parallel pathway for CDK-7 activation.

How is CHK-1 activated and regulated during mitosis?

My data suggest that CHK-1 is active during mitosis as evidenced by phospho-CHK-1 localization to the mitotic spindle. Active CDK-1 also localizes to the mitotic spindle. The results presented in Chapter 3 indicate that CHK-1 phosphorylates TLK-1 at T610 to promote CYB-3/CDK-1 binding. Therefore, TLK-1 may serve as a platform for CHK-1 and CYB-3/CDK-1 signaling to promote SAC silencing when microtubules are correctly attached to kinetochores. This mechanism may be especially crucial for holocentric chromosomes that likely rely on tension-generated changes in microtubule dynamics and/or structure as a prerequisite for SAC silencing. Accumulating evidence suggests that monocentric sister centromeres and kinetochores are stretched concomitant with the generation of tension (273). However, holocentric chromosomes are relatively stiff, bar-like structures that do not exhibit robust tension-generated separation of sister centromeres or kinetochores (38). Therefore, I propose that changes in microtubule dynamics or rigidity is a key readout of spindle tension at metaphase and therefore speculate that CHK-1 and CDK-1 activity at prometaphase and metaphase correlates with the fidelity of K-Mt attachments.

If CHK-1 and CDK-1 activity is linked to mitotic microtubule dynamics, what is a good experimental approach to determine the validity of this assumption? Immunostaining embryos treated with nocodazole or taxol with P-CHK-1 and P-CDK-1 antibodies might give some indication of changes to their catalytic activity. However, fixed embryo analyses would not reveal the temporality of kinase activity changes. Also, these specific phosphorylation sites in CHK-1 and CDK-1 may be poor indicators of their kinase activity. To determine the spatial and temporal changes of CHK-1 and CDK-1 kinase activity elicited by altered K-Mt dynamics, an *in vivo* approach similar to

the method used to monitor aurora B activity in human cells should be performed (187, 293). This method uses a phosphorylation-sensitive fluorescent sensor to determine the *in vivo* catalytic activity of kinases.

The fluorescence intensity of phosphorylation sensors depends on the efficiency of intramolecular energy transfer between CFP and YFP in the sensor (187). The CFP and YFP moieties are separated by the substrate and an FHA2 phospho-threonine binding domain (293). Therefore, phosphorylation of the substrate results in intramolecular FHA2 domain binding and emission of lower wavelengths of the sensor (293). The substrate peptide used in the Aurora B and Plk1 sensors were ~ 13 amino acids in length. Therefore, the CHK-1 and CDK-1 sensors should contain a short region of known substrates that contain the consensus sequence [(K/R)-X-X-T)] and [T-P], respectively. The mitotic spindle localization of CHK-1 and CDK-1 suggest that an untargeted, cytosolic sensor may be suitable for determining the influence microtubule dynamics have on kinase activity. However, the sensor can be tethered to a histone protein and targeted to chromosomes to determine kinase activity at the centromere and kinetochore. The sensor constructs can be introduced into *C. elegans* to obtain transgenic animals for live-cell imaging. The specificity of the sensors for CHK-1 and CDK-1 phosphorylation could be confirmed via RNAi-depletion of the kinases and their positive regulators.

Does TLK-1 contribute to the *cyb-3(RNAi)* phenotype?

The data presented in Chapter 4 reveal multiple mitotic defects in embryos depleted of CYB-3 during the first embryonic divisions. The results from Chapter 3 suggest that TLK-1 and CYB-3 interact during mitosis. However, embryos depleted of TLK-1 do not display mitotic defects until the ~ 16 cell stage. At this stage, *tlk-1(RNAi)* results in prometaphase and metaphase delays due to SAC activation. Therefore, the functionality of this interaction remains inconclusive given the distinct phenotypic severity caused by *cyb-3(RNAi)* and *tlk-1(RNAi)*. The pleiotropic mitotic alterations exhibited in *cyb-3(RNAi)* embryos suggests that TLK-1 likely modulates one or a few CYB-3-related functions. To molecularly assign the contribution TLK-1 has on CYB-3 function, genetic interactions between *tlk-1* and *cyb-3* should be explored. Since TLK-1

activates AIR-2, increased AIR-2 function in *cyb-3(RNAi)* embryos may reflect AIR-2 activation by TLK-1 due to metaphase kinetochore architectural changes. If increased AIR-2 activity destabilizes K-Mt attachments in embryos depleted of CYB-3, co-depleting TLK-1 may bring AIR-2 activity closer to wild-type levels and stabilize K-Mt attachments. Therefore, live-cell imaging may reveal partial suppression of the prometaphase defects in *cyb-3(RNAi)* embryos co-treated with *tlk-1(RNAi)*. To determine if the suppression is due to dampened AIR-2 activity, embryos can be fixed and stained with AIR-2 phospho-substrate antibodies. Alternatively, performing live-cell imaging with transgenic animals expressing an AIR-2 phosphorylation sensor would discern changes in AIR-2 activity in more precise terms.

Finally, Chapter 3 revealed that TLK-1 phosphorylated at T610 binds CYB-3. Thus, modification of TLK-1 at T610 may influence CYB-3/CDK-1 function. To determine the *in vivo* consequence of TLK-1 T610 phosphorylation, transgenic animals expressing GFP-tagged TLK-1(T610A) and TLK-1(T610E) mutants will reveal if P-T610 alters the localization or function of TLK-1 and/or CYB-3.

What subunits of dynein are regulated by CYB-3/CDK-1-mediated phosphorylation?

The results presented in Chapter 4 suggest that CYB-3 positively influences dynein activity. Although preliminary co-immunoprecipitation experiments revealed that dynein and CYB-3 may associate *in vivo*, the dynein subunit(s) that mediate this interaction are unknown. As the dynein complex consists of 13 subunits, educated guesses of the subunits that may interact with CYB-3 would facilitate a molecular understanding of CDK-1-mediated dynein regulation. Firstly, mammalian Cdk1 phosphorylates the dynein light intermediate chain to influence dynein function (184). Therefore, *C. elegans* dynein light intermediate chains may be subject to CDK-1 phosphorylation. Secondly, the published research and the work presented in Chapter 3 indicate that RXL motifs interact with the cyclin-box fold domains of cyclins. For instance, cyclin A binds RXL motifs of Rb to promote Cdk1 phosphorylation of Rb at [(S/T)/P] residues and entry into the cell cycle (229). Therefore, dynein subunits that interact with CYB-3 are expected to have RXL motifs and contain (S/T)/P residues for

CDK-1 phosphorylation. Interestingly, 8 dynein subunits have at least one (and up to three) RXL motifs and all but DYBR-1 have at least one potential Cdk1 phosphorylation site (Table 2). Out of the 5 subunits that do not have RXL motifs, only DYLT-2 has a Cdk1 site. The other 4 have neither RXL motifs nor Cdk1 phosphorylation sequences suggesting the coexistence of RXL motifs and [(S/T)/P] sequences in most dynein subunits. Therefore, DYCI-1 and DLI-1 are the most likely CYB-3-interacting dynein intermediate light chains and should be prioritized as potential CYB-3/CDK-1 substrates.

Once the dynein subunits that bind CYB-3 are identified, it will be critical to determine the residue(s) targeted by CDK-1 phosphorylation. The residue(s) of the dynein light chain(s) that are phosphorylated by CDK-1 may be efficiently revealed by *in vitro* kinase assays given their small size and predictable CDK-1 phosphorylation sites (Table 2). Alternatively, a quantitative mass spectrometry approach such as the SILAC technique (294) would reveal the CDK-1 phosphorylation sites that could subsequently be verified by *in vitro* and *in vivo* techniques. One key approach will be to raise phospho-specific antibodies to determine the spatial and temporal phosphorylation of dynein by CDK-1. We hypothesize that CYB-3 provides the substrate specificity of the CYB-3/CDK-1 complex toward dynein. Therefore, the immunoreactivity of the phospho-dynein antibody should be decreased in embryos treated with *cdk-1(RNAi)* and *cyb-3(RNAi)* but not *cyb-1(RNAi)*. It will also be vital to determine how dynein phosphorylation is affected by altered K-Mt dynamics. In this line of investigation, embryos treated with nocodazole or depleted of kinetochore microtubule interactors will reveal if dynein phosphorylation by CDK-1 is influenced by the state of K-Mt attachment. Moreover, the generation of transgenic animals expressing fluorophore-tagged phospho-null or phospho-mimetic dynein subunits will determine the *in vivo* consequence of CDK-1 phosphorylation of dynein.

Impacts from these studies

The research presented here has offered key insight into mechanisms governing chromosome segregation during *C. elegans* embryogenesis. Two critically important perspectives can be drawn from this research. Firstly, I have identified candidate TLK-1

Subunit name	Protein size (kD)	RXL motifs	[(S/T)P] sites
DHC-1	522	31	29
DLC-1	10	0	0
DLC-2	11	0	0
DLC-3	13	0	0
DLC-4	16	2	1
DLC-5	22	2	3
DLC-6	15	1	2

Subunit name	Protein size (kD)	RXL motifs	[(S/T)P] sites
DLI-1	49	3	4
DYCI-1	72	3	5
DYLT-1	12	0	0
DYLT-2	14	0	1
DYLT-3	19	1	2
DYRB-1	11	2	0

interactors that may be involved in transcriptional events by regulating RNA pol II and chromatin assembly factor function. Asf1 is the only known Tlk1 substrate, so the discovery of additional S-phase TLK-1 substrates will lead to a better understanding of Tousled function related to chromatin. Secondly, my research has revealed that the orphan B-type cyclin CYB-3 influences many aspects of dynein function especially dynein-dependent silencing of the SAC.

Until now, B3-type cyclins have not been adequately characterized in any organism perhaps due to cyclin b3 expression predominantly in mouse and human spermatocytes (264). However, the profound influence CYB-3 has on SAC silencing through dynein regulation suggests that the cyclin b3 family has unrecognized crucial functions. Research performed with mouse models and human neoplastic tissues has confirmed that the spindle assembly checkpoint is required to maintain chromosome stability during development and in dividing adult somatic cells (1). The deletion of one *MAD2* allele in human cancer cells and murine primary embryonic fibroblasts results in defective SAC signaling and chromosome missegregation, while $Mad2^{+/-}$ mice develop lung cancers (295). Also, sequencing of *BUB1* from 19 independent colorectal cell lines revealed a variety of mutations in the cancer but not adjacent wild-type cells that cause premature exit from mitosis (296). However, the inability to silence the SAC may be as detrimental to changes in ploidy and tumor onset. Mad2 overexpression in mice induces chromosome instability, aneuploidy, and tumor growth in a wide range of tissues (297). Importantly, Mad2 overexpression is common in human tumors and is associated with poor prognosis (297). CYB-3 influences the generation of stable K-Mt attachments and stimulates dynein-dependent SAC silencing. Therefore, decreased cyclin b3 levels in cancer cells may eliminate SAC silencing leading to the absence of sister chromatid separation and massive changes in ploidy. Increased cyclin b3 levels may inactivate the SAC by facilitating dynein-dependent silencing and may phenocopy *MAD2* and *BUB1* loss-of-function phenotypes (295, 296). Lastly, searching for aberrant cyclin B3 expression in human tumors by using the ONCOMINE database that contains microarray gene expression profiles (http://www.oncomine.org/) (298) revealed some interesting results. The expression level of cyclin B3 in many cell lines including Aaboe (bladder) and Adib (ovarian) has not been measured. In fact, cyclin B3 expression was

the only cyclin out of twenty (including cyclins A, D, E, F, and B1 and B2) that was not analyzed. However, the Adai cell lines revealed increased cyclin B3 expression in breast carcinoma, bronchioloalveolar carcinoma, large cell lung carcinoma, and non-small cell lung carcinoma among others. These revelations indicate that changes in cyclin b3 protein level or function in cancer cells remains an outstanding and important area of future investigation.

CHAPTER SIX: MATERIALS AND METHODS

Chapter Two

Yeast Strains, Plasmids, and Growth Conditions

Yeast strains used in this study were: SBY1730 (ura3-1, leu2-3,112, his3-11pCUP1GFP12-Lac12:HIS3, trp1-1 256lacO:TRP1, lys2^, bar1, can1-100, ade2-1, IPL1-myc13:KAN)(from S.Biggins, Fred Hutchinson Cancer Center, Seattle,WA), DBY5301 (a ade2, his3-Δ 200, ura3-52, leu2Δ101::URA3::leu2Δ102,lys2Δ101 ::HIS3::lys2-Δ102ipl1-2) and DBY4962 (a corresponding isogenic wild type strain to DBY5301), CCY914-10D (a ura3-52, lys2-801, his3-d200, leu2-3,112, ipl1-1) and CCY914-6B (corresponding isogenic wild type strain to CCY914-10D but alpha mating type). The DBY and CCY strains were provided by C. Chan, University of Texas at Austin. Yeast were propagated according to standard procedures in either rich media (YPD) or appropriate selective media (SC).

The entire coding sequences of *C. elegans* TLK-1 (C07A9.3), ICP-1 (Y39G10AR.13), and AIR-2 (B0207.4) were cloned into Xba I and Not I sites of the yeast expression vectors pYC2NTB or pYESNTB (Invitrogen, Carlsbad, CA) to create translational fusions with a 5' V5 epitope tag. TLK-1 mutants (S634A, S634E, and kinase-dead (KD) (D802A)) were PCR amplified from previously described constructs (20) and subcloned into the Xba I and Not I sites of pYC2NTB or pYESNTB. The construction of GST-ASF-1 was described previously (20). All constructs were verified by automated DNA sequencing (MDACC DNA Analysis Core Facility (M. D. Anderson CCSG Grant, NCI CA-16672(DAF)).

Immunoprecipitation and western blotting

Cell extracts were prepared from 500 ml cells grown in –ura media + 2% galactose for 6 hr to induce V5-TLK-1 expression (from a starting OD600 of 0.4). Cells were collected by centrifugation, washed once with water, and resuspended in 5 ml lysis buffer (50 mM Tris 8.0, 150 mM NaCl, 0.1% Triton-X100, 1 mM PMSF). Cell suspensions were flash frozen in liquid nitrogen and ground into powder in a coffee mill with dry ice. After thawing on ice, cellular debris was pelleted by centrifugation at 5000

g for 10 min. Supernatants were then clarified by incubating with 100 ul Protein G Sepharose (GE Healthcare, Piscataway, NJ) at 4°C for 1 hr. V5-TLK-1 was then immunoprecipitated (IPed) with 2 ug monoclonal V5 antibody (Invitrogen) at 4°C overnight. V5-TLK-1 immunoprecipitates (IPs) were isolated by adding 25 ul Protein G Sepharose at 4°C for 2 hr. Bound material was washed five times with lysis buffer, and resuspended and boiled in 25 ul loading buffer. Proteins were resolved by 10% SDS-PAGE and transferred to nitrocellulose. The membranes were blocked for 30 min in Tris-buffered saline (TBS) supplemented with 0.1% Tween 20 and 2% BSA, followed by overnight incubation with the antimyc mouse monoclonal 9E10 antibody (Santa Cruz Biotechnology, Santa Cruz, CA) at a final dilution of 1/1000. After incubation with antimouse horseradish peroxidase-conjugated secondary antibodies (Biorad, Irvine, CA), proteins were detected by chemiluminescence (GE Healthcare). Following detection of myc-Ipl1 with an anti-myc monoclonal 9E10 antibody (Santa Cruz Biotechnology, Santa Cruz, CA), membranes were stripped (2.2 M glycine pH 4.0, 0.5 M NaCl) and reprobed with the anti-V5 antibody at a final dilution of 1/5000.

Kinase Assays

IP of V5-TLK-1 was performed as above. Concurrently, myc-Ipl1 was IPed from parallel cultures with 1 ug anti-myc antibody at 4°C overnight. Myc-Ipl1 IPs were isolated and washed as above for V5-TLK-1 IPs. After the final wash, a 27 1/2 gauge needle was used to remove all traces of wash buffer from the Protein G Sepharose pellets. V5-TLK-1 IPs were then resuspended in 20.5 ul kinase reaction buffer (20 mM HEPES (pH7.6), 5 mM EGTA, 1 mM DTT, 25 mM β-glycerophosphate), whereas the myc-Ipl1 IPs were resuspended in 60 ul of the same buffer. Increasing amounts of the myc-Ipl1 IPs were transferred to individual tubes and the final volumes adjusted to 20.5 ul by addition of kinase buffer. 500 ng myelin basic protein (MYBP; Sigma, St. Louis, MO) and a cocktail of 30 uCi [3 Ci/umol] [γ-32P], 10 nM cold ATP, and 7.5 mM magnesium chloride were added and each reaction incubated at RT for 15 mins. The samples were boiled in loading buffer, separated by SDS-PAGE, transferred to nitrocellulose, and [^{32}P] incorporation into MYBP assessed by phosphoimaging. MYBP protein loading was determined by Ponceau S staining (Sigma). Western blotting with

anti-V5 and anti-myc antibodies was performed as above. Phosphorylation of GST-ASF-1 was assayed by IP of V5-TLK-1 and V5-TLK-1KD as above followed by kinase assays with GST-ASF-1 substituted for MYBP. [^{32}P] incorporation into GST-ASF-1 was assessed by phosphoimaging and GST-ASF-1 protein loading by Ponceau S staining (Sigma).

Kinase-Assay Quantitation

[^{32}P] incorporation into myelin basic protein (MYBP) (as visualized by phosphoimaging) and MYBP, V5-TLK-1, and myc-Ipl1 loading (as visualized by western analysis and chemiluminescence or Ponceau S staining) were measured with KodakID3.1 quantification software (Eastman Kodak, Rochester, NY). Phosphorylation of MYBP by Ipl1 in the presence of V5-TLK-1 was calculated as [((^{32}P-MYBP)/MYBP load (LD)) – (^{32}P-MYBP for vector alone/MYBP LD))/myc-Ipl1 LD] X (Avg. V5 LD/V5 LD per lane). Phosphorylation of MYBP by Ipl1 in the absence of V5-TLK-1 was calculated as ((^{32}P-MYBP)/MYBP LD)/myc-Ipl1 LD.

Chapter Three

Plasmids construction

The entire coding sequence of AIR-2 (excluding the stop codon) was subcloned into the EcoR1 and Sal1 MCS of pAS2.1 to create an N-terminal fusion with a Gal4 DBD. TLK-1 (1810 – 1992) with a C-terminal HA tag and 5' Sal1 and 3' Pst1 sites was generated by PCR from previously described constructs (123) and subcloned into AIR-2::pAS2.1 to generate the bait construct for the Y-2-H screen. Site-directed mutagenesis was utilized to generate the S/T → A and RXL → LXR constructs. All constructs were verified by automated DNA sequencing (MDACC DNA Analysis Core Facility (M. D. Anderson CCSG Grant, NCI CA-16672(DAF)).

Yeast two-hybrid screening procedure

Strain pJ694a (299) transformed with the Wt-S construct was grown in 5 ml –trp medium O/N at RT. Culture was diluted in 50 ml –trp and grown O/N at RT. Next a.m., cultures were diluted to OD_{600} = 0.35 in 125 ml YPD, grown 4 hr at 30°C, and centrifuged 5,000 rpm for 10 min. Pellet was washed with 100 ml sterile water, centrifuged, R/S in 12.5 ml LiSORB, and nutated at 30°C for 30 min. Yeast were pelleted, R/S in 156 μl LiSORB, and put on ice. Carrier DNA was prepared by boiling 100 μl SS DNA (10 mg/ml) for 5 min. 150 μl LiSORB was added to the SS DNA, mixed by pipetting, cooled to RT, and 10 μg of the *C. elegans* cDNA pACTII library (obtained from Caldwell lab) was added. 75 μl DNA mixture was added to 100 μl yeast in each of three eppendorf tubes and nutated 30 min at 30°C. Cells were pooled and washed twice with 1 ml sterile water. Pellet was R/S in 1.5 ml –leu, -trp, -his medium and plated on (5) 150 mm –leu, -trp, -his plates (300 μl each). Colonies for further analysis were obtained from plates after incubation at 30°C for 5 days.

DNA was isolated from colonies that grew on –leu, -trp, -his medium (after growth in –leu liquid medium to select for the prey pACTII plasmid) and was electroporated into DH5α cells. Three colonies from each DH5α plate were mini-prep'd and the DNA was used for PCR analysis with primers JMS 311 and JMS 545 to guarantee the absence of the bait construct. DNA preparations that did not contain the bait construct were cut with XhoI O/N to assess band migration during agarose gel electrophoresis. DNA isolated from three bacterial colonies from the same plate was expected to display similar-sized restriction fragments. However, if one of the three restriction digestions displayed unique bands, the constructs were considered unique and treated as independent potential bait interactors. pJ694a was co-transformed with pAS2.1 or Wt-S::pAS2.1 and the potential bait interactor constructs for the second round of screening.

Yeast transformation for plate-spot assays

Yeast were transformed by the Lithium Acetate procedure. 5 ml O/N culture was centrifuged in a 50 ml conical at 3500 rpm for 10 min. Yeast pellet was washed with 25 ml sterile water, centrifuged as above, R/S in 1 ml sterile water, transferred to 1.5 ml eppendorf tubes, and centrifuged at 6,000 rpm, 1 min. Pellet was R/S in 1 ml of 1X

LiAc/TE (made from 10X LiAc and 10X TE recipes below) and centrifuged at 6,000 g, 1 min. Pellet was R/S in 250-500 μl 1X LiAc/TE (corresponding to 50 μl per transformation, with 5-10 transformations respectively) and 50 μl yeast were allocated to eppendorf tubes. ~ 1 μg (in 1-8 μl) transforming DNA and 16 μl SS carrier DNA (Salmon sperm DNA (10 mg/ml); boil 5 min followed by 2 min incubation on ice prior to addition) were added to yeast suspension and mix by flicking. 600 μl PEG/LiAc/TE (960 μl 50% PEG, 120 μl 10X LiAc, 120 μl 10X TE) was added and gently R/S by pipetting. Tubes were incubated at RT for 2.5 – 3 hr, followed by centrifugation (6,000 g) and two washes with 1 ml sterile water. Pellets were R/S in 250 μl sterile water and plated on the appropriate medium. 10X Lithium Acetate: 1M, pH 7.5; 10X TE: 100mM Tris pH 7.5, 10 mM EDTA; 50% PEG (3500-4000). 100 μl 10X TE, 100 μl 10X LiAc, and 800 μl sterile water were mixed to make 1ml of 1X LiAc/TE.

Plate spot assays

Yeast were grown in 5 ml of appropriate selective medium 2 O/N at RT. Cell cultures were diluted 1:100 (2 μl O/N culture + 198 μl water) and spotted on a hemocytometer to count cell number (Z). A sterile 96-well PCR plate was used for the following dilutions. The initial dilution was (4000/Z) + sterile water to 200 μl. Cells were diluted 1:5 (with sterile water) from the initial dilution with a multi-pipettor. 3 μl from each dilution were spotted on the appropriate medium. Plates were incubated at 30°C for 3 days (his+ medium) or 5 days (his- medium).

Immunoprecipitation

5 ml –trp cultures grown O/N at RT in a 50 ml conical were diluted in 50 ml –trp and grown O/N. The OD_{600} was determined and cultures were diluted to 0.4 in 125 ml –trp medium. Cultures were incubated at 30°C for 4 hr followed by centrifugation at 12,000 rpm for 10 min. Pellets were washed with 50 ml water, R/S in 5 ml lysis buffer (as Chapter 2, but including the following 10X phosphatase inhibitor cocktail (diluted to 1X with lysis buffer): 375 mM sodium pyrophosphate, 1 M sodium azide, 1 M sodium fluoride, 50 mM sodium orthovanadate, 1 M β-glycerophosphate)). 1,500 μg of protein

extract in 1 ml total volume (diluted with lysis buffer) and 1 μg of a purified TLK-1 P-S634 antibody was used for O/N precipitation. Western analysis was performed with a polyclonal HA antibody (HA.11, Covance, Berkeley, CA).

In vitro phospho-peptide binding assays

Phospho-TLK-1 peptides (40 residues H604 – D643) with biotin conjugated at the N-terminus were generated **(**Small Scale Peptide Synthesis, W.M. Keck Biotechnology Resource Center, Yale U, New Haven, CT). 10 mg (~1/6 of product received) was dissolved in 1 ml TEN (10 mM Tris pH 7.5, 1 mM EDTA, 1 M NaCl) to give a 10 μg/μl peptide stock. The pH was very acidic and NaOH was added to obtain pH 7-8. 1 μl peptide stock was diluted with 49 μl PBS and incubated with 20 μl (50/50 slurry) Ultralink Immobilized Streptavidin resin (Pierce; Rockford, IL) O/N at 4°C on 360° tube rotator. Beads were pelleted (6000 g) and washed twice with PBS. 10 μl CYB-3 (~ 500 ng) expressed and purified from *E. coli* (MBP tag cleaved with TEV protease site between MBP and CYB-3 coding sequence) was incubated with 20 μl immobilized peptides diluted with 480 μl TEN_{150} (150 mM Nacl) on a nutator for 30 min at RT. Beads were pelleted, washed 4 times with 500 μl TEN_{150} (each wash on ice for 2 mins followed by brief slow centrifugation), and R/S in 15 μl 5X protein loading buffer for subsequent western analysis with the CYB-3 antibody used in Chapter Four.

Kinase assays

The assay conditions were similar to Chapter Two, except recombinant protein was used and the total reaction volume was 22.5 μl. 5 μl recombinant active human CHK1 (500ng) (Active Motif) and MBP::TLK-1 peptide (23 residues from H604 – H626) was used for the Chk1 kinase assays. 5 μl of AIR-2/ICP-1 purified from *E. coli* polycistronic expression and full-length MBP::TLK-1 was used for the AIR-2 kinase assays.

Immunostaining

Immunostaining was performed as Chapter Four. Phospho-Chk1 (Ser345) (Cell Signaling cat no 2341) was used at 1:250. Purified P-S634 and P-T610 antibodies were used at 1:500.

Chapter Four

C. elegans strains

C. elegans strains were maintained at 15°C as described (300). The following strains were used: N2 (wt), OD57 (GFP::α-tubulin; mCherry::Histone H2B) (301), OD110 (GFP::MDF-2; mCherry::Histone H2B) (154), OD203 (GFP::DHC-1; mCherry::Histone H2B) (286), OD204 (GFP::DNC-2; mCherry::Histone H2B) (286), OD11 (GFP::KBP-4) (286), TH32 (GFP::γ-tubulin; GFP::Histone H2B), and *dhc-1(or195ts)* (Strome 2005). To create the GFP::AIR-2; mCherry::Histone H2B strain (JS713), WH371 (GFP::AIR-2) (122) and OD56 (mCherry::Histone H2B) strains were crossed and animals homozygous for both transgenes were isolated. The same method was used to create the GFP::HCP-3; mCherry::Histone H2B strain (JS967) by crossing OD101 (GFP::HCP-3) (56) and OD56 (mCherry::Histone H2B) animals.

RNAi-Mediated Interference (RNAi)

RNAi plasmids CYB-3, MDF-1, SAN-1, BUB-1, and DYLT-1 were obtained from the Geneservice Ltd. *C. elegans* feeding library (302). The L4440 RNAi vector (*T7*) was used as an RNAi control. To deplete CYB-3 alone, a 3 ml LB + 100 μg/μl ampicillin liquid culture was seeded with a single colony of HT115 bacteria transformed with the *cyb-3(RNAi)* L4440 plasmid and shaken overnight (O/N) at 37°C . The next day, the O/N culture was expanded to 50 ml with the same media and grown for ~ 2 hrs until the OD600 of the culture was between 0.6 – 0.8. IPTG was added to a final concentration of 1mM and the culture was grown an additional 3 hrs at 37°C to induce *cyb-3* dsRNA expression. The culture was then centrifuged at 5000 rpm for 10 mins, and the pellet was resuspended (R/S) in 800 μl LB. 200 μl of the R/S pellet was plated on nematode growth (NG) plates containing 100 μg/μl ampicillin and 3 mM ITPG (NG/AMP/IPTG). Plates were incubated at 37°C O/N and then seeded with L4 larvae.

Seeded plates were incubated at 25°C overnight and young adult worms were utilized for experiments.

To co-deplete CYB-3 and MDF-1, SAN-1, or BUB-1, the induction conditions were as described above. However, after R/S the pellets in 800 μl LB, 200 μl of each R/S pellet (i.e. *cyb-3* and *mdf-1* dsRNA-expressing bacteria) were thoroughly mixed and transferred to NG/AMP/IPTG plates, incubated at 37°C O/N, and then seeded with L4 larvae. To generate dilute *cyb-3(RNAi)* conditions for the *dhc-1ts* experiments and the GFP::AIR-2 overexpression assays, *T7* and *cyb-3(RNAi)* bacteria were induced, pelleted, and R/S as above. 10 μl bacteria expressing *cyb-3* dsRNA and 190 μl *T7* bacteria were mixed in a 15 ml conical, vortexed, and briefly centrifuged at low speed. The pellet was R/S in the same supernatant and plated as above. For the dilute *cyb-3(RNAi)* plus *dylt-1(RNAi)* experiments, 10 ul bacteria expressing *cyb-3* dsRNA and 190 ul *dylt-1* dsRNA-expressing bacteria were plated. For *cyb-1&2(RNAi)* analyses, sense and anti-sense mRNAs corresponding to ZC168.4 (CYB-1) were transcribed from linearized templates using a T7 *in vitro* transcription kit (Ambion, Austin, TX), mixed, heated at 90°C for five minutes, and annealed at room temperature (RT). *cyb-3* dsRNA was also generated in this manner for direct comparison of injected animals. dsRNAs were injected into the gonads of OD57 L4 larvae and the injected animals incubated at 25°C O/N.

Immunostaining

Embryos from adult hermaphrodites were fixed and stained as previously described (303). Primary antibodies used were anti-α-tubulin (1:2000; Sigma, St. Louis, MO), anti-HCP-1 (1:500) (62), anti-BUB-1 (1:5000) (304), 3F3/2 (1:250) (305), anti-GFP (1:500) (Invitrogen, Eugene OR), anti-pICP-1(1:500) (150), anti-Phospho-cdc2 (Thr161) (1:500; Cell Signaling), and anti-Cdk1 ($pTpY^{14/15}$ 1:500; Invitrogen, Carlsbad, CA). Secondary antibodies were: Alexa Fluor 488 goat anti-mouse IgG and Alexa Fluor 555 goat anti-rabbit IgG (both at 1:1000) (Invitrogen Molecular Probes, Eugene, OR). For HCP-3 and BUB-1 co-staining experiments, anti-HCP-3 (304) and anti-BUB-1 antibodies were directly conjugated to fluorophores utilizing the Zenon Tricolor Rabbit IgG labeling kit (Invitrogen Molecular Probes, Eugene, OR) as per the manufacturer's instructions. The labeled antibodies were incubated on slides with fixed embryos for 3

hrs at RT. Slides were washed three times with PBSTb (PBS, 0.1% TritonX-100, 0.1% BSA) and mounted with ProLong Gold with DAPI (Invitrogen Molecular Probes, Eugene, OR).

For MAP staining, experiments were performed using control or *cyb-3(RNAi)*-treated gravid hermaphrodites reared at 25°C. Embryo fixation and antibody application was performed as previously described (306), albeit with these slight modifications: approximately 20 worms were placed on each slide and embryos were not excised from the adult worms. The slides were incubated with the a-tubulin antibody (1:2000) and either anti-DNC-1 (1:400) (306) or anti-BMK-1 (1:500) (278) antibodies O/N at 4°C. The following secondary antibodies were applied for 2 hrs at RT: Alexa Fluor 488 goat anti-mouse IgG and Alexa Fluor 555 goat anti-rabbit IgG (both at 1:1000) (Invitrogen Molecular Probes, Eugene, OR). After washing, slides were mounted with ProLong Gold with DAPI (Invitrogen Molecular Probes, Eugene, OR).

The following procedure was used for taxol treatment of embryos. All steps were performed at RT. ~ 30 adult hermaphrodites were cut open into a 30μl 1:9 bleach solution (diluted from a 6.15% sodium hypochlorite stock with M9) on a microscope slide. After 3 min incubation, embryo concoctions were R/S in 1 ml M9 and centrifuged at 1,500 g for 1 min. The embryo pellet was R/S in 30 ul chitinase (1 μg/μl), incubated for 5 min, and centrifuged 10,000 rpm for 20 sec. Pellet was R/S in 10 μl Taxol (100 μM in (M9 + 1% EtOH); Oregon Green 488 paclitaxel Molecular Probes) or vehicle (M9 + 1% EtOH) and incubated on a microscope slide for 4 min. A coverslip was placed on the slide and slight pressure was applied followed by 1 min incubation to facilitate Taxol entry. Slides were then placed on a metal plate chilled with dry ice and immunostained as above.

Image Analysis/Immunoquantitation

Immunofluorescent images were acquired on a Nikon 2000U inverted microscope equipped with a Photometrics Coolsnap HQ camera. Metamorph software was used for image acquisition. Z-sections were acquired at 0.2 μm steps using a 60X/1.49 NA objective. Z stacks were projected and deconvolved for 10 iterations using Autodeblur (Autoquant Media Cybernetics, Bethesda, MD). For immunoquantitation of

pICP-1 levels, deconvolved images were imported into Imaris x64 software (Bitplane, St. Paul, MN). 3D isosurfaces were generated based on minimal threshold values within the experimental set, and corresponding sum voxel intensity values were collected for each embryo within the data set. Since *cyb-3(RNAi)* embryos are defective in meiosis II and have increased DNA content, the ratio of the sum intensity values of (pICP-1/DAPI) was computed and used for quantitative analysis.

Live Imaging

Embryos from control and RNAi-treated (by feeding or dsRNA microinjection) animals were mounted on 2% agarose pads and imaged using a spinning disk confocal (Perkin Elmer, Waltham, MA) attached to a Nikon TE2000U inverted microscope. Images were acquired using an ORCA-ER digital camera (Hamamatsu, Bridgewater, NJ) and a 60X 1.45 NA Plan Apo VC lens. Ultraview software (Perkin Elmer) was used to control the confocal, microscope, and camera. Images from JS967 embryos were taken at 15 sec intervals while 30 sec intervals were generated for all other strains; Z-sections were 1 μm.

Immunoprecipitation and Western Analysis

Gravid N2 *C. elegans* hermaphrodites treated with control or *cyb-3(RNAi)* were subjected to the alkaline hypochlorite method to isolate embryos (151). Embryos were briefly washed in PBS and resuspended (R/S) in lysis buffer (PBS, 20mM HEPES, 1% NP-40, 50 μM β-glycerophosphate, 1 mM Na_3VO_4, 1 mM dithiothreitol [DTT], 1 mM EDTA, 1 mM PMSF + complete protease inhibitors (Roche Diagnostics, Indianapolis, IN) and sonicated 3 times over ice for 30 sec each. Following centrifugation at 12,000 rpm for 10 min, the clarified lysates were immediately used for immunoprecipitation. A 1/10 volume of Protein G-Sepharose beads (GE Healthcare, Piscataway, NJ) was added to the lysates and rocked at 4°C for 1 hr to preclear the extracts. The supernatant was isolated after a brief low-speed spin to pellet the beads. Protein concentration was determined by Bradford assay (Bio-Rad, Hercules, CA).

For immunoprecipitations, 500 μg embryo extract was incubated with 3 μl CYB-3 antibody (270) O/N at 4°C. 1 μg GFP antibody (Invitrogen, Eugene OR cat no

A11122) was used for GFP::DHC-1 immunoprecipitation. 50 μl protein G-Sepharose beads (in a 50:50 slur) were added and the extract incubated at 4°C for an additional 2 hr. The beads and isolated immunocomplexes pelleted via low-speed centrifugation and washed four times in lysis buffer without NP-40. Samples were separated by SDS-PAGE, transferred to nitrocellulose, and the membranes probed with the CYB-3 antibody (1:1000) or α-tubulin antibody (1:3000). Western analysis was performed as previously described (151).

REFERENCES

1. Rao, C. V., H. Y. Yamada, Y. Yao, and W. Dai. 2009. Enhanced genomic instabilities caused by deregulated microtubule dynamics and chromosome segregation: a perspective from genetic studies in mice. Carcinogenesis 30:1469-1474.
2. Thompson, S. L., and D. A. Compton. 2008. Examining the link between chromosomal instability and aneuploidy in human cells. The Journal of cell biology 180:665-672.
3. Baker, D. J., J. Chen, and J. M. van Deursen. 2005. The mitotic checkpoint in cancer and aging: what have mice taught us? Curr Opin Cell Biol 17:583-589.
4. Eitoku, M., L. Sato, T. Senda, and M. Horikoshi. 2008. Histone chaperones: 30 years from isolation to elucidation of the mechanisms of nucleosome assembly and disassembly. Cell Mol Life Sci 65:414-444.
5. Van Hooser, A. A., Ouspenski, II, H. C. Gregson, D. A. Starr, T. J. Yen, M. L. Goldberg, K. Yokomori, W. C. Earnshaw, K. F. Sullivan, and B. R. Brinkley. 2001. Specification of kinetochore-forming chromatin by the histone H3 variant CENP-A. J Cell Sci 114:3529-3542.
6. Sullivan, K. F. 2001. A solid foundation: functional specialization of centromeric chromatin. Curr Opin Genet Dev 11:182-188.
7. Carroll, C. W., and A. F. Straight. 2006. Centromere formation: from epigenetics to self-assembly. Trends Cell Biol 16:70-78.
8. Blow, J. J., and T. U. Tanaka. 2005. The chromosome cycle: coordinating replication and segregation. Second in the cycles review series. EMBO Rep 6:1028-1034.
9. Stear, J. H., and M. B. Roth. 2002. Characterization of HCP-6, a C. elegans protein required to prevent chromosome twisting and merotelic attachment. Genes Dev 16:1498-1508.
10. Hirano, T. 2005. Condensins: organizing and segregating the genome. Curr Biol 15:R265-275.
11. Cheeseman, I. M., and A. Desai. 2008. Molecular architecture of the kinetochore-microtubule interface. Nat Rev Mol Cell Biol 9:33-46.

12. Sampath, S. C., R. Ohi, O. Leismann, A. Salic, A. Pozniakovski, and H. Funabiki. 2004. The chromosomal passenger complex is required for chromatin-induced microtubule stabilization and spindle assembly. Cell 118:187-202.
13. Jallepalli, P. V., and C. Lengauer. 2001. Chromosome segregation and cancer: cutting through the mystery. Nat Rev Cancer 1:109-117.
14. Sathananthan, A. H., W. D. Ratnasooriya, A. de Silva, and P. Randeniya. 2006. Rediscovering Boveri's centrosome in Ascaris (1888): its impact on human fertility and development. Reprod Biomed Online 12:254-270.
15. Swedlow, J. R., and T. Hirano. 2003. The making of the mitotic chromosome: modern insights into classical questions. Mol Cell 11:557-569.
16. Li, G., G. Sudlow, and A. S. Belmont. 1998. Interphase cell cycle dynamics of a late-replicating, heterochromatic homogeneously staining region: precise choreography of condensation/decondensation and nuclear positioning. The Journal of cell biology 140:975-989.
17. Watson, J. D., and F. H. Crick. 1953. The structure of DNA. Cold Spring Harb Symp Quant Biol 18:123-131.
18. Prigent, C., and S. Dimitrov. 2003. Phosphorylation of serine 10 in histone H3, what for? J Cell Sci 116:3677-3685.
19. Maddox, P. S., N. Portier, A. Desai, and K. Oegema. 2006. Molecular analysis of mitotic chromosome condensation using a quantitative time-resolved fluorescence microscopy assay. Proc Natl Acad Sci U S A 103:15097-15102.
20. Fischle, W., B. S. Tseng, H. L. Dormann, B. M. Ueberheide, B. A. Garcia, J. Shabanowitz, D. F. Hunt, H. Funabiki, and C. D. Allis. 2005. Regulation of HP1-chromatin binding by histone H3 methylation and phosphorylation. Nature 438:1116-1122.
21. Hirota, T., J. J. Lipp, B. H. Toh, and J. M. Peters. 2005. Histone H3 serine 10 phosphorylation by Aurora B causes HP1 dissociation from heterochromatin. Nature 438:1176-1180.
22. Maison, C., and G. Almouzni. 2004. HP1 and the dynamics of heterochromatin maintenance. Nat Rev Mol Cell Biol 5:296-304.

23. Anderson, D. E., A. Losada, H. P. Erickson, and T. Hirano. 2002. Condensin and cohesin display different arm conformations with characteristic hinge angles. The Journal of cell biology 156:419-424.
24. Hudson, D. F., K. M. Marshall, and W. C. Earnshaw. 2009. Condensin: Architect of mitotic chromosomes. Chromosome Res 17:131-144.
25. Kimura, K., M. Hirano, R. Kobayashi, and T. Hirano. 1998. Phosphorylation and activation of 13S condensin by Cdc2 in vitro. Science 282:487-490.
26. Hagstrom, K. A., V. F. Holmes, N. R. Cozzarelli, and B. J. Meyer. 2002. C. elegans condensin promotes mitotic chromosome architecture, centromere organization, and sister chromatid segregation during mitosis and meiosis. Genes Dev 16:729-742.
27. Lipp, J. J., T. Hirota, I. Poser, and J. M. Peters. 2007. Aurora B controls the association of condensin I but not condensin II with mitotic chromosomes. J Cell Sci 120:1245-1255.
28. Wang, J. C. 2002. Cellular roles of DNA topoisomerases: a molecular perspective. Nat Rev Mol Cell Biol 3:430-440.
29. Rattner, J. B., M. J. Hendzel, C. S. Furbee, M. T. Muller, and D. P. Bazett-Jones. 1996. Topoisomerase II alpha is associated with the mammalian centromere in a cell cycle- and species-specific manner and is required for proper centromere/kinetochore structure. The Journal of cell biology 134:1097-1107.
30. Ackerman, P., C. V. Glover, and N. Osheroff. 1985. Phosphorylation of DNA topoisomerase II by casein kinase II: modulation of eukaryotic topoisomerase II activity in vitro. Proc Natl Acad Sci U S A 82:3164-3168.
31. Sahyoun, N., M. Wolf, J. Besterman, T. Hsieh, M. Sander, H. LeVine, 3rd, K. J. Chang, and P. Cuatrecasas. 1986. Protein kinase C phosphorylates topoisomerase II: topoisomerase activation and its possible role in phorbol ester-induced differentiation of HL-60 cells. Proc Natl Acad Sci U S A 83:1603-1607.
32. Belmont, A. S. 2006. Mitotic chromosome structure and condensation. Curr Opin Cell Biol 18:632-638.

33. Heck, M. M., W. N. Hittelman, and W. C. Earnshaw. 1989. In vivo phosphorylation of the 170-kDa form of eukaryotic DNA topoisomerase II. Cell cycle analysis. The Journal of biological chemistry 264:15161-15164.
34. Hudson, D. F., P. Vagnarelli, R. Gassmann, and W. C. Earnshaw. 2003. Condensin is required for nonhistone protein assembly and structural integrity of vertebrate mitotic chromosomes. Dev Cell 5:323-336.
35. Brinkley, B. R., and E. Stubblefield. 1966. The fine structure of the kinetochore of a mammalian cell in vitro. Chromosoma 19:28-43.
36. Rattner, J. B., and D. P. Bazett-Jones. 1989. Kinetochore structure: electron spectroscopic imaging of the kinetochore. The Journal of cell biology 108:1209-1219.
37. McEwen, B. F., C. E. Hsieh, A. L. Mattheyses, and C. L. Rieder. 1998. A new look at kinetochore structure in vertebrate somatic cells using high-pressure freezing and freeze substitution. Chromosoma 107:366-375.
38. Maddox, P. S., K. Oegema, A. Desai, and I. M. Cheeseman. 2004. "Holo"er than thou: chromosome segregation and kinetochore function in C. elegans. Chromosome Res 12:641-653.
39. Albertson, D. G., and J. N. Thomson. 1982. The kinetochores of Caenorhabditis elegans. Chromosoma 86:409-428.
40. Pathak, S., B. J. Dave, and S. Gagos. 1994. Chromosome alterations in cancer development and apoptosis. In Vivo 8:843-850.
41. Clarke, L., and J. Carbon. 1980. Isolation of a yeast centromere and construction of functional small circular chromosomes. Nature 287:504-509.
42. Mann, C., and R. W. Davis. 1986. Structure and sequence of the centromeric DNA of chromosome 4 in Saccharomyces cerevisiae. Mol Cell Biol 6:241-245.
43. Meluh, P. B., P. Yang, L. Glowczewski, D. Koshland, and M. M. Smith. 1998. Cse4p is a component of the core centromere of Saccharomyces cerevisiae. Cell 94:607-613.
44. Furuyama, S., and S. Biggins. 2007. Centromere identity is specified by a single centromeric nucleosome in budding yeast. Proc Natl Acad Sci U S A 104:14706-14711.

45. Dernburg, A. F. 2001. Here, there, and everywhere: kinetochore function on holocentric chromosomes. The Journal of cell biology 153:F33-38.
46. Zinkowski, R. P., J. Meyne, and B. R. Brinkley. 1991. The centromere-kinetochore complex: a repeat subunit model. The Journal of cell biology 113:1091-1110.
47. Buchwitz, B. J., K. Ahmad, L. L. Moore, M. B. Roth, and S. Henikoff. 1999. A histone-H3-like protein in C. elegans. Nature 401:547-548.
48. Yuen, K. W., B. Montpetit, and P. Hieter. 2005. The kinetochore and cancer: what's the connection? Curr Opin Cell Biol 17:576-582.
49. Sorger, P. K., F. F. Severin, and A. A. Hyman. 1994. Factors required for the binding of reassembled yeast kinetochores to microtubules in vitro. The Journal of cell biology 127:995-1008.
50. Masumoto, H., M. Nakano, and J. Ohzeki. 2004. The role of CENP-B and alpha-satellite DNA: de novo assembly and epigenetic maintenance of human centromeres. Chromosome Res 12:543-556.
51. Ohzeki, J., M. Nakano, T. Okada, and H. Masumoto. 2002. CENP-B box is required for de novo centromere chromatin assembly on human alphoid DNA. The Journal of cell biology 159:765-775.
52. Okada, T., J. Ohzeki, M. Nakano, K. Yoda, W. R. Brinkley, V. Larionov, and H. Masumoto. 2007. CENP-B controls centromere formation depending on the chromatin context. Cell 131:1287-1300.
53. Amor, D. J., and K. H. Choo. 2002. Neocentromeres: role in human disease, evolution, and centromere study. Am J Hum Genet 71:695-714.
54. Hayashi, T., Y. Fujita, O. Iwasaki, Y. Adachi, K. Takahashi, and M. Yanagida. 2004. Mis16 and Mis18 are required for CENP-A loading and histone deacetylation at centromeres. Cell 118:715-729.
55. Zhang, Y., H. H. Ng, H. Erdjument-Bromage, P. Tempst, A. Bird, and D. Reinberg. 1999. Analysis of the NuRD subunits reveals a histone deacetylase core complex and a connection with DNA methylation. Genes Dev 13:1924-1935.

56. Maddox, P. S., F. Hyndman, J. Monen, K. Oegema, and A. Desai. 2007. Functional genomics identifies a Myb domain-containing protein family required for assembly of CENP-A chromatin. J Cell Biol 176:757-763.
57. Stoler, S., K. Rogers, S. Weitze, L. Morey, M. Fitzgerald-Hayes, and R. E. Baker. 2007. Scm3, an essential Saccharomyces cerevisiae centromere protein required for G2/M progression and Cse4 localization. Proc Natl Acad Sci U S A 104:10571-10576.
58. Camahort, R., B. Li, L. Florens, S. K. Swanson, M. P. Washburn, and J. L. Gerton. 2007. Scm3 is essential to recruit the histone h3 variant cse4 to centromeres and to maintain a functional kinetochore. Mol Cell 26:853-865.
59. Pidoux, A. L., E. S. Choi, J. K. Abbott, X. Liu, A. Kagansky, A. G. Castillo, G. L. Hamilton, W. Richardson, J. Rappsilber, X. He, and R. C. Allshire. 2009. Fission yeast Scm3: A CENP-A receptor required for integrity of subkinetochore chromatin. Mol Cell 33:299-311.
60. Sanchez-Pulido, L., A. L. Pidoux, C. P. Ponting, and R. C. Allshire. 2009. Common ancestry of the CENP-A chaperones Scm3 and HJURP. Cell 137:1173-1174.
61. Foltz, D. R., L. E. Jansen, B. E. Black, A. O. Bailey, J. R. Yates, 3rd, and D. W. Cleveland. 2006. The human CENP-A centromeric nucleosome-associated complex. Nat Cell Biol 8:458-469.
62. Moore, L. L., M. Morrison, and M. B. Roth. 1999. HCP-1, a protein involved in chromosome segregation, is localized to the centromere of mitotic chromosomes in Caenorhabditis elegans. The Journal of cell biology 147:471-480.
63. Liao, H., R. J. Winkfein, G. Mack, J. B. Rattner, and T. J. Yen. 1995. CENP-F is a protein of the nuclear matrix that assembles onto kinetochores at late G2 and is rapidly degraded after mitosis. The Journal of cell biology 130:507-518.
64. Moore, L. L., and M. B. Roth. 2001. HCP-4, a CENP-C-like protein in Caenorhabditis elegans, is required for resolution of sister centromeres. The Journal of cell biology 153:1199-1208.

65. Oegema, K., A. Desai, S. Rybina, M. Kirkham, and A. A. Hyman. 2001. Functional analysis of kinetochore assembly in Caenorhabditis elegans. The Journal of cell biology 153:1209-1226.

66. Sonnichsen, B., L. B. Koski, A. Walsh, P. Marschall, B. Neumann, M. Brehm, A. M. Alleaume, J. Artelt, P. Bettencourt, E. Cassin, M. Hewitson, C. Holz, M. Khan, S. Lazik, C. Martin, B. Nitzsche, M. Ruer, J. Stamford, M. Winzi, R. Heinkel, M. Roder, J. Finell, H. Hantsch, S. J. Jones, M. Jones, F. Piano, K. C. Gunsalus, K. Oegema, P. Gonczy, A. Coulson, A. A. Hyman, and C. J. Echeverri. 2005. Full-genome RNAi profiling of early embryogenesis in Caenorhabditis elegans. Nature 434:462-469.

67. Desai, A., S. Rybina, T. Muller-Reichert, A. Shevchenko, A. Hyman, and K. Oegema. 2003. KNL-1 directs assembly of the microtubule-binding interface of the kinetochore in C. elegans. Genes Dev 17:2421-2435.

68. Pagliuca, C., V. M. Draviam, E. Marco, P. K. Sorger, and P. De Wulf. 2009. Roles for the conserved spc105p/kre28p complex in kinetochore-microtubule binding and the spindle assembly checkpoint. PLoS One 4:e7640.

69. Cheeseman, I. M., and A. Desai. 2005. A combined approach for the localization and tandem affinity purification of protein complexes from metazoans. Sci STKE 2005:pl1.

70. Cheeseman, I. M., S. Niessen, S. Anderson, F. Hyndman, J. R. Yates, 3rd, K. Oegema, and A. Desai. 2004. A conserved protein network controls assembly of the outer kinetochore and its ability to sustain tension. Genes Dev 18:2255-2268.

71. Cheeseman, I. M., J. S. Chappie, E. M. Wilson-Kubalek, and A. Desai. 2006. The conserved KMN network constitutes the core microtubule-binding site of the kinetochore. Cell 127:983-997.

72. Cheeseman, I. M., C. Brew, M. Wolyniak, A. Desai, S. Anderson, N. Muster, J. R. Yates, T. C. Huffaker, D. G. Drubin, and G. Barnes. 2001. Implication of a novel multiprotein Dam1p complex in outer kinetochore function. The Journal of cell biology 155:1137-1145.

73. Westermann, S., A. Avila-Sakar, H. W. Wang, H. Niederstrasser, J. Wong, D. G. Drubin, E. Nogales, and G. Barnes. 2005. Formation of a dynamic kinetochore-

microtubule interface through assembly of the Dam1 ring complex. Mol Cell 17:277-290.

74. Westermann, S., H. W. Wang, A. Avila-Sakar, D. G. Drubin, E. Nogales, and G. Barnes. 2006. The Dam1 kinetochore ring complex moves processively on depolymerizing microtubule ends. Nature 440:565-569.

75. Gestaut, D. R., B. Graczyk, J. Cooper, P. O. Widlund, A. Zelter, L. Wordeman, C. L. Asbury, and T. N. Davis. 2008. Phosphoregulation and depolymerization-driven movement of the Dam1 complex do not require ring formation. Nat Cell Biol 10:407-414.

76. Gaitanos, T. N., A. Santamaria, A. A. Jeyaprakash, B. Wang, E. Conti, and E. A. Nigg. 2009. Stable kinetochore-microtubule interactions depend on the Ska complex and its new component Ska3/C13Orf3. EMBO J 28:1442-1452.

77. Welburn, J. P., E. L. Grishchuk, C. B. Backer, E. M. Wilson-Kubalek, J. R. Yates, 3rd, and I. M. Cheeseman. 2009. The human kinetochore Ska1 complex facilitates microtubule depolymerization-coupled motility. Dev Cell 16:374-385.

78. Schmidt, D. J., D. J. Rose, W. M. Saxton, and S. Strome. 2005. Functional analysis of cytoplasmic dynein heavy chain in Caenorhabditis elegans with fast-acting temperature-sensitive mutations. Mol Biol Cell 16:1200-1212.

79. Gennerich, A., and R. D. Vale. 2009. Walking the walk: how kinesin and dynein coordinate their steps. Curr Opin Cell Biol 21:59-67.

80. Gennerich, A., A. P. Carter, S. L. Reck-Peterson, and R. D. Vale. 2007. Force-induced bidirectional stepping of cytoplasmic dynein. Cell 131:952-965.

81. Yen, T. J., D. A. Compton, D. Wise, R. P. Zinkowski, B. R. Brinkley, W. C. Earnshaw, and D. W. Cleveland. 1991. CENP-E, a novel human centromere-associated protein required for progression from metaphase to anaphase. EMBO J 10:1245-1254.

82. Howell, B. J., B. F. McEwen, J. C. Canman, D. B. Hoffman, E. M. Farrar, C. L. Rieder, and E. D. Salmon. 2001. Cytoplasmic dynein/dynactin drives kinetochore protein transport to the spindle poles and has a role in mitotic spindle checkpoint inactivation. The Journal of cell biology 155:1159-1172.

83. Rieder, C. L., E. A. Davison, L. C. Jensen, L. Cassimeris, and E. D. Salmon. 1986. Oscillatory movements of monooriented chromosomes and their position relative to the spindle pole result from the ejection properties of the aster and half-spindle. The Journal of cell biology 103:581-591.
84. Hays, T. S., D. Wise, and E. D. Salmon. 1982. Traction force on a kinetochore at metaphase acts as a linear function of kinetochore fiber length. The Journal of cell biology 93:374-389.
85. Powers, J., D. J. Rose, A. Saunders, S. Dunkelbarger, S. Strome, and W. M. Saxton. 2004. Loss of KLP-19 polar ejection force causes misorientation and missegregation of holocentric chromosomes. The Journal of cell biology 166:991-1001.
86. Brouhard, G. J., and A. J. Hunt. 2005. Microtubule movements on the arms of mitotic chromosomes: polar ejection forces quantified in vitro. Proc Natl Acad Sci U S A 102:13903-13908.
87. Nicklas, R. B. 1997. How cells get the right chromosomes. Science 275:632-637.
88. Andrews, P. D., E. Knatko, W. J. Moore, and J. R. Swedlow. 2003. Mitotic mechanics: the auroras come into view. Curr Opin Cell Biol 15:672-683.
89. Musacchio, A., and E. D. Salmon. 2007. The spindle-assembly checkpoint in space and time. Nat Rev Mol Cell Biol 8:379-393.
90. Vader, G., C. W. Cruijsen, T. van Harn, M. J. Vromans, R. H. Medema, and S. M. Lens. 2007. The chromosomal passenger complex controls spindle checkpoint function independent from its role in correcting microtubule kinetochore interactions. Mol Biol Cell 18:4553-4564.
91. Hunter, T. 1995. Protein kinases and phosphatases: the yin and yang of protein phosphorylation and signaling. Cell 80:225-236.
92. Nigg, E. A. 2001. Mitotic kinases as regulators of cell division and its checkpoints. Nat Rev Mol Cell Biol 2:21-32.
93. Quintas-Cardama, A., and J. Cortes. 2009. Chronic myeloid leukemia in the tyrosine kinase inhibitor era: what is the best therapy? Curr Oncol Rep 11:337-345.

94. Carter, S. L., A. C. Eklund, I. S. Kohane, L. N. Harris, and Z. Szallasi. 2006. A signature of chromosomal instability inferred from gene expression profiles predicts clinical outcome in multiple human cancers. Nat Genet 38:1043-1048.
95. Malumbres, M., and M. Barbacid. 2007. Cell cycle kinases in cancer. Curr Opin Genet Dev 17:60-65.
96. Morgan, D. O. 1997. Cyclin-dependent kinases: engines, clocks, and microprocessors. Annu Rev Cell Dev Biol 13:261-291.
97. De Bondt, H. L., J. Rosenblatt, J. Jancarik, H. D. Jones, D. O. Morgan, and S. H. Kim. 1993. Crystal structure of cyclin-dependent kinase 2. Nature 363:595-602.
98. Jeffrey, P. D., A. A. Russo, K. Polyak, E. Gibbs, J. Hurwitz, J. Massague, and N. P. Pavletich. 1995. Mechanism of CDK activation revealed by the structure of a cyclinA-CDK2 complex. Nature 376:313-320.
99. Miller, M. E., and F. R. Cross. 2001. Cyclin specificity: how many wheels do you need on a unicycle? J Cell Sci 114:1811-1820.
100. Malumbres, M., and M. Barbacid. 2005. Mammalian cyclin-dependent kinases. Trends Biochem Sci 30:630-641.
101. Feaver, W. J., J. Q. Svejstrup, N. L. Henry, and R. D. Kornberg. 1994. Relationship of CDK-activating kinase and RNA polymerase II CTD kinase TFIIH/TFIIK. Cell 79:1103-1109.
102. Th'ng, J. P., P. S. Wright, J. Hamaguchi, M. G. Lee, C. J. Norbury, P. Nurse, and E. M. Bradbury. 1990. The FT210 cell line is a mouse G2 phase mutant with a temperature-sensitive CDC2 gene product. Cell 63:313-324.
103. Peter, M., J. Nakagawa, M. Doree, J. C. Labbe, and E. A. Nigg. 1990. In vitro disassembly of the nuclear lamina and M phase-specific phosphorylation of lamins by cdc2 kinase. Cell 61:591-602.
104. Izumi, T., D. H. Walker, and J. L. Maller. 1992. Periodic changes in phosphorylation of the Xenopus cdc25 phosphatase regulate its activity. Mol Biol Cell 3:927-939.
105. Carmena, M., and W. C. Earnshaw. 2003. The cellular geography of aurora kinases. Nat Rev Mol Cell Biol 4:842-854.

106. Chan, C. S., and D. Botstein. 1993. Isolation and characterization of chromosome-gain and increase-in-ploidy mutants in yeast. Genetics 135:677-691.
107. Girdler, F., K. E. Gascoigne, P. A. Eyers, S. Hartmuth, C. Crafter, K. M. Foote, N. J. Keen, and S. S. Taylor. 2006. Validating Aurora B as an anti-cancer drug target. J Cell Sci 119:3664-3675.
108. Fu, J., M. Bian, J. Liu, Q. Jiang, and C. Zhang. 2009. A single amino acid change converts Aurora-A into Aurora-B-like kinase in terms of partner specificity and cellular function. Proc Natl Acad Sci U S A 106:6939-6944.
109. Adams, R. R., M. Carmena, and W. C. Earnshaw. 2001. Chromosomal passengers and the (aurora) ABCs of mitosis. Trends Cell Biol 11:49-54.
110. Kitajima, T. S., T. Sakuno, K. Ishiguro, S. Iemura, T. Natsume, S. A. Kawashima, and Y. Watanabe. 2006. Shugoshin collaborates with protein phosphatase 2A to protect cohesin. Nature 441:46-52.
111. Cheeseman, I. M., S. Anderson, M. Jwa, E. M. Green, J. Kang, J. R. Yates, 3rd, C. S. Chan, D. G. Drubin, and G. Barnes. 2002. Phospho-regulation of kinetochore-microtubule attachments by the Aurora kinase Ipl1p. Cell 111:163-172.
112. Andrews, P. D., Y. Ovechkina, N. Morrice, M. Wagenbach, K. Duncan, L. Wordeman, and J. R. Swedlow. 2004. Aurora B regulates MCAK at the mitotic centromere. Dev Cell 6:253-268.
113. Romano, A., A. Guse, I. Krascenicova, H. Schnabel, R. Schnabel, and M. Glotzer. 2003. CSC-1: a subunit of the Aurora B kinase complex that binds to the survivin-like protein BIR-1 and the incenp-like protein ICP-1. The Journal of cell biology 161:229-236.
114. Severson, A. F., D. R. Hamill, J. C. Carter, J. Schumacher, and B. Bowerman. 2000. The aurora-related kinase AIR-2 recruits ZEN-4/CeMKLP1 to the mitotic spindle at metaphase and is required for cytokinesis. Curr Biol 10:1162-1171.
115. Bishop, J. D., and J. M. Schumacher. 2002. Phosphorylation of the carboxyl terminus of inner centromere protein (INCENP) by the Aurora B Kinase

stimulates Aurora B kinase activity. The Journal of biological chemistry 277:27577-27580.

116. Francisco, L., W. Wang, and C. S. Chan. 1994. Type 1 protein phosphatase acts in opposition to IpL1 protein kinase in regulating yeast chromosome segregation. Mol Cell Biol 14:4731-4740.

117. Hsu, J. Y., Z. W. Sun, X. Li, M. Reuben, K. Tatchell, D. K. Bishop, J. M. Grushcow, C. J. Brame, J. A. Caldwell, D. F. Hunt, R. Lin, M. M. Smith, and C. D. Allis. 2000. Mitotic phosphorylation of histone H3 is governed by Ipl1/aurora kinase and Glc7/PP1 phosphatase in budding yeast and nematodes. Cell 102:279-291.

118. Kelly, A. E., S. C. Sampath, T. A. Maniar, E. M. Woo, B. T. Chait, and H. Funabiki. 2007. Chromosomal enrichment and activation of the aurora B pathway are coupled to spatially regulate spindle assembly. Dev Cell 12:31-43.

119. Sessa, F., M. Mapelli, C. Ciferri, C. Tarricone, L. B. Areces, T. R. Schneider, P. T. Stukenberg, and A. Musacchio. 2005. Mechanism of Aurora B activation by INCENP and inhibition by hesperadin. Mol Cell 18:379-391.

120. Mollinari, C., C. Reynaud, S. Martineau-Thuillier, S. Monier, S. Kieffer, J. Garin, P. R. Andreassen, A. Boulet, B. Goud, J. P. Kleman, and R. L. Margolis. 2003. The mammalian passenger protein TD-60 is an RCC1 family member with an essential role in prometaphase to metaphase progression. Dev Cell 5:295-307.

121. Rosasco-Nitcher, S. E., W. Lan, S. Khorasanizadeh, and P. T. Stukenberg. 2008. Centromeric Aurora-B activation requires TD-60, microtubules, and substrate priming phosphorylation. Science 319:469-472.

122. Heallen, T. R., H. P. Adams, T. Furuta, K. J. Verbrugghe, and J. M. Schumacher. 2008. An Afg2/Spaf-related Cdc48-like AAA ATPase regulates the stability and activity of the C. elegans Aurora B kinase AIR-2. Dev Cell 15:603-616.

123. Han, Z., G. M. Riefler, J. R. Saam, S. E. Mango, and J. M. Schumacher. 2005. The C. elegans Tousled-like kinase contributes to chromosome segregation as a substrate and regulator of the Aurora B kinase. Curr Biol 15:894-904.

124. Riefler, G. M., S. Y. Dent, and J. M. Schumacher. 2008. Tousled-mediated activation of Aurora B kinase does not require Tousled kinase activity in vivo. The Journal of biological chemistry 283:12763-12768.
125. Roe, J. L., C. J. Rivin, R. A. Sessions, K. A. Feldmann, and P. C. Zambryski. 1993. The Tousled gene in A. thaliana encodes a protein kinase homolog that is required for leaf and flower development. Cell 75:939-950.
126. Sillje, H. H., K. Takahashi, K. Tanaka, G. Van Houwe, and E. A. Nigg. 1999. Mammalian homologues of the plant Tousled gene code for cell-cycle-regulated kinases with maximal activities linked to ongoing DNA replication. Embo J 18:5691-5702.
127. Sillje, H. H., and E. A. Nigg. 2001. Identification of human Asf1 chromatin assembly factors as substrates of Tousled-like kinases. Curr Biol 11:1068-1073.
128. Carrera, P., Y. M. Moshkin, S. Gronke, H. H. Sillje, E. A. Nigg, H. Jackle, and F. Karch. 2003. Tousled-like kinase functions with the chromatin assembly pathway regulating nuclear divisions. Genes Dev 17:2578-2590.
129. Pilyugin, M., J. Demmers, C. P. Verrijzer, F. Karch, and Y. M. Moshkin. 2009. Phosphorylation-mediated control of histone chaperone ASF1 levels by Tousled-like kinases. PLoS One 4:e8328.
130. Krause, D. R., J. C. Jonnalagadda, M. H. Gatei, H. H. Sillje, B. B. Zhou, E. A. Nigg, and K. Khanna. 2003. Suppression of Tousled-like kinase activity after DNA damage or replication block requires ATM, NBS1 and Chk1. Oncogene 22:5927-5937.
131. Groth, A., J. Lukas, E. A. Nigg, H. H. Sillje, C. Wernstedt, J. Bartek, and K. Hansen. 2003. Human Tousled like kinases are targeted by an ATM- and Chk1-dependent DNA damage checkpoint. Embo J 22:1676-1687.
132. Bakkenist, C. J., and M. B. Kastan. 2003. DNA damage activates ATM through intermolecular autophosphorylation and dimer dissociation. Nature 421:499-506.
133. Han, Z., J. R. Saam, H. P. Adams, S. E. Mango, and J. M. Schumacher. 2003. The C. elegans Tousled-like kinase (TLK-1) has an essential role in transcription. Curr Biol 13:1921-1929.

134. Korber, P., S. Barbaric, T. Luckenbach, A. Schmid, U. J. Schermer, D. Blaschke, and W. Horz. 2006. The histone chaperone Asf1 increases the rate of histone eviction at the yeast PHO5 and PHO8 promoters. The Journal of biological chemistry 281:5539-5545.
135. Sunkel, C. E., and D. M. Glover. 1988. polo, a mitotic mutant of Drosophila displaying abnormal spindle poles. J Cell Sci 89 (Pt 1):25-38.
136. Kumagai, A., and W. G. Dunphy. 1996. Purification and molecular cloning of Plx1, a Cdc25-regulatory kinase from Xenopus egg extracts. Science 273:1377-1380.
137. Elia, A. E., P. Rellos, L. F. Haire, J. W. Chao, F. J. Ivins, K. Hoepker, D. Mohammad, L. C. Cantley, S. J. Smerdon, and M. B. Yaffe. 2003. The molecular basis for phosphodependent substrate targeting and regulation of Plks by the Polo-box domain. Cell 115:83-95.
138. Watanabe, N., H. Arai, Y. Nishihara, M. Taniguchi, T. Hunter, and H. Osada. 2004. M-phase kinases induce phospho-dependent ubiquitination of somatic Wee1 by SCFbeta-TrCP. Proc Natl Acad Sci U S A 101:4419-4424.
139. Jackman, M., C. Lindon, E. A. Nigg, and J. Pines. 2003. Active cyclin B1-Cdk1 first appears on centrosomes in prophase. Nat Cell Biol 5:143-148.
140. Lane, H. A., and E. A. Nigg. 1996. Antibody microinjection reveals an essential role for human polo-like kinase 1 (Plk1) in the functional maturation of mitotic centrosomes. The Journal of cell biology 135:1701-1713.
141. Feng, Y., D. R. Hodge, G. Palmieri, D. L. Chase, D. L. Longo, and D. K. Ferris. 1999. Association of polo-like kinase with alpha-, beta- and gamma-tubulins in a stable complex. Biochem J 339 (Pt 2):435-442.
142. Sumara, I., E. Vorlaufer, P. T. Stukenberg, O. Kelm, N. Redemann, E. A. Nigg, and J. M. Peters. 2002. The dissociation of cohesin from chromosomes in prophase is regulated by Polo-like kinase. Mol Cell 9:515-525.
143. Wong, O. K., and G. Fang. 2007. Cdk1 phosphorylation of BubR1 controls spindle checkpoint arrest and Plk1-mediated formation of the 3F3/2 epitope. The Journal of cell biology 179:611-617.

144. Kotani, S., S. Tugendreich, M. Fujii, P. M. Jorgensen, N. Watanabe, C. Hoog, P. Hieter, and K. Todokoro. 1998. PKA and MPF-activated polo-like kinase regulate anaphase-promoting complex activity and mitosis progression. Mol Cell 1:371-380.

145. van Vugt, M. A., and R. H. Medema. 2005. Getting in and out of mitosis with Polo-like kinase-1. Oncogene 24:2844-2859.

146. Adams, R. R., A. A. Tavares, A. Salzberg, H. J. Bellen, and D. M. Glover. 1998. pavarotti encodes a kinesin-like protein required to organize the central spindle and contractile ring for cytokinesis. Genes Dev 12:1483-1494.

147. Goto, H., T. Kiyono, Y. Tomono, A. Kawajiri, T. Urano, K. Furukawa, E. A. Nigg, and M. Inagaki. 2006. Complex formation of Plk1 and INCENP required for metaphase-anaphase transition. Nat Cell Biol 8:180-187.

148. Boxem, M., D. G. Srinivasan, and S. van den Heuvel. 1999. The Caenorhabditis elegans gene ncc-1 encodes a cdc2-related kinase required for M phase in meiotic and mitotic cell divisions, but not for S phase. Development (Cambridge, England) 126:2227-2239.

149. Chase, D., C. Serafinas, N. Ashcroft, M. Kosinski, D. Longo, D. K. Ferris, and A. Golden. 2000. The polo-like kinase PLK-1 is required for nuclear envelope breakdown and the completion of meiosis in Caenorhabditis elegans. Genesis 26:26-41.

150. Burrows, A. E., B. K. Sceurman, M. E. Kosinski, C. T. Richie, P. L. Sadler, J. M. Schumacher, and A. Golden. 2006. The C. elegans Myt1 ortholog is required for the proper timing of oocyte maturation. Development (Cambridge, England) 133:697-709.

151. Schumacher, J. M., A. Golden, and P. J. Donovan. 1998. AIR-2: An Aurora/Ipl1-related protein kinase associated with chromosomes and midbody microtubules is required for polar body extrusion and cytokinesis in Caenorhabditis elegans embryos. The Journal of cell biology 143:1635-1646.

152. Rogers, E., J. D. Bishop, J. A. Waddle, J. M. Schumacher, and R. Lin. 2002. The aurora kinase AIR-2 functions in the release of chromosome cohesion in Caenorhabditis elegans meiosis. The Journal of cell biology 157:219-229.

153. Kaitna, S., P. Pasierbek, M. Jantsch, J. Loidl, and M. Glotzer. 2002. The aurora B kinase AIR-2 regulates kinetochores during mitosis and is required for separation of homologous Chromosomes during meiosis. Curr Biol 12:798-812.
154. Essex, A., A. Dammermann, L. Lewellyn, K. Oegema, and A. Desai. 2009. Systematic analysis in Caenorhabditis elegans reveals that the spindle checkpoint is composed of two largely independent branches. Mol Biol Cell 20:1252-1267.
155. Arnaoutov, A., and M. Dasso. 2003. The Ran GTPase regulates kinetochore function. Dev Cell 5:99-111.
156. Mishra, R. K., P. Chakraborty, A. Arnaoutov, B. M. Fontoura, and M. Dasso. The Nup107-160 complex and gamma-TuRC regulate microtubule polymerization at kinetochores. Nat Cell Biol 12:164-169.
157. Zhou, J., J. Yao, and H. C. Joshi. 2002. Attachment and tension in the spindle assembly checkpoint. J Cell Sci 115:3547-3555.
158. Pinsky, B. A., and S. Biggins. 2005. The spindle checkpoint: tension versus attachment. Trends Cell Biol 15:486-493.
159. Li, R., and A. W. Murray. 1991. Feedback control of mitosis in budding yeast. Cell 66:519-531.
160. Kulukian, A., J. S. Han, and D. W. Cleveland. 2009. Unattached kinetochores catalyze production of an anaphase inhibitor that requires a Mad2 template to prime Cdc20 for BubR1 binding. Dev Cell 16:105-117.
161. Fang, G., H. Yu, and M. W. Kirschner. 1998. The checkpoint protein MAD2 and the mitotic regulator CDC20 form a ternary complex with the anaphase-promoting complex to control anaphase initiation. Genes Dev 12:1871-1883.
162. Luo, X., Z. Tang, G. Xia, K. Wassmann, T. Matsumoto, J. Rizo, and H. Yu. 2004. The Mad2 spindle checkpoint protein has two distinct natively folded states. Nat Struct Mol Biol 11:338-345.
163. Sudakin, V., G. K. Chan, and T. J. Yen. 2001. Checkpoint inhibition of the APC/C in HeLa cells is mediated by a complex of BUBR1, BUB3, CDC20, and MAD2. The Journal of cell biology 154:925-936.
164. Millband, D. N., and K. G. Hardwick. 2002. Fission yeast Mad3p is required for Mad2p to inhibit the anaphase-promoting complex and localizes to kinetochores

in a Bub1p-, Bub3p-, and Mph1p-dependent manner. Mol Cell Biol 22:2728-2742.

165. Encalada, S. E., J. Willis, R. Lyczak, and B. Bowerman. 2005. A spindle checkpoint functions during mitosis in the early Caenorhabditis elegans embryo. Mol Biol Cell 16:1056-1070.

166. Yamamoto, T. G., S. Watanabe, A. Essex, and R. Kitagawa. 2008. SPDL-1 functions as a kinetochore receptor for MDF-1 in Caenorhabditis elegans. The Journal of cell biology 183:187-194.

167. Griffis, E. R., N. Stuurman, and R. D. Vale. 2007. Spindly, a novel protein essential for silencing the spindle assembly checkpoint, recruits dynein to the kinetochore. J Cell Biol 177:1005-1015.

168. Pinsky, B. A., C. Kung, K. M. Shokat, and S. Biggins. 2006. The Ipl1-Aurora protein kinase activates the spindle checkpoint by creating unattached kinetochores. Nat Cell Biol 8:78-83.

169. Cimini, D., X. Wan, C. B. Hirel, and E. D. Salmon. 2006. Aurora kinase promotes turnover of kinetochore microtubules to reduce chromosome segregation errors. Curr Biol 16:1711-1718.

170. Sandall, S., F. Severin, I. X. McLeod, J. R. Yates, 3rd, K. Oegema, A. Hyman, and A. Desai. 2006. A Bir1-Sli15 complex connects centromeres to microtubules and is required to sense kinetochore tension. Cell 127:1179-1191.

171. Ditchfield, C., V. L. Johnson, A. Tighe, R. Ellston, C. Haworth, T. Johnson, A. Mortlock, N. Keen, and S. S. Taylor. 2003. Aurora B couples chromosome alignment with anaphase by targeting BubR1, Mad2, and Cenp-E to kinetochores. The Journal of cell biology 161:267-280.

172. Famulski, J. K., and G. K. Chan. 2007. Aurora B kinase-dependent recruitment of hZW10 and hROD to tensionless kinetochores. Curr Biol 17:2143-2149.

173. Elowe, S., S. Hummer, A. Uldschmid, X. Li, and E. A. Nigg. 2007. Tension-sensitive Plk1 phosphorylation on BubR1 regulates the stability of kinetochore microtubule interactions. Genes Dev 21:2205-2219.

174. Meraldi, P., and P. K. Sorger. 2005. A dual role for Bub1 in the spindle checkpoint and chromosome congression. EMBO J 24:1621-1633.

175. Logarinho, E., T. Resende, C. Torres, and H. Bousbaa. 2008. The human spindle assembly checkpoint protein Bub3 is required for the establishment of efficient kinetochore-microtubule attachments. Mol Biol Cell 19:1798-1813.
176. Kiyomitsu, T., C. Obuse, and M. Yanagida. 2007. Human Blinkin/AF15q14 is required for chromosome alignment and the mitotic checkpoint through direct interaction with Bub1 and BubR1. Dev Cell 13:663-676.
177. Kops, G. J., Y. Kim, B. A. Weaver, Y. Mao, I. McLeod, J. R. Yates, 3rd, M. Tagaya, and D. W. Cleveland. 2005. ZW10 links mitotic checkpoint signaling to the structural kinetochore. The Journal of cell biology 169:49-60.
178. Janke, C., J. Ortiz, J. Lechner, A. Shevchenko, M. M. Magiera, C. Schramm, and E. Schiebel. 2001. The budding yeast proteins Spc24p and Spc25p interact with Ndc80p and Nuf2p at the kinetochore and are important for kinetochore clustering and checkpoint control. EMBO J 20:777-791.
179. Matsuura, S., Y. Matsumoto, K. Morishima, H. Izumi, H. Matsumoto, E. Ito, K. Tsutsui, J. Kobayashi, H. Tauchi, Y. Kajiwara, S. Hama, K. Kurisu, H. Tahara, M. Oshimura, K. Komatsu, T. Ikeuchi, and T. Kajii. 2006. Monoallelic BUB1B mutations and defective mitotic-spindle checkpoint in seven families with premature chromatid separation (PCS) syndrome. Am J Med Genet A 140:358-367.
180. Hanks, S., K. Coleman, S. Reid, A. Plaja, H. Firth, D. Fitzpatrick, A. Kidd, K. Mehes, R. Nash, N. Robin, N. Shannon, J. Tolmie, J. Swansbury, A. Irrthum, J. Douglas, and N. Rahman. 2004. Constitutional aneuploidy and cancer predisposition caused by biallelic mutations in BUB1B. Nat Genet 36:1159-1161.
181. Yang, M., B. Li, D. R. Tomchick, M. Machius, J. Rizo, H. Yu, and X. Luo. 2007. p31comet blocks Mad2 activation through structural mimicry. Cell 131:744-755.
182. Mao, Y., A. Desai, and D. W. Cleveland. 2005. Microtubule capture by CENP-E silences BubR1-dependent mitotic checkpoint signaling. The Journal of cell biology 170:873-880.

183. Mische, S., Y. He, L. Ma, M. Li, M. Serr, and T. S. Hays. 2008. Dynein light intermediate chain: an essential subunit that contributes to spindle checkpoint inactivation. Mol Biol Cell 19:4918-4929.
184. Sivaram, M. V., T. L. Wadzinski, S. D. Redick, T. Manna, and S. J. Doxsey. 2009. Dynein light intermediate chain 1 is required for progress through the spindle assembly checkpoint. EMBO J 28:902-914.
185. Kardon, J. R., and R. D. Vale. 2009. Regulators of the cytoplasmic dynein motor. Nat Rev Mol Cell Biol 10:854-865.
186. Daum, J. R., J. D. Wren, J. J. Daniel, S. Sivakumar, J. N. McAvoy, T. A. Potapova, and G. J. Gorbsky. 2009. Ska3 is required for spindle checkpoint silencing and the maintenance of chromosome cohesion in mitosis. Curr Biol 19:1467-1472.
187. Liu, D., G. Vader, M. J. Vromans, M. A. Lampson, and S. M. Lens. 2009. Sensing chromosome bi-orientation by spatial separation of aurora B kinase from kinetochore substrates. Science 323:1350-1353.
188. Pinsky, B. A., C. R. Nelson, and S. Biggins. 2009. Protein phosphatase 1 regulates exit from the spindle checkpoint in budding yeast. Curr Biol 19:1182-1187.
189. Vanoosthuyse, V., and K. G. Hardwick. 2009. A novel protein phosphatase 1-dependent spindle checkpoint silencing mechanism. Curr Biol 19:1176-1181.
190. Oegema, K., and A. A. Hyman. 2006. Cell division. WormBook:1-40.
191. Couzin, J. 2006. Nobel Prize in Physiology or Medicine. Method to silence genes earns loud praise. Science 314:34.
192. Hubbard, E. J., and D. Greenstein. 2000. The Caenorhabditis elegans gonad: a test tube for cell and developmental biology. Dev Dyn 218:2-22.
193. Greenstein, D. 2005. Control of oocyte meiotic maturation and fertilization. WormBook:1-12.
194. Gonczy, P., and L. S. Rose. 2005. Asymmetric cell division and axis formation in the embryo. WormBook:1-20.
195. Service, R. F. 2008. Nobel Prize in chemistry. Three scientists bask in prize's fluorescent glow. Science 322:361.

196. Kelly, W. G., and A. Fire. 1998. Chromatin silencing and the maintenance of a functional germline in Caenorhabditis elegans. Development (Cambridge, England) 125:2451-2456.
197. Praitis, V., E. Casey, D. Collar, and J. Austin. 2001. Creation of low-copy integrated transgenic lines in Caenorhabditis elegans. Genetics 157:1217-1226.
198. Robert, V. J., I. Katic, and J. L. Bessereau. 2009. Mos1 transposition as a tool to engineer the Caenorhabditis elegans genome by homologous recombination. Methods 49:263-269.
199. Bartek, J., and J. Lukas. 2003. Chk1 and Chk2 kinases in checkpoint control and cancer. Cancer Cell 3:421-429.
200. Roe, J. L., J. L. Nemhauser, and P. C. Zambryski. 1997. TOUSLED participates in apical tissue formation during gynoecium development in Arabidopsis. Plant Cell 9:335-353.
201. Ozlu, N., M. Srayko, K. Kinoshita, B. Habermann, T. O'Toole E, T. Muller-Reichert, N. Schmalz, A. Desai, and A. A. Hyman. 2005. An essential function of the C. elegans ortholog of TPX2 is to localize activated aurora A kinase to mitotic spindles. Dev Cell 9:237-248.
202. Alder, M. N., S. Dames, J. Gaudet, and S. E. Mango. 2003. Gene silencing in Caenorhabditis elegans by transitive RNA interference. RNA 9:25-32.
203. Li, Y., R. DeFatta, C. Anthony, G. Sunavala, and A. De Benedetti. 2001. A translationally regulated Tousled kinase phosphorylates histone H3 and confers radioresistance when overexpressed. Oncogene 20:726-738.
204. Biggins, S., F. F. Severin, N. Bhalla, I. Sassoon, A. A. Hyman, and A. W. Murray. 1999. The conserved protein kinase Ipl1 regulates microtubule binding to kinetochores in budding yeast. Genes Dev 13:532-544.
205. Clarke, D. J., and J. Bachant. 2008. Kinetochore structure and spindle assembly checkpoint signaling in the budding yeast, Saccharomyces cerevisiae. Front Biosci 13:6787-6819.
206. Puig, O., F. Caspary, G. Rigaut, B. Rutz, E. Bouveret, E. Bragado-Nilsson, M. Wilm, and B. Seraphin. 2001. The tandem affinity purification (TAP) method: a general procedure of protein complex purification. Methods 24:218-229.

207. Warner, S. L., S. Bashyam, H. Vankayalapati, D. J. Bearss, H. Han, D. Mahadevan, D. D. Von Hoff, and L. H. Hurley. 2006. Identification of a lead small-molecule inhibitor of the Aurora kinases using a structure-assisted, fragment-based approach. Mol Cancer Ther 5:1764-1773.

208. Kotwaliwale, C. V., S. B. Frei, B. M. Stern, and S. Biggins. 2007. A pathway containing the Ipl1/aurora protein kinase and the spindle midzone protein Ase1 regulates yeast spindle assembly. Dev Cell 13:433-445.

209. Bayliss, R., T. Sardon, I. Vernos, and E. Conti. 2003. Structural basis of Aurora-A activation by TPX2 at the mitotic spindle. Mol Cell 12:851-862.

210. Cheetham, G. M., R. M. Knegtel, J. T. Coll, S. B. Renwick, L. Swenson, P. Weber, J. A. Lippke, and D. A. Austen. 2002. Crystal structure of aurora-2, an oncogenic serine/threonine kinase. The Journal of biological chemistry 277:42419-42422.

211. Walter, A. O., W. Seghezzi, W. Korver, J. Sheung, and E. Lees. 2000. The mitotic serine/threonine kinase Aurora2/AIK is regulated by phosphorylation and degradation. Oncogene 19:4906-4916.

212. Eyers, P. A., E. Erikson, L. G. Chen, and J. L. Maller. 2003. A novel mechanism for activation of the protein kinase Aurora A. Curr Biol 13:691-697.

213. Honda, R., R. Korner, and E. A. Nigg. 2003. Exploring the functional interactions between Aurora B, INCENP, and survivin in mitosis. Mol Biol Cell 14:3325-3341.

214. Li, Z., S. Gourguechon, and C. C. Wang. 2007. Tousled-like kinase in a microbial eukaryote regulates spindle assembly and S-phase progression by interacting with Aurora kinase and chromatin assembly factors. J Cell Sci 120:3883-3894.

215. Gesellchen, F., O. Bertinetti, and F. W. Herberg. 2006. Analysis of posttranslational modifications exemplified using protein kinase A. Biochim Biophys Acta 1764:1788-1800.

216. Cheng, K. Y., E. D. Lowe, J. Sinclair, E. A. Nigg, and L. N. Johnson. 2003. The crystal structure of the human polo-like kinase-1 polo box domain and its phospho-peptide complex. Embo J 22:5757-5768.

217. Liu, M. Y., S. Cai, A. Espejo, M. T. Bedford, and C. L. Walker. 2002. 14-3-3 interacts with the tumor suppressor tuberin at Akt phosphorylation site(s). Cancer Res 62:6475-6480.

218. Holland, A. J., and S. S. Taylor. 2006. Cyclin-B1-mediated inhibition of excess separase is required for timely chromosome disjunction. J Cell Sci 119:3325-3336.

219. Fields, S., and R. Sternglanz. 1994. The two-hybrid system: an assay for protein-protein interactions. Trends Genet 10:286-292.

220. Guo, D., T. R. Hazbun, X. J. Xu, S. L. Ng, S. Fields, and M. H. Kuo. 2004. A tethered catalysis, two-hybrid system to identify protein-protein interactions requiring post-translational modifications. Nat Biotechnol 22:888-892.

221. Krogan, N. J., M. Kim, A. Tong, A. Golshani, G. Cagney, V. Canadien, D. P. Richards, B. K. Beattie, A. Emili, C. Boone, A. Shilatifard, S. Buratowski, and J. Greenblatt. 2003. Methylation of histone H3 by Set2 in Saccharomyces cerevisiae is linked to transcriptional elongation by RNA polymerase II. Mol Cell Biol 23:4207-4218.

222. Albert, T. K., M. Lemaire, N. L. van Berkum, R. Gentz, M. A. Collart, and H. T. Timmers. 2000. Isolation and characterization of human orthologs of yeast CCR4-NOT complex subunits. Nucleic Acids Res 28:809-817.

223. Le Bot, N., M. C. Tsai, R. K. Andrews, and J. Ahringer. 2003. TAC-1, a regulator of microtubule length in the C. elegans embryo. Curr Biol 13:1499-1505.

224. Bellanger, J. M., and P. Gonczy. 2003. TAC-1 and ZYG-9 form a complex that promotes microtubule assembly in C. elegans embryos. Curr Biol 13:1488-1498.

225. Kim, M. H., D. R. Cooper, A. Oleksy, Y. Devedjiev, U. Derewenda, O. Reiner, J. Otlewski, and Z. S. Derewenda. 2004. The structure of the N-terminal domain of the product of the lissencephaly gene Lis1 and its functional implications. Structure 12:987-998.

226. Grieco, M., A. Cerrato, M. Santoro, A. Fusco, R. M. Melillo, and G. Vecchio. 1994. Cloning and characterization of H4 (D10S170), a gene involved in RET rearrangements in vivo. Oncogene 9:2531-2535.

227. Gandhi, M., L. W. Dillon, S. Pramanik, Y. E. Nikiforov, and Y. H. Wang. DNA breaks at fragile sites generate oncogenic RET/PTC rearrangements in human thyroid cells. Oncogene.

228. Noble, M. E., J. A. Endicott, N. R. Brown, and L. N. Johnson. 1997. The cyclin box fold: protein recognition in cell-cycle and transcription control. Trends Biochem Sci 22:482-487.

229. Adams, P. D., X. Li, W. R. Sellers, K. B. Baker, X. Leng, J. W. Harper, Y. Taya, and W. G. Kaelin, Jr. 1999. Retinoblastoma protein contains a C-terminal motif that targets it for phosphorylation by cyclin-cdk complexes. Mol Cell Biol 19:1068-1080.

230. Latham, J. A., and S. Y. Dent. 2007. Cross-regulation of histone modifications. Nat Struct Mol Biol 14:1017-1024.

231. Campbell, M. S., and G. J. Gorbsky. 1995. Microinjection of mitotic cells with the 3F3/2 anti-phosphoepitope antibody delays the onset of anaphase. The Journal of cell biology 129:1195-1204.

232. Zachos, G., E. J. Black, M. Walker, M. T. Scott, P. Vagnarelli, W. C. Earnshaw, and D. A. Gillespie. 2007. Chk1 is required for spindle checkpoint function. Dev Cell 12:247-260.

233. Tang, J., R. L. Erikson, and X. Liu. 2006. Checkpoint kinase 1 (Chk1) is required for mitotic progression through negative regulation of polo-like kinase 1 (Plk1). Proc Natl Acad Sci U S A 103:11964-11969.

234. Kim, S. H., A. H. Holway, S. Wolff, A. Dillin, and W. M. Michael. 2007. SMK-1/PPH-4.1-mediated silencing of the CHK-1 response to DNA damage in early C. elegans embryos. The Journal of cell biology 179:41-52.

235. Gartner, A., S. Milstein, S. Ahmed, J. Hodgkin, and M. O. Hengartner. 2000. A conserved checkpoint pathway mediates DNA damage--induced apoptosis and cell cycle arrest in C. elegans. Mol Cell 5:435-443.

236. Brauchle, M., K. Baumer, and P. Gonczy. 2003. Differential activation of the DNA replication checkpoint contributes to asynchrony of cell division in C. elegans embryos. Curr Biol 13:819-827.

237. Ehsan, H., J. P. Reichheld, T. Durfee, and J. L. Roe. 2004. TOUSLED kinase activity oscillates during the cell cycle and interacts with chromatin regulators. Plant Physiol 134:1488-1499.
238. Seroz, T., J. R. Hwang, V. Moncollin, and J. M. Egly. 1995. TFIIH: a link between transcription, DNA repair and cell cycle regulation. Curr Opin Genet Dev 5:217-221.
239. Strome, S. 2005. Specification of the germ line. WormBook:1-10.
240. He, X., S. Asthana, and P. K. Sorger. 2000. Transient sister chromatid separation and elastic deformation of chromosomes during mitosis in budding yeast. Cell 101:763-775.
241. van den Heuvel, S. 2005. Cell-cycle regulation. WormBook:1-16.
242. Murray, A. W. 2004. Recycling the cell cycle: cyclins revisited. Cell 116:221-234.
243. Li, J., A. N. Meyer, and D. J. Donoghue. 1997. Nuclear localization of cyclin B1 mediates its biological activity and is regulated by phosphorylation. Proc Natl Acad Sci U S A 94:502-507.
244. Maldonado-Codina, G., and D. M. Glover. 1992. Cyclins A and B associate with chromatin and the polar regions of spindles, respectively, and do not undergo complete degradation at anaphase in syncytial Drosophila embryos. The Journal of cell biology 116:967-976.
245. Alfa, C. E., B. Ducommun, D. Beach, and J. S. Hyams. 1990. Distinct nuclear and spindle pole body population of cyclin-cdc2 in fission yeast. Nature 347:680-682.
246. Pines, J., and T. Hunter. 1991. Human cyclins A and B1 are differentially located in the cell and undergo cell cycle-dependent nuclear transport. The Journal of cell biology 115:1-17.
247. Cahu, J., A. Olichon, C. Hentrich, H. Schek, J. Drinjakovic, C. Zhang, A. Doherty-Kirby, G. Lajoie, and T. Surrey. 2008. Phosphorylation by Cdk1 increases the binding of Eg5 to microtubules in vitro and in Xenopus egg extract spindles. PLoS One 3:e3936.

248. Miyamoto, D. T., Z. E. Perlman, K. S. Burbank, A. C. Groen, and T. J. Mitchison. 2004. The kinesin Eg5 drives poleward microtubule flux in Xenopus laevis egg extract spindles. The Journal of cell biology 167:813-818.
249. Crasta, K., P. Huang, G. Morgan, M. Winey, and U. Surana. 2006. Cdk1 regulates centrosome separation by restraining proteolysis of microtubule-associated proteins. EMBO J 25:2551-2563.
250. Beaudouin, J., D. Gerlich, N. Daigle, R. Eils, and J. Ellenberg. 2002. Nuclear envelope breakdown proceeds by microtubule-induced tearing of the lamina. Cell 108:83-96.
251. Salina, D., K. Bodoor, D. M. Eckley, T. A. Schroer, J. B. Rattner, and B. Burke. 2002. Cytoplasmic dynein as a facilitator of nuclear envelope breakdown. Cell 108:97-107.
252. Galy, V., W. Antonin, A. Jaedicke, M. Sachse, R. Santarella, U. Haselmann, and I. Mattaj. 2008. A role for gp210 in mitotic nuclear-envelope breakdown. J Cell Sci 121:317-328.
253. Nigg, E. A. 1993. Cellular substrates of p34(cdc2) and its companion cyclin-dependent kinases. Trends Cell Biol 3:296-301.
254. Bentley, A. M., G. Normand, J. Hoyt, and R. W. King. 2007. Distinct sequence elements of cyclin B1 promote localization to chromatin, centrosomes, and kinetochores during mitosis. Mol Biol Cell 18:4847-4858.
255. Chen, Q., X. Zhang, Q. Jiang, P. R. Clarke, and C. Zhang. 2008. Cyclin B1 is localized to unattached kinetochores and contributes to efficient microtubule attachment and proper chromosome alignment during mitosis. Cell research 18:268-280.
256. Stemmann, O., H. Zou, S. A. Gerber, S. P. Gygi, and M. W. Kirschner. 2001. Dual inhibition of sister chromatid separation at metaphase. Cell 107:715-726.
257. Gorr, I. H., D. Boos, and O. Stemmann. 2005. Mutual inhibition of separase and Cdk1 by two-step complex formation. Mol Cell 19:135-141.
258. Dahmann, C., and B. Futcher. 1995. Specialization of B-type cyclins for mitosis or meiosis in S. cerevisiae. Genetics 140:957-963.

259. Fitch, I., C. Dahmann, U. Surana, A. Amon, K. Nasmyth, L. Goetsch, B. Byers, and B. Futcher. 1992. Characterization of four B-type cyclin genes of the budding yeast Saccharomyces cerevisiae. Mol Biol Cell 3:805-818.

260. Richardson, H., D. J. Lew, M. Henze, K. Sugimoto, and S. I. Reed. 1992. Cyclin-B homologs in Saccharomyces cerevisiae function in S phase and in G2. Genes Dev 6:2021-2034.

261. Sigrist, S., H. Jacobs, R. Stratmann, and C. F. Lehner. 1995. Exit from mitosis is regulated by Drosophila fizzy and the sequential destruction of cyclins A, B and B3. EMBO J 14:4827-4838.

262. McCleland, M. L., J. A. Farrell, and P. H. O'Farrell. 2009. Influence of cyclin type and dose on mitotic entry and progression in the early Drosophila embryo. J Cell Biol 184:639-646.

263. Brandeis, M., I. Rosewell, M. Carrington, T. Crompton, M. A. Jacobs, J. Kirk, J. Gannon, and T. Hunt. 1998. Cyclin B2-null mice develop normally and are fertile whereas cyclin B1-null mice die in utero. Proc Natl Acad Sci U S A 95:4344-4349.

264. Nguyen, T. B., K. Manova, P. Capodieci, C. Lindon, S. Bottega, X. Y. Wang, J. Refik-Rogers, J. Pines, D. J. Wolgemuth, and A. Koff. 2002. Characterization and expression of mammalian cyclin b3, a prepachytene meiotic cyclin. J Biol Chem 277:41960-41969.

265. Nieduszynski, C. A., J. Murray, and M. Carrington. 2002. Whole-genome analysis of animal A- and B-type cyclins. Genome Biol 3:RESEARCH0070.

266. Lozano, J. C., E. Perret, P. Schatt, C. Arnould, G. Peaucellier, and A. Picard. 2002. Molecular cloning, gene localization, and structure of human cyclin B3. Biochem Biophys Res Commun 291:406-413.

267. Wallenfang, M. R., and G. Seydoux. 2002. cdk-7 Is required for mRNA transcription and cell cycle progression in Caenorhabditis elegans embryos. Proc Natl Acad Sci U S A 99:5527-5532.

268. Sonneville, R., and P. Gonczy. 2004. Zyg-11 and cul-2 regulate progression through meiosis II and polarity establishment in C. elegans. Development 131:3527-3543.

269. Lyczak, R., L. Zweier, T. Group, M. A. Murrow, C. Snyder, L. Kulovitz, A. Beatty, K. Smith, and B. Bowerman. 2006. The puromycin-sensitive aminopeptidase PAM-1 is required for meiotic exit and anteroposterior polarity in the one-cell Caenorhabditis elegans embryo. Development 133:4281-4292.
270. Shirayama, M., M. C. Soto, T. Ishidate, S. Kim, K. Nakamura, Y. Bei, S. van den Heuvel, and C. C. Mello. 2006. The Conserved Kinases CDK-1, GSK-3, KIN-19, and MBK-2 Promote OMA-1 Destruction to Regulate the Oocyte-to-Embryo Transition in C. elegans. Curr Biol 16:47-55.
271. van der Voet, M., M. A. Lorson, D. G. Srinivasan, K. L. Bennett, and S. van den Heuvel. 2009. C. elegans mitotic cyclins have distinct as well as overlapping functions in chromosome segregation. Cell Cycle 8:4091-4102.
272. Maresca, T. J., and E. D. Salmon. 2009. Intrakinetochore stretch is associated with changes in kinetochore phosphorylation and spindle assembly checkpoint activity. The Journal of cell biology 184:373-381.
273. Uchida, K. S., K. Takagaki, K. Kumada, Y. Hirayama, T. Noda, and T. Hirota. 2009. Kinetochore stretching inactivates the spindle assembly checkpoint. The Journal of cell biology 184:383-390.
274. Ahonen, L. J., M. J. Kallio, J. R. Daum, M. Bolton, I. A. Manke, M. B. Yaffe, P. T. Stukenberg, and G. J. Gorbsky. 2005. Polo-like kinase 1 creates the tension-sensing 3F3/2 phosphoepitope and modulates the association of spindle-checkpoint proteins at kinetochores. Curr Biol 15:1078-1089.
275. Waters, J. C., R. H. Chen, A. W. Murray, and E. D. Salmon. 1998. Localization of Mad2 to kinetochores depends on microtubule attachment, not tension. The Journal of cell biology 141:1181-1191.
276. Kitagawa, R., and A. M. Rose. 1999. Components of the spindle-assembly checkpoint are essential in Caenorhabditis elegans. Nat Cell Biol 1:514-521.
277. Skop, A. R., and J. G. White. 1998. The dynactin complex is required for cleavage plane specification in early Caenorhabditis elegans embryos. Curr Biol 8:1110-1116.

278. Bishop, J. D., Z. Han, and J. M. Schumacher. 2005. The Caenorhabditis elegans Aurora B kinase AIR-2 phosphorylates and is required for the localization of a BimC kinesin to meiotic and mitotic spindles. Mol Biol Cell 16:742-756.
279. Cockell, M. M., K. Baumer, and P. Gonczy. 2004. lis-1 is required for dynein-dependent cell division processes in C. elegans embryos. J Cell Sci 117:4571-4582.
280. O'Rourke, S. M., M. D. Dorfman, J. C. Carter, and B. Bowerman. 2007. Dynein modifiers in C. elegans: light chains suppress conditional heavy chain mutants. PLoS Genet 3:e128.
281. Hoffman, D. B., C. G. Pearson, T. J. Yen, B. J. Howell, and E. D. Salmon. 2001. Microtubule-dependent changes in assembly of microtubule motor proteins and mitotic spindle checkpoint proteins at PtK1 kinetochores. Mol Biol Cell 12:1995-2009.
282. de Carvalho, C. E., S. Zaaijer, S. Smolikov, Y. Gu, J. M. Schumacher, and M. P. Colaiacovo. 2008. LAB-1 antagonizes the Aurora B kinase in C. elegans. Genes Dev 22:2869-2885.
283. Tschop, K., G. A. Muller, J. Grosche, and K. Engeland. 2006. Human cyclin B3. mRNA expression during the cell cycle and identification of three novel nonclassical nuclear localization signals. FEBS J 273:1681-1695.
284. Gallant, P., and E. A. Nigg. 1994. Identification of a novel vertebrate cyclin: cyclin B3 shares properties with both A- and B-type cyclins. EMBO J 13:595-605.
285. Li, J. J., and S. A. Li. 2006. Mitotic kinases: the key to duplication, segregation, and cytokinesis errors, chromosomal instability, and oncogenesis. Pharmacology & therapeutics 111:974-984.
286. Gassmann, R., A. Essex, J. S. Hu, P. S. Maddox, F. Motegi, A. Sugimoto, S. M. O'Rourke, B. Bowerman, I. McLeod, J. R. Yates, 3rd, K. Oegema, I. M. Cheeseman, and A. Desai. 2008. A new mechanism controlling kinetochore-microtubule interactions revealed by comparison of two dynein-targeting components: SPDL-1 and the Rod/Zwilch/Zw10 complex. Genes Dev 22:2385-2399.

287. Whyte, J., J. R. Bader, S. B. Tauhata, M. Raycroft, J. Hornick, K. K. Pfister, W. S. Lane, G. K. Chan, E. H. Hinchcliffe, P. S. Vaughan, and K. T. Vaughan. 2008. Phosphorylation regulates targeting of cytoplasmic dynein to kinetochores during mitosis. The Journal of cell biology 183:819-834.

288. Nystul, T. G., J. P. Goldmark, P. A. Padilla, and M. B. Roth. 2003. Suspended animation in C. elegans requires the spindle checkpoint. Science 302:1038-1041.

289. Csankovszki, G., K. Collette, K. Spahl, J. Carey, M. Snyder, E. Petty, U. Patel, T. Tabuchi, H. Liu, I. McLeod, J. Thompson, A. Sarkesik, J. Yates, B. J. Meyer, and K. Hagstrom. 2009. Three distinct condensin complexes control C. elegans chromosome dynamics. Curr Biol 19:9-19.

290. DeLuca, J. G., W. E. Gall, C. Ciferri, D. Cimini, A. Musacchio, and E. D. Salmon. 2006. Kinetochore microtubule dynamics and attachment stability are regulated by Hec1. Cell 127:969-982.

291. Chan, Y. W., L. L. Fava, A. Uldschmid, M. H. Schmitz, D. W. Gerlich, E. A. Nigg, and A. Santamaria. 2009. Mitotic control of kinetochore-associated dynein and spindle orientation by human Spindly. J Cell Biol 185:859-874.

292. Lee, K. M., I. Miklos, H. Du, S. Watt, Z. Szilagyi, J. E. Saiz, R. Madabhushi, C. J. Penkett, M. Sipiczki, J. Bahler, and R. P. Fisher. 2005. Impairment of the TFIIH-associated CDK-activating kinase selectively affects cell cycle-regulated gene expression in fission yeast. Mol Biol Cell 16:2734-2745.

293. Fuller, B. G., M. A. Lampson, E. A. Foley, S. Rosasco-Nitcher, K. V. Le, P. Tobelmann, D. L. Brautigan, P. T. Stukenberg, and T. M. Kapoor. 2008. Midzone activation of aurora B in anaphase produces an intracellular phosphorylation gradient. Nature 453:1132-1136.

294. Ong, S. E., L. J. Foster, and M. Mann. 2003. Mass spectrometric-based approaches in quantitative proteomics. Methods 29:124-130.

295. Michel, L. S., V. Liberal, A. Chatterjee, R. Kirchwegger, B. Pasche, W. Gerald, M. Dobles, P. K. Sorger, V. V. Murty, and R. Benezra. 2001. MAD2 haplo-insufficiency causes premature anaphase and chromosome instability in mammalian cells. Nature 409:355-359.

296. Cahill, D. P., C. Lengauer, J. Yu, G. J. Riggins, J. K. Willson, S. D. Markowitz, K. W. Kinzler, and B. Vogelstein. 1998. Mutations of mitotic checkpoint genes in human cancers. Nature 392:300-303.

297. Sotillo, R., E. Hernando, E. Diaz-Rodriguez, J. Teruya-Feldstein, C. Cordon-Cardo, S. W. Lowe, and R. Benezra. 2007. Mad2 overexpression promotes aneuploidy and tumorigenesis in mice. Cancer Cell 11:9-23.

298. Rhodes, D. R., J. Yu, K. Shanker, N. Deshpande, R. Varambally, D. Ghosh, T. Barrette, A. Pandey, and A. M. Chinnaiyan. 2004. ONCOMINE: a cancer microarray database and integrated data-mining platform. Neoplasia 6:1-6.

299. James, P., J. Halladay, and E. A. Craig. 1996. Genomic libraries and a host strain designed for highly efficient two-hybrid selection in yeast. Genetics 144:1425-1436.

300. Brenner, S. 1974. The genetics of Caenorhabditis elegans. Genetics 77:71-94.

301. McNally, K., A. Audhya, K. Oegema, and F. J. McNally. 2006. Katanin controls mitotic and meiotic spindle length. J Cell Biol 175:881-891.

302. Kamath, R. S., and J. Ahringer. 2003. Genome-wide RNAi screening in Caenorhabditis elegans. Methods 30:313-321.

303. Seydoux, G., and M. A. Dunn. 1997. Transcriptionally repressed germ cells lack a subpopulation of phosphorylated RNA polymerase II in early embryos of Caenorhabditis elegans and Drosophila melanogaster. Development 124:2191-2201.

304. Monen, J., P. S. Maddox, F. Hyndman, K. Oegema, and A. Desai. 2005. Differential role of CENP-A in the segregation of holocentric C. elegans chromosomes during meiosis and mitosis. Nat Cell Biol 7:1248-1255.

305. Daum, J. R., and G. J. Gorbsky. 1998. Casein kinase II catalyzes a mitotic phosphorylation on threonine 1342 of human DNA topoisomerase IIalpha, which is recognized by the 3F3/2 phosphoepitope antibody. J Biol Chem 273:30622-30629.

306. Dinkelmann, M. V., H. Zhang, A. R. Skop, and J. G. White. 2007. SPD-3 is required for spindle alignment in Caenorhabditis elegans embryos and localizes to mitochondria. Genetics 177:1609-1620.

VITA

Early childhood life was a challenge from the start for me, being born two months premature and weighing 3lbs 6oz. However, I quickly gained weight and showed no sign of permanent complications due to my premature birth (at least outwardly LOL). I was a sensitive child that loved animals and was brought up in a family that valued education, both academically and musically. My mother was a music teacher and taught me piano at an early age. However, I quickly became aware of my talent with singing and began concentrating on learning appropriate vocal technique in my early teenage years. I also succeeded in school, hardly ever getting less than an "A" in all subjects. Throughout my life, however, was an absence of parental figures, especially a father. My mother and father divorced when I was a year old as he was unwilling to work to support his family and was an alcoholic. So, my mother, brother, and I moved in and out of my grandparent's house (maternal side). When not living with my grandparents, we lived in trailers. Luckily, my grandparents were terrific people who supported me and ingrained the value of education in me. However, the disparity between what I felt inside as my unlimited potential as an intelligent and talented person maturing into adulthood and the confinement of the outside world due to financial difficulties was very distressing to me. Also, my family taught me that people are untrustworthy and they did not allow me the physical or mental freedom to get close to anyone. I was basically "secluded" my entire childhood until I graduated high school in 1996 at which time a swift onset of depersonalization disorder kicked in and has remained with me today (although the "symptoms" are nearly non-existent and lie somewhere in the background).

Many people may have acted out in violence or opposition to a childhood full of disappointments. However, I must have made the decision early in life to learn subjects that interested me (i.e. Science, Math, and Music), focus on but then forget material that I could care less about (i.e. History), and disconnect at some level from the

daily confusion that was my childhood. I graduated in the top 20 students of my high school class of over 400, was a member of the National Honors Society, Who's Who Among American High School Students, and Tri-M Music Honor Society. I was also involved in chorus and musical theater during high school, often having the lead male role in musicals… I guess those *gay* genes were my saving grace! After high school I enrolled at a local college (Stockton College) due to financial difficulties with an intended major in psychology and minor in music. Chris Narcisco entered my life full-time when I started college (I had known him in high school when I was convinced that he had stolen his brand new Nissan Maxima from an elderly woman at the nursing home he had worked at) and he took me under his wing to guide me in the right direction. If a God exists, It brought Chris and I together at that time in my life to show me true love and support. Turns out, he was and remains a very hard worker and did not mug an elderly woman after all! :) After two years at the local college, I decided that obtaining student loans and getting a better education at a higher accredited university (Rutgers) was a necessity due to the limitations of the local college. The Rutgers biology department was fantastic, and many of my classes centered on neuroscience. I changed my major to Biology, with a minor in Psychology. Also, I was fortunate to join one of the choruses at Rutgers and enrolled in vocal training with several music professors. I entered Dr. Bonnie Firestein's lab toward the end of my education at Rutgers to obtain lab experience. I was so fortunate to have contacted her at that time since she had just started her lab in the neuroscience department. The hands-on laboratory training she gave offered me the rare opportunity to work directly with an experienced scientist.

I am proud to admit that I am the first person in my family to obtain an advanced degree beyond a Bachelor's degree. Although my mother's B.A. was in early childhood education, other than teaching music to children she never capitalized on her degree. My grandmother obtained her B.A. in library science around the age of 50 and was a librarian for many years. Lastly, I have legally changed my last name within the past year to my grandmother's maiden name (Deyter) in honor of her memory and for personal gratification.

Virtual address: gmdeyter@gmail.com